Université de Caen Basse-Normandie

U.F.R. : Institut de Biologie Fondamentale et Appliquée

École doctorale Normande de Biologie Intégrative, Santé, Environnement

Thèse

Présentée par

Mr Martin Ubertini

Soutenue le

11 décembre 2012

En vue de l'obtention du

Doctorat de l'Université de Caen

Spécialité : Physiologie, Biologie des organismes, Populations, Interactions

(Arrêté du 07 août 2006)

Déterminisme de la remise en suspension des diatomées benthiques au travers du couplage benthos-pelagos dans les écosystèmes côtiers conchylicoles bas-normands

MEMBRES DU JURY :

Mr Jacques Clavier	Professeur, UBO-IUEM, Brest	Rapporteur
Mr Lionel Denis	Professeur, USTL-LOG, Wimereux	Rapporteur
Mr Dominique Davoult	Professeur, UPMC-SBR, Roscoff	Président
Mr Antoine Grémare	Professeur, UBX1, Bordeaux	Examinateur
Mr Francis Orvain	Maître de conférences, UCBN, Caen	Encadrant scientifique
Mr Sébastien Lefebvre	Professeur, USTL-LOG, Wimereux	Co-directeur
Mr Jean-Paul Robin	Professeur, UCBN, Caen	Directeur

Ces travaux de recherches ont été réalisés au sein de l'Ecole Doctorale Normande de Biologie Intégrative, Santé et Environnement, dans le laboratoire de Biologie des Mollusques marins et des Ecosystèmes Associés (BioMEA, FRE3484 – CNRS INEE) de l'Université de Caen basse-Normandie, sous la direction du Professeur Jean-Paul Robin

Cette thèse a été financée par le Conseil Régional de Basse-Normandie.

Je dédie cette thèse à ma mère.

Sans elle je n'en serais pas là (bon ça c'est sûr…) ; c'est grâce à ton amour, ton éducation, ta dévotion et tes conseils. Les mots sont bien peu de chose en comparaison de tout ce que tu m'as donné.

Merci maman.

Je remercie tout d'abord les Professeurs Jacques Clavier et Lionel Denis pour avoir accepté de prendre de leur précieux temps afin d'être rapporteur de ce travail.

Après m'avoir accueilli au sein de ses cours d'écologie marine en Master d'Océanographie et Environnements Marins à Paris VI, je suis heureux d'accueillir le Professeur Dominique Davoult au sein de ce jury de thèse et le remercie d'avoir accepté d'y participer.

Je remercie également le Professeur Antoine Grémare pour sa participation à ce jury de thèse.

Je remercie mon directeur, le Professeur Jean-Paul Robin, pour avoir accepté de diriger ma thèse à la thématique bien lointaine de la sienne. Merci également au Professeur Pascal Sourdaine pour m'avoir accueilli au sein du laboratoire BioMEA.

J'adresse bien sûr mes remerciements et ma reconnaissance à mon encadrant scientifique, Francis Orvain, pour ses conseils et la qualité de ses enseignements mais également pour son optimisme et son côté humain. Merci beaucoup Francis. Merci également à mon co-directeur, Sébastien Lefebvre, pour ses conseils éclairés, sa rigueur et sa facilité d'accès. Merci Sébastien.

Merci à tous les enseignants-chercheurs du laboratoire, et particulièrement Karine Grangeré (j'ai un peu hésité à te mettre chez les profs ;o), Pascal Claquin et Anne-Sophie Martinez, pour leurs conseils et leur bienveillance (et pour le reste !o).

Je remercie également le Docteur jérôme LeDauphin pour ses précieuses explications et aides en chimie.

Merci à Madame jeanne Mathieu pour son implication dans l'ensemble des démarches administratives liées à ma thèse au cours de ces 3 dernières années.

Je remercie également les techniciens permanents pour leur travail et leur sympathie : Christophe Roger, toujours le sourire et l'envie de rendre service, un grand merci à toi. Merci également à Bertrand, Sandra, Fabienne et Béatrice pour leur travail et leur courtoisie.

Merci aux personnels de la Station de Luc sur Mer et particulièrement Jean-Paul Lehodey pour son temps et son aide astucieuse dans les expériences.

Merci à tous les stagiaires également qui m'ont beaucoup aidé dans la tâche qui m'était dévolue : Christiane (la nerveuse), Sébastien (le consciencieux), Manu (le sportif), Ludovic (le jeunot), Georges (« Nous les Cap-Verdiens ont vous explose au Calva les Bretons et Normands »… Le comique) ; mais aussi Loris, Fan (FAN !)…

Un grand merci à mes collègues (et maintenant amis) de thèse, sans qui je n'aurais pu vivre ces 3 années de thèse exceptionnelles. Au programme mes collègues de ce bureau 100% testostérone : Le Gras Michael pour son côté gros ours gentil quand même, Antoine la motte pour rendre l'atmosphère de la pièce si agréable… et Charles la blonde pour son côté bougon mais gentil quand même (j'ai l'impression d'avoir déjà dit ça…). Et puis tous les autres : Paupau bien évidemment (Trainée !), Camille (et ma raclette alors !), Elmina (le pinson), Christelle (qui ne manque pas d'air non plus), Céline (je suis un elfe sylvain), Stéphanie (… Moi aussi !), Laetitia (la Tia-Tia), Maxine (Mireille), Marie (…Robert !), Valérie (Une fois), Margot (Concessionnaire Renault Traffic), Emilie (Tarot ?), Cécile (La râleuse), Anne-Flore (Mais achète-toi une vraie raquette de bad…), Virginie (miam miam la Rouelle de Porc), Jéhane (Ciseaux !), Nadège (La dévergondée introvertie), Thomas (Cherbourg tu peux pas test…), Georges (Lélé), Jeremy (le geek de la mécanique) Alex (mon débauché), Adrien (La touffe), Saïd (zébi !), Alban (Papa) et Antoine (La blonde « originale », et oui Charles tu n'es qu'une bonne imitation…), Nico (Le Roux), Rémi (Mojito ou Mojito ?!), Sutin (L'œil du tigre aura raison du Thaï Style).

Merci également à mes amis de toujours, des gens sur qui on peut compter, des gens qui ont grandi avec moi : Calfuego (baby !) Toubiak (le créatif), Nus (l'autre brun), Neuf (Le podologue), Max (le couillon), mais également Marin d'eau douce, Mariep, Nanas, Manue, Youlie, Mymy, Carolina, Simon, Dav (mon p'tit frère), Robin, François, Toinou, Divad, Toinou M, Thomas L, Axel (mon collègue zikos) etc… Désolé pour les oublis ou manques, mais vous êtes tous au meilleur endroit, dans mon cœur (waouh quel poète !).

Bien sûr je remercie ma Paupau à moi, ma coloc pendant ces 3 années de thèse mais surtout une amie comme peu en ont … Juste merci pour tout.

Je remercie également mon père ainsi que mes petits frères et sœurs : Léa, Nil, Félix et Zoé qui complètent cette famille formidable qui m'a tant apporté. Merci à vous, et j'espère vous rendre fiers autant que vous me rendez fier tous les jours.

Enfin merci à Michèle pour sa gentillesse, son soutien et son amour. Je t'aime.

Table des matières

Table des matières 1

Introduction générale 3

Ecosystèmes côtiers et productivité primaire 5

Les diatomées 6

Microphytobenthos, remise en suspension et réseau trophique 7

Microphytobenthos, apports autochtones ou allochtones ? 8

Etat de l'art, objectifs 11

Les appareils de mesure de la remise en suspension 13

La remise en suspension des diatomées benthiques 18

Couplage benthos-pelagos et interactions trophiques 18

Influence de l'hydrodynamisme sur l'érosion sédimentaire 20

Influence du type de sédiment sur la stabilité sédimentaire 22

Influence des organismes benthiques sur la stabilité sédimentaire 23

Etude de la remise en suspension *in situ* : les sites d'étude 31

La Baie des Veys 31

Lingreville sur mer 32

Objectifs 34

Variabilité spatiale du couplage benthos-pelagos dans un écosystème estuarien : Conséquences pour le phénomène de remise en suspension du microphytobenthos 37

Influence des bivalves cultivés sur le couplage benthos-pelagos d'un système marin côtier 59

Impact de la structure du sédiment et de l'âge du biofilm sur la remise en suspension du microphytobenthos : Etude en canal 87

Evaluation de l'impact du bioturbateur Cerastoderma edule sur la remise en suspension du sédiment et du microphytobenthos associé : étude en canal 113

Discussion générale, perspectives 139

Remise en suspension des diatomées benthiques et couplage benthos-pelagos 141

Les processus de remise en suspension/bio-déposition dans l'écosystème 142

Le processus de remise en suspension à micro-et méso-échelle 143

Mieux intégrer la macrofaune benthique dans les modèles écosystémiques 144

Diversité des organismes et diversité de la bioturbation 146

Bibliographie, liste des figures, liste des tableaux 151

Bibliographie 153

Liste des figures 177

Liste des tableaux 179

Chapitre I

Introduction générale

«Nos connaissances sont une goutte, notre ignorance, un océan…»

Isaac Newton

Ecosystèmes côtiers et productivité primaire

Les écosystèmes marins côtiers, interfaces entre les milieux continentaux et marins, sont parmi les plus productifs au monde (Marcus and Boero, 1998). En effet, l'apport continu de sels nutritifs (phosphates, nitrates et silice principalement) par le continent permet à ces zones d'être rarement limitées par ces derniers (Nixon et al., 1986). De plus, la profondeur relativement faible de ces écosystèmes permet des échanges rapides entre la colonne d'eau (ou compartiment pélagique) et le fond (ou compartiment benthique), particulièrement dans les écosystèmes caractérisés par un cycle tidal de forte amplitude. La faible profondeur de ces écosystèmes entraîne également l'absence d'une thermocline permanente qui, à l'instar de systèmes marins ouverts, limite la diffusion des sels nutritifs dans la zone euphotique, autrement dit la zone exposée à une lumière suffisante pour que la photosynthèse se produise (Nybakken and Bertness, 2004). La photosynthèse permet la production de matière organique végétale (biomasse), par des organismes autotrophes, dits producteurs primaires. Contrairement aux océans ouverts où la production primaire relève essentiellement des microalgues pélagiques ou phytoplancton, les écosystèmes marins côtiers sont également caractérisés par des producteurs primaires benthiques au niveau de la zone intertidale que sont les macro-algues mais aussi les microalgues ou microphytobenthos (MPB). Les biomasses de producteurs primaires sont très rapidement utilisées avec des taux de renouvellement élevés de par (i) des processus physiques contraignants (érosion, arrachage) et (ii) une forte diversité des consommateurs primaires se partageant rapidement les ressources trophiques (Herman et al., 2001). La régénération rapide des sels nutritifs au niveau du sédiment profite directement au MPB. En effet, les nutriments régénérés en profondeur diffusent à l'interface eau-sédiment pendant l'immersion, tandis qu'en période d'émersion le MPB a accès à une plus forte quantité de lumière permettant une production élevée (Stevenson et al., 1991). L'interface eau-sédiment est renouvelée régulièrement par les processus d'érosion/sédimentation liés à l'hydrodynamisme ainsi que par les processus de broutage par les consommateurs primaires. Ainsi, la production associée au MPB, bien que longtemps sous-estimée, participe largement à la forte productivité de ces écosystèmes, avec une contribution allant jusqu'à 50% de la production primaire totale des écosystèmes côtiers (Underwood and Kromkamp, 1999).

Les diatomées

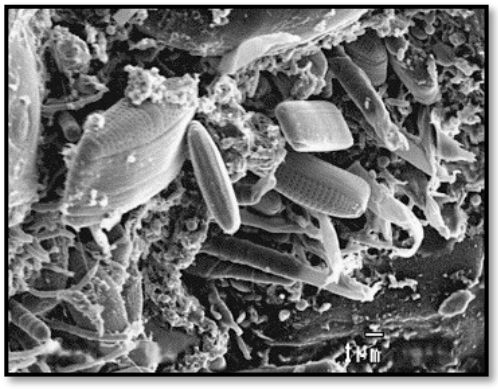

Figure 1 : Biofilm de surface avec diatomées épipéliques (Source : Barreto et Meyer, 2006).

Les diatomées benthiques constituent le groupe dominant du MPB (Smith and Underwood, 1998; Underwood and Kromkamp, 1999), et sont divisées en deux groupes fonctionnels : les diatomées dites « épipéliques », capables de se déplacer activement dans la couche de surface et les diatomées « épipsammiques », peu mobiles et restant attachées aux grains de sédiments sableux (Mitbavkar and Anil, 2004). Les diatomées benthiques forment des biofilms (Fig. 1) plus ou moins compacts à la surface du sédiment. Les stress générés par les forçages physiques au niveau de la zone intertidale se traduisent par une remise en suspension plus ou moins élevée du sédiment de surface avec les diatomées associées, perturbant la communauté microphytobenthique (Mitbavkar and Anil, 2004). Les diatomées benthiques épipéliques ont un rythme de migration verticale considéré comme un comportement chronobiologique avec une horloge interne (Serôdio et al., 1997). On considère la lumière et le cycle de marée comme étant les deux facteurs clés gouvernant la migration verticale (Smith and Underwood, 1998; Mitbavkar and Anil, 2004). En effet, dans les zones intertidales, les diatomées migrent vers la surface en période d'émersion lorsque la photosynthèse est possible et en profondeur en période d'immersion et/ou en période d'obscurité (Thornton et al., 2002), optimisant ainsi leurs rendements photosynthétiques (Fig. 2).

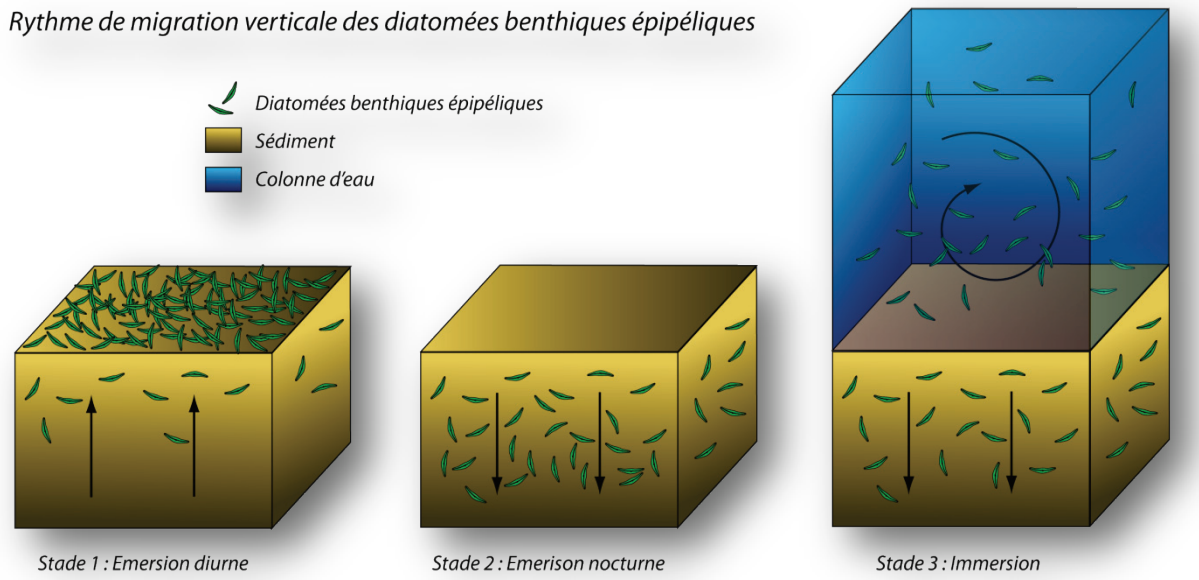

Figure 2 : Rythme de migration verticale des diatomées benthiques épipéliques, adapté de Gérard et al. (2006)

La migration des diatomées épipéliques leur permet également de régénérer leurs quotas internes de sels nutritifs qui peuvent devenir très vite limitants dans les biofilms autotrophes (Kingston, 2002; Saburova and Polikarpov, 2003). Les communautés épipsammiques ne peuvent migrer verticalement, et utilisent le cycle de la xanthophylle pour leur photorégulation (Jesus et al., 2005).

Microphytobenthos, remise en suspension et réseau trophique

La forte production primaire des écosystèmes côtiers marins profite aux consommateurs primaires benthiques et pélagiques. En plus des apports d'origine pélagique, le macrozoobenthos et particulièrement les mollusques suspensivores accèdent à de multiples sources de nourriture d'origine benthique (microalgues benthiques, détritus de macroalgues, bactéries, détritus de plantes des marais, protozoaires). La proximité des compartiments benthique et pélagique induit en effet un brassage de la colonne d'eau sous l'influence de facteurs physiques tels que le vent ou la marée, entraînant la remise en suspension des sédiments superficiels et des organismes associés. Par le biais de la remise en suspension, le MPB constitue une source de nourriture importante pour les mollusques filtreurs sauvages comme la coque *Cerastoderma edule*, mais aussi cultivés tels que les huîtres creuses *Crassostrea gigas* ou les moules *Mytilus edulis* (Dubois et al., 2007; Marín Leal et al., 2008; Lefebvre et al., 2009). Cependant, la remise en suspension des micro-algues benthiques est un phénomène complexe puisque ces dernières sont capables de contrôler en partie aussi leur propre remise en suspension vers la colonne d'eau en modifiant les propriétés du sédiment (Tolhurst et al., 2002). Si les caractéristiques de forte productivité des écosystèmes côtiers en font des lieux de prédilection pour les activités conchylicoles, les zones conchylicoles ne sont pourtant pas toujours propices à des productivités primaires importantes, comme cela a été mis en évidence en baie du Mont-Saint-Michel. En effet, la présence des structures conchylicoles peut créer un frein hydrodynamique limitant la remise en suspension du MPB (Davoult et al., 2009; Kervella et al., 2010). En conséquence, des niveaux de biomasse de MPB très élevés sont observés de manière quasi permanente sous ces structures. En l'absence de facteurs liés à l'exportation de la biomasse physique (par remise en suspension) ou trophique (consommation), le niveau de productivité devient alors très faible (Blanchard et al., 2001). Par ailleurs, l'accumulation de bio-dépôts sous les structures conchylicoles enrichit les sédiments en matière organique et finit par perturber durablement la structure de la macrofaune benthique, avec une raréfaction des bivalves filtreurs et une forte colonisation par des annélides (Dubois, et al., 2007). A l'inverse, les zones de vasières nues comme celles de la Baie de Marennes-Oléron sont des zones protégées où l'hydrodynamisme peut être maintenu à un niveau relativement modéré en l'absence de structures conchylicoles. Les échanges érosifs maintiennent alors une productivité primaire élevée dans les biofilms, avec des pertes de

biomasses par consommation/érosion conduisant à des niveaux de biomasses relativement faibles (Blanchard et al., 2001). Les activités intenses de bioturbation sur les zones de vasières nues (associées à des biomasses de macrofaunes très fortes et typiques de ces zones) participent fortement à une exportation quotidienne de MPB, et participent au maintien des biomasses de MPB à des niveaux faibles mais très productifs (Orvain et al., 2004, 2007).

Microphytobenthos, apports autochtones ou allochtones ?

Le rôle trophique que jouent ces micro-algues dans la colonne d'eau dépend donc directement de leur remise en suspension à partir des sédiments de surface qu'elles colonisent et l'environnement physique local est essentiel à considérer, tout comme les processus de consommation primaire et de bioturbation par la faune endogée. En effet, ceux-ci semblent jouer un rôle significatif dans ces échanges érosifs (Orvain et al., 2007). Cependant, il a souvent été démontré que les croissances des huîtres cultivées repose partiellement sur le MPB remis en suspension (Riera et al., 1999; Perissinotto et al., 2003; Kang et al., 2006; Lefebvre et al., 2009). Si les sédiments locaux sous les parcs à huîtres sont peu favorables à une productivité primaire soutenue malgré des fortes biomasses (Davoult et al., 2009), il est très fortement probable que l'origine de cette matière organique soit allochtone, provenant des zones adjacentes aux parcs à huîtres qui viendraient alimenter les huîtres en MPB remis en suspension. Les caractéristiques des masses d'eau et de leurs mouvements (intensité et direction des courants) doivent donc être prises en compte en tant que vecteur physique de transfert de la biomasse microphytobenthique exportée depuis des zones adjacentes. Cette source trophique pourrait donc être essentiellement d'origine allochtone dans les écosystèmes conchylicoles. L'advection du MPB peut se faire à différentes échelles, puisque la remise en suspension du MPB peut avoir lieu dans les rivières, les havres ou les embouchures d'estuaires, avant d'alimenter les échelons trophiques supérieurs au niveau des écosystèmes marins côtiers. Par exemple, lors d'années humides, les écosystèmes côtiers de l'Ouest Cotentin reçoivent des apports en sels nutritifs plus élevés qui vont augmenter la part des apports allochtones pour l'alimentation des filtreurs. Durant les années sèches l'alimentation de ces derniers repose principalement sur des sources alimentaires d'origine pélagique, alors que durant les années humides elle consiste en un mélange de sources alimentaires pélagiques et benthiques (Grangeré et al., 2012).

Le caractère autochtone ou allochtone de la matière organique issue du sédiment ajoute donc un degré de complexité au couplage benthos-pelagos. Le rôle trophique du MPB peut donc varier d'un écosystème à l'autre mais également d'une saison à l'autre, puisque la disponibilité est conditionnée par les contraintes du milieu : température, salinité, hydrodynamisme, lumière, sels

nutritifs, nature sédimentaire, pression trophique. La prise en compte des différentes échelles spatio-temporelles impliquées dans le fonctionnement des écosystèmes marins côtiers est donc primordiale pour une meilleure compréhension de leur fonctionnement. Le chapitre suivant correspond à un état de l'art permettant d'introduire les notions associées à l'étude de la remise en suspension des diatomées benthiques dans le couplage benthos-pelagos. Une première partie permet d'avoir un aperçu des différents appareils de mesure de la remise en suspension, et des variables de mesures associées. Une seconde partie traite de la remise en suspension des diatomées benthiques. Le contexte de couplage benthos-pelagos dans lequel intervient la remise en suspension est tout d'abord explicité, puis les différents compartiments impliqués dans ce processus, à savoir l'hydrodynamisme, le sédiment, la macrofaune benthique et les diatomées elles-mêmes, sont abordés. Les substances exopolymériques (EPS) secrétées par les diatomées font également l'objet de cette deuxième partie. Enfin, les écosystèmes choisis comme modèle durant ce travail de thèse sont décrits. Cet état de l'art est clôturé par les objectifs de ce travail de thèse.

Chapitre II

Etat de l’art, objectifs

« La connaissance s'acquiert par l'expérience, tout le reste n'est que de l'information. »

Albert Einstein

Les appareils de mesure de la remise en suspension

Divers appareillages permettent de mesurer les paramètres d'érodabilité en laboratoire (Jonsson et al., 2006). Cependant chaque système possède des avantages et inconvénients, le choix d'un appareil plutôt qu'un autre dépendant des besoins spécifiques de l'expérience.

Le CSM (Cohesive Strength Meter)

Cet appareil mesure le seuil critique d'érosion ou « Bed Shear Stress » des sédiments intertidaux, en envoyant des jets d'eau à vitesse d'impulsion croissante jusqu'à ce que la force de l'impulsion dépasse la force de cohésion des sédiments de surface testés (Paterson, 1989a). Le dispositif se compose d'une chambre posée sur le sédiment et soigneusement remplie d'eau. La pression du jet est augmentée systématiquement, induisant une remise en suspension qui est détectée par une réduction de la transmission de la lumière infrarouge dans la chambre. Le CSM est calibré en termes de pression de jet nécessaire pour remettre en suspension une taille spécifique de grains de sable avec une contrainte de cisaillement critique connue. Une équation empirique est utilisée pour convertir la pression d'érosion en une contrainte de cisaillement horizontale. L'appareil ne permet cependant pas d'évaluer les flux d'érosion en réponse à des contraintes de cisaillement. Il s'agit de l'appareil de mesure d'érodabilité le plus répandu *in situ* (Paterson, 1989a; Tolhurst et al., 1999; Lubarsky et al., 2010).

Le MAGPI

Le principe du MAGPI repose sur l'induction de particules magnétiques (Larson et al., 2009; Lubarsky et al., 2010). Un volume connu de particules ferromagnétiques fluorescentes est déposé sur une surface connue de sédiment. Les particules sont ensuite attirées par un électro-aimant sus-jacent (Fig. 3), et la force (le flux magnétique) nécessaire pour extraire les particules permet de mesurer la capacité de rétention du substrat, un proxy de l'adhésion des particules. La force électromagnétique appliquée est contrôlée et les mouvements des particules peuvent être contrôlés à chaque palier de courant/voltage. Un des points forts du MAGPI est le contrôle total du sédiment en termes de taille de grain et de cohésion de base.

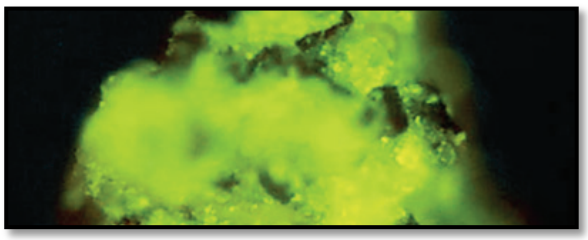

Figure 3 : Particules ferromagnétiques fluorescentes remises en suspension lors d'une expérimentation au MAGPI (Source : http://www.partrac.com)

Cependant, à l'instar du CSM, il ne permet pas d'évaluer les flux d'érosion en réponse à des contraintes de cisaillement. Le MAGPI ne mesure pas le seuil critique d'érosion mais la force critique d'érosion.

Les canaux

Les canaux hydrauliques existent sous différentes formes et différentes tailles (Fig. 4). Ils permettent de faire circuler un flux laminaire à vitesse régulée. Des capteurs de turbidité permettent de mesurer à la fois le seuil critique et les flux d'érosion pour un sédiment cohésif. Ces canaux selon leur taille (mini-canaux) peuvent être utilisés sur le terrain (Schaaff et al., 2006). Toutefois, les canaux ne permettent pas de différencier la fraction vaseuse de la fraction sableuse lors des flux d'érosion. De plus, la tension de frottement n'est pas directement mesurée lors d'un essai d'érosion. Seul le débit est contrôlé et des courbes d'étalonnage de la contrainte sont utilisées pour estimer indirectement la tension de frottement appliquée au fond. Il existe 3 types de calibration de la contrainte de cisaillement :

- Mesure de particules à différentes tensions critiques. Quand l'initiation du mouvement a lieu, la tension de frottement inconnue est égale à celle des grains dont la tension critique est connue. Le diagramme de Shields sert alors de référence pour connaître la tension critique en fonction de la taille et densité des particules (Guizien et al., 2012)
- Mesure directe à l'aide d'une sonde à film chaud (Andersen, 2001)
- Pour les canaux benthiques de grande dimension, établissement d'un profil vertical complet de $U_{(z)}$ et déduction de U^* (et donc τ) à partir de la droite de regression entre $ln(z)$ et U (Amos et al., 1992; Denis et al., 1996; Orvain, et al., 2003). Ces calibrations sont faites une fois pour l'ensemble d'une série d'expériences, et ne peuvent donc pas prendre en compte les modifications de rugosité qui peuvent avoir lieu d'une expérience à l'autre.

La méthode récente de Guizien et al. (2012) est basée sur la perte de charge, en se référant à la relation débit-pression et en comparant à une courbe de référence basée sur un fond lisse. La tension n'est donc plus calculée à partir du débit, et la tension de frottement exacte est estimée en tenant compte des modifications de rugosité.

D'autres techniques permettent de mesurer la tension de frottement, comme la Vélocimétrie par Image de Particules (VIP, qui mesure la vitesse de particules entraînées par l'écoulement à partir de deux photos successives prises à un très court intervalle de temps (Trevethan et al., 2010), ou encore l'Energie cinétique turbulente « TKE » (van Duren et al., 2006).

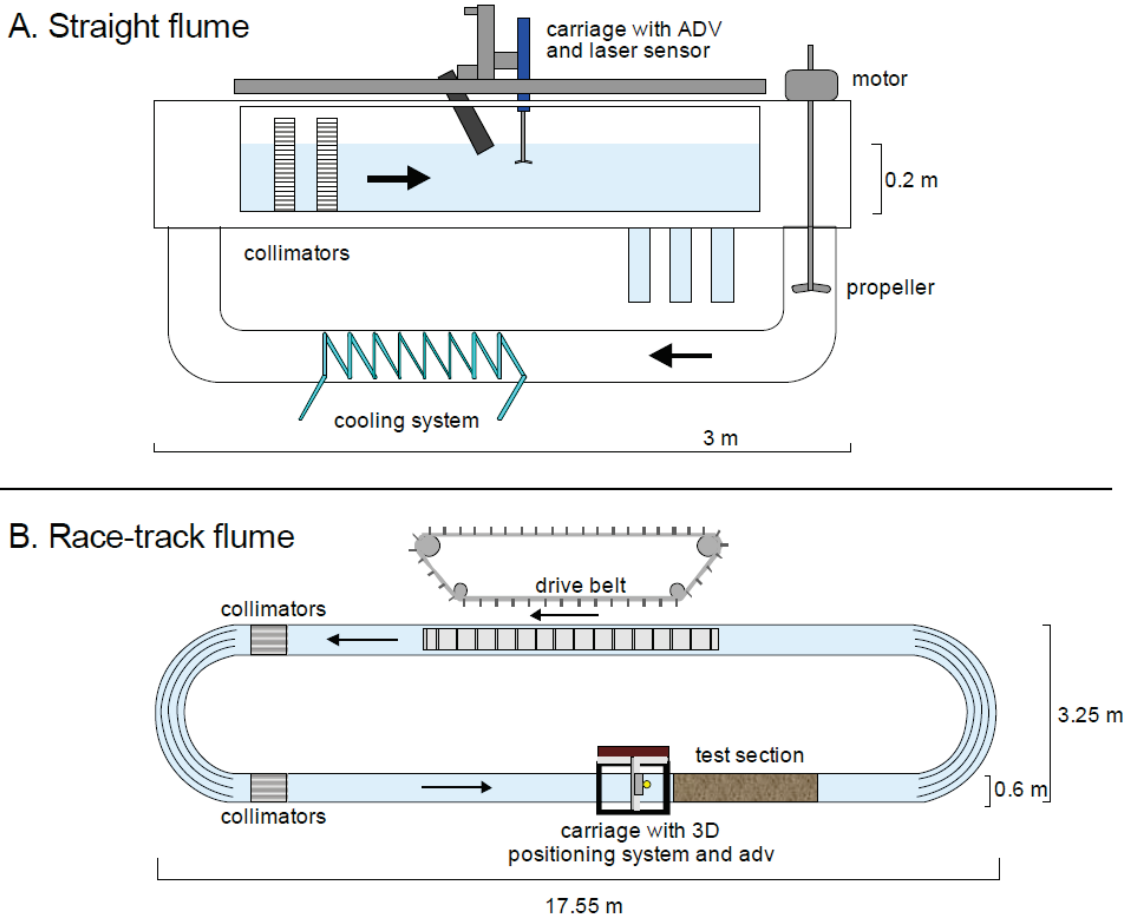

Figure 4 : Illustration des différents types de dispositifs d'étude de la remise en suspension (Source : Jonsson et al., 2006)

L'érodimètre

L'ensemble des outils cités en amont souffre d'un manque : la non-prise en compte de la rugosité du sédiment (Tableau 1). En effet, les sédiments naturels sont rarement lisses, induisant des turbulences dans la colonne d'eau sus-jacente. Or, les courbes de calibrations sont en général établies pour des fonds lisses. La contrainte réelle des sédiments naturels est donc systématiquement minimisée en utilisant de telles courbes de calibration. L'érodimètre est un canal vertical permettant de mesurer l'ensemble des paramètres d'érodabilité (seuil et flux d'érosion) en laboratoire ou *in situ* et de différencier l'érosion des fractions fines et grossières pour le cas des mélanges sablo-vaseux. Il permet, par une mesure de pression différentielle entre l'amont et l'aval de l'échantillon de sédiment, d'estimer la tension de frottement réelle (et ce même si la rugosité varie), évitant donc de se référer à des courbes d'étalonnage qui ne restent valides que si le fond est lisse (Orvain et al., 2007; Guizien et al., 2012).

Tableau 1 : Les différents types de systèmes permettant de mesurer l'érosion du sédiment

	Mesures directes disponibles					
Système	Seuil d'érosion critique	Flux d'érosion global	Flux d'érosion selon fraction (vase/sable)	Tension de frottement	Flux d'érosion chl *a*	Seuil d'érosion chl *a*
CSM	✓					
MAGPI	✓					
EROMES	✓	✓				
Canal droit	✓	✓			✓	✓
Canal circulaire	✓	✓			✓	✓
Canal en hippodrome	✓	✓			✓	✓
Canal de terrain	✓	✓			✓	✓
EFA	✓	✓	✓	✓	✓	✓
Erodimètre	✓	✓	✓	✓	✓	✓

L'érodimètre est un petit canal en circuit fermé d'une contenance de 15L, où l'eau circule grâce à une pompe munie d'un variateur de fréquence. L'échantillon de sédiment artificiel ou naturel vient affleurer la base de l'érodimètre, et subit un écoulement incrémenté par palier, un capteur de turbidité à rétrodiffusion optique permettant de mesurer la quantité de matières en suspension

(MES) et ainsi déterminer les paramètres de l'érosion. Le variateur de fréquence permet d'augmenter la vitesse du courant et le BSS au niveau du fond. Ainsi, les échantillons sont soumis à l'augmentation du BSS en fonction du temps, et ce dernier peut être mesuré avec précision pour chaque expérience grâce un capteur de pression qui permet de calculer la tension de frottement à la surface de l'échantillon.

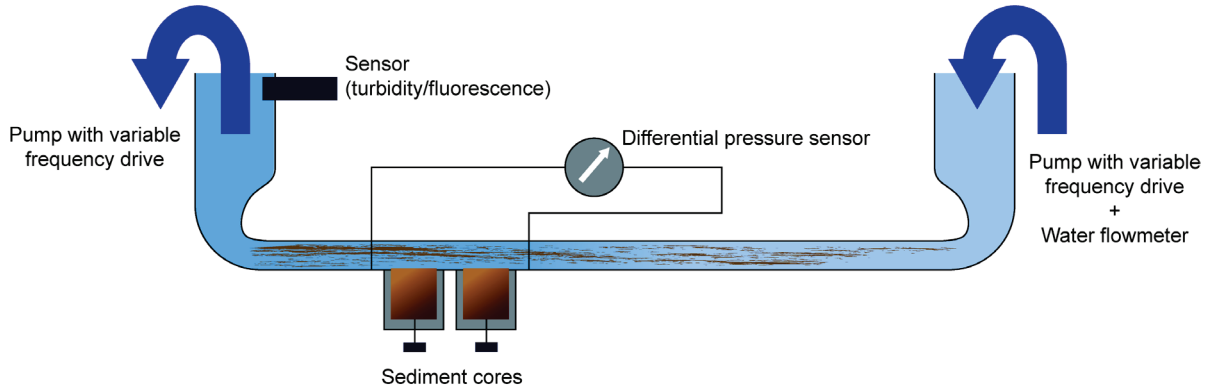

Figure 5 : Schéma simplifié du fonctionnement de l'érodimètre développé par IFREMER

Dans la section droite de l'érodimètre (Fig. 5), le courant est entièrement contrôlé : les dimensions du chenal, le débit et la rugosité de surface sont connus. Le courant vient affleurer la surface de l'échantillon (possibilité d'utiliser 2 échantillons) et entraîne l'érosion et le transport des particules par charriage et/ou suspension. La fraction non-cohésive du sédiment tombe par gravitation dans le piège à sable situé en aval de l'échantillon, tandis que la fraction cohésive remise en suspension est maintenue dans le courant. Le volume de sable récupéré est noté à la fin de chaque palier, tandis qu'en fin de test la masse totale de sable est pesée. Après passage du coude en aval de l'échantillon le capteur de turbidité quantifie les MES. Un capteur additionnel de fluorescence permettant de quantifier la concentration de Chl *a* en suspension dans le cas d'un sédiment naturel avec biofilm. Dans ce cas l'érosion (et les paramètres inhérents) du sédiment et du biofilm peuvent être différenciées.

La remise en suspension des diatomées benthiques

Couplage benthos-pelagos et interactions trophiques

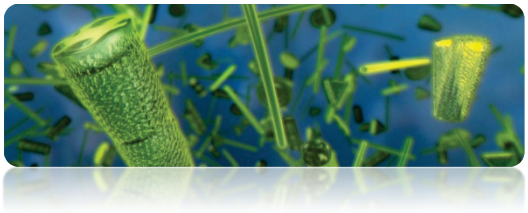

Le terme de couplage benthos-pelagos fait généralement référence au *cycle des éléments ou sels nutritifs entre les sédiments du fond et la colonne d'eau sus-jacente*. De façon plus générale il correspond aux *connections entre les processus écologiques dans la colonne d'eau et au niveau du fond* (Graf, 1992). Smith et al. (2006) utilisent même une définition plus générale où le couplage benthos-pélagos correspond à une *relation causale entre les processus benthiques et pélagiques*. L'équilibre de ces échanges entre compartiments benthiques et pélagiques varie d'un écosystème à l'autre mais aussi d'une saison à l'autre, conduisant à un contrôle plus élevé d'un des 2 compartiments sur l'autre. Lorsque les processus pélagiques exercent un contrôle sur le benthos, la production du compartiment benthique est dépendante de processus tels que la bio-déposition de matière organique ou de sels nutritifs. A l'inverse, quand les processus benthiques exercent un contrôle sur le pelagos, la production pélagique sera dépendante de phénomènes tels que la remise en suspension de sels nutritifs ou de matière organique. L'intensité du couplage benthos-pelagos est plus élevée dans les environnements côtiers qu'en océan ouvert (Marcus and Boero, 1998). En effet, l'action des vagues et des courants tidaux sur les flux de remise en suspension/déposition augmente au niveau des écosystèmes côtiers.

Traditionnellement, les modèles de production et de dynamique de population accordaient un grand rôle au couplage benthos-pelagos au niveau des cycles biogéochimiques, sans inclure les cycles de vie des organismes benthiques et pélagiques (Marcus and Boero, 1998). Depuis plusieurs années, l'importance des processus d'érosion du sédiment a été réévaluée au niveau des écosystèmes côtiers, soulignant l'importance des interactions entre le biofilm benthique et le réseau trophique pélagique. Le MPB est en effet susceptible de contribuer très significativement à la croissance des consommateurs primaires dans la colonne d'eau, ou encore de contrôler le couplage benthos-pelagos de certains écosystèmes au niveau de l'initiation de blooms (MacIntyre et al., 2004). Le rôle du MPB est donc primordial ; outre sa consommation directe par le benthos, il alimente une fois remis en suspension le réseau trophique pélagique mais aussi benthique via la consommation des organismes benthiques suspensivores. Ainsi, le couplage benthos-pelagos est désormais envisagé pour l'ensemble du réseau trophique, d'où l'apparition de modèles de réseaux trophiques couplés benthos-pelagos (Leguerrier et al., 2003). Les forçages hydrodynamiques à l'interface eau-sédiment,

la remise en suspension, la bioturbation, les flux trophiques sont autant d'éléments à intégrer pour l'étude fonctionnelle des écosystèmes marins côtiers.

Différentes interactions trophiques naissent de l'existence du couplage benthos-pelagos, à l'image de la facilitation trophique[1]. En effet, le remaniement actif de la surface sédimentaire par la faune locale peut faciliter la remise en suspension d'une fine couche superficielle riche en diatomées benthiques (Orvain et al., 2007). Par exemple, les coques *Cerastoderma edule* sont susceptibles de stimuler l'exportation des diatomées vers la colonne d'eau et faciliter ainsi la croissance des autres filtreurs en élevage (Ubertini et al., 2012). Les huîtres, par l'émission de pseudo-fèces, enrichissent le sédiment en matière organique, favorisant l'envasement et indirectement la croissance du MPB (Cognie and Barillé, 1998). Certaines espèces, comme *Macoma balthica* ou *Scrobicularia plana*, sont des acteurs et profitent dans le même temps des processus de remise en suspension et de biodéposition. Elles sont en effet anatomiquement capables de se nourrir, à marée haute, d'éléments en suspension et, à marée basse, d'éléments déposés sur le sédiment (Taghon et al., 1980; Riisgårdet and Kamermans, 2001; Rossi et al., 2004). L'influence des bivalves cultivés peut induire des processus de facilitation par le processus de biodéposition également (Fig. 6).

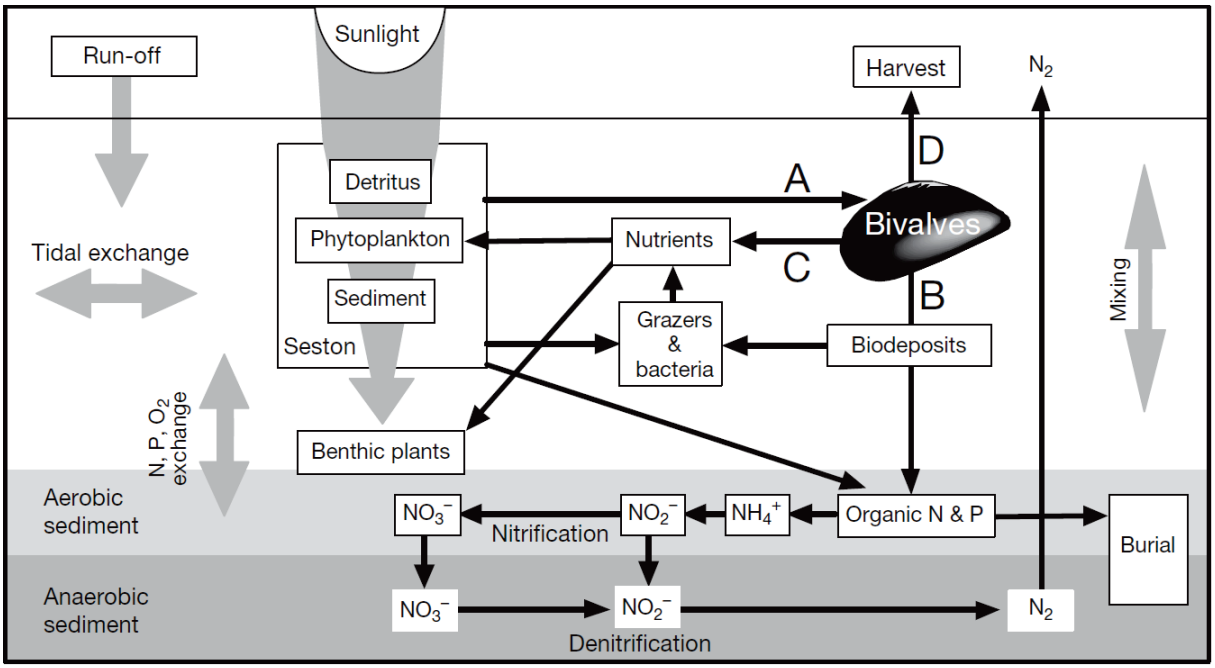

Figure 6 : Diagramme conceptuel des interactions entre les bivalves cultivés et l'écosystème, en lien avec : (A) l'impact de la filtration sur la déplétion en MES (seston); (B) la biodéposition de la matière organique non digérée dans les fèces et pseudofèces; (C) l'excrétion d'ammonium et d'azote; and (D) l'enlèvement de matériaux (sels nutritifs) lors de la récolte des bivalves (Cranford et al. 2006).

[1]**Facilitation trophique** : Des interactions facilitatrices ou positives sont rencontrées entre des organismes quand un au moins bénéficie d'une ou plusieurs de ces interactions sans qu'aucun n'en pâtisse. Cette facilitation apparaît par exemple quand un organisme rend son environnement plus favorable à un autre organisme, de façon directe ou indirecte (Bruno et al., 2003).

Influence de l'hydrodynamisme sur l'érosion sédimentaire

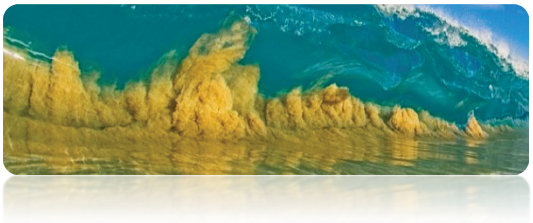

Les conditions hydrodynamiques au niveau du fond sous l'action des vagues et courants tidaux affectent l'érosion ainsi que les processus de mélange/transport de la colonne d'eau. Les différents mécanismes permettant de déplacer les particules solides sont le charriage (les grains roulent ou glissent sur le fond) et la suspension (Fig. 7). L'interaction des courants et des vagues a pour conséquences (i) un changement du coefficient de viscosité turbulente[1] (« eddy viscosity coefficient») et (ii) une augmentation de la contrainte de cisaillement[2] (« bed shear stress ») provoqué par l'augmentation des turbulences (Jing and Ridd, 1996).

L'écoulement d'un fluide est défini par quatre grandeurs physiques : la vitesse de l'écoulement U, la masse volumique ρ, la viscosité moléculaire ν et la longueur caractéristique de l'écoulement (longueur de mélange). On différencie 2 types d'écoulements : l'écoulement « laminaire », lisse et régulier, et l'écoulement « turbulent ». Le nombre de Reynolds (R_e, **1**) permet de déterminer la nature de l'écoulement :

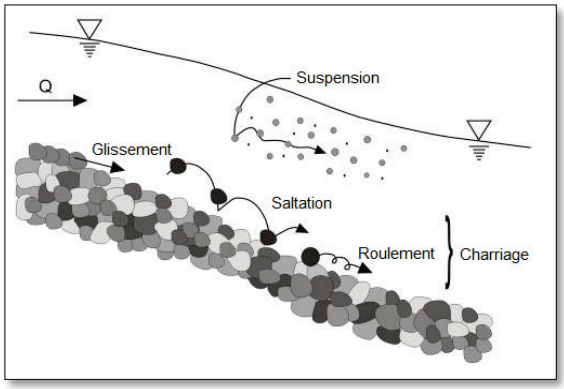

Figure 7 : Modes de déplacement des particules solides lors d'épisodes d'érosion (Source : Blanckaert, 2005).

$$R_e = \frac{UL}{\nu} = \frac{\rho UL}{\mu} \qquad \textbf{1}$$

Avec μ la viscosité cinématique du fluide et L la longueur caractéristique

En fonction des nombres de Reynolds croissants on distingue quatre régimes principaux : régime de Stokes ($R_e \approx 0$), régime laminaire ($R_e < 500$), régime transitoire ($500 < R_e < 2000$), régime turbulent ($R_e \geq 2000$).

[1]**Coefficient de viscosité turbulente** = Coefficient caractérisant le transfert turbulent de quantité de mouvement par des tourbillons au sein d'un fluide. Ce phénomène donne lieu à un frottement interne au sein du liquide, analogue à celui qui résulte de la viscosité laminaire dans un écoulement laminaire, mais se produit à une échelle beaucoup plus grande. La valeur du coefficient de viscosité turbulente de l'eau de mer est de l'ordre de 10 000 c^2/s.

[2]**Contrainte de cisaillement « τ »** = Force exercée par unité de surface d'un fluide (Newton/m^2), lorsque les efforts s'exercent en sens opposés, tangentiellement aux surfaces : $\tau = F/S$

Les processus d'érosion à l'interface eau-sédiment considèrent les lois classiques de Parthéniades (**2**). La viscosité d'un fluide joue seulement un rôle très près de la paroi, et ce d'autant plus que le nombre de Reynolds est grand (couche infiniment mince pour nombre de Reynolds infini). Cette zone est appelée couche limite benthique, et est régie selon la « loi de la paroi » émise par Karman-Prandtl (**3**). C'est cette loi qui permet notamment de calculer la vitesse de frottement (**4**). Le frottement de l'eau sur le fond a pour effet de diminuer la vitesse du fluide depuis la surface jusqu'au fond où s'exerce τ (Fig. 8). A partir d'un seuil critique τ_c, la vitesse de frottement ou cisaillement devient supérieure à la force de résistance exercée par le sédiment. A ce moment, le sédiment est mis en mouvement par charriage ou suspension (Fig. 9).

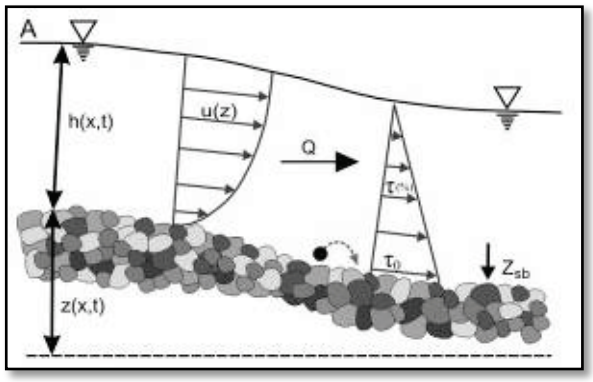

Figure 8 : Illustration des vitesses et tensions inhérentes au niveau du fond pendant un écoulement de fluide turbulent (Source : Blanckaert, 2005).

$$E = M\left[\left(\frac{\tau}{\tau_c}\right) - 1\right] \qquad \textbf{2}$$

Avec E = flux d'érosion surfacique (kg.m^{-2}.s^{-1}) ; M = coefficient d'érodabilité (kg.m^{-2}.s^{-1}) ; τ_c = contrainte critique de cisaillement (« erosion critical shear stress »)

$$U = (U^*/K)Ln(z/z_0) \qquad \textbf{3}$$

Avec K la constante de Karman (~0,41, sans dimension), U^* la vitesse de frottement, z la hauteur au dessus du fond et $z_0$le paramètre de rugosité

$$U^* = \sqrt{\tau/\rho} \qquad \textbf{4}$$

Avec ρ la densité du fluide

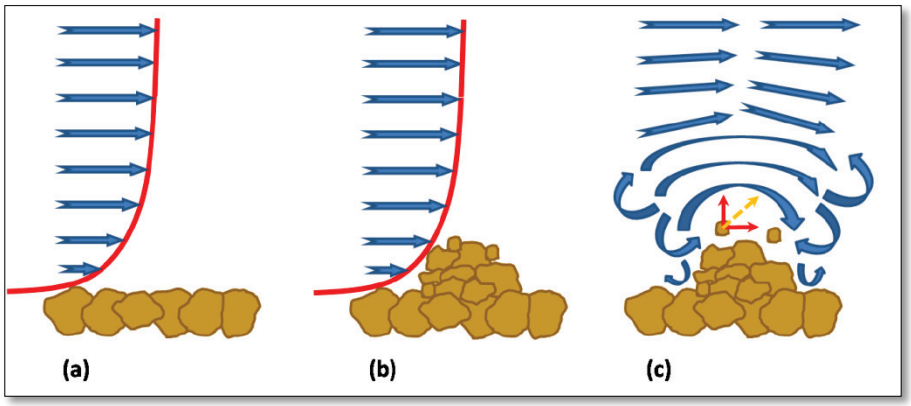

Figure 9 : Écoulement sur surface lisse (A), avec un profil de vitesse logarithmique caractéristique. Lorsqu'il rencontre des irrégularités de surface (b), l'écoulement devient turbulent (c) et une combinaison de forces de poussée et traction entraîne les particules de sédiments à s'éroder (Trotsenburg, 2011).

Influence du type de sédiment sur la stabilité sédimentaire

L'érodabilité d'un sédiment varie selon les caractéristiques du sédiment (taille des grains, densité, cohésion). Les sédiments sont généralement décrits en référence à l'échelle de Wentworth (1922), divisant les types de sédiments en 6 classes. Les sédiments sableux ont une taille de grain allant de 63µm à 2mm de diamètre, de forme plutôt sphérique, présentant peu de cohésion entre les particules. Les sédiments vaseux (<63µm) présentent des particules de forme plus allongée, avec un rapport de surface sur volume plus important, induisant une cohésion entre les particules (Paterson, 1982). Pour les sédiments homogènes, les sédiments sableux (non-cohésifs) sont plus facilement mobilisables que les sédiments vaseux (cohésifs). Cependant, les sédiments vaseux sont remis en suspension plus facilement que les sédiments sableux qui sont simplement charriés, et nécessitent des vitesses plus fortes pour être maintenus en suspension.

Dans le cas de sédiments cohésifs, l'érosion va entraîner un flux, appelé flux d'érosion, correspondant à la quantité de sédiment remis en suspension par unité de surface et par unité de temps ($kg.m^{-2}.s^{-1}$). Ce flux dépend de la contrainte de cisaillement τ et du seuil critique d'érosion τ_c. Après un épisode de remise en suspension, les sédiments retombent au fond sous l'effet de la gravité. Les sédiments non cohésifs (sables, graviers, galets) ne se tassent pratiquement pas. Au contraire, les flocons de sédiments cohésifs se tassent en perdant leur eau interstitielle et celle liée par les forces électrostatiques. Si la vitesse des phénomènes de tassements peut varier selon les caractéristiques du sédiment ou de l'eau, le tassement n'en reste pas moins un phénomène lent. Pour les sédiments cohésifs, on distingue deux types d'érosion en fonction de ce tassement. Lors d'une cinétique d'érosion avec des contraintes de cisaillement τ augmentant progressivement, on observe des libérations successives de sédiment par palier. Ce type d'érosion est appelé « érosion de type I » (Amos et al., 1992) et correspond à des lits de sédiments déposés (Mehta and Partheniades, 1982). Pendant une cinétique analogue, si peu de sédiment est libéré dans la colonne d'eau – correspondant à un gradient de tension critique très faible – on observe une libération massive de sédiment, linéaire pendant un palier à tension de cisaillement constante. On parle alors d'une « érosion de type II » (Amos et al., 1992), apparaissant pour des sédiments tassés (Mehta and Partheniades, 1982). De façon indirecte, les sédiments cohésifs sont moins facilement érodés que les sédiments non-cohésifs dans le milieu naturel, et ce phénomène est potentiellement amplifié par la présence d'un biofilm en surface. Les mélanges sablo-vaseux se comportent comme du sable pur, mais il ya une fraction de vase critique (typiquement 30%), au-dessus de laquelle le comportement

du mélange est entièrement cohésif (Le Hir et al., 2011). Au-dessus de cette valeur critique, la résistance au cisaillement du mélange dépend de la concentration de vase (Migniot, 1989; Waeles et al., 2008).

Influence des organismes benthiques sur la stabilité sédimentaire

Bien que l'érodabilité du sédiment soit généralement considérée comme uniquement dépendante des processus physiques (équilibre entre contrainte de frottement et tension critique pour l'érosion), les processus de remise en suspension peuvent être fortement influencés par les composantes biologiques benthiques (Le Hir et al., 2007a).

Microorganismes et stabilité sédimentaire

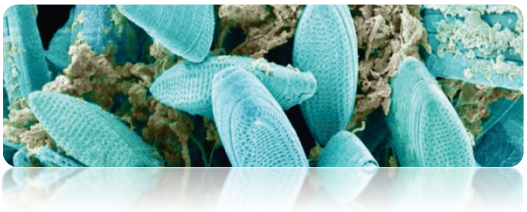

Les microorganismes et notamment les diatomées benthiques exercent une action stabilisatrice sur le sédiment, par l'établissement d'un biofilm en surface (Fig. 10). La migration des diatomées benthiques épipéliques se fait par l'extrusion de longues chaînes d'hétéropolymères riches en hydrates de carbone produits par le raphé, appelés communément Substances Polymériques Extracellulaires (EPS). Les EPS ont des fonctions multiples au sein du biofilm (Tableau 2). Les EPS peuvent être séparés en 2 fractions (Liu and Fang, 2003) : (i) les EPS liés, constitués de polymères capsulaires (fortement liés aux cellules) et de substances visqueuses plus faiblement liées qui entourent les cellules (slime EPS), et (ii) les EPS colloïdaux, macromolécules solubles. Au sein de chacune de ces fractions, les EPS sont constitués d'un mélange de différentes macromolécules (protéines, polysaccharides, lipides, ADN), les protéines et polysaccharides (~95%) étant les composants majoritaires. Les polysaccharides sont composés de sucres neutres, d'acides uroniques, de sucres sulfonatés ou de groupes pyruvates (Sutherland, 2001). Les rôles principaux des EPS au sein du biofilm sont multiples (Tableau 2) et ont été revus par Flemming and Wingender (2010).

Les EPS enveloppent les cellules en constituant des structures floculées reliées par des cations. Une étape d'extraction est donc nécessaire à l'analyse de ces derniers. Ces méthodes d'extraction peuvent être divisées en 2 groupes avec (i) les méthodes physiques : ultra-sons, centrifugation, thermique et (ii) les méthodes chimiques : résine Dowex cationique, éthylène diamine tétraacétique acide, NaOH, formaldéhyde, formaldéhyde+NAOH. Ces techniques ont été souvent comparées (Frølund et al., 1996; Liu and Fang, 2002; Comte et al., 2006; Pan et al., 2010; Takahashi et al., 2010), mais chacune agit différemment afin de déstructurer les liaisons retenant les EPS dans la matrice biologique. La résine échangeuse d'ions Dowex est actuellement la plus utilisée et permet

Tableau 2 : Fonctions des EPS dans les biofilms, tiré de Flemming and Wingender (2010).

Fonction	Rôle pour les biofilms	Composants des EPS impliqués
Adhésion	Permet les premières étapes de la colonisation des surfaces abiotiques et biotiques par les cellules planctoniques, et l'attachement à long terme de biofilms sur des surfaces.	Polysaccharides, protéines, ADN et molécules amphiphiles
Agrégation des cellules bactériennes	Permet l'attachement des cellules, l'immobilisation temporaire de populations bactériennes et le développement de fortes densités cellulaires ainsi que la reconnaissance de cellule à cellule.	Polysaccharides, protéines et ADN
Cohésion du biofilm	Forme un réseau de polymères hydratés (la matrice du biofilm), régulant la stabilité mécanique des biofilms (souvent en collaboration avec des cations multivalents) et détermine l'architecture du biofilm à travers la structure EPS (capsule, glue ou gaine), tout en permettant la communication de cellule à cellule.	Polysaccharides neutres et chargés, protéines (amyloïdes et lectines), et ADN
Rétention d'eau	Maintient un microenvironnement fortement hydraté autour des organismes du biofilm, ce qui conduit à leur tolérance de dessiccation dans les milieux déficitaires en eau.	Polysaccharides hydrophiles, rôle soupçonné des protéines
Barrière protectrice	Confère une résistance aux défenses immunitaires spécifiques et non spécifiques au cours de l'infection, confère une tolérance à divers agents anti-microbiens (par exemple, les désinfectants et les antibiotiques), protège des cyanobactéries nitrogénase contre les effets nocifs de l'oxygène et protège contre le broutage de certains protozoaires.	Polysaccharides et protéines
Sorption de composés organiques	Permet l'accumulation d'éléments nutritifs dans l'environnement et la sorption des xénobiotiques (contribuant ainsi à la détoxication de l'environnement).	Polysaccharides chargés ou hydrophobes et protéines
Sorption de composés inorganiques	Favorise la formation de gel de polysaccharides, l'échange d'ions, ainsi que la formation minérale et l'accumulation d'ions métalliques toxiques (ce qui contribue à la détoxification de l'environnement).	Polysaccharides et protéines chargées, y compris des substi-tuants inorganiques tels que le phosphate et le sulfate
Activités enzymatiques	Permet la digestion de macromolécules exogènes pour l'acquisition des éléments nutritifs et la dégradation des EPS structurelles, ce qui permet la libération des cellules du biofilm.	Protéines
Source de nutriment	Fournit une source de carbone, d'azote et de composés contenant du phosphore pour utilisation par la communauté du biofilm.	Potentiellement tous les composants EPS
Échange de d'information génétique	Facilite le transfert horizontal de gènes entre les cellules du biofilm.	ADN
Donneur d'électrons ou accepteur	Permet l'activité redox dans la matrice du biofilm.	Protéines et potentiellement les substances humiques
Exportation de composants cellulaires	Evacue le matériel cellulaire à la suite du renouvellement métabolique.	Vésicules membranaires contenant des acides nucléiques, enzymes, lipopolysaccharides et phospho-lipides
Puits pour énergie excédentaire	Stocke l'excès de carbone quand les ratios carbone-azote deviennent déséquilibrés.	Polysaccharides
Attachement des enzymes	Résultats de l'accumulation, de la rétention et de la stabilisation des enzymes par leur interaction avec les polysaccharides	Polysaccharides et enzymes

une très bonne extraction des EPS, avec peu de lyse selon les conditions de l'extraction (Frølund et al., 1996; Takahashi et al., 2010).Les EPS extraits peuvent être caractérisées par (i) chromatographie d'exclusion par taille, (ii) spectroscopie infrarouge, (iii) spectroscopie classique (Avella Vasquez, 2010). Cette dernière permet de quantifier les espèces majoritaires des EPS, à savoir les protéines et polysaccharides. Pour la quantification des protéines, les techniques suivantes sont utilisées (Avella Vasquez, 2010): la méthode de Bradford (1976), de Lowry (Lowry et al.,1951) ou encore de l'acide Bicinchonique BCA (Smith et al., 1985). En ce qui concerne la quantification des polysaccharides, les techniques suivantes sont utilisée (Avella Vasquez, 2010): Les polysaccharides sont hydrolysés à travers le chauffage d'acide sulfurique, puis réagissent avec du phénol (Dubois et al., 1956) ou de l'Anthrone (Dreywood, 1946).

En plus de jouer un rôle dans la migration verticale (Underwood and Smith, 1998; Decho, 2000), ces EPS ont un rôle de stabilisation biogénique des sédiments inter et subtidaux, limitant potentiellement l'érosion de ce dernier (Holland et al., 1974; Grant et al., 1986; Paterson, 1989a; Smith and Underwood, 1998; Friend et al., 2008, Tableau 3). Le microphytobenthos peut également stabiliser le sédiment en diminuant la rugosité de surface de ce dernier (Friend et al., 2008). En effet, Les diatomées possèdent un frustule siliceux qui, associé aux EPS, pourrait jouer un rôle d'« armure » pour la surface du sédiment, retardant l'érosion et augmentant les seuils d'érodabilité (Tolhurst et al., 2003). Certains biofilms de diatomées ne migrent pas, restant à la surface du sédiment durant l'immersion (Hay et al., 1993). De cette façon les diatomées stabiliseraient le sédiment selon les espèces, leur taille ou leur comportement de migration, ainsi que leur sécrétion d'EPS (Tolhurst et al., 2003). La production d'EPS pourrait également avoir pour effet un lissage de l'interface eau-sédiment, diminuant ainsi les forces de frottement et les taux d'érosion (Friend et al., 2008). La taille moyenne des particules du sédiment peut être modifiée par la simple production d'EPS qui augment l'adhésion entre les grains (Johnson and Azetsu-Scott, 1995).

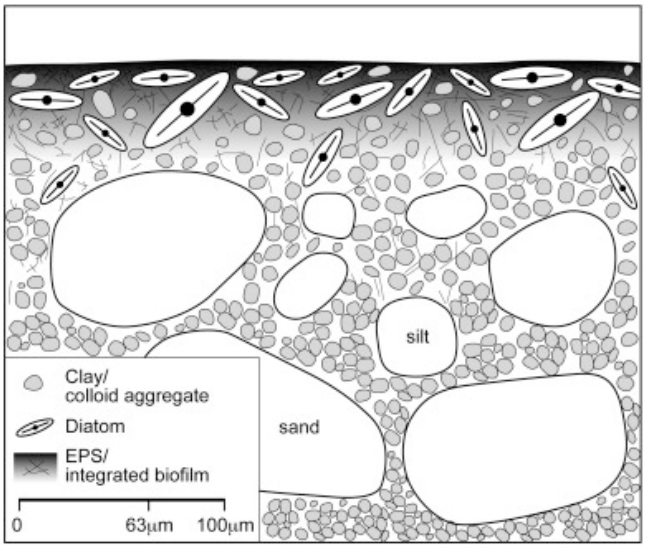

Figure 10 Microstructure d'un sédiment cohésif, montrant les matrices créées par les composants biotiques et abiotiques (Source : Grabowsky, 2011)

Tableau 3 : Travaux menés depuis 2000 concernant l'influence du microphytobenthos sur la stabilité sédimentaire

Auteurs	Instrument(s) utilisé(s)	Corrélation « + » avec la stabilité sédimentaire	Méthode d'extraction des EPS	Sédiment cohésif ■ /non-cohésif ■		Profondeur de prélèvement
Lubarsky et al. (2010)	CSM, MAGPI	Chl *a*, EPS colloïdaux (c & p)	Eau distillée et NaOH	■		5 mm
Gerbersdorf et al. (2009)	CSM, MAGPI	Chl *a*, EPS colloïdaux (c & p)	Eau distillée et centrifugation	■		3 mm
Friend et al. (2008)	CSM	Chl *a*, EPS colloïdaux (c)	Eau distillée		■	1 mm
Spears et al. (2008)	CSM	EPS totaux (c)	Eau distillée	■		×
Tolhurst et al. (2008)	CSM	Chl *a*, EPS colloïdaux (c)	Eau distillée	■		2 mm
Gerbersdorf et al. (2007)	SETEG-Flume	EPS (c) colloïdaux	Résine échangeuse de cation	■		5 mm
Tolhurst et al. (2006)	CSM	Chl *a*, EPS colloïdaux (c)	EDTA	■		5 mm
Paarlberg et al. (2005)	*Sand-mud-bio* model	Diatoms	×	■	■	×
de Brouwer et al. (2005)	rheological device	Diatoms	×		■	2 mm
Lucas et al. (2003)	Annular flume	Chl *a*, EPS colloïdaux (c)	×		■	2 mm
Tolhurst et al. (2003)	CSM	Chl *a*	×	■		2 mm
Lelieveld et al. (2003)	*In situ*	Chl *a*, EPS liés et colloïdaux (c)	×	■	■	5 mm
Friend et al., (2003)	CSM	Chl *a*, EPS colloidaux (c)	Eau distillée	■	■	1-2 mm
Andersen and Pejrup (2002)	EROMES	Chl *a*	×	■		1-2 mm
Yallop et al. (2000)	CSM	Chl *a*, EPS colloïdaux (c)	Eau distillée et EDTA	■		2 mm

Macrofaune et stabilité sédimentaire

La macrofaune benthique peut influencer de façon active ou passive la stabilité sédimentaire. En effet, les organismes peuvent par leur simple présence en surface changer la rugosité de surface, et ainsi induire des changements de contrainte de cisaillement (Whitehouse et al., 2000). Ils peuvent de façon active, via les activités de bioturbation, changer les flux d'érosion/déposition (Graf and Rosenberg, 1997). La bioturbation, en milieu marin, correspond au *brassage de sédiment résultant de processus biologiques, par l'action de l'endofaune et de l'épifaune benthique, ainsi que du necton* (Cadée, 2001). Le concept de bioturbation a été récemment revu par Kristensen et al. (2012) : *Tous les processus de transport effectués par des animaux qui affectent directement ou indirectement les matrices sédimentaires. Ces processus comprennent le remaniement des particules et la ventilation par creusement*. Au niveau des sédiments intertidaux, les taxons retrouvés sont les Mollusques (Bivalves, Gastéropodes), les Crustacés (Amphipodes, Isopodes) et les Annélides (Oligochètes, Achètes). La macrofaune benthique peut à la fois stabiliser et déstabiliser le substrat (Tableau 4, Fig. 11), par des comportements de recherche de nourriture, construction de terrier, déplacement, etc. (Andersen, 2001).

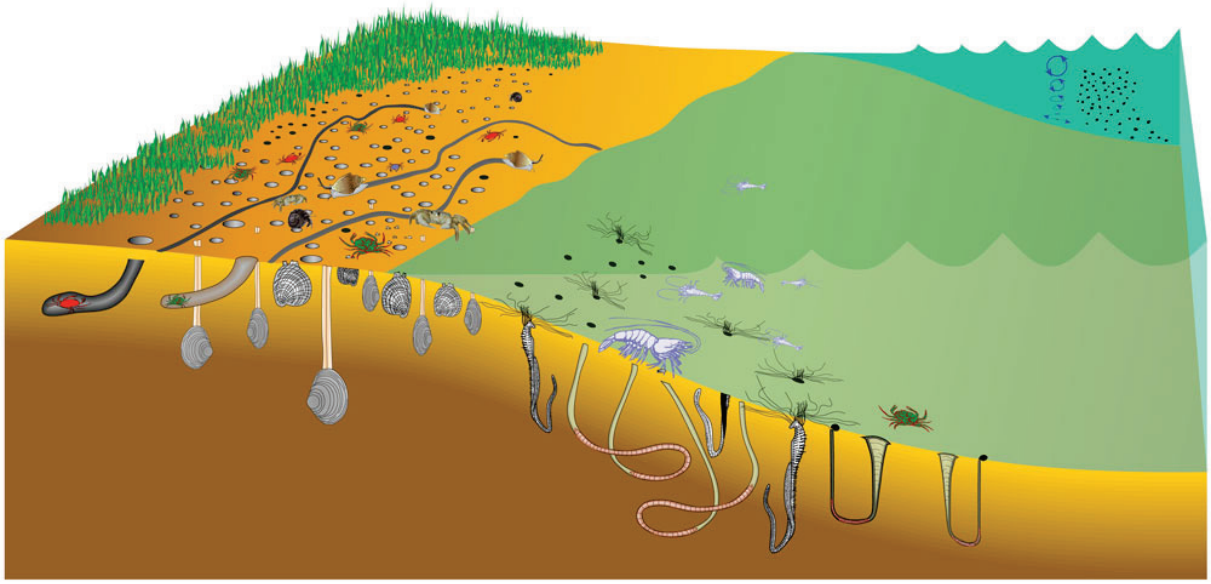

Figure 11 : Illustration du phénomène de bioturbation au niveau de la zone intertidale. On y observe les différents taxons ainsi que les différents types de perturbation du sédiment par la faune endogée.
(Source : http://www.waikato.ac.nz/wfass/subjects/geography/people/max/TidalGraphics.shtml)

Selon les effets que la bioturbation entraîne sur la dynamique sédimentaire, on classe les macro-invertébrés en grands groupes fonctionnels. Ces groupes étaient au nombre de 5 (François et al., 1999) avant d'être récemment ramenés à 4 grands groupes fonctionnels (Kristensen et al., 2012, Fig. 12) :

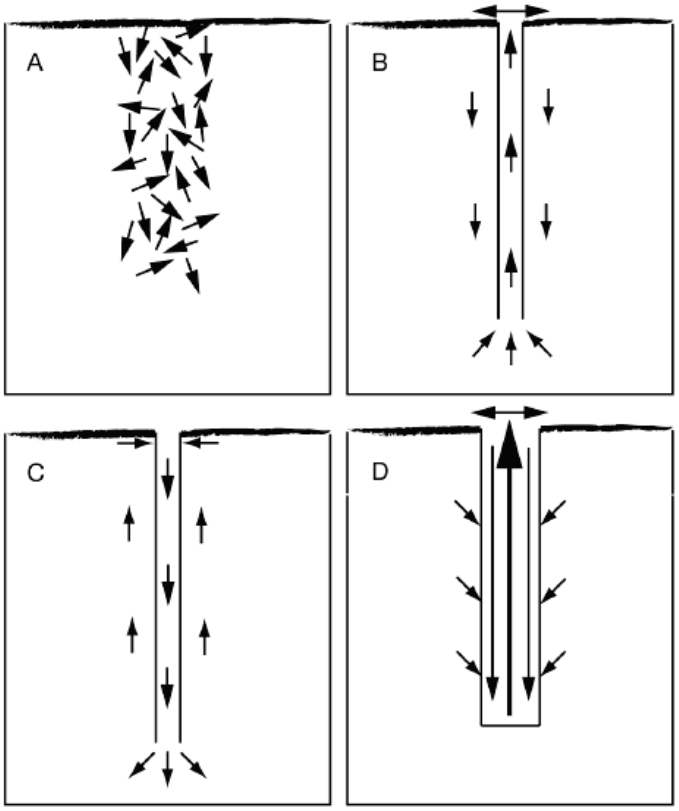

Figure 12 : Les 4 types de remaniements sédimentaires par la macrofaune benthique. A. Biodiffuseurs, B. Convoyeurs vers le haut, C. Convoyeurs vers le bas, D. Régénérateurs (Source : Kristensen et al., 2012)

• **Biodiffuseurs** : Organismes déplaçant aléatoirement (dans les trois dimensions) les particules dans les premiers cm de sédiment ; on parle d'un transport diffusif, par homogénéisation. Ce groupe est divisé en 3 sous-groupes : Les biodiffuseurs de l'épifaune benthique, c'est le cas des crabes ou poissons épibenthiques ; les biodiffuseurs de surface, c'est le cas de bivalves comme *Ruditapes decussatus* et *Venerupis aurea* (François et al., 1999), *Cerastoderma edule* (Mermillod-Blondin et al., 2004) ou *Mya arenaria* et *Macoma balthica* (Michaud et al., 2005), et de certains amphipodes comme *Corophium volutator* (Mermillod-Blondin et al., 2005) ; et les biodiffuseurs à galeries, comme pour l'annélide polychète *Nereis diversicolor* (François et al., 2002).

• **Bioconvoyeurs vers le haut** : Organismes orientés verticalement dans le sédiment, partie antérieure orientée vers le bas, ingérant des particules sédimentaires en profondeur et rejetant leurs pelotes fécales à la surface du sédiment. De plus, un transport advectif passif autour de l'organisme s'effectue par recouvrement du sédiment à l'interface eau-sédiment. On observe ce type de mélange chez *Arenicola marina* par exemple (Valdemarsen et al., 2011).

• **Bioconvoyeurs vers le bas** : Même fonctionnement que le groupe précédent, mais orientation inverse (on parle de convoyeurs « inverses »). On retrouve ce type de remaniement sédimentaire chez certains invertébrés marins comme les Sipunculidae (Smith et al., 1986).

• **Régénérateurs** : Organismes fouisseurs creusant des terriers larges à l'interface eau/sédiment. Ce type de mélange se retrouve lorsque les terriers sont abandonnés : après une phase active de mélange biodiffusif (expulsion du sédiment pendant le creusement du terrier), une phase passive consiste en l'écroulement du terrier. Ce mode de mélange a été décrit chez le crabe violoniste *Uca pugnax* (Gardner et al., 1987).

L'érodabilité des sédiments dépend de l'interaction entre les processus physiques, chimiques et biologiques, particulièrement la balance entre les processus de biostabilisation et biodéstabilisation (Ciutat et al., 2007). Les organismes vivants jouent donc un rôle important en tant qu'« ingénieurs écosystémiques » (Jones et al., 1994), en modifiant l'hydrodynamisme à l'interface eau-sédiment et la dynamique sédimentaire des habitats inter- et sub-tidaux (Widdows and Brinsley, 2002). L'impact de la bioturbation dans la stabilité et l'érosion du sédiment et du biofilm associé peut s'avérer très importante (Tableau 4).

Erosion de la chl *a*

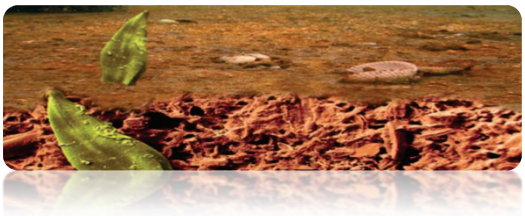

La remise en suspension de la chl *a* benthique est un phénomène complexe du fait des interactions entre le sédiment et la faune benthique. En effet, la macrofaune benthique modifie les seuils critiques d'érosion par les processus de bioturbation et la production de mucus (Blanchard et al., 1997). De plus, la taille des cellules entraîne des différences dans leur remise en suspension. Ainsi, les grosses diatomées (*ex Coscinodiscus spp.*) nécessitent des tensions de frottement plus élevées pour être érodées que les petites diatomées de type *Navicula* (Lucas et al., 2001). Les diatomées benthiques selon les taxons peuvent être remises en suspension à des seuils critiques variables (Shimeta et al., 2002), et semblent être plus résistantes à l'érosion que les communautés bactériennes ou d'euglènes (Shimeta et al., 2003). La formation d'un biofilm en surface peut induire une différence d'érosion entre la matrice biogène et le sédiment sous-jacent (Ubertini et al., 2012). Shimeta et al. (2003) trouvent des valeurs de U^* proches pour les matières en suspension et la Chla (1,79 et 1,87 respectivement), mais cette différence peut varier selon la composition du sédiment et/ou de la microflore benthique.

Tableau 4 : Etudes menées depuis les années 2000 quant aux effets de la bioturbation sur les paramètres d'érodabilité à l'interface eau-sédiment

Auteur(s)	Année	Instrument(s) utilisé(s)	Espèce étudiée	Activité de bioturbation Effet stabilisateur / déstabilisateur	Sédiment cohésif ■ /non-cohésif ■
Soares and Sobral	2009	Annular flume	*Scrobicularia plana*	Modification de vitesse critique de l'érosion, augmentation de la biostabilisation avec l'augmentation de la fraction sableuse	■ (mélange)
Escapa et al.	2008	*in situ*	*Neohelice granulata*	Construction de terriers produisant des monticules biogènes facilement remis en suspension Les terriers jouent le rôle de trappes à sédiment passives	■
Pillay et al.	2007	*in situ*	*Callianassa kraussi*	Augmentation de la remise en suspension par destruction du biofilm lors de la construction de terriers	■2 µm
Volkenborn	2007	*in situ*	*Arenicola marina*	Augmente la rugosité de surface. Nutrition sur le pool de microphytobenthos.	■200-340 µm
Orvain et al.	2007	Model	*Scrobicularia plana* *Hydrobia ulvae*	Diminue le seuil d'érosion par son activité de bioturbation etproduction de biodépôts de surface Augmente la remise en suspension du biofilm de surface	■<63 µm
Ciutat et al.	2007	Annular flume	*Cerastoderma edule*	Construction de terrier et adduction de la coquille Augmentation de la rugosité de surface	■
Lumborg et al.	2006	Model	*Hydrobia ulvae*	Modification de la force de cisaillement	■<63 µm
Orvain	2005	Model	*Scrobicularia plana*	Augmente l'érosion du sédiment par 2 influences : production de biodépots facilement érodables en surface et augmentation de l'érodabilité du sédiment en profondeur par action du terrier et des siphons	■<63 µm
Fernandes et al.	2006 2009	Annular flume	*Nereis diversicolor*	Augmentation de la remise en suspension du sédiment par compression latérale de la paroi des galeries. Réduction du biofilm algal par déplacement. Augmentation de la force de cisaillement et de la vitesse critique d'érosion	■10 µm
Wood and Widdows	2002	Model	*Macoma balthica*	Déstabilise les vasières intermédiaires (concentration de population élevée), augmente le niveau du lit des vasières hautes)	■<63 µm
Deckere et al.	2001	CSM	*Communauté macro-benthique*	Augmentation de la teneur en eau, réduction de la microtopographie et prédation sur le microphytobenthos	■16 µm
Andersen	2001	EROMES	*Hydrobia ulvae*	Déstabilise le sédiment par sa nutrition sur le microphytobenthos	■10 µm

Etude de la remise en suspension in situ : les sites d'étude

La Baie des Veys

La Baie des Veys est un estuaire situé dans la partie occidentale de la Baie de Seine à la jonction des départements du Calvados et de la Manche (Fig. 13). Présentant une ouverture de 6 km de large et une profondeur de 5 à 7 km du large vers les terres, la Baie est orientée Nord-Nord-Est, relativement protégée des vents dominants par la péninsule du Cotentin à l'Ouest. Le bassin versant associé à la Baie s'étend sur 3500 km^2, et comprend deux couples de rivières, l'Aure et la Vire ainsi que la Douve et la Taute, qui se rejoignent pour former deux chenaux au niveau de la Baie : les chenaux d'Isigny (à l'Est) et de Carentan (à l'Ouest). Le débit des chenaux est relativement élevé en hiver et faible en été, avec des débits allant de 3,7 à 26,4 $m^3.s^{-1}$ pour le chenal de Carentan et de 23,9 à 40,4 $m^3.s^{-1}$ pour le chenal d'Isigny. La zone intertidale (Fig. 14) s'étend sur 37km^2 (Sylvand, 1995), et est caractérisée par un marnage d'une amplitude de 7-8m durant les marées de vives eaux et 2.5m durant les marées de mortes eaux. Le fond de la Baie est caractérisé par des vasières bordées par un schorre. Une transition de sédiments vaseux vers des sables moyens est observable selon un gradient de direction Nord-Nord-Est. La vitesse des courants peut atteindre 3 $m.s^{-1}$ pendant le flot et 1,5 $m.s^{-1}$ pendant le jusant. La courantologie générale de la Baie génère un déplacement circulaire des masses d'eau dans le sens contraire des aiguilles d'une montre. Il s'agit d'une Baie à forte dominance marine, puisque les volumes d'eau de mer entrant dans la baie à chaque marée moyenne représentent environ 15 millions de m^3, pour un volume d'eau douce moyen déversé en 6 heures d'environ 0,62 million de m^3. Des cultures d'huîtres et de moules s'étendent à l'Est du chenal d'Isigny, sur une surface d'environ 160 ha (Fig. 14).

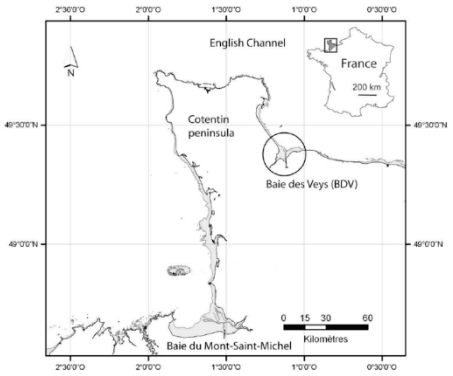

Figure 13 : Situation géographique de la baie des veys (Source : Lefebvre et al., 2009).

La température de la Baie varie entre 7,8 ± 1,2°C en hiver et 18,3 ± 1,1°C en été. La salinité moyenne de la Baie est de 33,3 ± 0,8, mais des épisodes de dessalure apparaissent à chaque marée descendant jusqu'à 10-15. La dynamique saisonnière de la Baie au niveau du phytoplancton est caractérisée par un bloom printanier important en avril-mai, lorsque la lumière devient non-limitante. Un deuxième bloom de moindre importance apparaît en septembre, lors de la régénération de l'ammonium.

Figure 14 : Vues d'altitude de la Baie des Veys. Les chenaux d'Isigny et Carentan apparaissent respectivement à gauche et à droite de la photo (Sources : http://www.basse-normandie.developpement-durable.gouv.fr pour l'image de gauche, Homeexhange.com pour l'image de droite).

La production ostréicole de la Baie des Veys est de 7000 tonnes par an, ce qui en fait le premier site de production ostréicole du Calvados et le troisième de Basse Normandie. Les apports permettant cette production sont de nature variée : phytoplancton, microphytobenthos, débris d'algues, matière organique terrigène, le phytoplancton constituant la ressource trophique majoritaire des huîtres (Marín Leal et al., 2008).

Lingreville sur mer

Lingreville sur Mer est situé sur la côte Ouest de la péninsule du Cotentin (Fig.15), en face du Havre de la Vanlée. Le havre de la Vanlée (Fig. 16) est une zone de 300 ha dont 60% est occupée par le schorre (Guillaumont, 1987). Le marnage de la zone de Lingreville peut atteindre jusqu'à 13 m (Lefebvre et al., 2009) lors des marées de vives eaux, et est d'environ 5m en période de mortes eaux. Il s'agit d'une zone exposée aux vents dominants d'Ouest et Nord-Ouest. Du fait de son ouverture sur la mer, la baie est fortement influencée par les courants marins. Les apports terrigènes proviennent de deux rivières : la Sienne, située plus au Nord de la zone avec un débit variant de 2,2 à 24,3 $m^3.s^{-1}$ pour un bassin versant de 759 km^2, et la Vanlée, caractérisée par un débit faible et dont le bassin versant occupe 60 km^2. Le sédiment est constitué majoritairement de sable et de sable coquillier (Lefebvre et al., 2009).

La température de la zone de Lingreville varie entre 8,8 ± 0,2°C en hiver et 19,4 ± 0,6°C en été (http://www.ifremer.fr/envlit, 2008). La salinité moyenne de la Baie est de 34,6 ± 0,5, les minima étant observés en mars et les maxima en octobre. Le bloom de printemps apparaît au mois de mai, suivi d'un bloom automnal de plus faible intensité au début du mois d'octobre.

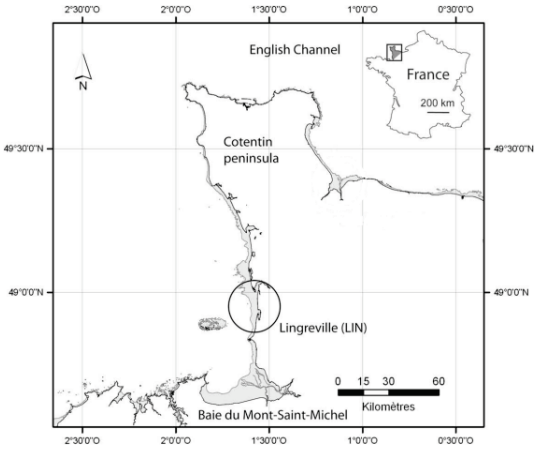

Figure 15 : Localisation géographique de Lingreville sur mer (Source : Lefebvre et al., 2009).

Figure 16 : A gauche, embouchure de la Sienne et en arrière plan embouchure de la Vanlée (Source : http://www.parachutisme-chutelibre.fr). A droite Havre de la Vanlée (Source : http://manche.fr).

De par sa situation géographique, la zone de Lingreville (Fig. 16) bénéficie des apports océaniques, de la Vanlée mais également de la Sienne (Fig. 17). La multiplicité des apports assure une production élevée de moules de bouchots.

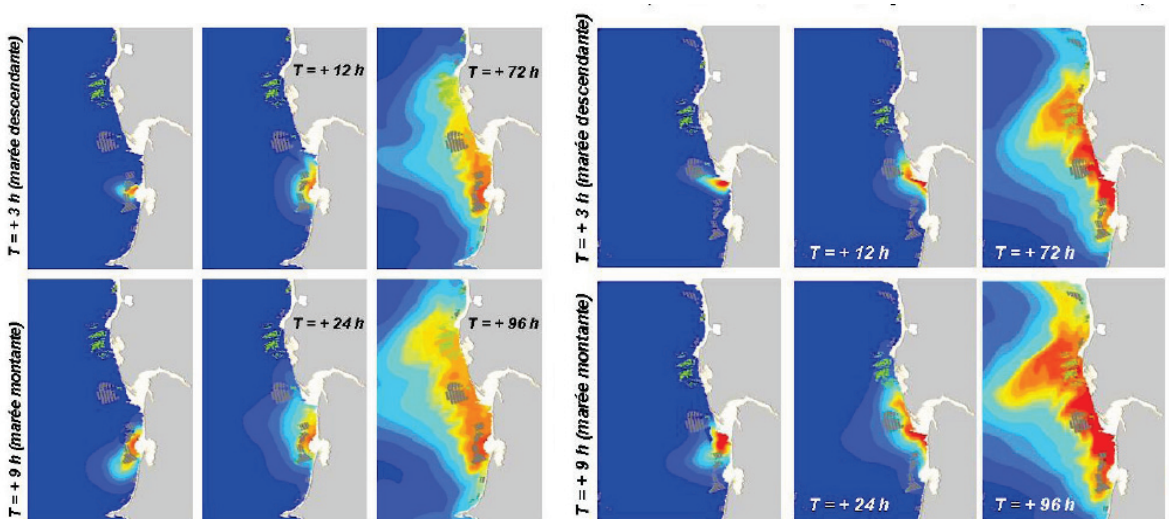

Figure 17 : Modélisation du panache de la Vanlée (à gauche) et de la Sienne (à droite). Simulation sans vent, coefficient de marée 75, rejet continu, lâché à pleine mer. L'échelle de dilution est symbolisée du rouge (moins dilué) au bleu (plus dilué) (Source : http://www.ifremer.fr/envlit, 2008).

Objectifs

L'objectif de cette thèse était donc de mieux quantifier et hiérarchiser les phénomènes de remise en suspension, afin de déterminer la capacité des diatomées benthiques à être remises en suspension et ainsi participer au pool de matière organique pouvant être filtré et consommé par les mollusques suspensivores cultivés ou non. Afin de répondre à ces questions, différentes approches on été utilisées, de l'approche écosystèmique globale *in situ* à l'étude fine des processus *ex situ* (Fig. 17).

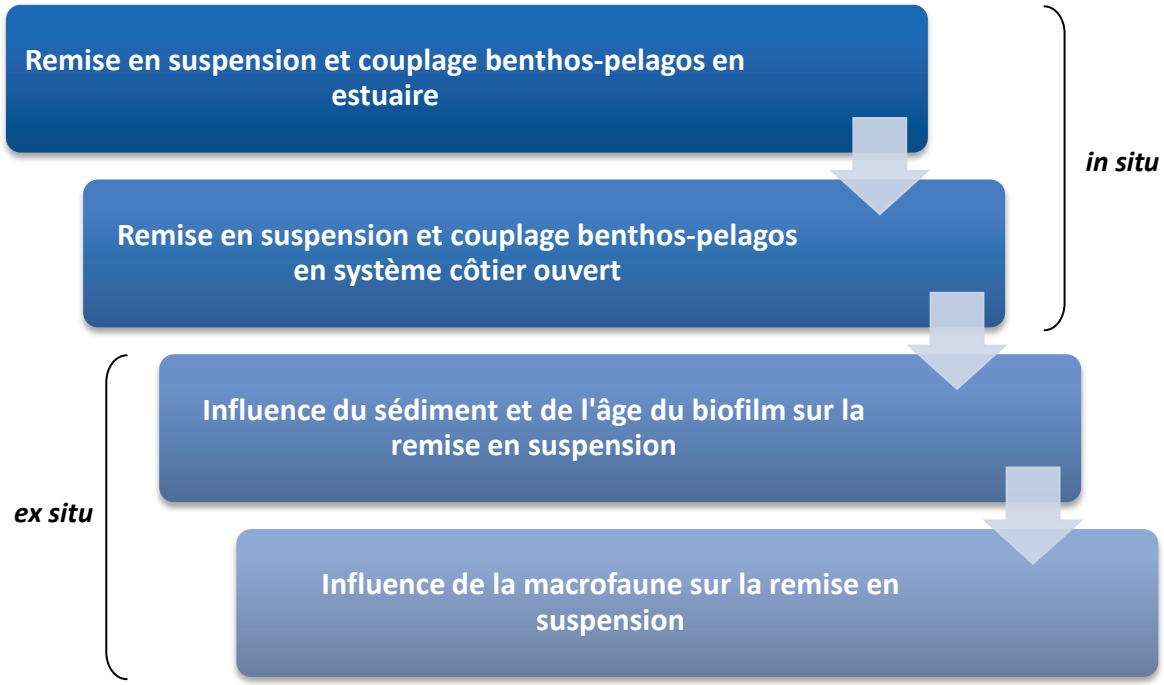

Figure 18 : Approches utilisées durant la thèse pour répondre à la problématique générale

Les études *in situ* ont permis d'explorer la remise en suspension au travers du couplage benthos-pelagos à l'échelle de l'écosystème, sans en contrôler les variables « forçantes ». Les études *ex situ* à méso-échelle quant à elles ont permis d'explorer la remise en suspension en contrôlant les variables « forçantes ».

Le plan de la thèse est construit tel que la question de la remise en suspension des diatomées benthiques a été envisagée. La première partie est un préambule correspondant à l'état de l'art concernant la remise en suspension des diatomées benthiques, et les moyens utilisés pour l'évaluer. Les sites étudiés pour répondre à la problématique de thèse sont également présentés, le choix des sites s'inscrivant plus largement dans l'intérêt de la remise en suspension des diatomées benthiques quant à leur devenir dans les échelons trophiques supérieurs.

La deuxième partie correspond au travail mené sur la remise en suspension au sein d'écosystèmes conchylicoles, par des études *in situ*. Les dimensions spatiales et temporelles de la remise en suspension ont ainsi pu être étudiées en relation avec les communautés benthiques des zones étudiées. Ainsi, la caractérisation de ces écosystèmes en termes de couplage benthos-pelagos et de communautés benthiques avait pour objectif de replacer la resuspension des diatomées benthiques dans un contexte écosystémique global, et de mieux quantifier/hiérarchiser les processus physiques et biologiques impliqués. Le choix des deux écosystèmes étudiés se justifie par des configurations différentes, permettant de mieux discriminer les processus (Tableau 5) :

Tableau 5 : Différences notoires entre les deux écosystèmes modèles étudiés pendant la thèse

Caractéristiques	Baie des Veys	Lingreville sur mer
Type d'écosystème	Estuaire ouvert	Côtier ouvert
Apports fluviatiles	Elevés	Faibles
Type de conchyliculture	Huîtres (Parcs)	Moules (Bouchots)
Couverture conchylicole	Partielle	Totale
Type sédimentaire	Gradient sablo-vaseux	Sable grossier

La troisième partie est axée sur les facteurs impliqués dans la remise en suspension des diatomées benthiques, en contrôlant aux mieux les paramètres par une approche *ex situ*. Les compartiments physiques (hydrodynamisme et sédiment), biologiques (microphytobenthos) et chimiques (EPS) ont donc pu être étudiés plus finement afin de quantifier leur impact dans le phénomène de remise en suspension. L'impact des mélanges sablo-vaseux a été particulièrement étudié, de nombreux écosystèmes étant caractérisés par des mélanges sablo-vaseux comme en Baie des Veys (Orvain et al., 2012).

Une dernière partie permet de faire la synthèse des principaux résultats obtenus au cours de cette thèse, et permet de faire le lien entre les approches *in situ* et *ex situ*. La combinaison des échelles ainsi explorées permet de revenir sur les écosystèmes étudiés pour proposer une intégration quantifiable de la remise en suspension dans le couplage bentho-pélagique. Les voies restant à explorer sont également abordées, notamment quant à l'intégration des données acquises dans des modèles.

Chapitre III

Variabilité spatiale du couplage benthos-pelagos dans un écosystème estuarien : Conséquences pour le phénomène de remise en suspension du microphytobenthos

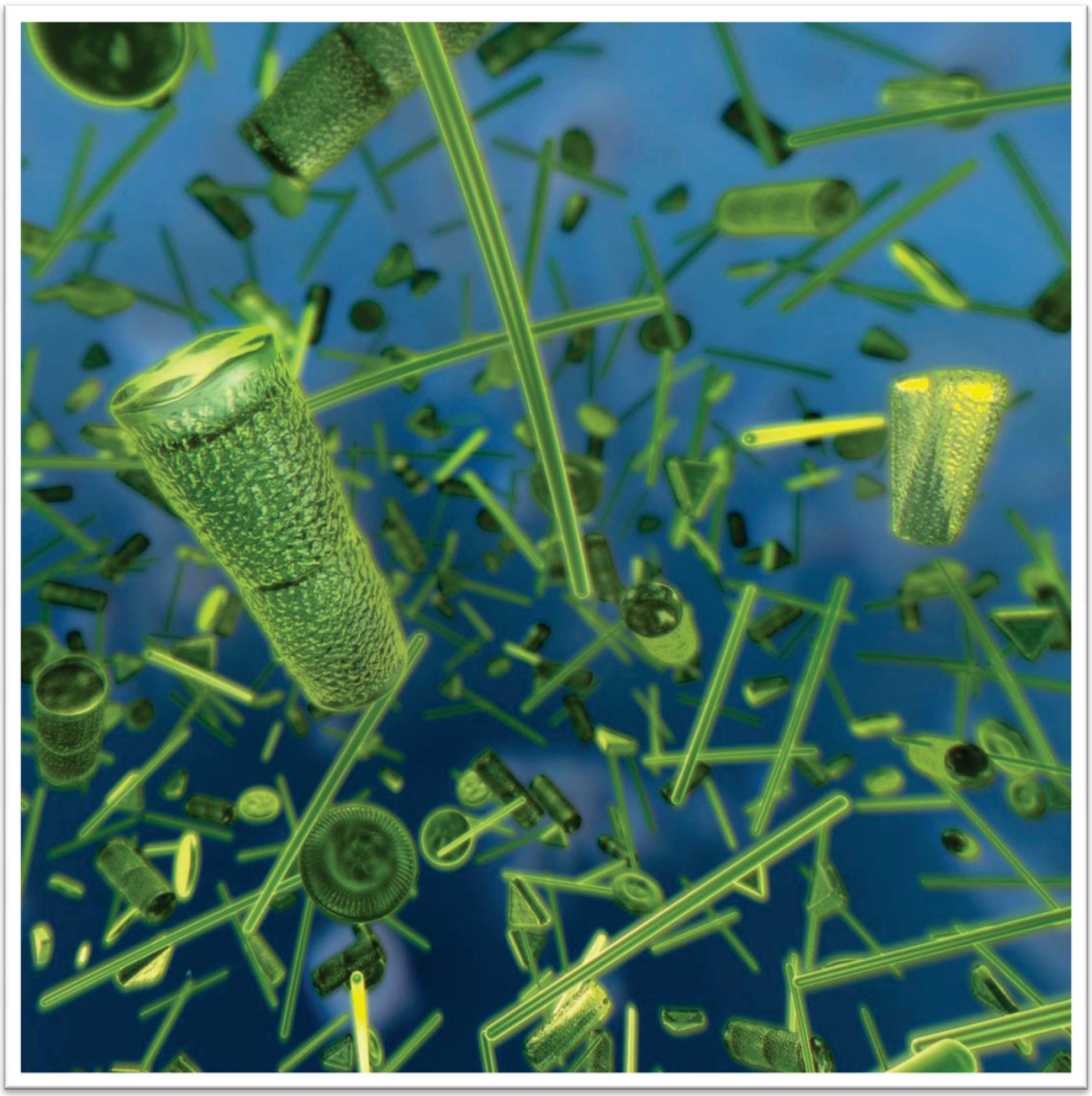

« Homme libre, toujours tu chériras la mer ! »

Charles Baudelaire

Spatial variability of benthic-pelagic coupling in an estuarine ecosystem: Consequences for microphytobenthos resuspension phenomenon

Martin Ubertini[1,2], Sébastien Lefebvre[3], Aline Gangnery[4], Karine Grangeré[1,2], Romain Le Gendre[4], Francis Orvain[1,2,5]

[1] *Université de Caen Basse-Normandie, FRE3484 BioMEA, Caen, France,*
[2] *CNRS INEE, FRE3484 BioMEA, Caen, France*
[3] *Université de Lille1, UMR CNRS 8187 LOG ''Laboratoire d'Océanologie et Géosciences'', Station Marine de Wimereux, Wimereux, France*
[4] *IFREMER, LERN, Port en Bessin, Franc*
[5] *CNRS, UMR 7208 BOREA, Muséum d'histoire naturelle, CRESCO, Dinard, France*

Publié dans le journal :

"**Plos One**"
IF=4.411

Résumé

L'importance des forçages physiques dans les écosystèmes intertidaux estuariens augmente les échanges entre les compartiments benthiques et pélagiques. Dans ces écosystèmes, la remise en suspension du microphytobenthos (MPB) est un phénomène majeur, puisque sa contribution aux niveaux trophiques supérieurs peut être très importante. Comprendre la remise en suspension du sédiment et MPB associé ainsi que son devenir dans la colonne d'eau est indispensable pour quantifier la nourriture disponible pour les réseaux trophiques benthiques et pélagiques. Afin d'identifier et de hiérarchiser les facteurs physiques/biologiques potentiellement impliqués dans la remise en suspension du MPB, l'ensemble de la zone intertidale ainsi que la colonne d'eau sus-jacente ont été échantillonnés au jusant dans un écosystème estuarien, la Baie des Veys. Un large éventail de paramètres physiques (régime hydrodynamique, granulométrie des sédiments et matières en suspension) et de paramètres biologiques (assemblages floristiques et faunistiques, chlorophylle) ont été analysés pour caractériser le couplage benthos-pelagos à l'échelle de la baie. Les échantillons ont été prélevés à deux périodes contrastées, le printemps et la fin de l'été, afin d'évaluer l'impact des variables « forçantes » sur le couplage benthos-pelagos. Une approche cartographique utilisant l'interpolation par krigeage nous a permis de superposer des cartes benthiques et pélagiques de variables physiques et biologiques, correspondant aux conditions hydrologiques et trophiques. La chlorophylle *a* pélagique fut le meilleur indice expliquant la distribution spatiale des mollusques suspensivores. Nos résultats suggèrent également une structure spatio-temporelle pérenne des deux compartiments benthiques et pélagiques dans l'écosystème, du moins lorsque le système n'est pas contraint par des vents intenses, la distribution du MPB étant contrôlée par la granulométrie du sédiment et la bathymétrie. La composante benthique semble contrôler la composante pélagique par des phénomènes de remise en suspension à l'échelle de la baie. L'analyse de co-inertie a montré un couplage benthos-pelagos plus fort entre les variables au printemps. L'observation d'une biomasse de MPB plus élevée en été suggère une plus grande contribution au régime des filtreurs, ce qui indique une remise en suspension plus élevée en été qu'au printemps, suggérant un rôle important de la bioturbation par la macrofaune et de la nutrition par filtration (*Cerastoderma edule*).

OPEN ACCESS Freely available online

PLOS ONE

Spatial Variability of Benthic-Pelagic Coupling in an Estuary Ecosystem: Consequences for Microphytobenthos Resuspension Phenomenon

Martin Ubertini[1,2], Sébastien Lefebvre[4], Aline Gangnery[3], Karine Grangeré[1,2], Romain Le Gendre[3], Francis Orvain[1,2,5]*

1 Université de Caen Basse-Normandie, FRE3484 BioMEA, Caen, France, **2** CNRS INEE, FRE3484 BioMEA, Caen, France, **3** IFREMER, LERN, Port en Bessin, France, **4** Université de Lille1, UMR CNRS 8187 LOG "Laboratoire d'océanologie et geosciences", Station Marine de Wimereux, Wimereux, France, **5** CNRS, UMR 7208 BOREA, Muséum d'histoire naturelle, CRESCO, Dinard, France

Abstract

The high degree of physical factors in intertidal estuarine ecosystem increases material processing between benthic and pelagic compartments. In these ecosystems, microphytobenthos resuspension is a major phenomenon since its contribution to higher trophic levels can be highly significant. Understanding the sediment and associated microphytobenthos resuspension and its fate in the water column is indispensable for measuring the food available to benthic and pelagic food webs. To identify and hierarchize the physical/biological factors potentially involved in MPB resuspension, the entire intertidal area and surrounding water column of an estuarine ecosystem, the Bay des Veys, was sampled during ebb tide. A wide range of physical parameters (hydrodynamic regime, grain size of the sediment, and suspended matter) and biological parameters (flora and fauna assemblages, chlorophyll) were analyzed to characterize benthic-pelagic coupling at the bay scale. Samples were collected in two contrasted periods, spring and late summer, to assess the impact of forcing variables on benthic-pelagic coupling. A mapping approach using kriging interpolation enabled us to overlay benthic and pelagic maps of physical and biological variables, for both hydrological conditions and trophic indicators. Pelagic Chl *a* concentration was the best predictor explaining the suspension-feeders spatial distribution. Our results also suggest a perennial spatio-temporal structure of both benthic and pelagic compartments in the ecosystem, at least when the system is not imposed to intense wind, with MPB distribution controlled by both grain size and bathymetry. The benthic component appeared to control the pelagic one via resuspension phenomena at the scale of the bay. Co-inertia analysis showed closer benthic-pelagic coupling between the variables in spring. The higher MPB biomass observed in summer suggests a higher contribution to filter-feeders diets, indicating a higher resuspension effect in summer than in spring, in turn suggesting an important role of macrofauna bioturbation and filter feeding (*Cerastoderma edule*).

Citation: Ubertini M, Lefebvre S, Gangnery A, Grangeré K, Le Gendre R, et al. (2012) Spatial Variability of Benthic-Pelagic Coupling in an Estuary Ecosystem: Consequences for Microphytobenthos Resuspension Phenomenon. PLoS ONE 7(8): e44155. doi:10.1371/journal.pone.0044155

Editor: Simon Thrush, National Institute of Water & Atmospheric Research, New Zealand

Received April 5, 2012; **Accepted** July 30, 2012; **Published** August 29, 2012

Funding: This work was funded by the Regional council of Basse-Normandie. The funders had no role in study design, data collection and analysis, decision to publish, or preparation of the manuscript.

Competing Interests: The authors have declared that no competing interests exist.

* E-mail: francis.orvain@unicaen.fr

Introduction

Estuaries are known to be among the most productive systems in the biosphere [1]. Their high productivity is mainly due to the presence of nutrients and of multiple food resources for the trophic web, coming from both riverine, marine planktonic and benthic compartments [2]. Moreover, in most of these shallow water environments, the intensity of the physical factors reinforces the connections between benthic and pelagic environments by increasing material processing, nutrient cycling and erosion/deposition exchanges. Among all these processes, microphytobenthos (MPB) resuspension is a major phenomenon involved in benthic-pelagic coupling since MPB can contribute up to 50% or more of the primary production for such ecosystems [3]. Consequently, MPB resuspension has major implications both for the food web and for ecosystem stability [4], [5][6].

Benthic-pelagic coupling and especially MPB resuspension are controlled by a complex set of interactions (Fig. 1) between biological, physical, and chemical components or processes [7]. Physical processes such as waves and tidal currents are responsible for erosion of the sediment, leading to sediment resuspension in the water column [8], and hence modifying the properties of the sediment. These mechanisms directly control sediment erodibility, especially sediment composition and compaction [9]. The associated MPB is resuspended at the same time, with wind effect being the major physical factor controlling its resuspension [4]. Even if MPB resuspension is directly controlled by bulk sediment properties related to erodibility, MPB is partly able to control its own resuspension behavior by producing exopolymeric substances (EPS), which reinforces the surface cohesion [10], [11], [12]. This biofilm structure may also cause physical armoring of the sediment, thus limiting its erosion [7]. Macrofauna may also affect the resuspension of MPB by bioturbation, affecting sediment

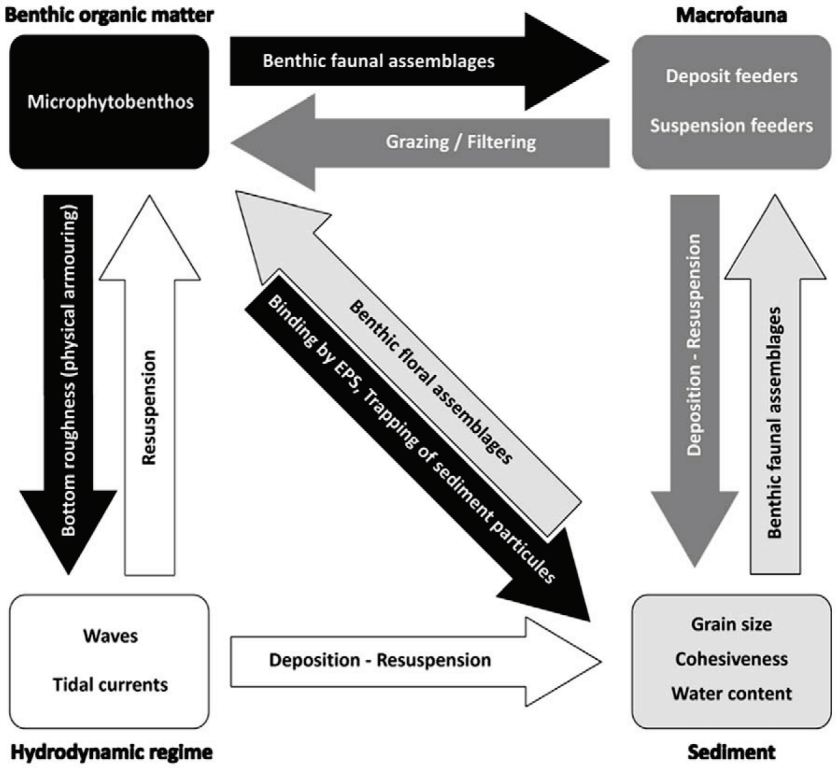

Figure 1. Factors involved in sediment resuspension and the associated microphytobenthos.
doi:10.1371/journal.pone.0044155.g001

erodibility by 1) releasing a material with a high concentration of microphytobenthos [13] and 2) reducing MPB biomass due to nutrition [14]. As a consequence of trophic interactions, MPB can influence long-term trends in benthic macrofauna composition [15], which in turn influence differently MPB resuspension by bioturbation.

MPB biomass always varies in space and over time at all scales in the sedimentary landscape. For instance, surface MPB biomass can double at a given site within one day [16], and MPB biofilms also oscillate in response to the tidal 14-day cycle [17], [18]. In intertidal areas, MPB biomass also varies with the season, and the lowest and highest biomass are found in winter and summer, respectively [16], [19]. Variation in MPB biomass from one year to the next appears to be low [19]. Physical variables such as light irradiance [20], temperature [21], nutrient concentration [22] or wind intensity [19], may be responsible for these seasonal variations in MPB biomass, and many of these time forcing variables can also cause variations at different spatial scales. Even if irradiance varies over the year, light availability is closely related to the bathymetry, and thus influences benthic production [18], [19]. Grain-size is not homogenous within the intertidal area, leading to differential distribution of sediments with different degrees of erodibility, and sediment composition could be the main factor that regulates the spatial patterns of MPB biomass [17]. These differences between sediment types lead to different diatom assemblages with epipsamic or epipelic diatoms causing related variation in MPB biomass. If the previously described physical variables act as a bottom-up control of MPB biomass [17], biological phenomena such as grazing can act as a top-down control [23]. Even if the spatio-temporal dynamics of microphytbenthos production and biomasses are now better understood, the extent to which the MPB biomass supplies the water column is poorly described and quantified.

Different approaches have been used to characterize benthic-pelagic exchanges caused by MPB resuspension phenomenon. This phenomenon has been widely studied using flume experiments, which enable quantification of the relationship between bed erodibility and sediment properties [24]. However, flume studies focus on the initial point of the erosion phenomenon, without tracking the source distribution of particles along Lagrangian movements of water bodies. Most of the time those data are used for model parameterization for a further evaluation of its fate in the water column. Although flume and small mesocosms experiments are useful to quantify resuspension rates at small scales, they do not enable assessment of the implications of resuspension processes for benthic-pelagic coupling and trophic redistribution at the ecosystem scale [25]. Bivalve farmings have often been recognized as habitats where microphytobenthic communities colonize rapidly the sediments in relation to deposit and bed flow properties mediation by the effect of farming structures and alimentary behavior of animals [17], [25].

Different proxies have been used to study the benthic-pelagic coupling and they can be used as well to better define the trophic routes of resuspended microphytobenthos within an ecosystem. Chlorophyll *a* (Chl *a*) biomass, which is often used as a proxy for phytoplankton biomass [26], can also be used as a proxy for resuspension [27], but this variable include both benthic and pelagic sources of Chl *a*. The taxonomic ratio of benthic to pelagic microalgae can be used as a quantitative indicator for resuspension phenomena [28], thus refining the Chl *a* concentration indicator. However, differences between benthic and pelagic diatoms are not that obvious since some species are tychopelagic, i.e. live in both environments. Like for Chl *a* concentration, particulate suspended

inorganic matter (SPiM) can be a good indicator of resuspension if both benthic and pelagic compartments are studied at the same time, but the time lag is difficult to avoid *in situ*, particularly when a whole ecosystem is being studied. Some authors used isotopic signatures with $\delta^{13}C$ and $\delta^{15}N$ values of suspension feeders to determine the MPB contribution to their diets [29], [30], [31]. In fact, they could be indirectly used as a proxy of amounts of resuspended MPB, but isotopic studies focus on the final point, i.e. consumption, without knowing whether the initial MPB primary production was autochthonous or allochthonous. Such information could be very useful to consider for coastal management and ecological implications in terms of habitat connection and trophic interaction. The use of phaeopigments as a grazing indicator has been discussed by several authors and judged to be useful for studies of the water column [32], [33]. Because *in situ* studies include many parameters and all these indices provide substantial information concerning different aspects of benthic-pelagic coupling, the combination of them is the best way to assess the implication of MPB resuspension and its redistribution in the pelagic ecosystem and along the trophic chain.

Understanding the set of multifactorial interactions at the ecosystem scale is of critical importance to quantify exports of MPB to the water column, its relative importance compared to the phytoplankton communities and to hierarchize the physical and biological factors potentially involved in MPB exportation. To our knowledge, field experiments have never included both benthic and pelagic compartments at a large scale to explore MPB resuspension phenomenon even though they are complementary and very difficult to separate in estuaries. Because MPB is simultaneously consumed and exported to the water column, in this study we overlaid benthic and pelagic maps of physical and biological variables, for both hydrological conditions and trophic indicators.

The multiple criteria approach we used to study the indices at all scales enabled us to explain the resuspension within the whole ecosystem approach and to cope with the absence of flux measurements (i.e. erosion as well as trophic fluxes). This study also included a spatial survey of MPB distribution, the factors explaining its resuspension and finally its consumption by filter feeders. To better assess the temporal variations in benthic-pelagic coupling, benthic and pelagic compartments were studied simultaneously at two contrasted seasons in terms of forcing variables and MPB and phytoplankton biomass within a temperate macrotidal and exploited coastal ecosystem, the "Baie des Veys" (BDV, France). The whole intertidal area was sampled to account for the spatial heterogeneity within the Bay including different spatial patterns of forcing factors (presence/absence of shellfish farmings, sediment composition, macrofauna distribution, bed shear stress, salinity). Concerning temporal variability, MPB production is normally low in early spring and high in late summer, but the spring phytoplankton bloom is normally higher than the late summer bloom, so resuspension and its relative contribution as a trophic resource in the water column is expected to be higher in late summer. Bioturbation activities that could lead to the resuspension of microphytobenthos from intertidal sediments are also expected to be amplified at the end of summer because of the high levels of biomass but also because of the positive effects of temperature.

Materials and Methods

1. Study Area

The *Baie des Veys* (BDV, Fig. 2) is an estuarine bay located in the western part of the Bay of Seine in the eastern English Channel. It is characterized by an intertidal area covering 37 km^2 and a macrotidal regime that reaches 7 m maximum tidal amplitude during spring tides and 2.5 m during neap tides [34]. The bay is quite well protected from the prevailing wind by the Cotentin peninsula. Current velocity can reach 3 $m.s^{-1}$ during flood tides and 1.5 $m.s^{-1}$ during ebb tides [29]. Four rivers flow into the BDV through two channels, the Isigny channel in the east and the Carentan channel in the west. Freshwater runoff is low in summer and high in winter, with flows ranging from 3.7 to 26.4 $m^3.s^{-1}$ in the Carentan Channel and from 23.9 to 40.4 $m^3.s^{-1}$ for the Isigny Channel. The oyster farming area extends into the north-eastern part of the bay.

2. Sampling Strategy

Both benthic and pelagic variables were sampled during spring tides to better assess the contribution of resuspended MPB to the total Chl *a* content in the water column [4]. Benthic samples were collected within a week between March 29 and April 2, 2010, and water samples were collected on April 29 and 30, 2010. For the 2 sampling periods, the tidal amplitude was approximately 5.5 m. The same strategy was applied at the end of summer, to assess the impact of the increased number and activity of mollusks on the resuspension phenomenon. Benthic samples were collected from September 8 to 12, 2010, and water samples on the 13 and 14 of September. Because farming structures are located in the north-eastern part of the bay, they may benefit from both autochtonous and allochtonous resources coming from the south of the bay. As a consequence, water was sampled during spring ebb tides, to account for the flux of MPB from the southern part to the north part of the bay, potentially feeding the suspension-feeders reared in the bay. A systematic grid of 88 points was extended over the entire map of the intertidal area with a sampling interval of 500 m (Fig. 2). Heterogeneity in soil organism distribution occurs at nested scales, and is shaped by a spatial hierarchy of environmental factors, intrinsic population processes and disturbances [35]. To explore smaller scale distributions, a nested sampling design was applied [36], [17]. The intertidal area was divided into three sub-domains that were considered as distinct areas due to their separation by the Isigny and Carentan Channels. In each sub-domain, a semi-cross sampling design was applied with an interval of 100 m between each point (Fig. 2). Each semi-cross was placed on high gradient areas previously observed on the field [17].

3. Field Measurements

Sediment and benthos sampling. At low tide, four 20 cm diameter cores were collected at each sampling site. The first cm of each core was removed and placed in a separate plastic bag. At each site, macrofauna were harvested within a square of 0.25 m^2. The choice of a surface of 0.25 m^2 is appropriate when referring to several studies carried out on the benthos in the intertidal zone showing that this surface is sufficiently large and well suited for estimating the abundance of bivalves [37]. This surface allows a suitable and satisfactory sampling of the fauna whatever its distribution (contagious, regular, or random), even when populations are small in number [38].

The entire sediment was sampled to a depth of 10 cm by hand, and then sieved directly on the spot using a 1 mm mesh size sieve [39]. The depth of 10 cm was chosen in order to take in account most of the mollusk biomass potentially involved in resuspension phenomenon, assuming the fact that some bivalve species like *Mya arenaria* that was observed on the field live under this depth [40]. Sieved samples were placed in plastic bags for transport to the lab.

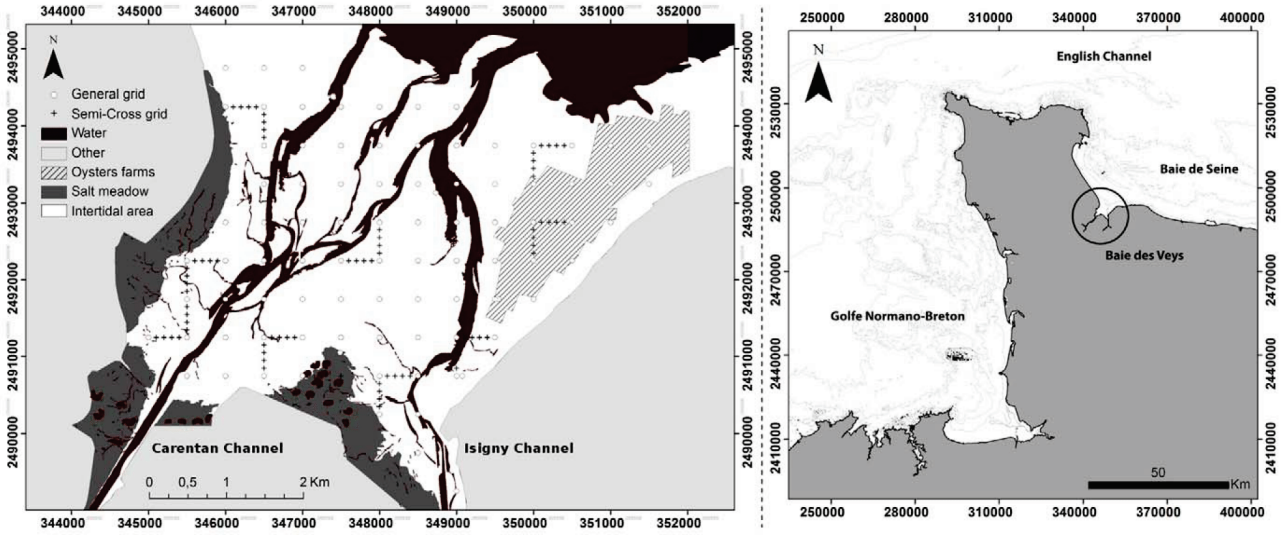

Figure 2. Location of the Baie des Veys and sampling grid.
doi:10.1371/journal.pone.0044155.g002

Animal sampling for isotopy. Six sampling sites were selected within the farming structures to assess the spatial variability of the suspension-feeder *Crassostrea gigas* diet by sampling the widest extent of the structures. The bathymetry of all sites was between +1.65 and +3.50 m. Sites 1 and 2 were on hard substrata, and other sites were on soft-bottom. At each sampling site, five oysters were sampled in the two seasons one month after the spring and late summer samplings, in order to investigate their diets by stable isotopic ratios of carbon and nitrogen.

Water column sampling. Surveys were carried out during ebb tide at all grid points, from one hour after high tide to one hour before low tide. For the 2 periods, the wind velocities were found to be relatively low and similar (3.44 and 4.67 m s^{-1} for April and September respectively), as well as the wind direction with dominant west-northwestern winds (213.33 and 251.46° in a 360° compass rose for April and September respectively). At each point, 5 L water samples were collected by pumping water at a height of 1 m above the seafloor, to ensure access to resuspended MPB. Water samples passed directly through a home-made device equipped with a multi-parameter sensor YSI 6600 (YSI, Yellow Springs, Ohio, USA), before being stored for laboratory measurements. Water subsamples were immediately preserved in Lugol solution for the determination of flora.

4. Laboratory Analyses

Sediment. Back at the laboratory, sediment samples were pooled and mixed thoroughly, and a 1.5 ml subsample was removed and stored at −20°C in the dark until Chl *a* analyses. The remaining sediment was also stored at −20°C until grain-size measurements. Each subsample of sediment was freeze-dried and then weighed to determine the sediment water content. Chl *a* was measured on freeze-dried subsamples using a fluorometric method to estimate algal biomass (µg.g^{-1} sediment). The Chl *a* content of the sediment was extracted in 90% acetone at 4°C for18 h in the dark. The chlorophyll extracts were measured after centrifugation on a Turner Designs TD 700 fluorimeter (USA) following the method of Welschmeyer [41]. Analysis of particle size distribution was performed by using a grain-size laser method. Sediment samples were dried at 60°C for 3 days and sieved (for coarse-grained particles >2000 µm). Organic matter was removed from the samples with H_2O_2, followed by soil dispersion with sodium hexametaphosphate. Then, grain-size analysis was performed using a laser granulometer (Coulter, LS200, USA). For the sake of simplicity, the size fractions obtained using the Wenworth scale were then classified in two groups: mud (0–63 µm) and sand (63–2000 µm).

Macrofauna. Samples were fixed in a 10% formaldehyde solution for 24 h and transferred to 70% ethanol for storage until further analyses. All samples were carefully sorted to separate organisms and the remaining sediment. The mollusk species were then determined [42]. Mollusk flesh was separated from the shell, dried at 60°C for 3 days and weighed without the shell. Small specimens with a tough shell (e.g. *Peringia ulvae*) were treated with a drop of 33% hydrochloric acid solution for a few minutes to dissolve the shell. The organisms were then dried in an oven at 450°C for 4 hours to obtain the ash free dry weight.

Freeze–dried, powdered, and homogenized oyster samples were analyzed using a CHN elemental analyzer (EuroVector, Milan, Italy) for particulate organic carbon (POC) and particulate nitrogen (PN) in order to calculate their C/N atomic ratio (Cat/Nat). The analytical precision of the experimental procedure was estimated to be less than 2% DW for POC and 6% DW for PN. The gas resulting from the elemental analyses was introduced online into an isotope ratio mass spectrometer (IRMS) (GV IsoPrime, UK) to determine carbon and nitrogen isotopes. Stable isotopic data are expressed as the relative per mil (‰) differences between the samples and the conventional standards, Pee Dee Belemnite (PDB) for carbon and atmospheric N_2 for nitrogen, according to the following equation:

$$\delta(‰) = \left[\left(\frac{R_{sample}}{R_{standard}}\right) - 1\right] \times 1000$$

where δ is ^{13}C or ^{15}N abundance and R is the ^{13}C: ^{12}C or ^{15}N:^{14}N ratio. The internal standard was the USGS 40 of the International Atomic Energy Agency ($\delta^{13}C = -26.2$; $\delta^{15}N = -4.5$). The typical analytical precision was ±0.05‰ for carbon and ±0.19‰ for nitrogen. The Phillips and Gregg mixing model [43] was used to estimate spatio-temporal variations in the contribution of suspended organic matter (OMS), including particulate organic

Table 1. Variogram models with their parameter values and cross-validation results.

Spring sampling						
Variable	**Benthic Chl *a***	**Mud fraction**	**Macrofauna biomass**	**Pelagic Chl *a***	**SPiM**	**Salinity**
Kriging type	Ordinary	Ordinary	Ordinary	Universal	Universal	Ordinary
Detrending order	None	None	None	First	First	None
Transformation	Log	Log	Log	Log	Log	None
Variogram model	Spherical	Gaussian	Exponential	Circular	Circular	Gaussian
Anisotropy	True	True	False	False	True	True
Nugget	0.132	0.469	0.080	0.136	0.163	1.655
Sill	0.894	1.460	1.232	0.419	0.489	6.953
Range	3122.358	2937.798	968.969	1273.001	423.666	3078.753
R^2 (variogram)	0.991	0.987	0.881	0.925	0,732	0,857
Mean std.	0.016	0.000	−0.024	−0.025	−0.046	-0.005
RMSS	0.951	1.198	0.968	1.122	0.946	1.054
Summer sampling						
Variable	**Benthic Chl *a***	**Mud fraction**	**Macrofauna biomass**	**Pelagic Chl *a***	**SPiM**	**Salinity**
Kriging type	Ordinary	Ordinary	Ordinary	Ordinary	Ordinary	Ordinary
Detrending order	None	None	None	None	None	None
Transformation	Log	None	Log	Log	None	Log
Variogram model	Gaussian	Circular	Exponential	Circular	Exponential	Spherical
Anisotropy	False	True	False	False	False	False
Nugget	0.319	37.4	0.040	0.037	0.865	0.002
Sill	0.677	101	1.46	0.174	18.0	0.347
Range	2242	3456	1101	2675	2714	2568
R^2 (variogram)	0.841	0.730	0.924	0.965	0.847	0.934
Mean std.	−0.002	−0.017	−0.050	−0.023	0.001	−0.022
RMSS	1.06	1.067	1.178	1.068	1.172	0.943

Mean std = Mean standardized; RMSS = Root Mean Square standardized.
doi:10.1371/journal.pone.0044155.t001

matter (POM), MPB, resuspended POM (rPOM), and macroalgae (ULV), to the suspension-feeders' diets, following the protocol of Lefebvre et al. [7] but with fractionation values of 1.85‰ for $\delta^{13}C$ and 3.79‰ for $\delta^{15}N$, obtained from Dubois et al. [44].

Water samples. To measure the concentration of suspended particulate matter, two subsamples (1L) were sieved and passed through weighed and dried glass-fiber filters (Whatman GF-C), washed with distilled water to avoid errors due to salt, packed in petrislides (Millipore, USA), and immediately stored at −20°C until analyses. The filters were dried in an oven at 60°C for 72 hours. For Chl *a* concentration measurements, two subsamples were sieved and passed through a glass-fiber filter (Whatman GF-C), folded and placed in a tube at −20°C before analyses. The Chl *a* content was extracted in 90% acetone for 18 h at 4°C in the dark. After short centrifugation (3500 G), the chlorophyll extracts were measured on a Turner Designs TD 700 fluorimeter (USA) following the method of Welschmeyer [41] and expressed as chlorophyll content ($\mu g.L^{-1}$) in the spring samples. The summer samples were analyzed using Lorenzen's method [45] in order to examine the phaeopigment content. Calibration was performed between the two methods to compare the result of the two samplings ($y = 0.9624x+1.5399$, $R^2 = 0.999$). Each sample preserved in Lugol was observed for quantitative/qualitative determination of microalgae flora, following the Utermohl method described in [46] using light microscopy on Sedgewick-Rafter cells. In some samples, 400 individual cells were counted whatever the total number of cells, following the European standard for phytoplankton counting (NF EN 15204, 2006). Finally, a list of diatoms and the ratio of benthic to pelagic diatom species were established for each site following the protocol of Kasim and Mukaï [28]. Actually, the quantity of larger species is underestimated using abundances, while of the smaller species is underestimated using biomass [47]. To get round this problem, log-transformed abundance scores were used to calculate this ratio [48].

5. Statistical Analyses

Geostatistical analyses were performed with the ArcGIS extension Geostatistical Analyst (ESRI, USA) in order to map the different variables measured on the field. Since there was a high spatial dependency in all the variables measured, kriging was chosen as the best interpolation method to predict values for the whole intertidal area. Normal distribution was checked before each analysis and log-transformation was applied as a function of the variable concerned. Global trends were also examined, to enable removal of the possible effect of the tidal circulation on the water column. If necessary, detrending was applied using a polynomial algorithm of chosen order. Each variable was studied

to find the best semivariogram model fitting for data, between circular, spherical, exponential and gaussian models (Table 1). Cross-validation enabled us to check the validity of the semivariogram models we selected. Nugget effect was always small and never reached up to 1/3 of the sill value (Table1), confirming the validity of the sampling scale and chosen nested design scale. If the prediction errors are not biased, the mean prediction error should be near zero. However, this value depends on the scale of the data; to standardize these, the standardized prediction errors give the prediction errors divided by their prediction standard errors. The mean of these, called "mean standardized", should also be near zero. If the prediction standard errors are valid, the root mean squared standardized error should be close to 1. If it is greater than 1, the variability of the predictions has been underestimated, and inversely. The MARS-3D hydrodynamic model [49] was used to obtain the mean bottom current velocities at the two sampling periods. The results were plotted using the ArcgiS Toolbox "MGET" [50].

Multivariate analysis using the R package ADE4 (R-project) were used to better identify spatial and seasonal effects and explore the benthic-pelagic coupling through correlations between the variables. Principal Components Analyses (PCA) were performed on benthic and pelagic log-transformed datasets for both seasons, completed with estimated data from the kriging matrices for the few numbers of points where there were some missing values. For these analyses, bathymetry was considered as an auxiliary variable because it can play a role in both benthic and pelagic compartments. Co-inertia analysis was used to explore the relationships between the benthic and pelagic compartments by coupling the previous PCA, and its validity was checked by performing a Monte-Carlo test on the sum of eigenvalues of the analysis [51]. Frequency distribution of the RV values for 100 random co-inertia simulations was tested to check the validity of the co-inertia analyses.

Regression analyses were performed using Minitab (Minitab inc., USA) in order to find the best model predicting variable distribution. Stepwise regression was used to identify the best subsets of predictors in sampled variables. A linear regression was then applied on the most appropriate subset of data, corresponding to the best Awaike Information Criterion (AIC), meaning the lowest values when comparing the different regression models.

Results

Benthos

Data for each measured variable were analyzed using a PCA (Fig. 3). Only the two first components were kept, and these explained 93.7% of the total variation. The correlation circle (Fig. 3A) showed a clear relationship between the mud fraction, Chl *a* content and the bathymetry of the intertidal area. These three variables were well represented in the 1st axis and explained 61.4% of the total variation, confirming that the distribution patterns for both the mud fraction and the Chl *a* concentration remained stable between the two seasons. Mollusk biomass distribution was not correlated with the above variables; it was well represented on the 2nd axis and explained 32.3% of the total variance.

The scatter plot of individuals (Fig. 3B) showed a clear spatial structure, and sampling points were merged into three groups, corresponding to three areas of the bay: the eastern part located on the east side of the Isigny channel, and the northern and southern areas to the west (Fig. 4H). Individual distribution was explained by the correlation circle, with a Chl *a* concentration gradient from north to south, and an eastern area with a lower mollusk biomass.

Geostatistical analysis and kriged maps confirmed that benthic Chl *a* concentration (Fig. 4A, B) was characterized by the same distribution patterns at the two seasons, with higher concentration close to the salt meadow particularly at the southern borders of the bay, and also under the farming structures in the east. Less concentration was found in the central and northern part of the bay, resulting in a decreasing gradient from the coast to the center of the bay. Regarding to the three areas determined by the PCA, the southern and eastern areas were characterized by relatively high Chl *a* concentration compared to the northern area. The mud fraction (Fig. 4C, D) was correlated with the previous parameter with a gradient from the southern part of the bay with muddy to mixed sediment to sandy areas in the north and east. There was a slight increase in the mud fraction in two patches in the eastern part of the bay sampled during summer. The Chl *a* concentration and mud fraction were both clearly linked to the bathymetry of the bay (Fig. 4G), with the shallower parts located close to the salt meadow and along the eastern coast. Ordinary kriging was required for the Chl *a* concentration and mud fraction (Table 1), and the variogram structure was close considering the range (ca. 3000 m), reflecting a similar patch size for these two variables.

In contrast, there was a change in mollusk biomass between the two sampling periods (Fig. 4E,F). Five major species were identified at each season, with the cockle *Cerastoderma edule* as the dominant species (Table 2). Only one of the major species changed between the two seasons: *S. plana* was present in spring but replaced by *Abra tenuis* in late summer (Table 2). Mean mollusks biomass increased 20-fold between the two seasons (Table 2). Despite these differences, the distribution type of mollusks remained the same for the two seasons since the variogram structure was similar in terms of kriging method (Ordinary), in terms of variogram model (Exponential) and range values (ca. 1 km). Maximum biomass increased 3-fold between the two sampling dates, from 87.6 g.m^2 in spring to 216.3 g.m^2 in summer. The spring map shows the three-parted intertidal area, with a high mollusk biomass in the south, a lower biomass in the north and a very low biomass in the east. The summer map shows a larger high biomass area, and a contrast between the eastern part with low biomass and the northern and southern areas characterized by high biomass. Two high biomass patches were present in spring, and were still present but far bigger in summer. Very low mollusk biomass was found under the farming structures in the east at both sampling dates.

Regression analysis (Table 3) revealed that benthic Chl *a* concentration can be predicted by the whole set of benthic and pelagic variables in spring and mud fraction, bathymetry and water Chl *a* concentration in summer. For both seasons, mollusk biomass was best predicted by the association of chl *a* water and bathymetry, with a better model adjustment for spring ($R^2 = 0.48$).

Pelagos

A PCA was applied to the pelagic variables and only the two first components were retained, which explained 81.6% of the total variation. The correlation circle (Fig. 5A) shows that SPiM was anti-correlated with the bathymetry and was well represented on the 1st axis, where it explains 57.3% of the total variation. There was also a good correlation between the pelagic Chl *a* concentration and the concentration of SPiM, even if the former was partly represented on the 2nd axis. Salinity was not correlated with the pelagic Chl *a* concentration, and was represented to the same extent on both axes, but poorly anti-correlated with the concentration of SPiM. This low or null relationship between salinity and both pelagic Chl *a* concentration and SPiM

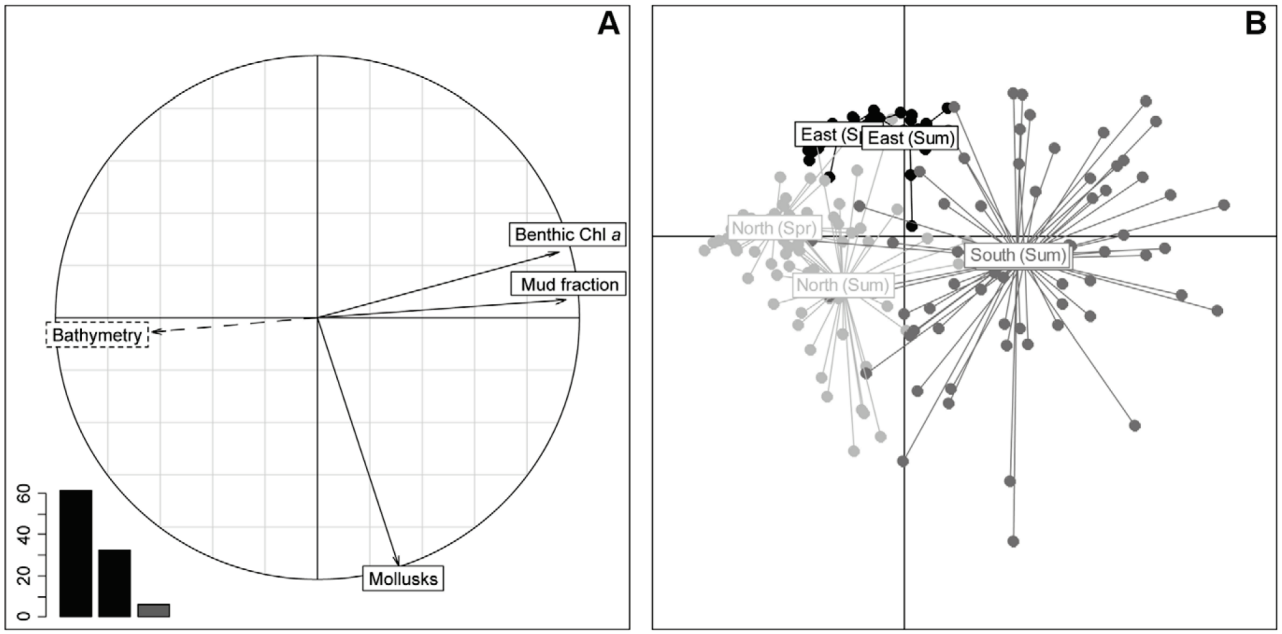

Figure 3. PCA results of the benthic log-transformed variables for the 2 seasons. Bathymetry (m), Chl *a* concentration (µg.g^{-1}), mud fraction (% of total sediment) and mollusk biomass (g AFDW.m^{-2}). Data used for the PCA resulted from the extraction of the corresponding kriged maps on the general sampling grid. Bathymetry was used as an auxiliary variable. A: Correlation circle; B: Scatter plot of individuals, "South (Spr)" and "South (Sum)" captions are confounded.
doi:10.1371/journal.pone.0044155.g003

concentration showed that these two variables were not entirely related to the river inlets.

In line with the results for benthos, the scatterplot of individuals (Fig. 5B) showed a clear spatial structure in the data: the sites were merged into three groups, corresponding to three spatial areas within the bay: eastern, northern and southern areas. The drift observed in the scatterplot of individuals between the two seasons was the same in all parts of the bay and appeared to be related to salinity. The southern area was characterized by the highest pelagic Chl *a* concentration while the eastern area had the lowest.

Kriged salinity maps (not shown) showed a common structure with a south to north gradient from low to high salinity. Salinity was twice lower in spring with stronger river inputs, particularly from the eastern channel. The southern part of the bay was characterized by high Chl *a* concentration and SPiM (Fig. 6), whereas the northern area showed lower concentrations. Both sampling periods were characterized by a depletion observed in the eastern area, which was stronger in spring. In late summer, Chl *a* concentration ranged from 2.78 to 18.8 µg.L^{-1}, and the area was smaller than that found in April (from 0.64 to 26.1 µg.L^{-1}). Like on the spring map, on the summer map, a large area at the north-east was characterized by a limited depletion of Chl *a* concentration in the water column. The quantity of SPiM was higher in the southern and north-western part of the bay than in the eastern part. Except in the area with the farming structures where SPiM was low, concentrations were related to the bathymetry of the bay, with lower concentrations in areas with deeper water. Mean currents at the bottom showed velocities of between 0.05 and 0.40 m.s^{-1}, with higher velocities along the two channels. The two sampling periods showed similar hydrodynamic conditions with a general field of current vectors oriented towards the north-north-west of the bay during this ebb tide causing the bay to empty. A small area with lower velocities was observed in the center of the bay.

Benthic-Pelagic Coupling

In order to examine the benthic-pelagic coupling at the bay scale, co-inertia analysis was performed on both benthic and pelagic variables. Correlation circles revealed the close link between the co-structure described by co-inertia axis F1/F2, and the structure of each dataset described by the respective components in each PCA. In fact, projected variances on axis F1/F2 of the co-inertia analysis were close to the values of maximum projected variances on the 1st and 2nd axis of the PCA (Table 4). Comparison between the co-inertia coefficient RV and its empirical distribution during the Monte-Carlo test showed a strong co-structure between the two tables (RV = 0.239). Next, the test procedure was run on the two seasons separately, to check for a seasonal impact on the co-structure between benthos and pelagos. Results were more significant in spring (RV = 0.500), even if the summer RV (RV = 0.110) remained good ($p<0.01$ for the 3 tests).

The cross-table resulting from the co-inertia (Fig. 7) confirmed the strong impact of the season on benthos-pelagos coupling. In spring, mollusks exhibited a negative correlation with salinity, and a positive correlation with SPiM and water Chl *a* concentration. The levels of correlations were much lower than in spring data. Spring benthic Chl *a* concentration showed a negative correlation with salinity, whereas it showed a positive correlation with SPiM in both seasons. The mud fraction was positively correlated with water Chl *a* concentration in spring, and negatively correlated with salinity at the same period. The same relationship was found in summer, but to a lesser degree. Finally, in both season, the mud fraction was negatively correlated with bathymetry and positively correlated with SPiM.

Diatom taxonomic analysis revealed a number of taxa originating from different environments - marine, brackish and benthic - and characterized by different shapes and sizes (Table 5). Even if the species composition was almost the same at the two

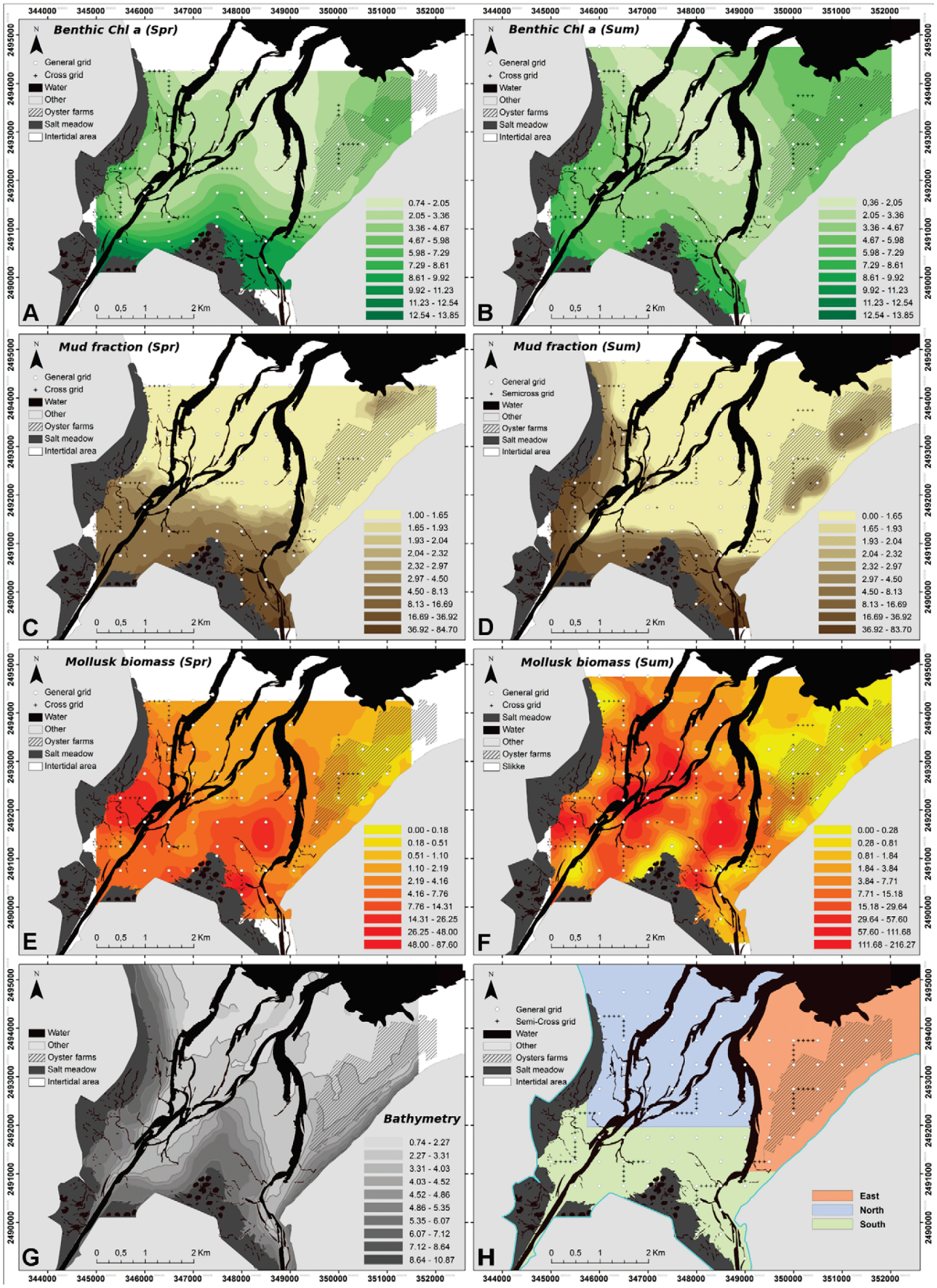
A
Benthic Chl a (Spr)
General grid
Cross grid
Water
Other
Oyster farms
Salt meadow
Intertidal area
0.74 - 2.05
2.05 - 3.36
3.36 - 4.67
4.67 - 5.98
5.98 - 7.29
7.29 - 8.61
8.61 - 9.92
9.92 - 11.23
11.23 - 12.54
12.54 - 13.85
B
Benthic Chl a (Sum)
0,36 - 2,05
C
Mud fraction (Spr)
1.00 - 1.65
1.65 - 1.93
1.93 - 2.04
2.04 - 2.32
2.32 - 2.97
2.97 - 4.50
4.50 - 8.13
8.13 - 16.69
16.69 - 36.92
36.92 - 84.70
D
Mud fraction (Sum)
Semicross grid
0.00 - 1.65
36.92 - 83.70
E
Mollusk biomass (Spr)
0.00 - 0.18
0.18 - 0.51
0.51 - 1.10
1.10 - 2.19
2.19 - 4.16
4.16 - 7.76
7.76 - 14.31
14.31 - 26.25
26.25 - 48.00
48.00 - 87.60
F
Mollusk biomass (Sum)
Slikke
0.00 - 0.28
0.28 - 0.81
0.81 - 1.84
1.84 - 3.84
3.84 - 7.71
7.71 - 15.18
15.18 - 29.64
29.64 - 57.60
57.60 - 111.68
111.68 - 216.27
G
Bathymetry
0.74 - 2.27
2.27 - 3.31
3.31 - 4.03
4.03 - 4.52
4.52 - 4.86
4.86 - 5.35
5.35 - 6.07
6.07 - 7.12
7.12 - 8.64
8.64 - 10.87
H
Semi-Cross grid
Oysters farms
East
North
South
0 0,5 1 2 Km
344000 345000 346000 347000 348000 349000 350000 351000 352000
2495000 2494000 2493000 2492000 2491000 2490000

Figure 4. BDV spring and summer kriged maps of benthic variables for the 2 seasons. All variables were kriged on different variogram models depending on the data (Table 1). Geometrical scales were used to maximize the visualization of both gradients and the patchiness of the different variables. Mollusk maps are at different scales to account for the discrepancy in the data between the 2 sampling campaigns. **A, B**: Chl *a* concentration ($\mu g.g^{-1}$); **C, D**: Mud fraction (%<63 μm of total sediment); **E, F**: Mollusks biomass (g AFDW $g.m^2$). **G**: Bathymetry of the BDV, from low to high tide spring tide levels (m). **H**: Representation of the 3 subdomains defined by the PCA.
doi:10.1371/journal.pone.0044155.g004

sampling periods, the relative proportions of the different species differed. The long-chain diatom *Asterionellopsis glacialis*, a brackish species observed at both sampling dates, was the dominant species in the Bay during the spring sampling (92.4%). The marine genus *Chaetoceros sp*. was dominant during the autumn sampling (73.4%) but was not identified in the spring samples. Benthic-pelagic ratios were calculated at several points distributed throughout the intertidal area, and represented on the Chl *a* concentration maps for both seasons (Fig. 5). At the first sampling date, the benthic-pelagic ratios were low throughout the Bay. However, benthic species reached 40% of the diatom community at two sampling points in the late summer sampling. Results showed that the benthic-pelagic ratios supported pelagic species over the entire map (Fig. 6), with percentages ranging between 60.2% and 100% in spring and between 59.6% and 100% except at two sites in summer. In fact, at these two sampling points, benthic diatoms species reached 47.0% and 47.2% of the diatom community. These two points corresponded to the area where the highest water Chl *a* concentration and SPiM were observed.

The benthic phaeopigment percentage map (Fig. 8) showed a higher concentration close to the channels, and a lower concentration under the farming structures and in the central area between the two channels. The water column phaeopigment map showed a negative relationship with the water column Chl *a* concentration map (Fig. 6, 8), whereas no relationship was observed with the benthic phaeopigments map. The two depletion areas previously seen for the pelagic Chl *a* concentration were the two areas with the maximum phaeopigment percentages, ranging from 21.50% to 30.39% of the total pigments.

Oysters sampled a month after each field campaign showed significant differences in isotopic signature (Fig. 9A). The $\delta_{13}C$ values ranged between −20 and −19‰, and $\delta_{15}N$ values between 9 and 10‰ in spring. These values increased in summer, ranging from −19 to −18‰ for $\delta_{13}C$ and from 9.5 to 11‰. After correction of the trophic step fractionation (Fig. 9B), these values were clearly distributed between particulate organic matter (POM) and MPB. There was an increased contribution of MPB to the oyster diets (paired t-test, P-value = 0.027), which increased from 18.0% in spring to 39.2% in summer on average (Fig. 9C). The spatial pattern of this contribution differed in the two seasons, with a decreasing south-to-north gradient in spring, whereas the maximum contribution was found at the OYST3 and OYST4 located the middle of the farming structures in summer (Fig. 9D). This area was found to be enriched in both mud and benthic Chl *a* concentration at the same season.

Discussion

MPB Spatial Distribution: Strong Effect of Mud Fraction and Bed Elevation

As shown in Orvain et al. [17] for this ecosystem, there was a clear relationship between MPB biomass and the grain-size of the sediment. Chl *a* concentration appeared to increase as a function of the mud fraction, in agreement to other studies ([52], [53]) which found higher Chl *a* content when expressed per mass unit. Moreover, both Chl *a* biomass and mud fraction were closely correlated with the bathymetry of the intertidal area, especially in area located on the west side of the Carentan channel. In fact, shallower water in areas with less hydrodynamic stress favored the silting up of these areas, and increased sunlight intensity, all of which favored MPB production [54]. Thus, in the present study, MPB biomass was well correlated to both mud fraction and bathymetry, as shown for other temperate estuarine ecosystems ([19], [55], [56]). In spite of the strong contrast between the two sampling periods in terms of temperature or light and nutrients availability, results revealed a perennial spatial structure of the intertidal sediments and MPB biomass in the bay (Fig. 4A, B, C, D) regarding to the stability of patterns between seasons at the year scale. The southern area close to the salt meadow was characterized by shallower waters, resulting in a muddy area because of the combination of direct river inputs and lower hydrodynamic conditions. Conversely, the northern part was under marine influence, with higher hydrodynamic conditions leading to sandy sediments. Finally, the eastern area appeared to be mainly influenced by the farming structures. The limited seasonal effect on the ranges of benthic Chl *a* concentration found in the BDV underlines the predominant effect of grain size and bathymetry on MPB distribution and biomass. As this bay is mostly made up of sandy sediments, these results correspond to those observed by van der Wal et al. [19], showing lower variability in sandy sediments than in muddy sediments. MPB distribution patterns were in close agreement with the results observed in April 2003 [17] even if the biomass levels were higher, certainly due to the much higher solar radiation observed during that exceptionally hot year.

Mollusk Spatial Distribution: Direct Linkage with Water Chl a Spatial Patterns

Distribution patterns of mollusk biomass, mainly represented by *Cerastoderma edule*, appeared to be related to the water Chl *a* concentration for the two seasons. Distribution of macrozoobenthos in response to microphytobenthos and sediment has been

Table 2. Mean weight and number of mollusks per m^2 in the 2 samplings.

Species	*C. edule*		*M. balthica*		*A. tenuis*		*H. ulvae*		*S. plana*	
Mean	ind.m^2	g. m^2	ind. m^2	g. m^2	ind. m^2	g. m^2	ind. m^2	g. m^2	ind. m^2	g. m^2
Spring	16.6	2.99	2.172	0.064			102	0.077	10.7	0.035
Summer	169	65.6	4.331	0.632	6.55	0.067	148	3.18		

doi:10.1371/journal.pone.0044155.t002

Table 3. Response of selected variables to log-transformed benthic and pelagic variables.

Variable	Linear predictor	R^2_{adj}	AIC
Benthic Chl a (SPR)	−2.60 −0.145 mollusks*** +0.546 mud fraction*** −0.513 bathymetry*** +0.319 SPiM* −0.235 chl *a* water** +2.26 salinity*	0.78	−211
Benthic Chl a (SUM)	0.943+0.325 mud fraction*** - 0.143 bathymetry* −0.346 chl *a* water***	0.76	−257
Mollusks (SPR)	0.339+0.725 chl *a* water*** −0.624 bathymetry***	0.48	−35.3
Mollusks (SUM)	−1.46+1.81 chl *a* water*** +0.826 bathymetry***	0.13	64.5

All variables included in linear predictor are significant (*p<0.05, **p<0.01, ***p<0.001). R^2 represents the percentage of response variable variation that is explained by its relationship with one or more predictor variables, adjusted for the number of predictors in the model. AIC (Akaike information criterion) is a measure of the relative goodness of fit of the models, best models (lower values) were kept.
doi:10.1371/journal.pone.0044155.t003

studied by van der Wal [57] at an intertidal area scale, finding good model predictors to describe surface and deep deposit-feeders biomass using benthic variables such as MPB biomass or median grain-size, but the model found for suspension feeders was less satisfying with no predictor terms of the model significant. Honkoop et al. [58] also found low relationship between abiotic factors and the distribution patterns of benthos, suggesting that they could be influenced or determined by biotic interactions which may be more important than the assumed abiotic structuring they measured.

Our results confirm their suggestions about including pelagic variables to improve comprehension and modeling of macrofauna abundance or biomass distribution. If benthic variables may explain biomass and/or distribution of deposit-feeders, both benthic and pelagic variables must be assessed to explain better suspension-feeders biomass and/or distribution, underlining the necessity of including food compartment associated with studied communities. As a consequence the reverse reasoning has to be considered too when studying Chl *a* concentration in the water column, with higher cockle densities leading to higher bioturbation and consequently higher MPB resuspension.

Benthic-pelagic Coupling: Impact of Resuspension Phenomenon

The same three part structure as for the benthic sampling was observed in the water column at two sampling seasons (Fig. 4G), showing on the one hand the fundamental influence of physical factors on benthic-pelagic coupling, and, on the other hand, its robustness over time in terms of both structure and resuspension phenomena. The pelagic structure is not perennial since water bodies are highly variable over time in terms of phytoplankton abundance and composition. As a consequence, the strong spatial structure of the benthic compartment influences the pelagic compartment through a domino effect controlled mainly by hydrodynamics and currents. Wind effect is well recognized as one of the first factor implicated in the temporal variation of resuspension phenomenon [4]. The results by de Jonge and van Beusekom focused on temporal dynamics in terms of resuspension

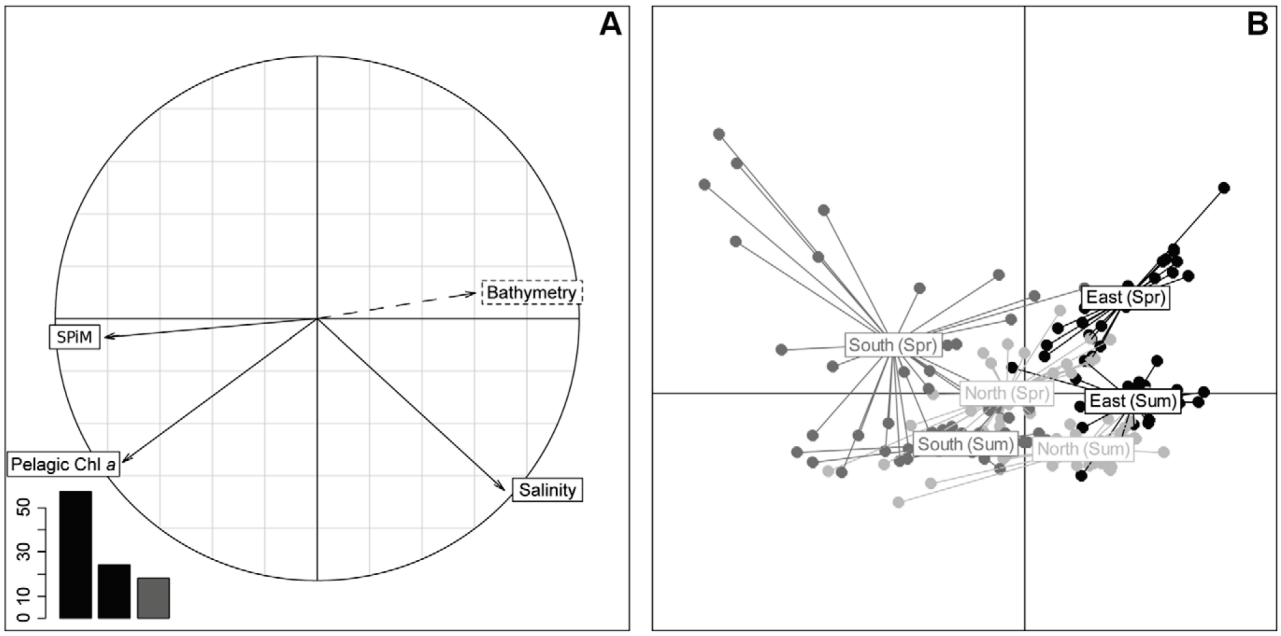

Figure 5. PCA results of the pelagic log-transformed variables for the 2 seasons. Bathymetry (m), Chl *a* concentration (µg.L^{-1}), SPIM (mg.L^{-1}) and salinity. Data used for the PCA resulted from the extraction of the corresponding kriged maps at the location of the general sampling grid. A: Correlation circle; B: Scatter plot of individuals (Spr = Spring; Sum = Summer).
doi:10.1371/journal.pone.0044155.g005

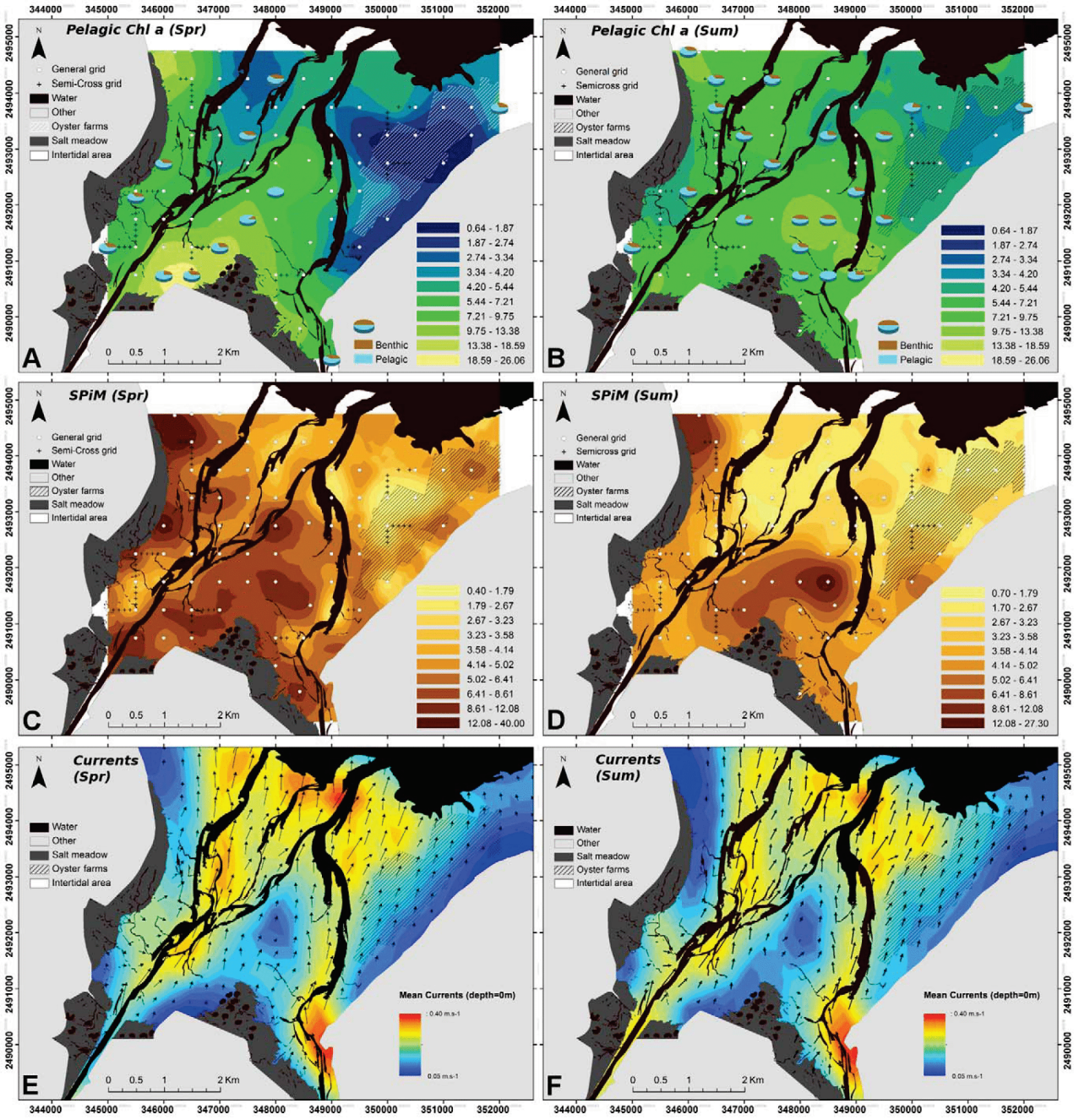

Figure 6. BDV spring and summer kriged maps of pelagic variables for the 2 seasons. All variables were kriged on different variogram models depending on the data (Table 1). Geometrical scales were used to maximize the visualization of both gradients and the patchiness of the different variables. Mollusk maps are at different scales to account for the discrepancy in the data between the 2 samplings. **A, B**: Chl *a* concentration ($\mu g.L^{-1}$); **C, D**: SPiM amount ($mg.L^{-1}$). **E, F**: Bottom mean current velocities and direction at the 2 sampling periods, calculated by the MARS-3D hydrodynamic model.
doi:10.1371/journal.pone.0044155.g006

phenomenon. By contrast, the present study was based on two samplings with similar hydrodynamic conditions but with a comprehensive number of stations to examine spatial patterns. Temporal detailed dynamics of the resuspension of microphytobenthos as well as wind effects were out of the scope of the present study which aims at describing spatial patterns of the benthic and pelagic variables without considering the wind. The results presented here and particularly the difference observed between the two samplings focus on other phenomena implicated in resuspension phenomenon. We must mention that contrary to more open estuarine ecosystems, BDV is relatively protected of wind effects by the geographical configuration of this basin, which is protected by southern and/or western dominant winds by the Cotentin Peninsula. Only northern (and especially north-eastern) winds can have an impact on the general functioning of this bay in terms of erosion.

Table 4. Comparison of inertia resulting from the separate analyses of each dataset.

Axis	InerBen	InerPel	InermaxBen	InermaxPel
F1	1.78	1.63	1.84	1.72
F2	1.02	0.738	0.967	0.731

Two co-inertia axes (F1 and F2) were selected. InerBen = inertia of the benthic table projected on co-inertia axes; InerPel = inertia of the pelagic table projected on co-inertia axes; InermaxBen = maximal projected inertia of the benthic table (1st and 2nd eigenvalue of the PCA); InermaxPel = maximum projected inertia of the pelagic table (1st and 2nd eigenvalue of the PCA).
doi:10.1371/journal.pone.0044155.t004

The pelagic Chl *a* concentration was closely correlated with the concentration of the SPiM, but the low or null relationship with salinity revealed the influence of resuspension events rather than river inputs. In fact, the two channels were characterized by low SPiM concentrations (Fig. 6E and F). Moreover, both Chl *a* concentration and SPiM concentration were inversely correlated with bed elevation (Fig. 5A), reinforcing the hypothesis of resuspension events from the muddier sediments with a higher impact in these shallow waters [59]. Similarly, good levels of correlation between SPiM and Chl a in the water column were obtained by Guarini et al. during large-scale [60] and long-term [48] samplings in another estuarine bay (Marennes-Oléron) where microphytobenthic communities are more developed than in BDV.

The significant co-structure found between the benthic and pelagic compartments confirms the hypothesis of a strong coupling, maintaining the 3-part structure in both compartments and at both seasons. The dominance of *Asterionelopsis glacialis* and *Chaetoceros spp.* during the respective sampling periods in this ecosystem has already been reported in the literature [61]. It reflects changes in the estuarine microalgae communities over the year, with dominance of brackish species in early spring and of marine species in late summer. However, resuspension phenomena appear to be relatively stable, given the range of the MPB ratios revealed by taxonomic identification. Only two locations showed a high MPB ratio during the late summer sampling, corresponding to a higher SPiM and an area of lower current velocities observed at the same period. According to the benthic:pelagic ratio of this patch and to microscopic observations, a part of this resuspended MPB is probably the result of inputs from the eastern channel. However, taxonomic analyses have to be interpreted with caution. The distinction between plankton and benthos is not perfectly clear because some microalgae are tychopelagic, i.e. they live in both environments [62]. Actually, in the surf zone (the zone extending from the outermost line of breakers to the limit of wave uprush) communities dominated by long chain diatoms like *Asterionellopsis glacialis* can be deposited on the sediment by the ebb tide, because mucus and particles attached to the cells increase their density, hence increasing sedimentation [63]. As a consequence, the number of living *A. glacialis* cells per sediment area behind the surf zone can be on average four orders of magnitude higher than the concentrations found in the respective water column [64].

The mollusk biomass was 20-fold higher in summer than in spring and macrofaunal activity is also known to increase between spring and summer because of the effects of temperature, so higher biological activity at the bay scale resulted in a higher phytoplankton consumption and subsequently in an increase in biodeposition. This high consumption rate was confirmed by

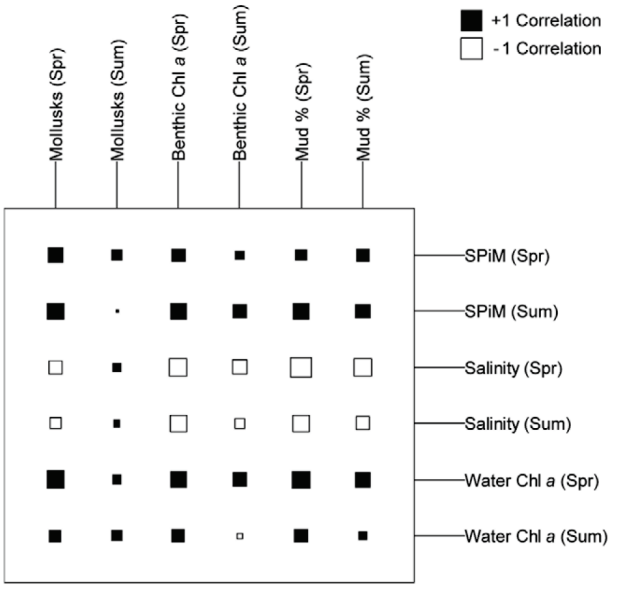

Figure 7. Cross-table resulting from the co-inertia analysis. Represents the correlation between the benthic and pelagic datasets.
doi:10.1371/journal.pone.0044155.g007

phaeopigments released in the water column (Fig. 8B). Finally, the isotopic signature of the diatom *Asterionellopsis glacialis* needs to be investigated since it could regulate its buoyancy in order to stay in the bay [65], since it belongs both to benthic and pelagic environment. Its presence, highest in spring, could help explain the good overlay of the benthic and pelagic maps.

In spring, resuspension phenomena were mainly under hydrodynamic influences resulting in an almost complete overlaying of benthic and pelagic compartment map, reflecting the close coupling between them. In summer, the increase in mollusk biomass increased the effects of bioturbation that could be involved in different chl *a* fluxes like consumption, biodeposition and bioresuspension processes. The role of bioturbators is well known as an important factor controlling microphytobenthos resuspension [13] [66]. Macrofauna activities and especially those of the cockle *Cerastoderma edule* must be better explored and evaluated because our results suggest that this is, when not considering wind effect, the prime factor controlling resuspension rates of microphytobenthos at the scale of the bay. This process must be thoroughly involved in the good relationship between suspension-feeder biomass and concentrations of resuspended chl *a*.

Impact of Cultivated Oysters in the Benthic-pelagic Coupling

The intertidal area is divided into two parts with respect to the Isigny channel, the two parts being clearly separated by the presence/absence of oysters farming structures. The spatial distribution of studied variables in the eastern part of the bay allows deciphering of the oyster impact on the benthic-pelagic coupling. Even if this area was characterized by sandy sediments with a very small mud fraction and a high depth, MPB biomass was high. Several explanations are possible and/or a combination of them.

First, microalgae communities can benefit from biological phenomena such as biodeposition under the farming structures, providing a favorable habitat for MPB assemblages [67]. Increased oyster filtration activity in late summer [68] led to

Table 5. List of determined microalgal taxa from Lugol fixed water samples.

Diatom species	Lifestyle	Shape	Size classes	Spring	Automn
Asterionellopsis glacialis	Tychopelagic	Pennate	Small ($<15.10^3$ µm^3.cell^{-1})	■	■
Chaetoceros spp.	Pelagic	Centric		□	■
Cyclotella spp.	Pelagic	Centric		■	■
Navicula spp.	Benthic	Pennate		■	■
Diploneis spp.	Benthic	Pennate	Medium (15.10^3 µm^3.cell^{-1}$<$ $x$$<150.10^3$ µm^3.cell^{-1})	■	□
Gyrosigma fasciola	Benthic	Pennate		■	■
Gyrosigma hippocampus	Benthic	Pennate		■	■
Nitzschia longissima	Benthic	Pennate		■	■
Pleurosigma spp.	Benthic	Pennate		■	■
Pseudo-nitzschia spp.	Benthic	Pennate		■	■
Paralia marina	Benthic	Centric		■	■
Thalassionema nitzschioides	Pelagic	Pennate		□	■
Thalassiosira rotula	Pelagic	Centric		■	■
Coscinodiscus wailesii	Pelagic	Centric	Large ($>150.10^3$ µm^3.cell^{-1})	■	■
Guinardia delicatula	Pelagic	Centric		■	■
Guinardia striata	Pelagic	Centric		■	■
Lauderia annulata	Pelagic	Centric		■	■
Odontella regia	Pelagic	Centric		■	■
Rhizosolenia imbricata	Pelagic	Centric		■	■

Each species is classified by living, shape, size class and presence/absence during the two samplings.
doi:10.1371/journal.pone.0044155.t005

a higher biodeposition, explaining two little patches with a higher mud fraction in the east in late summer (Fig. 4D) and the high phaeopigment percentages in the water column (Fig. 8B). Nevertheless, biodeposition was a local phenomenon which was mostly visible under the farming structures, and may be insufficient to significantly increase the mud fraction of the sediment at the scale of the eastern area. The two small patches could be explained by a combination of cultivated stocks, currents or bathymetry difference over farming structures [69]. Secondly, the high clearance rate of oysters significantly affected light availability by reducing water turbidity [18], thus enhancing MPB production.

Thirdly, the eastern area was characterized by very low concentrations of wild mollusks and biomass, in contrast to the western part of the bay. The exclusion of wild suspension-feeders under farming structures has already been observed at this site by Dubois et al. [70], showing that there was a shift in the trophic chain to high levels, with a predominance of predators, especially under farming structure. The primary consumption rate of MPB by grazers must therefore be low under the farming structures.

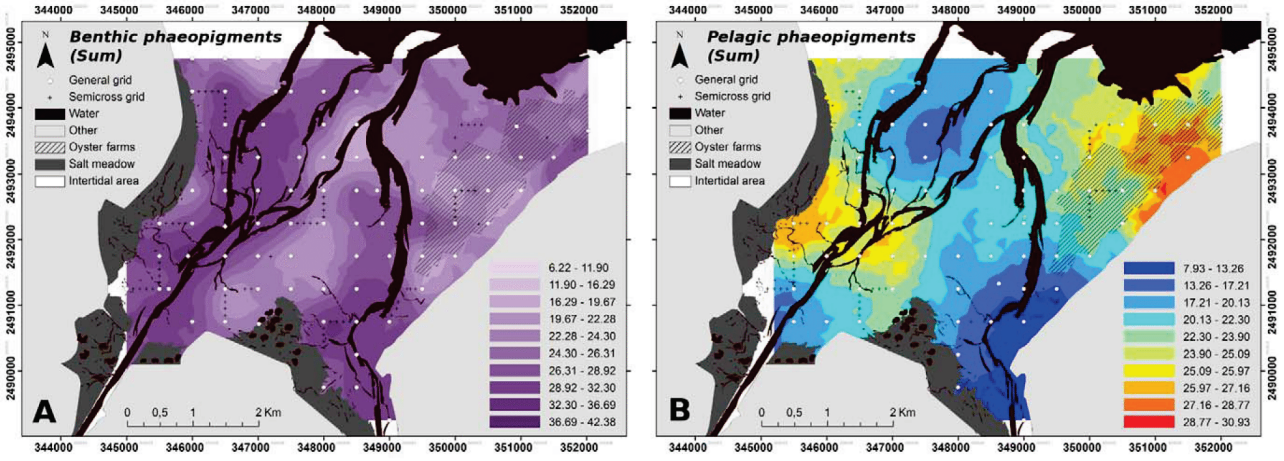

Figure 8. BDV summer kriged maps of both benthic (A) and pelagic (B) phaeopigments. Results are presented as % of total pigments.
doi:10.1371/journal.pone.0044155.g008

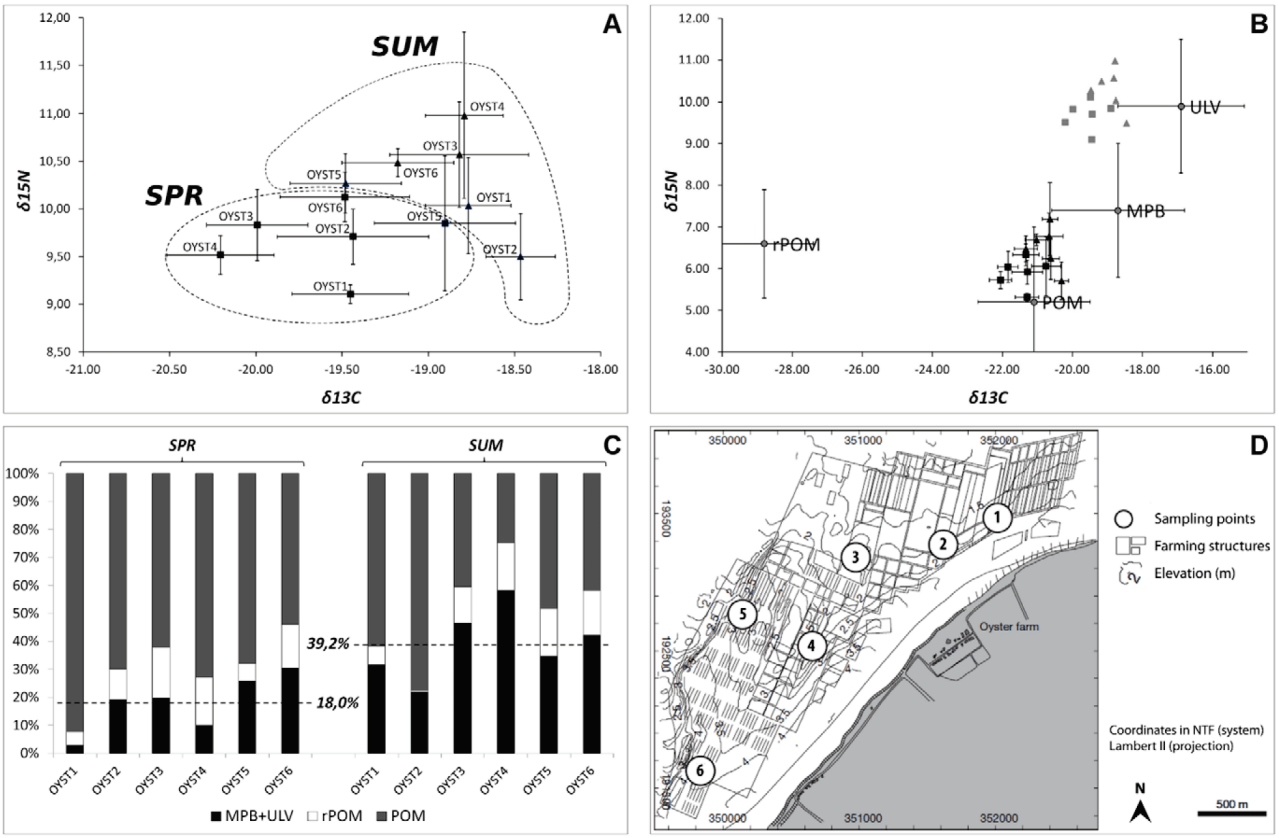

Figure 9. Temporal variations of δ13C and δ15N for *C. gigas* at 6 locations in the BDV. Isotopic signature (A), Isotopic signature before (gray) and after (black) fractionation (B), contribution of sources to oyster diets (C), location of oysters within the farming structures in the north-western part of the bay (D). Organic matter sources are plotted with standard deviations (see Lefebvre et al., 2009) to distinguish their relative contribution to the diets in the 2 sampling campaigns (B). Horizontal bars indicate the ±SD of the mean for n = 5.
doi:10.1371/journal.pone.0044155.g009

Finally, this part of the bay could be dominated by epipsammic species, explaining the contrast between the null or low mud fraction and the high Chl *a* concentration in both spring and summer. Sandy sediments have been reported to show more diverse assemblages than muddy sediments, including epipsammic diatoms, euglenids and cyanobacteria [71].

Porter et al. [25] found that a low degree of tidal resuspension is also responsible for a general shift from phytoplankton primary production to microphytobenthic primary production (by a cascade of effects where light and nutrient availabilities are also involved). Such effects must be implicated in the ecological functioning of this farming zone and this general shift must be still reinforced by the biodeposition fluxes due to oysters. Among the 4 hypotheses mentioned above for explaining the high concentrations of MPB biomass in this zone, none of them can be really excluded. A combination of all these processes must interfere in interactions with tidal hydrodynamics, and it appears very delicate to disentangle the relative contribution of each of these processes. The reduction in pelagic Chl *a* concentration observed above the farming structures highlighted the filtration efficiency of oysters, which was also confirmed by the percentage of water phaeopigment. The latter variable provides an argument in favour of the direct production of pseudofeces after consumption of microalgae and/or resuspension events of easily erodible sediments with high biodeposits under the farming structures [66]. However, the lack of match between benthic phaeopigments and both pelagic Chl *a* concentration and water phaeopigments suggests that it resulted mostly from the direct consumption of microalgae. These observations confirm the adequacy of the model proposed by Grangeré et al. [69], which represent ecosystem functioning with or without the presence of oysters, and revealed the prevailing effect of their top-down regulation in this area.

Since mollusk biomass was 20 times higher in summer than in spring, primary consumption would be expected to be higher in summer. However, the relative constancy of the MPB biomass levels between the two seasons suggests that the primary consumption is balanced by a higher primary production in summer. The eastern part of the bay was characterized by the absence of wild mollusks under farming structures, confirming the exclusion of suspension feeders already observed by Dubois et al. [70]. Suspension feeders may be disturbed by both biodeposition [72] and/or overconsumption of organic matter by the oysters. Thus, the lack of a correlation between the spatial patterns of MPB and macrofauna can be mainly attributed to the fact that most of the mollusk biomass was made up of suspension feeders and especially of *C. edule*, which widely dominated the mollusk assemblage, rather than deposit feeders that feed exclusively on MPB.

Impact of Resuspension for Higher Trophic Levels: Evidence for Allochtonous Feeding

Isotopic signatures showed that oysters consumed 2 times more MPB in summer than in spring, leading us to formulate three hypotheses: i) local feeding of autochtonous MPB directly associated with resuspended biodeposits under farming structures, ii) reduced phytoplankton abundance in late summer compared to spring, leading to a higher relative abundance of MPB in the potential food pool, iii) a higher resuspension at the bay scale and especially from the adjacent area in the south, that consequently supplies trophic resources to the cultivated oysters [73]. Regarding the limited differences between the two seasons in terms of benthic Chl *a* concentration, the first one can be ignored. Moreover, fluxes would not be expected to be very different since similar hydrodynamics and mollusk densities were found at both seasons under the farming structures, supporting the hypothesis of an allochtonous feeding of oysters. At 1 m depth Chl *a* concentration levels are similar in April and September, so that the second hypothesis seems unlikely. Taxonomic analyses revealed higher benthic-pelagic ratios for the 2 samplings in the adjacent area of the forming zone at the south/west, reinforcing the third hypothesis, which seems to be the most reliable one, when merging all data. A higher resuspension rate at the bay scale results from a change in the forcing variables, meaning one of the following compartments: hydrodynamics, sediment properties and/or macrofauna. Both samplings campaigns were conducted during spring tides with similar hydrodynamic conditions, and sediment properties revealed only slight differences between the two seasons. Higher resuspension could be explained by the huge increase in mollusk biomass between the two seasons. In fact, the cockles C*erastoderma edule* have been shown to increase resuspension phenomena via bioturbation [74]. Therefore, the better coupling between benthic and pelagic compartments in spring can probably be explained by a predominance of physical factors. The increase in mollusk biomass/activity in summer drastically altered the balance between benthic and pelagic Chl *a*, with an increased role for biological factors in resuspension phenomena.

Conclusion

To better assess resuspension phenomenon at an ecosystem scale, a special effort was made to study benthic and pelagic variables at the same time, to better unravel causes of resuspension between biotic and abiotic factors. This *in situ* study is the first to analyze benthic-pelagic coupling at a bay scale in terms of body masses advection and trophic routes. The spatial heterogeneity of this ecosystem enabled the predominant physical and/or biological processes to be highlighted as a function of the area and/or season. The perennial structure observed at the scale of the whole bay provides evidence for the significant involvement of resuspension phenomena at the bay scale. Although physical factors appeared to predominate during winter/spring, in summer, biological factors can significantly increase exchanges between benthic and pelagic compartments when not considering the wind. The use of a multicriteria approach (robust approach plus unusual indicators) to trophic/taxonomic indicators made it possible to strongly suggest a role for resuspension and benthic zonation in the spatial distribution of Chl *a* concentration in the water columns in two contrasting seasons and also that mollusks and particularly the cockle *Cerastoderma edule* play a role in microphytobenthic resuspension and its availability for oysters (*Crassostrea gigas*). When the biomass of these mollusks increases too much, this positive effect is masked by a high consumption rate leading to local depletion of Chl *a* concentration and SPiM. In fact, mollusk spatial distribution has a direct linkage with water Chl *a* concentration spatial patterns, which might have a structuring role on suspension-feeders. This highlights the fact that it is of critical importance to consider the connection between adjacent areas in terms of trophic relationships and microphytobenthos advection for farming structure management. These results underline the importance of taking biological phenomena into account in benthic-pelagic coupling to better evaluate the impact of resuspension for higher trophic levels.

Our study clearly suggests that there is not only a direct resuspension of microphytobenthos from the south of the bay but also an exportation from the water body of this habitat to another one at the north, then supplying food items to the cultivated oysters of the bay. Such trophic connections between adjacent habitat is of prime importance to consider because ecosystem models must consider these processes from the primary benthic production to the final consumption by suspension-feeders by including resuspension and advection in order to evaluate the real contribution of these areas as potential sink/sources of carbon [60].

Acknowledgments

We would particularly like to thank Jean-Paul Lehodey both for his help with innovative equipment during sampling and for his help in the field. We are grateful to Frédéric Guyon and Christophe Roger for their help in the field, and to Frank Maheux for his valuable help with organizing the water sampling. We thank Emmanuel Karakachian and Sébastien Lemaire for their help in the field and for their significant contribution to mollusk determination and grain-size analysis. We would also like to thank Pascal Claquin, Juliette Fauchot, Anne-Marie Russig, Isabelle Mussio, Clothilde Heudes, Olivier Desmur, Vincent Justome, Olivier Pierre-Duplessix, Emilie Rabiller, and Benjamin Simon as well as interns Olivier Goetz, Maxime Lafont for their help in the field. We are very grateful to Sandra Sritharan for her help with isotopic analysis, and to the GEOPHEN laboratory and especially to Laëtitia Birée for their help with grain-size analysis. We also thank METEOFRANCE for wind data. We would like to thank the two anonymous reviewers for their insightful and constructive comments.

Author Contributions

Conceived and designed the experiments: MU FO SL. Performed the experiments: MU FO AG KG. Analyzed the data: MU FO SL. Contributed reagents/materials/analysis tools: MU AG FO RL. Wrote the paper: MU.

References

1. Schelske CL, Odum EP (1962) Mechanisms maintaining high productivity in Georgia estuaries. Proc Gulf Caribb Fish Inst: 75–80.
2. Malet N, Sauriau P, Ryckaert M, Malestroit P, Guillou G (2008) Dynamics and sources of suspended particulate organic matter in the Marennes-Oléron oyster farming bay: Insights from stable isotopes and microalgae ecology. Estuar Coast Shelf Sci 78: 576–586.
3. Underwood G, Kromkamp J (1999) Primary production by phytoplankton and microphytobenthos in estuaries. Adv Ecol Res 29: 93–153.
4. De Jonge VN, Van Beusekom JEE (1995) Wind and tide induced resuspension of sediment and microphytobenthos in the Ems estuary. Limnol Oceanogr 40: 766–778.
5. Perissinotto R, Nozais C, Kibirige I, Anandraj A (2003) Planktonic food webs and benthic-pelagic coupling in three South African temporarily-open estuaries. Acta Oecol 24: 307–316.
6. Kang C, Lee Y, Choy E, Shin J, Seo I, et al. (2006) Microphytobenthos seasonality determines growth and reproduction in intertidal bivalves. Mar Ecol Prog Ser 315: 113–127.

7. Tolhurst TJ, Jesus B, Brotas V, Paterson DM (2003) Diatom migration and sediment armouring – an example from the Tagus Estuary, Portugal. Mar Ecol 503: 183–193.
8. Lucas CH, Widdows J, Brinsley MD, Salkeld PN, Herman PMJ (2000) Benthic-pelagic exchange of microalgae at a tidal flat: 1. Pigment analysis. Mar Ecol Prog Ser 196: 59–73.
9. Amos C, Feeney T, Sutherland T, Luternauer J (1997) The stability of fine-grained sediments from the Fraser River Delta. Estuar Coast Shelf Sci 45: 507–524.
10. Tolhurst TJ, Gust GM, Paterson D (2002) The influence of an extracellular polymeric substance (EPS) on cohesive sediment stability. Fine Sediment Dynamics in the Marine Environment. Elsevier, Vol. 5. 409–425.
11. Consalvey M, Jesus B, Perkins RG, Brotas V, Underwood GJC, et al. (2004) Monitoring Migration and Measuring Biomass in Benthic Biofilms: The Effects of Dark/far-red Adaptation and Vertical Migration on Fluorescence Measurements. Photosynth Res 81: 91–101.
12. Spears B, Saunders J, Davidson I, Paterson DM (2008) Microalgal sediment biostabilisation along a salinity gradient in the Eden Estuary, Scotland: unravelling a paradox. Mar Freshwater Res 59: 313–321.
13. Orvain F, Sauriau PG, Sygut A, Joassard L, Le Hir P (2004) Interacting effects of *Hydrobia ulvae* bioturbation and microphytobenthos on the erodibility of mudflat sediments. Mar Ecol Prog Ser 278: 205–223.
14. Austen I, Andersen TJ, Edelvang K (1999) The Influence of Benthic Diatoms and Invertebrates on the Erodibility of an Intertidal Mudflat, the Danish Wadden Sea. Estuar Coast Shelf Sci 49: 99–111.
15. Pillay D, Branch GM, Forbes AT (2007) Effects of *Callianassa kraussi* on microbial biofilms and recruitment of macrofauna : a novel hypothesis for adult – juvenile interactions. Mar Ecol Prog Ser 347: 1–14.
16. Koh CH, Khim JS, Araki H, Yamanishi H, Koga K (2007) Within-day and seasonal patterns of microphytobenthos biomass determined by co-measurement of sediment and water column chlorophylls in the intertidal mudflat of Nanaura, Saga, Ariake Sea, Japan. Estuar Coast Shelf Sci 72: 42–52.
17. Orvain F, Lefebvre S, Montepini J, Sébire M, Gangnery A, et al. (2012) Spatial and temporal interaction between sediment and microphytobenthos in a temperate estuarine macro-intertidal bay. Mar Ecol Prog Ser 458: 53–68.
18. Newell RIE, Cornwell JC, Owens MS (2002) Influence of simulated bivalve biodeposition and microphytobenthos on sediment nitrogen dynamics: A laboratory study. Limnol Oceanogr 47: 1367–1379.
19. van der Wal D, Wielemaker-van den Dool A, Herman PMJ (2010) Spatial Synchrony in Intertidal Benthic Algal Biomass in Temperate Coastal and Estuarine Ecosystems. Ecosystems 13: 338–351.
20. Serodio J, Coelho H, Vieira S, Cruz S (2006) Microphytobenthos vertical migratory photoresponse as characterised by light-response curves of surface biomass. Estuar Coast Shelf Sci 68: 547–556.
21. Colijn F, De Jonge V (1984) Primary production of microphytobenthos in the Ems-Dollard Estuary. Mar Ecol Prog Ser 14: 185–196.
22. Cibic T, Blasutto O, Falconi C, Fondaumani S (2007) Microphytobenthic biomass, species composition and nutrient availability in sublittoral sediments of the Gulf of Trieste (northern Adriatic Sea). Estuar Coast Shelf Sci 75: 50–62.
23. Blanchard GF, Guarini J-M, Orvain F, Sauriau P-G (2001) Dynamic behaviour of benthic microalgal biomass in intertidal mudflats. J Exp Mar Biol Ecol 264: 85–100.
24. Lucas C, Widdows J, Wall L (2003) Relating spatial and temporal variability in sediment chlorophyll a and carbohydrate distribution with erodibility of a tidal flat. Estuar Coast 26: 885–893.
25. Porter E, Mason R, Sanford L (2010) Effect of tidal resuspension on benthic–pelagic coupling in an experimental ecosystem study. Mar Ecol Prog Ser 413: 33–53.
26. Huot Y, Babin M, Bruyant F (2007) Does chlorophyll *a* provide the best index of phytoplankton biomass for primary productivity studies? Biogeosciences 4: 707–745.
27. de Jonge VD, van Beusekom JEE (1995) Wind-and tide-induced resuspension of sediment and microphytobenthos from tidal flats in the Ems estuary. Limnol Oceanogr 40: 766–778.
28. Kasim M, Mukai H (2006) Contribution of benthic and epiphytic diatoms to clam and oyster production in the Akkeshi-ko estuary. J Oceanogr 62: 267–281.
29. Dubois S, Orvain F, Marin-léal JC, Ropert M, Lefebvre S (2007) Small-scale spatial variability of food partitioning between cultivated oysters and associated suspension- feeding species, as revealed by stable isotopes. Mar Ecol Prog Ser 336: 151–160.
30. Lefebvre S, Marín Leal JC, Dubois S, Orvain F, Blin J-L, et al. (2009) Seasonal dynamics of trophic relationships among co-occurring suspension-feeders in two shellfish culture dominated ecosystems. Estuar Coast Shelf Sci 82: 415–425.
31. Choy EJ, Richard P, Kim K-R, Kang C-K (2009) Quantifying the trophic base for benthic secondary production in the Nakdong River estuary of Korea using stable C and N isotopes. J Exp Mar Biol Ecol 382: 18–26.
32. Carpenter SR, Elser MM, Elser JJ (1986) Chlorophyll production, degradation, and sedimentation: Implications for paleolimnology. Limnol Oceanogr 31: 112–124.
33. Spooner N, Harvey HR, Pearce GES, Eckardt CB, Maxwell JR (1994) Biological defunctionalisation of chlorophyll in the aquatic environment. II: Action of endogenous algal enzymes and aerobic bacteria. Org Geochem 22: 773–780.
34. Deroin J-P (2012) Combining ALOS and ERS-2 SAR data for the characterization of tidal flats. Case study from the Baie des Veys, Normandy, France. Int J Appl Earth Obs 18: 183–194.
35. Ettema CH, Wardle DA (2002) Spatial soil ecology. Trends Ecol Evol 17: 177–183.
36. Webster R, Welham SJ, Potts JM, Oliver MA (2006) Estimating the spatial scales of regionalized variables by nested sampling, hierarchical analysis of variance and residual maximum likelihood. Comput Geosci 32: 1320–1333.
37. Eleftheriou A, Holme NA (1984) Macrofauna techniques. N.A. Holme & A.D. McIntyre (Eds.), Methods for the study of marine benthos, Oxford, Blackwell Scientific. 140–216.
38. Underwood AJ, Chapman M (1996) Scales of spatial patterns of distribution of intertidal invertebrates. Oecologia 1996: 212–224.
39. Hammerstrom KK, Ranasinghe JA, Weisberg SB, Oliver JS, Fairey WR, et al. (2010) Effect of sample area and sieve size on benthic macrofaunal community condition assessments in California enclosed bays and estuaries. Integrated Environ Assess Manag: 1–10.
40. Hansen K, King GM, Kristensen E (1996) Impact of the soft-shell clam *Mya arenaria* on sulfate reduction in an intertidal sediment. Aquat Microb Ecol 10: 181–194.
41. Welschmeyer NA (1994) Fluorometric of chlorophyll a in the presence of analysis b and pheopigments chlorophyll. Limnol Oceanogr 39: 1985–1992.
42. Hayward PJ, Ryland JS (1990) The marine fauna of the British Isles and north West Wales. Clarendon Press, Oxford 1: 1–627.
43. Phillips DL, Gregg JW (2003) Source partitioning using stable isotopes: coping with too many sources. Oecologia 136: 261–269.
44. Dubois S, Jean-louis B, Bertrand B, Lefebvre S (2007) Isotope trophic-step fractionation of suspension-feeding species : Implications for food partitioning in coastal ecosystems. J Exp Mar Biol Ecol 351: 121–128.
45. Lorenzen CJ (1967) Determination of chlorophyll and phaeopigments: spectrophotometric equations. Limnol Oceanogr: 343–346.
46. Utermöhl von H (1931) Neue Wege in der quantitativen Erfassung des Planktons. (Mit besondere Beriicksichtigung des Ultraplanktons). Verh Int Verein Theor Angew Limnol 5: 567–595.
47. Snoeijs P, Busse S, Potapova M (2002) The importance of diatom cell size in community analysis. J Phycol 38: 265–281.
48. Guarini J-M, Gros P, Blanchard G, Richard P, Fillon A (2004) Benthic contribution to pelagic microalgal communities in two semi-enclosed, European-type littoral ecosystems (Marennes-Oléron Bay and Aiguillon Bay, France). J Sea Res 52: 241–258.
49. Lazure P, Dumas F (2008) An external–internal mode coupling for a 3D hydrodynamical model for applications at regional scale (MARS). Adv Water Resour 31: 233–250.
50. Roberts JJ, Best BD, Dunn DC, Treml EA, Halpin PN (2010) Environmental Modelling & Software Marine Geospatial Ecology Tools : An integrated framework for ecological geoprocessing with ArcGIS, Python, R, MATLAB, and C++. Environ Modell Softw 25: 1197–1207.
51. Dolédec S, Chessel D (1994) Co-inertia analysis: an alternative method for studying species-environment relationships. Freshwater Biol 31: 277–294.
52. Perkins R (2003) Changes in microphytobenthic chlorophyll a and EPS resulting from sediment compaction due to de-watering: opposing patterns in concentration and content. Cont Shelf Res 23: 575–586.
53. Cartaxana P, Mendes C, Vanleeuwe M, Brotas V (2006) Comparative study on microphytobenthic pigments of muddy and sandy intertidal sediments of the Tagus estuary. Estuar Coast Shelf Sci 66: 225–230.
54. Ní Longphuirt S, Clavier J, Grall J, Chauvaud L, Leloch F, et al. (2007) Primary production and spatial distribution of subtidal microphytobenthos in a temperate coastal system, the Bay of Brest, France. Estuar Coast Shelf Sci 74: 367–380.
55. Brotas V, Cabrita T, Portugal A, Serodio J, Catarino F (1995) Spatio-temporal distribution of the microphytobenthic biomass in intertidal flats of Tagus Estuary (Portugal). Hydrobiologia 300–301: 93–104.
56. Saburova M, Polikarpov I (1995) Spatial structure of an intertidal sandflat microphytobenthic community as related to different spatial scales. Mar Ecol Prog Ser 129: 229–239.
57. van der Wal D, Herman P, Forster R, Ysebaert T, Rossi F, et al. (2008) Distribution and dynamics of intertidal macrobenthos predicted from remote sensing: response to microphytobenthos and environment. Mar Ecol Prog Ser 367: 57–72.
58. Honkoop PJC, Pearson GB, Lavaleye MSS, Piersma T (2006) Spatial variation of the intertidal sediments and macrozoo-benthic assemblages along Eighty-mile Beach, North-western Australia. J Sea Res 55: 278–291.
59. Lund-Hansen LC, Petersson M, Nurjaya W (1999) Vertical sediment fluxes and wave-induced sediment resuspension in a shallow-water coastal lagoon. Estuaries 22: 39–46.
60. Guarini J-M, Sari N, Moritz C (2008) Modelling the dynamics of the microalgal biomass in semi-enclosed shallow-water ecosystems. Ecol Model 211: 267–278.
61. Pannard A, Bormans M, Lagadeuc Y (2008) Phytoplankton species turnover controlled by physical forcing at different time scales. Can J Fish Aquat Sci 65: 47–60.
62. Safi KA (2003) Microalgal populations of three New Zealand coastal locations: forcing functions and benthic-pelagic links. Mar Ecol Prog Ser 259: 67–78.
63. Odebrecht C, Abreu PC, Fugita C, Bergesch B (2003) The Impact of Mud Deposition on the Long Term Variability of the Surf-Zone Diatom *Asterionellopsis glacialis* (Castracane) Round at Cassino Beach, Brazil. J Coastal Res 35: 486–491.

64. Rörig LR, Garcia VMT (2003) Accumulations of the surf-zone diatom *Asterionellopsis glacialis* (CASTRACANE) ROUND in Cassino Beach, Southern Brazil, and its Relationship with Environmental Factors. J Coastal Res 35: 167–177.
65. Waite AM, Thompson PA, Harrisson PJ (1992) Does energy control the sinking rates of marine diatoms? Limnol Oceanogr 37: 468–477.
66. Orvain F, Sauriau PG, Bacher C, Prineau M (2006). The influence of sediment cohesiveness on bioturbation effects due to *Hydrobia ulvae* on the initial erosion of intertidal sediments: a study combining flume and model approaches. J Sea Res 55: 54–73.
67. Cognie B, Barille L (1998) Does bivalve mucus favour the growth of their main food source, microalgae? Oceanol Acta 22: 441–450.
68. Bougrier S, Geairon P, Deslous-Paoli J, Bacher C, Jonquières G (1995) Allometric relationships and effects of temperature on clearance and oxygen consumption rates of *Crassostrea gigas* (Thunberg). Aquaculture 134: 143–154.
69. Grangeré K, Lefebvre S, Bacher C, Cugier P, Ménesguen A (2010) Modelling the spatial heterogeneity of ecological processes in an intertidal estuarine bay: dynamic interactions between bivalves and phytoplankton. Mar Ecol Prog Ser 415: 141–158.
70. Dubois S, Marin-Léal JC, Ropert M, Lefebvre S (2007) Effects of oyster farming on macrofaunal assemblages associated with *Lanice conchilega* tubeworm populations : A trophic analysis using natural stable isotopes. Aquaculture 271: 336–349.
71. Underwood GJC, Barnett M (2006) What determines species composition in microphytobenthic biofilms? Functioning of microphytobenthos in estuaries. Kromkamp J, editor. Microphytobenthos symposium. Amsterdam, The Netherlands: Royal Netherlands Academy of Arts and Sciences. 121–138.
72. Callier MD, Richard M, McKindsey CW, Archambault P, Desrosiers G (2009) Responses of benthic macrofauna and biogeochemical fluxes to various levels of mussel biodeposition: an in situ "benthocosm" experiment. Mar Pollut Bull 58: 1544–1553.
73. Kon K, Hoshino Y, Kanou K, Okazaki D, Nakayama S, et al. (2012) Importance of allochthonous material in benthic macrofaunal community functioning in estuarine salt marshes. Estuar Coast Shelf Sci 96: 236–244.
74. Ciutat A, Widdows J, Readman JW (2006) Influence of cockle *Cerastoderma edule* bioturbation and tidal-current cycles on resuspension of sediment and polycyclic aromatic hydrocarbons. Mar Ecol Prog Ser 346: 114–126.

Chapitre IV

Influence des bivalves cultivés sur le couplage benthos-pelagos d'un système marin côtier

© Clarke little

«Les eaux ont beau couler dans tous les sens le sable restera toujours au fond »

Proverbe géorgien

Benthic-pelagic coupling of an open marine coastal system: Evidence for cultured bivalve top-down control

Martin Ubertini[1,2], Jean-Louis Blin[3], Sébastien Lefebvre[4], Gernez Pierre[5], Laurent Barillé[5], Olivier Basuyaux[3], Pascal Claquin[1,2], Aline Gangnery[6], Francis Orvain[1,2,7]

[1] *Université de Caen Basse-Normandie, FRE3484 BioMEA, Caen, France,*
[2] *CNRS INEE, FRE3484 BioMEA, Caen, France*
[3] *Syndicat Mixte pour l'Équipement du Littoral (SMEL), 50560 Blainville sur Mer, France*
[4] *Université de Lille1, UMR CNRS 8187 LOG ''Laboratoire d'Océanologie et Géosciences'', Station Marine de Wimereux, Wimereux, France*
[5] *LUNAM université, Université de Nantes, Mer Molécules Santé EA 2160, Faculté des Sciences et des Techniques, 2 rue de la Houssinière, 44322 Nantes cedex 3, France*
[6] *IFREMER, LERN, Port en Bessin, Franc*
[7] *CNRS, UMR 7208 BOREA, Muséum d'histoire naturelle, CRESCO, Dinard, France*

En préparation pour :

"**Marine Ecology Progress Series**"
IF = 2.711

Résumé

Les mollusques cultivés peuvent induire des modifications radicales à l'échelle des écosystèmes, en exerçant une forte influence sur la colonne d'eau à travers leur activité de filtration. Ainsi, les écosystèmes exploités pour la culture des bivalves sont souvent caractérisées par un appauvrissement du seston et par une biodéposition intense via les fèces et pseudofèces, l'approvisionnement de seston par la marée étant insuffisant pour le renouvellé. L'évaluation de l'impact sur la culture des bivalves sur le couplage benthique-pélagique a donc une importance primordiale pour quantifier la capacité de l'écosystème à s'autoréguler, et donc évaluer la capacité de charge des écosystèmes pour les bivalves suspensivores cultivés. Nous avons donc utilisé une approche multi-critères pour étudier les indices de couplage benthique-pélagique à différentes échelles spatiales et temporelles. Afin de mieux évaluer le rôle de la conchyliculture sur le fonctionnement des écosystèmes, les compartiments benthiques et pélagiques ont été étudiés simultanément au sein d'un écosystème tempéré macrotidal et exploité, « Lingreville sur mer » (LIN, France). Deux saisons contrastées en termes de variables de forçage et de biomasse phytoplanctonique ont été choisies. Toute la zone intertidale a été échantillonnée afin de tenir compte de l'hétérogénéité des différentes structures spatiales en termes de facteurs de forçage (présence / absence de la conchyliculture, composition des sédiments, distribution de la macrofaune, salinité, etc.). Des indices isotopiques ont été utilisées afin de déterminer dans quelle mesure les mollusques cultivés peuvent bénéficier des différentes sources pélagiques et benthiques de chl *a* disponibles. L'hypothèse d'une boucle de rétro-contrôle permettant de stimuler la croissance du microphytobenthos via les biodépôts, puis de profiter de ce dernier via la remise en suspension a été explorée. Les cultures de moules semblent dominer l'écosystème à travers le processus de biodéposition, conduisant à la facilitation trophique pour les déposivores de surface comme *Nassarius reticulatus* et l'exclusion compétitive des espèces sauvages filtreurs comme *Cerastoderma edule*. Le microphytobenthos ne semble pas être bien impliqués dans l'auto-régulation du système, du moins pendant les années sèches.

Abstract

Shellfish cultures can induce radical changes at an ecosystem scale, exerting a strong influence on the water column through their filtering activity. Thus, ecosystems exploited for the culture of bivalves are often characterized by a seston depletion and subsequent biodeposition of feces and pseudofeces, tidal supply being insufficient to replace it. The assessment of bivalve culture impact on benthic-pelagic coupling is of prime importance to quantify the capacity of shellfish cultured ecosystem to auto-regulate without exceed their carrying capacity, and thus evaluate the carrying capacity of ecosystems for bivalve suspension feeders. We thus used a multiple criteria approach to study the benthic-pelagic coupling indices. To better assess the role of mussel culture on the ecosystem functioning, benthic and pelagic compartments were studied simultaneously within a temperate macrotidal and exploited coastal ecosystem ''*Lingreville sur mer*" (LIN, France). Two contrasted seasons in terms of forcing variables and MPB and phytoplankton biomass were chosen. The whole intertidal area was sampled to account for the spatial heterogeneity within the intertidal area including different spatial patterns of forcing factors (presence/absence of shellfish farming, sediment composition, macrofauna distribution, bed shear stress, salinity). Isotopic indices were used to determine, to what extent cultivated mollusks can benefit from the different available pelagic and benthic chl *a* sources. The hypothesis of a feed-back regulation including microphytobenthos enhancement through biodeposition and inherent resuspension which could participate to the mussel diet was explored. Mussel cultures appeared to dominate the ecosystem through biodeposition process, leading to trophic facilitation for deposit-feeders such as *Nassarius reticulatus* and competitive exclusion of wild filter-feeders like *Cerastoderma edule*. Microphytobenthos did not appear to be strongly implicated in the self-organization of the system.

Introduction

The close coupling between benthic and pelagic compartments and the allochthonous influx of nutrients by rivers are responsible for the high productivity of coastal marine ecosystems (Cloern, 1987). These characteristics make them ideal for farming of suspension cultured bivalves, which directly benefit from the enhanced coastal primary production. Shellfish cultures can induce radical changes at an ecosystem scale. The food availability for the community in these ecosystems is strongly affected by the relative abundances of cultured bivalves (de Montaudouin et al., 1999; Riera et al., 2002; Grangeré et al., 2010). Dense cultivated bivalve populations may exert a strong influence on the water column by their filtering activity. By a modeling approach, Jiang and Gibbs (2005) showed that introduction of the large-scale bivalve culture could result in a decrease of the mean trophic level of the ecosystem, with bivalves replacing zooplankton as the major grazers in the modelled system. Ecosystems exploited for the culture of bivalves are often characterized by a seston depletion and subsequent biodeposition of feces and pseudofeces, tidal supply being insufficient to remove it (Grant et al., 2005). As a consequence, food depletion leads to interspecific and/or intraspecific competition for food (Franke and Janke, 1998; Decottignies et al., 2007). However, bivalves can also stimulate growth of particular functional groups by feedback mechanisms in terms of nutrient recycling (Newell, 2004). The changes can have positive effects by increasing nutrient availability for primary production (Prins et al., 1994) or negative effects by altering ecosystem structure through a reduction of its carrying capacity (Decottignies et al., 2007; Guyondet et al., 2010). Introduced bivalves in shellfish cultures can also lead to facilitation processes through biodeposition . In fact, mollusk biodeposition can significantly affect grain-size distribution (Ysebaert et al., 2009), and the latter is an indicator of both hydrodynamic transport and sedimentation which influence benthic fauna distribution (Grebmeier et al., 2006).

If the influence of mussel culture on low energy soft-bottom benthic environments have been well studied (McKindsey et al., 2011), its influence in high energy intertidal systems did not receive the same interest (Grant et al., 2012). Open marine coastal systems are subject to higher hydrodynamics, with shorter residence times. Allochthonous supplies depend on each site configuration, but in absence of major rivers inlets these systems are less productive than estuaries. Moreover, ecosystems characterized by fine sediments such as estuaries often benefit from microphytobenthos (MPB) resuspension which significantly contributes to cultivated bivalves diets (Underwood and Kromkamp, 1999; Ubertini et al., 2012). On the contrary, sandy sediments are known to be colonized by epipsammic species, which stick at the sand grains to prevent them for being resuspended far away in those unstable environments (De Jonge, 1985). As a consequence,

estuarine cultivated bivalves can benefit from autochtonous MPB resuspension (Kang et al., 2006; Ubertini et al., 2012), whereas open coastal ecosystem cultivated bivalves should mostly rely on phytoplankton and allochtonous organic matter support (Grangeré et al., 2012). The limited food support may lead to competition for food between wild and cultivated suspension-feeders in these ecosystems, while biodeposition process may lead to facilitation processes for deposit feeders. However, if sandy sediments are generally characterized by a lower Chl *a* concentration than muddy sediments, the greater depth of sediment erosion during bedload transport exposes more Chl *a* to the surface (Lucas et al., 2000). Moreover, the turnover of nutrients in non-cohesive sediments has been found to be faster than for cohesive sediments (Peninsula et al., 1995). Shellfish farming introduction changes interactions between benthic and pelagic compartments, leading to a number of positive and negative feedbacks (Prins et al., 1998). High amount of cultivated suspensive suspension-feeders in cultivated shellfish ecosystems increases the biodeposition process fluxes enhancing MPB biomass by enriching the sediment with nutrients, and leading to a potential shift from episammic to epipelic communities with a cascade effect on the shift of macrofaunal communities (Dubois et al., 2007; Ubertini et al., 2012). Biodeposition leads to increase the fine fraction of the sediment, making possible the installation of epipelic species under farming structures. The fresh biodeposits are easily erodible, allowing autochtonous organic matter to fuel cultivated bivalve growth.

As a consequence, there is still a paradox to elucidate in cultivated open ecosystems. In an estuarine bay with limited tidal flow, Widdows et al. (2009) stressed a direct effect of self-organized mussel beds, leading to enhance microphytobenthos resuspension that can supply food for mussel growth, and serves to offset the phytoplankton depletion. Thus, in open ecosystems with higher degrees of tidal flow, these effects should occur to a higher extent, in order to supply MPB food items to mussels each year. On the other hand, a recent study (Grangeré et al., 2012) stressed that the contribution of MPB to bivalve diet is limited to wet years in this ecosystem (and all along the Western coast of Cotentin peninsula). If MPB resuspension from biodeposits does not contribute to bivalve diet whatever the humidity is, biodeposits should strongly impact benthic MPB and macrofaune spatial structure. By sampling both benthic and pelagic components of this ecosystem and examine examining their spatial structure, this study attempted to clarify the impact of mussels on the ecosystem, and the possibility of a feed-back enhancing both MPB biomass, and deposit-feeders biomass and thus MPB resuspension.

The assessment of bivalve culture impact on benthic-pelagic coupling is of prime importance to quantify the capacity of shellfish cultured ecosystem to auto-regulate without exceed their

carrying capacity, and thus evaluate the carrying capacity of ecosystems for bivalve suspension feeders (Prins et al., 1998). For an appropriate estimation of carrying capacity, all sources of primary production must be considered, i.e. planktonic as well as benthic. We thus sampled with the same effort benthic and pelagic compartments, which were studied simultaneously within a temperate macrotidal and exploited coastal ecosystem ''*Lingreville sur mer*" (LIN, France). Two seasons (winter vs. summer) with contrasted forcing variables, MPB and phytoplankton biomass were analyzed. The whole intertidal area was sampled to account for the spatial heterogeneity within the intertidal area including different spatial patterns of forcing factors (presence/absence of shellfish farming, sediment composition, macrofauna distribution, bed shear stress, salinity). As for a previously studied estuarine ecosystem (Ubertini et al., 2012), we used a multiple criteria approach and we combined the spatial patterns of benthic/pelagic coupling to isotopic indices of bivalve diets.

Materials and methods

1. Study area

Lingreville sur mer (LIN, Fig. 1) is a macrotidal coastal system located in the western coast of the Cotentin peninsula in the English Channel. This area faces the haven of Vanlée, an area of 300 ha of which 60% is occupied by salt marsh. The tidal amplitude of *Lingreville* is up to 13 m during spring tides, and is about 5m during neap tides. The area is exposed to the prevailing winds from the west and north-west (NAO^- year). Because of its opening to the sea, the bay is strongly influenced by ocean currents. Terrigenous inputs come from two rivers: *La Sienne*, located further north of the area, with a flow rate ranging from 2.2 to 24.3 $m^3.s^{-1}$ for a watershed of 759 km^2, and *La Vanlée*, characterized by a lower flow and whose watershed occupies 60 km^2. The sediment consists mainly of sand and coarse shell sand (Lefebvre et al., 2009).

2. Sampling strategy

Both benthic and pelagic variables were sampled during spring tides to better assess the contribution of resuspended MPB to the total Chl *a* content in the water column (de Jonge et van Beusekom, 1995) and the trophic interactions between macrofaunal communities. Samples were collected in spring within a week, benthic samples between the 1st March and the 3rd April, 2010, and water samples between the 4th March and the 5th March, 2010. The same strategy was applied in autumn, to assess the impact of the increased number and activity of benthic mollusks on the resuspension phenomenon. Benthic samples were collected from October 10 to 12, 2010, and water samples on the 13 and 14 of October.

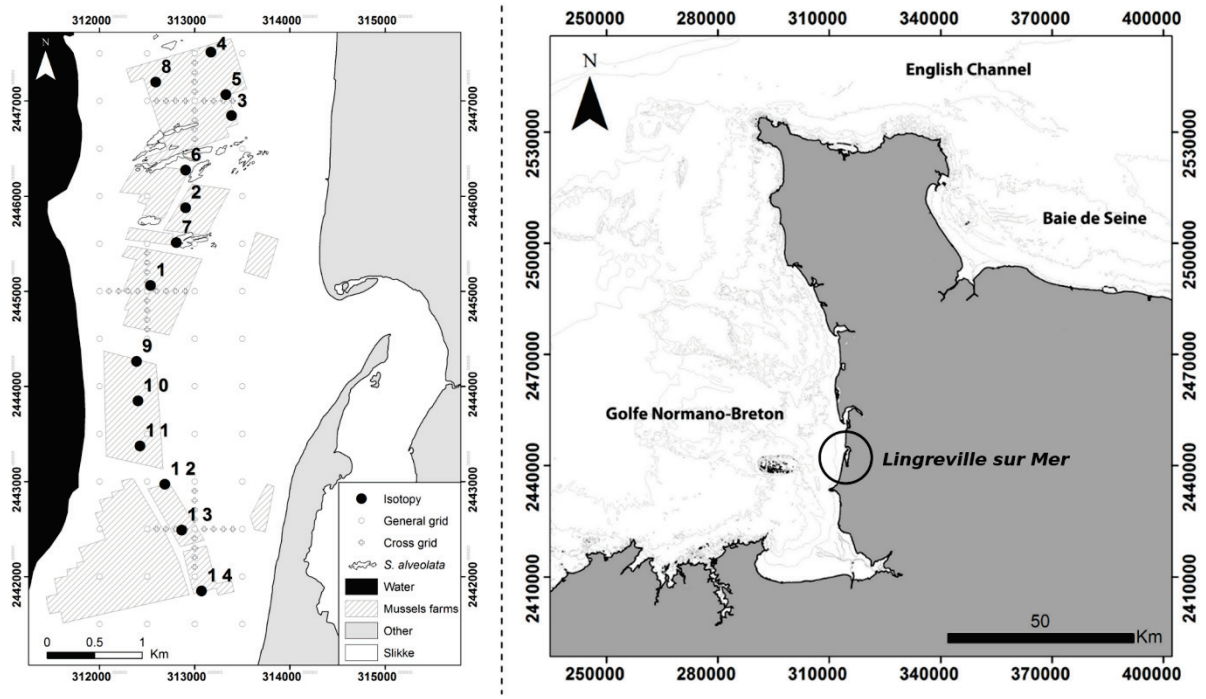

Figure 1: Location of the Lingreville ecosystem coastal system and sampling grid.

Two sampling periods were chosen, with tidal amplitude of 12 m during spring tidal cycles. Because farming structures are located all over the studied area, they may benefit from both phytoplankton primary production and allochtonous resources through microphytobenthos resuspension coming from *La Vanlée*. As a consequence, water was sampled during ebb tides, to account for the flux of MPB from *La Vanlée*, potentially feeding the suspension-feeders reared in the bay A systematic grid of 52 points was extended over the entire map of the intertidal area with a sampling interval of 500 m (Fig. 1). Heterogeneity in sediment organic matter distribution occurs at nested scales, and is shaped by a spatial hierarchy of environmental factors, intrinsic population processes and disturbances (Ettema and Wardle, 2002). To explore smaller scale distributions, a nested sampling design was applied (Webster et al., 2006),(Orvain et al., 2012). A semi-cross sampling design was applied with an interval of 100 m between each point (Fig. 1). Each semi-cross was placed on high gradient areas previously observed on the field as suggested by Orvain et al. (2012) in another coastal area.

3. Field measurements

Sediment and benthos sampling. At low tide, four 20 cm diameter cores were collected at each sampling site. This sampled surface is above the minimum surface that must be sampled to properly estimate MPB standing stocks in the first cm (Spilmont et al., 2011). The first cm of each core was removed and placed in a separate plastic bag. At each site, macrofauna were harvested within a square of 0.25 m^2. The choice of a surface of 0.25 m^2 is appropriate when referring to several studies carried out on the benthos in the intertidal zone showing that this surface is sufficiently large and well suited for estimating the abundance of mollusks (Eleftheriou, A., Holme, 1984). This surface allows a suitable and satisfactory sampling of the fauna whatever its distribution (contagious, regular, or random), even when populations are small in number (Underwood and Chapman, 1996).The entire sediment was sampled to a depth of 10 cm by hand, and then sieved directly in the field using a 4 mm mesh size sieve. This size was chosen because of the coarse sediment of the area. The depth of 10 cm was chosen in order to take into account most of the mollusk biomass potentially involved in resuspension phenomenon. Sieved samples were placed in plastic bags for transport waiting further sample analyses at a small distance from the sampled site.

Animal sampling for isotopy. Fourteen sampling sites were selected within the farming structures to assess the spatial variability of the suspension-feeder *Mytilus edulis* diet by sampling the widest extent of the structures (Fig. 1). At each sampling site, six mussels were sampled in April one month after the sampling, in order to investigate their diets by stable isotopic ratios of carbon and nitrogen.

Water column sampling. Surveys were carried out during ebb tide at all grid points, from one hour after high tide to one hour before low tide. At each point, 5 L water samples were collected by pumping water at a height of 1m above the seafloor, to ensure access to resuspended MPB. Water samples were immediately placed in the dark and then brought back for laboratory measurements. March sampling has been done between the 2 blooms observed between March and April at 8°C water temperature, and October sampling during the fall bloom (Fig. 2). A multispectral SPOT image was acquired during the field measurement campaign on October 11th at 11:20 UTC. It was processed for amospheric correction with the FLAASH method (Fast Line of sight Atmospheric Analysis of Spectral Hypercubes), available in ENVI® software and using MODTRAN4 transfer codes, to calculate the reflectance at the sea and obtain a qualitative estimation of the turbidity spatial distribution.

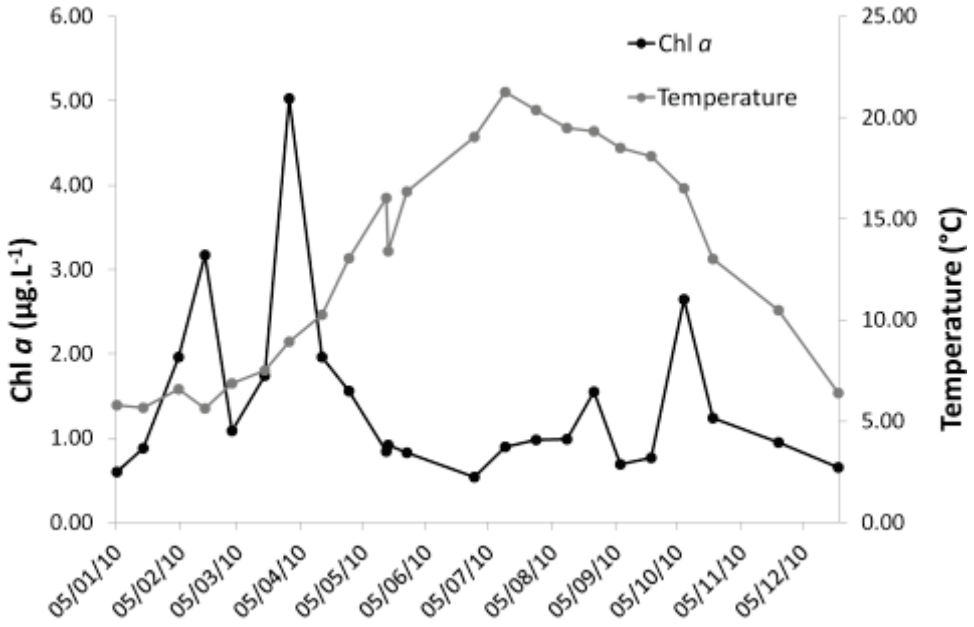

Figure 2: Temporal variations of chlorophyll *a* (Chl *a*) concentration and temperature. Data were measured at the Lingreville station twice a month (Hydrobiological monitoring HYDRONOR, SMEL, *Lingreville* station).

4. Laboratory analyses

Sediment samples. Back at the laboratory, sediment samples were immediately pooled and mixed thoroughly, and a 5ml subsample was removed and stored at -20°C in the dark until Chl *a* analyses. The remaining sediment was also stored at -20°C until grain-size measurements. Each subsample of sediment was freeze-dried and then weighed to determine the sediment water content. Chl *a* was measured on freeze-dried subsamples using afluorometric method to estimate algal biomass (µg.g^{-1} sediment). The Chl *a* content of the sediment was extracted in 90% acetone at 4°C for 18 h in the dark. The chlorophyll extracts were measured after centrifugation on a Turner Designs TD 700 fluorimeter (USA) following the method of Welschmeyer (Welschmeyer, 1994). One replicate of sediment sample was selected for the analyses of sediment grain-size distribution. First, a wet sieve analysis was performed to collect the finest fraction. The sediment sample was gently mixed in freshwater, which was agitated with a brush to remove the salt and break the aggregates. Particles were sieved through a 40 µm mesh to retain the coarse fraction. The particles remaining on each sieve were collected and weighed on scales to the nearest mg. After multiplying by 1.3 (to convert from a grain-size of particles sieved on a squared mesh into an equivalent spherical grain-size), the weights were recorded. Mud fraction was calculated from the sediment mass cumulative percentage.

Macrofauna samples. Samples were fixed in a 10% formaldehyde solution for 24h and transferred to 70% ethanol for storage until further analyses. All samples were carefully sorted to separate organisms and the remaining sediment. The mollusk species were then determined (Hayward and Ryland, 1990). Mollusk flesh was separated from the shell, dried at 60 °C for 3 days and weighed without the shell. Small specimens with a tough shell (e.g. *Peringia ulvae*) were treated with a drop of 33% hydrochloric acid solution for a few minutes to dissolve the shell. The organisms were then dried in an oven at 450 °C for 4 hours to obtain the ash free dry weight. The bioreef study was conducted between 2009 and 2011 on the west facade of the department *La Manche* by Olivier Basuyeaux (SMEL). The observations were made in situ from aerial view. GPS mapping provided surface sizes with an accuracy of 0.5 m. For each surface, the height was measured (10 by 10 cm), and the recovery rate was evaluated by direct observation. The area of spots observed is calculated as the area "covered" which takes into account the coverage of the surface observed.

Freeze–dried, powdered, and homogenized mussel samples were analyzed using a CHN elemental analyzer (EuroVector, Milan, Italy) for particulate organic carbon (POC) and particulate nitrogen (PN) in order to calculate their C/N atomic ratio (Cat/Nat). The analytical precision of the experimental procedure was estimated to be less than 2% DW for POC and 6% DW for PN. The gas resulting from the elemental analyses was introduced online into an isotope ratio mass spectrometer (IRMS) (GV IsoPrime, UK) to determine carbon and nitrogen isotopes. Stable isotopic data are expressed as the relative per mil (‰) differences between the samples and the conventional standards, Pee Dee Belemnite (PDB) for carbon and atmospheric N_2 for nitrogen, according to the following equation:

$$\delta(‰) = \left[\left(\frac{R_{sample}}{R_{standard}} \right) - 1 \right] \times 1000$$

where δ is ^{13}C or ^{15}N abundance and R is the ^{13}C: ^{12}C or ^{15}N:^{14}N ratio. The internal standard was the USGS 40 of the International Atomic Energy Agency ($\delta^{13}C$ = -26.2; $\delta^{15}N$ = -4.5). The typical analytical precision was ±0.05‰ for carbon and ±0.19‰ for nitrogen. The Phillips and Gregg mixing model (Phillips and Gregg, 2003) was used to estimate spatio-temporal variations in the contribution of suspended organic matter (OMS), including particulate organic matter (POM), MPB, resuspended POM (rPOM), and macroalgae (ULV), to the mussel diets, following the protocol of (Lefebvre et al., 2009) but with fractionation values of 1.85‰ for $\delta^{13}C$ and 3.79‰ for $\delta^{15}N$, obtained from Dubois et al. (Dubois, Jean-louis, et al., 2007).

Water samples. To measure the concentration of Suspended Particulate Matter (SPM), two subsamples (1L) were sieved and passed through weighed and burned glass-fiber filters (Whatman GF-C), rinsed with distilled water, packed in petri slides (Millipore, USA), and immediately stored at -20 °C until analyses. The filters were dried in an oven at 60 °C for 72 hours. For Chl *a* concentration measurements, two subsamples were filtered through a glass-fiber filter (Whatman GF-C), folded and placed in a tube at -20°C before analyses. The Chl *a* content was extracted in 90% acetone for 18 h at 4 °C in the dark. After short centrifugation (3500 g), the chlorophyll extracts were measured on a Turner Designs TD 700 fluorimeter (USA) following the method of Welschmeyer (Welschmeyer, 1994) and expressed as chlorophyll concentration ($\mu g.L^{-1}$) in the spring samples. The summer samples were analyzed using Lorenzen's method (Lorenzen, 1967) in order to obtain the phaeopigment content. Calibration was performed between the two methods to compare the result of the two samplings ($y = 0.9624x + 1.5399$, $R^2 = 0.99$).

5. Statistical analyses

Geostatistical analyses were performed with the ArcGIS extension Geostatistical Analyst (ESRI, USA) in order to map the different variables measured on the field. Since there was a high spatial dependency in all the variables measured, kriging was chosen as the best interpolation method to predict values for the whole intertidal area. Normal distribution was checked before each analysis and log-transformation was applied as a function of the variable concerned. Global trends were also examined, to enable removal of the possible effect of the tidal circulation on the water column. If necessary, detrending was applied using a polynomial algorithm of chosen order (Orvain et al., 2012). Each variable was studied to find the best semi-variogram model fitting for data, between circular, spherical, exponential and gaussian models (Table 1). Cross-validation enabled us to check the validity of the semi-variogram models we selected. If the prediction errors are not biased, the mean prediction error should be near zero. However, this value depends on the scale of the data; to standardize these, the standardized prediction errors give the prediction errors divided by their prediction standard errors. The mean of these, called "mean standardized", should also be near zero. If the prediction standard errors are valid, the root mean squared standardized error should be close to 1. If it is greater than 1, the variability of the predictions has been underestimated, and inversely.

Multivariate analysis using the R package ADE4 (R-project) were used to better identify spatial and seasonal effects and explore the benthic-pelagic coupling through correlations between the variables. Principal Components Analyses (PCA) were performed on benthic and pelagic log-transformed datasets for both seasons, completed with estimated data from the kriging matrices for the few numbers of points where there were some missing values. For these analyses, bathymetry

was considered as an auxiliary variable because it can play a role in both benthic and pelagic compartments.

Table 1: Variogram models with their parameter values and cross-validation results.

March sampling					
Variable	**Benthic Chl *a***	**Median grain-size**	**Mollusk biomass**	**Pelagic Chl *a***	**SPM**
Kriging type	Ordinary	Ordinary	Ordinary	Ordinary	Ordinary
Detrending order	None	None	None	None	None
Transformation	Log	None	Log	None	Log
Variogram model	Spherical	Spherical	Spherical	Spherical	Spherical
Anisotropy	False	False	False	False	False
Nugget	0.151	0.000	0.004	0.014	0.080
Sill	0.395	2.001	0.005	0.077	0.670
Range	618.381	1632.58	6192.745	1663.515	2472.025
R^2 (variogram)	0.656	0.595	0.270	0.900	0.957
Mean std.	0.007	-0.032	-0.009	0.004	-0.070
RMSS	0.871	1.379	1.025	1.076	1.233
October sampling					
Variable	**Benthic Chl *a***	**Median grain-size**	**Mollusk biomass**	**Pelagic Chl *a***	**SPM**
Kriging type	Ordinary	Ordinary	Ordinary	Ordinary	Ordinary
Detrending order	None	None	None	None	None
Transformation	None	Log	None	Log	Log
Variogram model	Spherical	Exponential	Exponential	Circular	Spherical
Anisotropy	False	False	False	False	False
Nugget	1.133	0.000	0.010	0.105	0.152
Sill	7.163	0.154	0.031	0.481	0.961
Range	1164.191	634.152	719.266	1310.615	1.113
R^2 (variogram)	0.959	0.747	0.435	0.320	0.949
Mean std.	-0.018	-0.028	-0.007	0.001	-0.056
RMSS	0.886	1.222	1.031	1.293	1.123

Mean std = Mean standardized; RMSS = Root Mean Square standardized.

Results

March sampling - A PCA was performed on the spring variables, with the two first components explaining 67.17% of the total variation. The correlation circle (Fig. 3A) showed a clear relationship between the benthic Chl *a* and mud fraction.

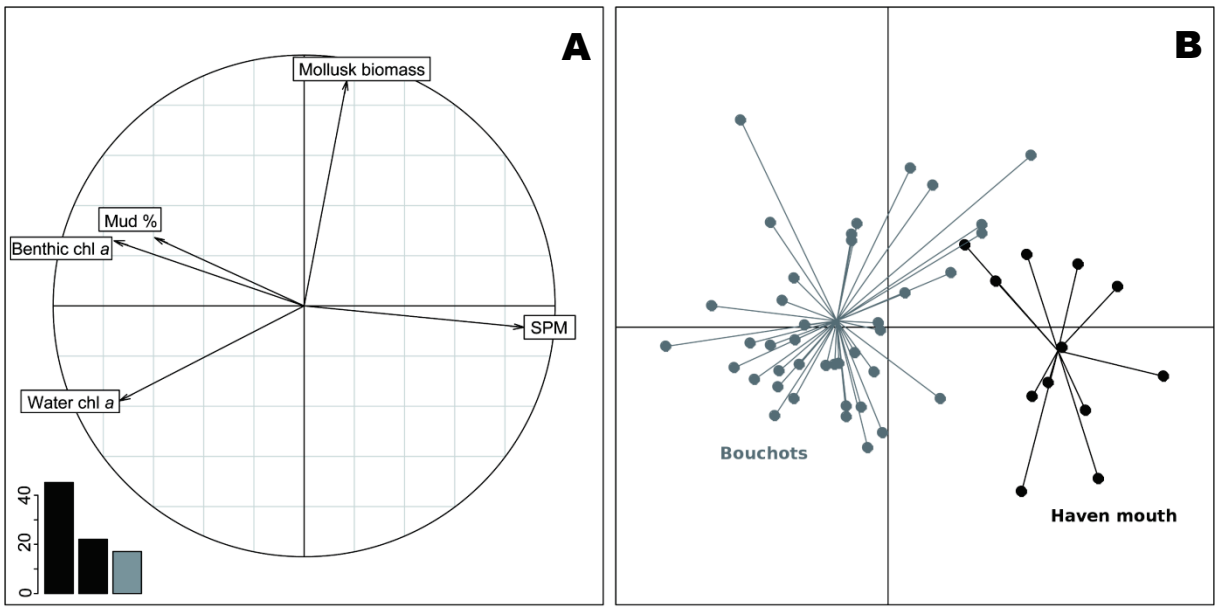

Figure 3: PCA results of the benthic and pelagic log-transformed variables for the March sampling. SPM (mg.L^{-1}), benthic Chl *a* concentration (µg.g^{-1}), water Chl *a* concentration (µg.L^{-1}), mud fraction (%) and wild mollusk biomass (g AFDW.m^{-2}). Data used for the PCA resulted from the extraction of the corresponding kriged maps on the general sampling grid. A: Correlation circle; B: Scatter plot of individuals, with a group distinction corresponding to the area in front of the haven called "Haven mouth" and the rest of the area corresponding to the shellfish structures called "Bouchots".

These two variables were also quite well related to the water Chl *a*. These three variables were inversely related to SPM, all these variables being well represented by the 1st axis and explained 45.16% of the total variation. Mollusk biomass had no relationship with the previous variables and was well represented on the 2nd axis, explaining 22.01% of the total variance. The scatter plot of individuals (Fig. 3B) showed a clear spatial structure, and the individuals were merged into 2 groups: the area located in front of the haven mouth, and the other area with the rest of the stations. The haven mouth was characterized by the strongest SPM concentration and lowest Chl *a*.

Geostatistical analysis and kriged maps showed the clear spatial structure of the area, separating the haven mouth from the rest of the area. Benthic Chl a (Fig. 4) showed concentrations starting from 0.67 to 12.94 µg.g-1, the haven mouth being characterized by the lowest values of the

studied area. Two patches of higher concentration appeared respectively at the north and south of the haven mouth. Regarding to mud fraction distribution, the finer sediments were located under the mussel structures ranging from 5 to 7% of the total amount of sediment, the haven mouth being characterized by the lowest mud fractions. A systematic relationship did appear between the physical structures of the area and sediment patterns, i.e. the mussel beds and the bioreef beds (Sabellaria alveolata reefs) and the mud fraction of the underlying sediment. The south and the north of the field showed a homogenous distribution of the mud fraction.

For benthic mollusk biomass, the haven mouth is characterized by the lowest biomass of the area. Higher levels of biomass were located at the north of the study area and in the southern part of the haven mouth. The kriged map of mollusk biomass let appear a latitudinal division of the foreshore into 3 parts. A first zone situated in front of the mouth is characterized by the total absence of mollusks. The areas located at the north and south of the haven mouth, especially at the edges of mussel culture areas, are characterized by higher biomass ranging between 0 and 2.30 g.m2 (g AFDW) especially at the edges of mussel culture areas. Biomasses were low, between 0 and 2.30 g.m2 (g AFDW).

The biomass distribution map of suspension and deposit feedersconsumers' feeding type (Figure 5) showed that deposit- feeders were associated to mussel bed cultures while suspension-feeders were mainly found outside mussel-farming structures sites. These features significantly affect the distribution of deposit- feeders in these areas (ANOVA, p-value <0.001). The species distribution map indicated that Nassarius reticulatus was distributed exclusively under mussel-farming structures. The bivalve *Cerastoderma edule* was only present at the borders of the haven mouth.

Water Chl *a* was characterized by low values for the entire area, the haven mouth being characterized by almost no Chl *a*. The mussel cultures located at the North-East showed lower Chl *a* concentrations than the other structures. SPM map was inversely distributed, with the highest concentration found at the haven mouth between 21.90 and 33.71 $mg.L^{-1}$. The north and south areas were characterized by homogeneous concentrations ranging from 1.65 to 5.54 $mg.L^{-1}$. The south area was characterized by the lowest SPM values, relatively homogeneously distributed.

Mussels sampled a month after March campaign showed no significant differences in isotopic signature between sites. The respective average values for $\delta_{13}C$ and $\delta_{15}N$ were -19.01±0.13 and 6.47±0.31 ‰, indicating that the diet of mussels in March was almost exclusively composed of phytoplankton (Lefebvre et al., 2009).

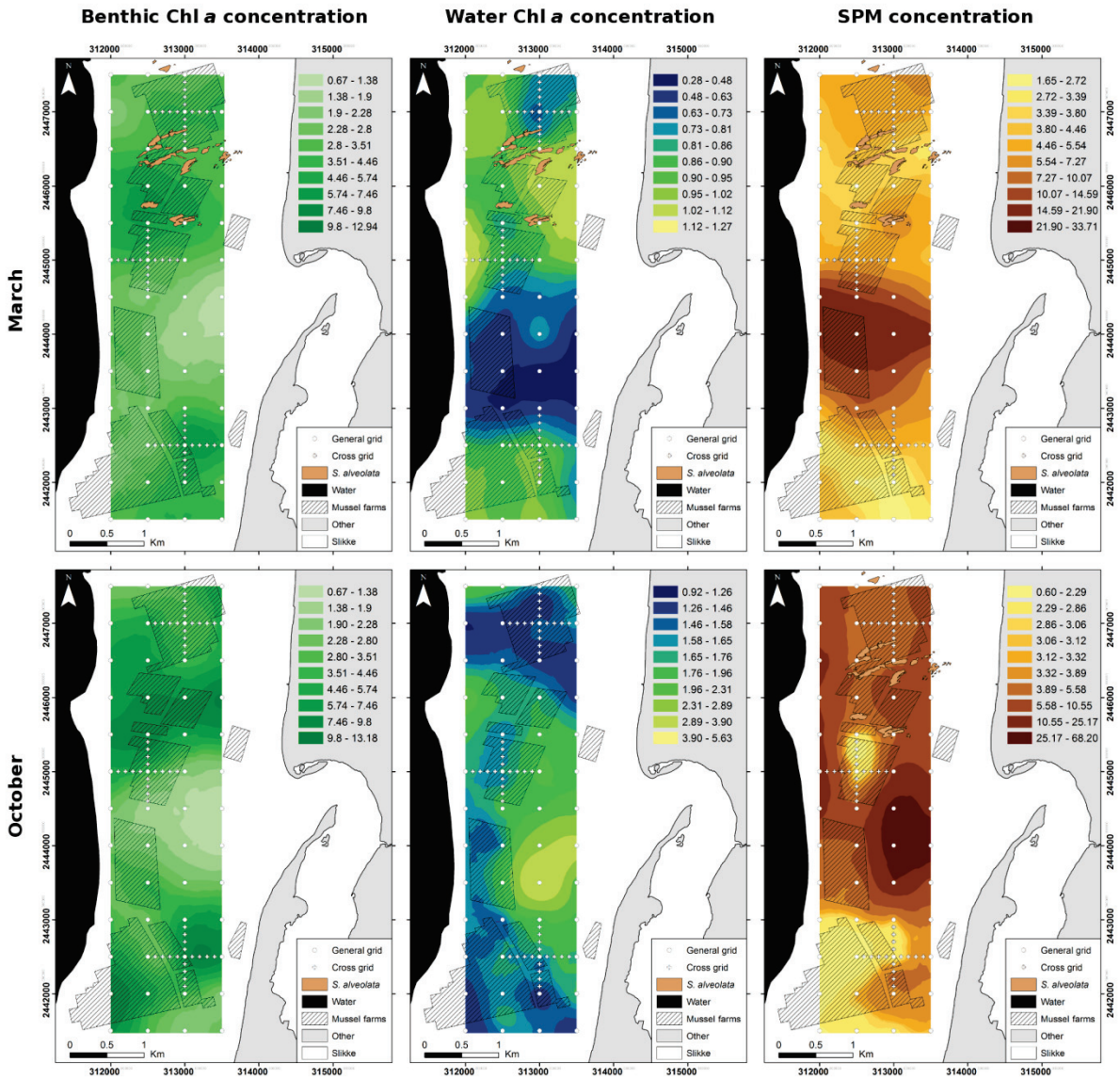

Figure 4: LIN March and October kriged maps of pelagic variables. All variables were kriged on different variogram models depending on the data (Table 1). Geometrical scales were used to maximize the visualization of both gradients and the patchiness of the different variables. **Benthic Chl *a* concentration**: Chl *a* concentration (µg.g^{-1}); **Water Chl *a* concentration**: Chl *a* concentration (µg.L^{-1}). **SPM concentration**: Suspended Particulate Matter (mg.L^{-1}).

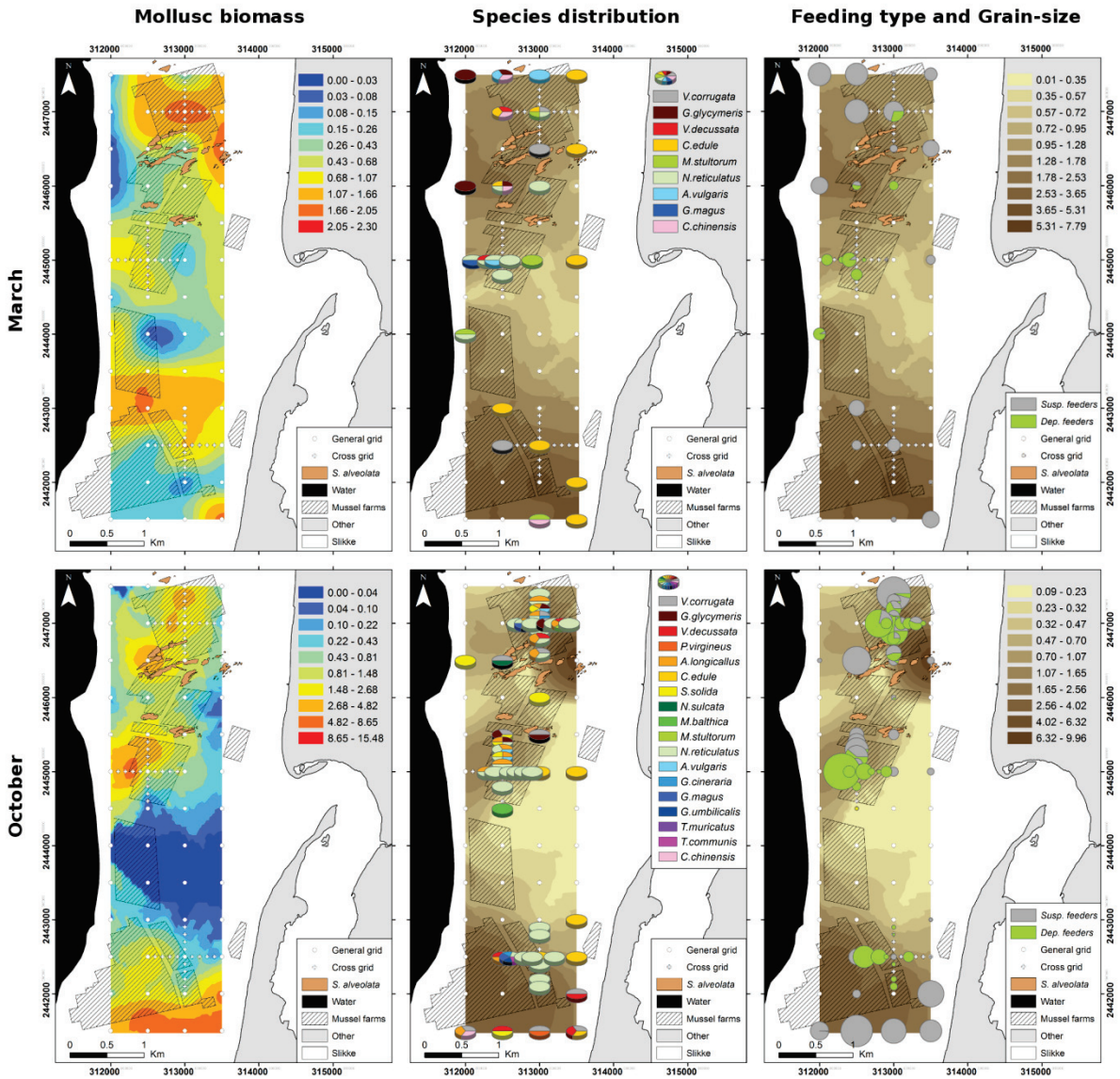

Figure 5: LIN March and October kriged maps of benthic variables. All variables were kriged on different variogram models depending on the data (Table 1). Geometrical scales were used to maximize the visualization of both gradients and the patchiness of the different variables. Mollusk maps are at different scales to account for the discrepancy in the data between the 2 sampling campaigns. **Mollusk biomass**: g AFDW g.m^2; **Species distribution**: Pie charts represent the presence of a species without taking acirrespectivecount of its relative biomass or numberabundance; **Feeding type and Grain-size**: Pie charts represent the relative ratio of deposit or suspension feeders, the size of the pie chart is relative to the biomass of each feeding type. Grain-size represents the mud fraction distribution.

October sampling - A PCA was realized on the fall variables, with the two first component explaining 73.60% of the total variation. The correlation circle (Fig. 6A) showed a clear relationship between the water Chl *a*, SPM and mud fraction. SPM and water Chl *a* variables were negatively correlated to the mud fraction of the sediment, all these variables being well represented by the 1st

axis and explained 54.52% of the total variation. Even if there is still a negative relationship between water Chl *a* and mud fraction, it is opposite to the spring results where water Chl *a* and mud fraction were positively correlated. Benthic and pelagic variables were clearly uncoupled. Benthic Chl *a* was also not related to the mud fraction, on the opposite of their strong relationship during the spring sampling. Mollusk biomass, as for the spring sampling, had no relationship with the previous variables and was quite well represented on the 2nd axis, explaining 19.08% of the total variance. The scatter plot of individuals (Fig. 6B) showed the same clear spatial structure than for the spring sampling, with a separation between the areas located in front of the haven mouth and the rest of the stations characterized by mussel cultures. Contrary to spring data, the haven mouth was characterized by the strongest Chl *a* and SPM concentration, with the sampling done during the autumnal bloom (Fig. 3).

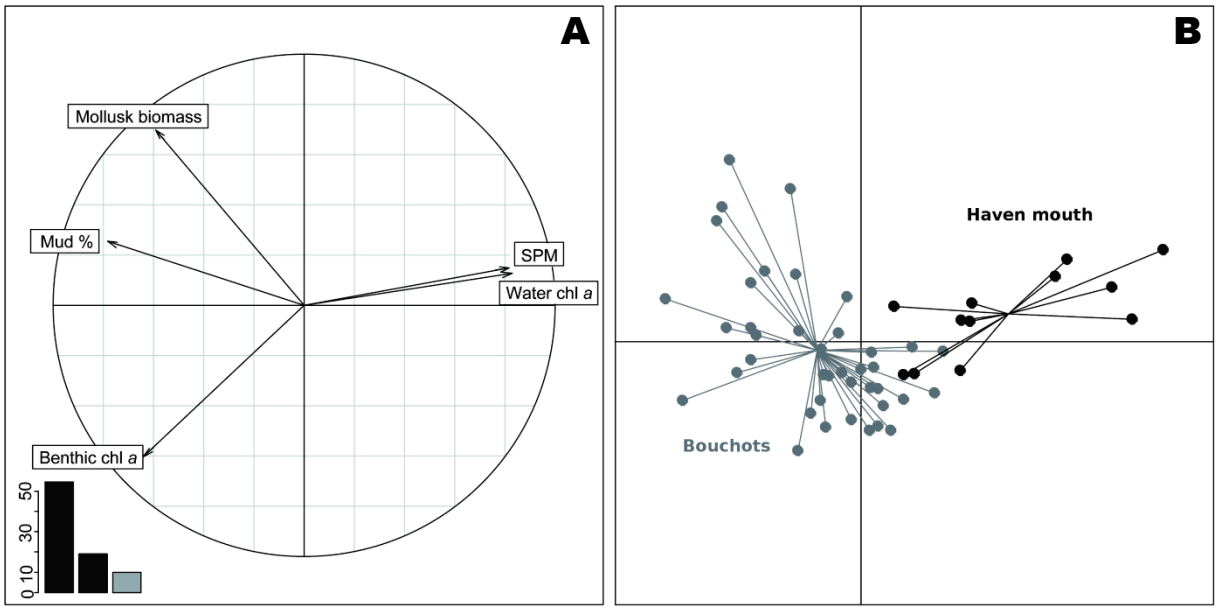

Figure 6: PCA results of the benthic and pelagic log-transformed variables for the October sampling. SPM (mg.L^{-1}), benthic Chl *a* concentration (µg.g^{-1}), water Chl *a* concentration (µg.L^{-1}), mud fraction (%) and wild mollusk biomass (g AFDW.m^{-2}). Data used for the PCA resulted from the extraction of the corresponding kriged maps on the general sampling grid. A: Correlation circle; B: Scatter plot of individuals.

Geostatistical analysis and kriged maps showed again the clear spatial structure of the area, separating the haven mouth from the rest of the area. Benthic Chl *a* (Fig. 4) showed similar concentrations than for the spring sampling, from 0.67 to 13.18 µg.g^{-1}. The benthic Chl *a* distribution was similar for the 2 sampling seasons, the haven mouth being characterized by the lowest values of the study area. Conversely to the spring sampling, the north of the field showed a heterogeneous distribution of the mud fraction. A mud patch was observed near next to the Sabellaria alveolata bioreefs.

Mollusc biomass was low at the haven mouth, and ranged from 0 to 15.48 $g.m^{-2}$, with a higher biomass than in spring. The same 3 parts latitudinal division of the foreshore appeared in autumn. The biomass distribution map of suspension and deposit feeders (Fig. 7) showed that deposit-feeders were associated to mussel-farming structures sites while suspension- feeders felt were observed mainly outside mussel structures. These structures significantly affected the distribution of deposit- feeders in these areas (ANOVA, p-value <0.001). The mollusk biomass was apportioned according to the mud fraction of the sediment, with biomasses increasing as a function of the mud fraction ($R^2 = 0.237$, $p< 0.001$).

The species distribution map indicated that *Nassarius reticulatus* was the dominant species of the area in terms of coverage and was distributed exclusively under mussel structures. Another deposit-feeder, *Abra longicallus*, was present under mussel structures. Both number of individuals and biomass increased a lot for the species *Venerupis corrugata* between March and October, and their number were multiplied by two whereas their biomass was multiplied by ten resulting in bigger individual size (Table 2). *Venerupis decussata* population did increase too, but in a lower extent, multiplying both biomass and individuals by two times. On the contrary, the species *Glycimeris glycimeris* was characterized by high biomass for the 2 seasons but smaller individuals in october (Table 2). The biomass of *Crepidula fornicata*, which was limited to the bouchots, decreased between March and October. As in spring, the bivalve *Cerastoderma edule* was again mostly present at the borders of the haven mouth.

Water Chl *a* was characterized by higher values than spring sampling for the entire area, the haven mouth being characterized by the highest concentrations of Chl *a*, opposite to the spring sampling. The mussel bed located at the North-East showed lower Chl *a* concentrations than the other structures, as for the spring sampling. SPM map showed higher concentrations at the haven mouth, as for the spring sampling, ranging from 25.17 to 68.20 $mg.L^{-1}$. At the north there was a longitudinal depletion over the mussel structures and the borders of the north area was characterized by higher SPM concentrations. As for the spring sampling, the south area was characterized by the lowest SPM values, relatively homogeneously distributed. The high tide RVB SPOT image (Fig. 7) showed two plumes of water coming from both *La Sienne* and *La Vanlée* havens, with a Northern-Western direction. Plume did not extend in the mussel culturearеas at the north or the south of the haven mouth (Fig. 8). Bathymetry showed a homogeneous gradient of increasing depth from the coast to the sea (Fig. 9).

Table 2: Mean mollusk biomass (g AFDW.m^{-2}) for the 2 sampling season.

Reign	Species	Trophic group	March (g.m^2)	October (g.m^2)	March (ind.m^2)	October (ind.m^2)
Bivalvia	*Venerupis corrugata*	Suspension-feeder	0.059	0.627	0.119	1.931
	Glycimeris glycimeris	Suspension-feeder	0.278	0.135	0.317	0.379
	Venerupis decussata	Suspension-feeder	0.080	0.146	0.356	0.551
	Polititapes virgineus	Suspension-feeder		0.012		0.206
	Abra longicallus	Deposit-feeder		0.028		1.551
	Cerastoderma edule	Suspension-feeder	0.395	0.030	0.673	0.551
	Spisula solida	Suspension-feeder		0.035		0.517
	Nucula sulcata	Deposit-feeder		0.001		0.068
	Macoma balthica	Suspension-feeder Deposit-feeder		0.002		0.034
	Mactra sultorum	Suspension-feeder	0.016	0.001	0.158	0.034
Gasteropodia	*Nassarius reticulatus*	Deposit-feeder	0.192	0.881	0.713	10.862
	Gibbula magus	Deposit-feeder	0.016	0.016	0.040	0.137
	Gibbula cineraria	Deposit-feeder		0.002		0.068
	Gibulla umbilicalis	Deposit-feeder		0.002		0.517
	Trophonopsis muricatus	Deposit-feeder		0.001		0.011
	Turitella communis	Suspension-feeder		0.001		0.172
	Crepidula fornicata	Suspension-feeder	0.561	0.253	6.373	1.620
	Calyptraea chinensis	Suspension-feeder	0.010	0.001	0.198	0.103
Scaphopodia	*Antalis vulgaris*	Deposit-feeder	0.050	0.007	0.158	0.275

The benthic phaeopigment percentage map (Fig. 9) showed a patch of higher concentration in the north of the sampled area, as well as a high concentration in the south between 20 and 30% of total pigments. The central area was characterized by low concentrations ranging from 0 to 10% of total pigments. The water column phaeopigment map showed a negative relationship with the water column Chl *a* concentration map (Fig. 6, 9), whereas it showed no relationship with the benthic phaeopigments map. The haven mouth was the less concentrated area in phaeopigments, whereas it was characterized by the higher water Chl *a* on the area. The locations characterized by a Chl *a* depletion over the farming structures were characterized by high water phaeopigment concentrations in the water column, between 30 and 40% of the total pigments.

Figure 7: Composite colour (RGB) SPOT image of Lingreville (October 11, 2010 at 11:20 UTC) showing the turbid plumes exiting La Sienne and La Vanlée haven, with a Northern-Western direction.

Figure 8: Composite colour (RGB) SPOT image of Lingreville (October 11, 2010 at 11:20 UTC) showing the turbid plumes exiting La Vanlée haven, with a Northern-Western direction.

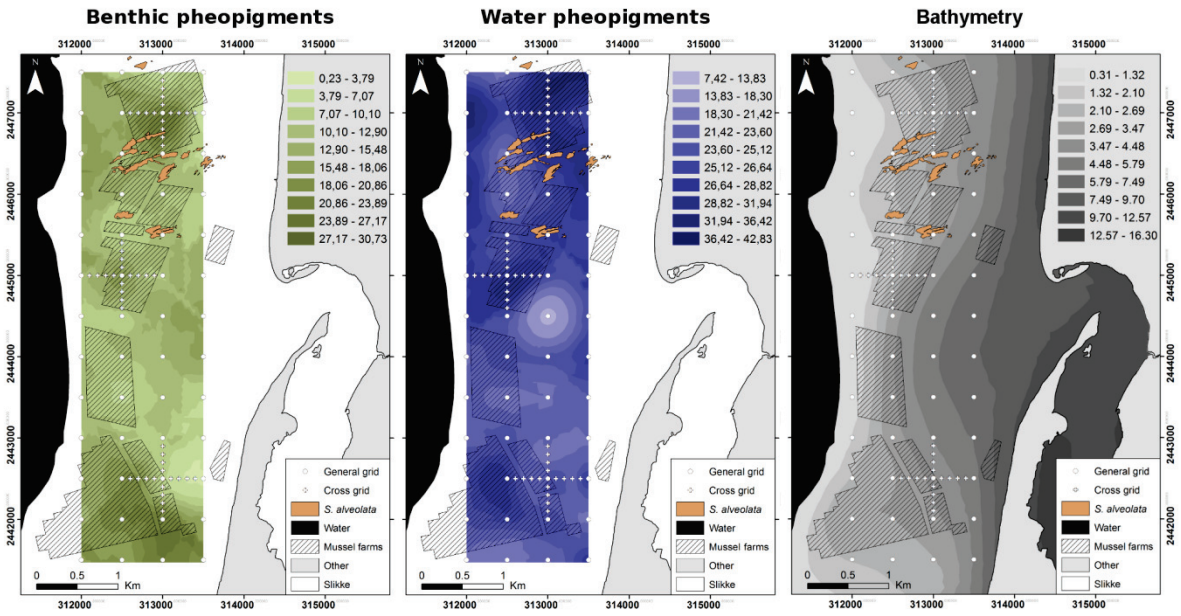

Figure 9: LIN kriged maps of benthic/water pheopigments and bathymetry. Phaeopigments measurements have been done in October only. Results are presented as % of total pigments.

Discussion

Impact of cultivated mussels in the benthic-pelagic coupling. The annual mean of water chl *a* was 1.41 ± 1.03 µg. L^{-1}, lower than the value of 2.7 ± 1.3 µg. L^{-1} found by Marín Leal et al. (2008) for a wet year in 2004, classifying the sampling year of the present study as a dry year. Sampling has been done between the 2 small peaks observed between March and April at 8°C water temperature (Fig. 2), with typical low values associated to dry years, when comparing to data in the same site during dry years (Marín Leal et al., 2008) or wet years (Blin, com pers). Despite the strong contrast between the two seasons sampled in terms of temperature or mollusk biomass, the result showed a perennial distribution of MPB within the sampled area. This result confirms other results of the literature (van der Wal et al., 2010; Ubertini et al., 2012). Benthic Chl *a* is often related to mud fraction of the sediment (Perkins, 2003; Cartaxana et al., 2006; Orvain et al., 2012; Ubertini et al., 2012). The haven mouth is an extremely dynamic area, characterized by a structure of temporary micro-channels with high flow coming from the haven mouth; as a consequence there is a permanent perturbation and the microphytobenthos installation seems difficult. Moreover, the absence of mollusk in this area make the sediment more homogeneous, with mainly sand whereas the rest of the area is characterized by coarse shell sand, with heterogeneous material from shell fragments toward bouchots to mud enrichment between them. This typical sediment distribution has already been shown by Grant (2010) and Grant et al. (2012) for similar ecosystems. Besides, the mud fraction of the sediment is higher under the farming structure, as a consequence of the biodeposition

process generated by mussels. The *Sabellaria alveolata* reefs must contribute to the higher mud fraction in this area too. In fact, MPB participates to the diet of *S. alveolata* (Lefebvre et al., 2009) ; thus we can emphasize that mussel structures could facilitate the maintaining of the *S. alveolata* reefs in this area, by fueling them through : 1) biodeposits which may enhance fine fraction of the sediment, 2) MPB growth favored by these biodeposits and 3) Resuspension of these MPB. The fine sediments favor the epipelic MPB development under the mussel structures. As a consequence, benthic Chl *a* biomass was related to the mud fraction of the sediment. However, the biodeposit accumulation (and dispersion) in October did not enhance the microphytobenthic biomasses compared to March. This relationship was clearer in March, the weaker relationship in October being probably due to the apparition of euglenid patches observed in the field over sandy sediments. In spite of the high flow regime in this open ecosystem, there is an accumulation of biodeposits in the area surrounding mussel cultures. It seems unlikely that the resuspension of MPB from biodeposits that has been mentioned by Widdows et al. (2009) did occur during this study. Indeed, MPB did not contribute to mussel diet during this dry year, but remained attached to the bottom substrat.

Distribution patterns of mollusk biomass appeared to be related to the farming structures. As the degree of biodeposition increases, typical soft-sediment communities dominated by large filter-feeders are replaced by deposit-feeding organisms (Callier et al., 2008; McKindsey et al., 2011; Ubertini et al., 2012). The deposit-feeders were mainly located within mussel-farming sites while suspension-feeders were mainly distributed outside mussel structures, showing on one hand the trophic facilitation of mussels for deposit-feeders through biodeposition, and the competition between wild and cultivated suspension-feeders for phytoplankton. High bivalve abundance leads to higher clearance rates and intra/inter-competition for food (Newell, 2004). Moreover, *S. alveolata* reefs probably contributed to the trophic pressure on the water column through the polychaete's clearance rate (Dubois et al., 2003). The increased activity of mussels in autumn compared to spring facilitated the installation of deposit-feeders whose biomass increased a lot between the two seasons, whereas the higher filtration rate of mussels in autumn leaded to increased competition with indigenous suspension-feeders whose biomass decreased between the two seasons. In fact, as well as reducing available resources such as food for competitors, the mussels may also reduce other species'recruitment by feeding on their larvae (Alfaro, 2006; Porri et al., 2008). Indeed, in March where a lot of juveniles were globally observed, the spatial distribution of suspension-feeders, was negatively affected by the presence of mussels. The distribution of *Glycimeris glycimeris* probably illustrated the trophic depletion linked to the mussel-farming structures. We can hypothesize that in March, this species was distributed outside the mussel cultures, and in October it was found within

the cultures with the same biomass but more individuals, only smaller individuals being able to survive in low food conditions imposed by mussels.

Autochthonous versus allochtonous trophic sources. Filter-feeding by cultivated mussels may result in phytoplankton depletion in the water column. The high influence of mussel filtration efficiency of mussels is confirmed by both high phaeopigments and low Chl *a* concentrations in the water column, as shown by Ubertini et al. (2012) for another cultivated ecosystem. If consumption exceeds phytoplankton renewal by tidal flushing and phytoplankton growth, the ecosystem becomes food limited with a carrying capacity being strongly affected. McKindsey et al. (2006) have reviewed the "carrying capacity" of cultured bivalves in order to limit negative impacts on ecosystem dynamics. The use of culture farming on vertical sticks is currently restricted to France (McKindsey et al., 2011), thus direct comparison of fluxes induced by off-bottom cultures is difficult. Nevertheless, observation on the field showed large amount of fine sediment deposits toward these structures colonized by deposit-feeders also seen by Grant (2010), all the more so that the friction coefficient owing to culture farming structures can be 10 times higher compared to those of open sandy areas (Allard et al. 2008). The role of biodeposition could possibly be favorable to bioreefs of *Sabellaria alveolata*, whose diet is largely related to MPB (Lefebvre et al., 2009). Thus, cultivated mussels may be trophic facilitators for *S. alveolata*, all the more that they could benefit from resuspension before mussels because of their proximity to the seafloor compared to the mussels. The tubiculous annelid *S. alveolata* is a filter-feeder, which has been demonstrated to compete with cultivated mussels in terms of filtration efficiency and food sources (Dubois et al., 2009), thus the possibility for accessing MPB from the uppermost sediment could explain the possibility of mussels and *S. alveolata* to co-exist without exceeding the carrying capacity of the ecosystem. However, populations of the latter are in drastic decrease since 2011, indicating that the carrying capacity of the system could have been reached after a second dry year in 2011.

The primary production seasonal variability induces changes in suspension-feeding at the ecosystem scale. As a consequence mussels are ecosystem key-engineers (Crowe et al., 2011), modifying vertical and benthic fluxes in the water column. The stepped-up consumption in autumn increases biodeposition, but since chl *a* concentrations seem to be relatively stable between the two contrasted sampled seasons, the hypothesis of autochthonous feeding on resuspended MPB can be ruled out for this ecosystem, at least during the studied period (i.e. a dry year). The phytoplankton overconsumption by mussels leads to exceed the carrying capacity of this ecosystem, with a clear exclusion of other suspension feeder in the cultivated area. Normandy west coast ecosystems display inter-annual variability in hydrobiological variables with differences between wet and dry years,

ecosystems with limited eutrophication being sensitive to nutrient enrichment (Grangeré et al., 2012). The year 2010 was a dry year, increasing the prevalence of phytoplankton in the mussel diets as shown by the isotopic values of sampled mussels, hence confirming results by Lefebvre et al., (2009) who studied bivalve diets during dry years (2004-2005) too with similar findings. Oyster diet was shifting from phytoplankton total contribution during dry years (2004-2006) in this ecosystem to a mixture of phytoplankton and resuspended MPB during wet years (2007-2008, Grangeré et al., 2012). We can emphasize that mussel diet are subjected to the same kind of balance between dry years and wet years. Chl *a* inlets from *La Vanlée* were clearly reduced (Fig. 8) probably lower than during wet years, modifying the balance between autochthonous and allochtonous MPB coming from the haven. When phytoplankton becomes low in the water column, the suspension-feeder diet may rely on organic matter inlets coming from *La Vanlée* or *La Sienne*. Conversely, *Sabellaria alveolata* diet relies on resuspended MPB in majority, even during dry years when examining the results by Lefebvre et al. (2009). This species is maybe able to provoke local MPB resuspension by an active bioturbation and an effect on bed roughness through local field turbulences as often observed for tubiculous annelids (Friedrichs et al., 2000; Peine et al., 2009).

Our results cannot explain the MPB contribution (up to 50%) to mussel diet during wet years (2007-2008). Indeed, we can imagine 2 alternative assumptions: First, these food items can come from autochthonous material. The strong currents and the dominance of western winds during wet years must enhance the turbulence regime and biodeposits with associated MPB that are not highly resuspended during a dry year, could be resuspended at high erosion rates during a wet year. There is a strong alternative explanation, concerning the haven inlets that can supply chl *a* biomass enriched in MPB during wet year in this ecosystem. We observed that the plume is impoverished in chl *a* in March and the plume extension in October did not reach the cultivated areas. If the biomass within the plume is enriched in MPB, this material cannot supply food for cultivated bivalves during the sampled periods (even if the fall sampling was performed during a marked bloom). During wet years, the high rainfall regime and river flows must be very high and certainly enriched in resuspended riverine MPB. In such conditions, we can easily emphasize that plume extension from haven mouth extends over wider areas than during dry years, and this material must contribute to suspension-feeder diets. A similar study should be repeated during a wet year to better decipher the contribution of the 2 alternative hypothesis and to better refine the factors that control the Lingreville ecosystem functioning.

Our study clearly stressed the dependence of MPB biomass and benthic deposit-feeders on mussel cultures in this ecosystem. We can also emphasize that the decrease of bio-reefs observed in 2011 could be linked to a trophic cascade effect, the year 2010 being a dry year with poor

phytoplankton populations and also poor biodeposition that could provoke poor benthic chl *a* concentration and a reduction in MPB resuspension rates. These 2 processes must entail the ecosystem to overpass its carrying capacity rapidly and reducing mussel growth. Thus, biodeposition should have decreased, reducing the food potentially available for bioreefs.

Conclusion

The present study aimed to explore the mussel culture impacts on benthic-pelagic coupling and the capacity or the system to auto-regulate without allochtonous support by studying both compartments simultaneously. Biodeposition processes appeared to be predominant in this ecosystem, controlling fine sediment enrichment, in association to MPB, both factors hence affecting wild mollusk distribution. Seasonal variation in mussel activity led to mud enrichment under farming structure, and as a consequence the biomass of deposit feeders with a typical exclusion of suspension-feeders. Wild suspension-feeders must suffer from trophic competition with the mussels and were preferentially found outside or on the borders of farming structures. We can emphasize that bioreef installation of *Sabellaria alveolata* has probably been facilitated by the biodeposition process induced my mussels in the past. The installation of farming structures leaded the system to be food limited at least for dry years, exceeding the carrying capacity of the ecosystem.

Acknowledgements

We would particularly like to thank Jean-Paul Lehodey both for his help with innovative equipment during sampling and for his help in the field. We are grateful to Frédéric Guyon, Christophe Roger and Karine Grangeré for their help in the field. We thank Ludovic Hermabessière and Emmanuel Karakachian for their significant contribution to mollusk determination and grain-size analysis, and the latter his help of the field. We would also like to thank Jean-Louis Lesoif, Thibaut Gauquelin, Sébastien Pien, Claire Châtaigner and Bertrand Bouchaud for their help in the field. We are grateful to Sandra Sritharan for her help with isotopic analysis.

Chapitre V

Impact de la structure du sédiment et de l'âge du biofilm sur la remise en suspension du microphytobenthos : Etude en érodimètre

© Clarke little

« La mer joint les régions qu'elle sépare. »

Alexander Pope

Impact of sediment grain-size and biofilm age on microphytobenthos resuspension

Martin Ubertini[1,2], Christiane Rakotomalala[1,2], Francis Orvain[1,2,3*]

[1] *Université de Caen Basse-Normandie, FRE3484 BioMEA, Caen, France*
[2] *CNRS INEE, FRE3484 BioMEA, Caen, France*
[3] *CNRS, UMR 7208 BOREA, Muséum d'histoire naturelle, CRESCO, Dinard, France*

*Corresponding author

Soumis au journal :

"**Journal of Sea Research**"
IF = 2,598

Résumé

Les zones intertidales sont des zones de haute énergie, et l'hydrodynamique est responsable de la remise en suspension des sédiments et du microphytobenthos associé. La composition des sédiments et l'âge du biofilm sont deux éléments majeurs impliqués dans cette remise en suspension. Cependant, le rôle respectif de ces deux paramètres par rapport au phénomène de remise en suspension a rarement été étudié simultanément dans des conditions contrôlées. Afin de mieux évaluer les rôles des mélanges sablo-vaseux et de l'âge du biofilm sur la remise en suspension du microphytobenthos, différentes conditions ont été testées en utilisant un canal benthique, l'érodimètre. Des conditions allant de la vase pure jusqu'à des mélange sablo-vaseux ont été testés en présence d'un biofilm microphytobenthique, et les cultures de biofilm en mésocosme ont été contrôlées pour évaluer le stade de développement du biofilm en réglant l'intensité lumineuse et les périodes d'immersion. Les paramètres photosynthétiques du biofilm ont été suivis, ainsi que la teneur en eau et la concentration des sels nutritifs dans les sédiments. Une augmentation du débit a été appliquée sur des carottes de sédiments, et l'influence induite par la contrainte de cisaillement sur l'érosion a été évaluée par la turbidité et la chl *a* via des capteurs. Entre les 3 et 9 premiers jours du développement du biofilm, l'âge du biofilm a affecté significativement les seuils d'érosion critiques de la chl *a* et du sédiment pour les mélanges sablo-vaseux. Les caractéristiques de l'érosion de la chl *a* et du sédiment diffèrent selon les traitements, le biofilm pouvant être érodé avant sédiments quand ils sont bien constitués (en particulier dans la vase pure). La remise en suspension des sédiments semble être principalement due aux contraintes physiques comme la compaction différentielle et de la ségrégation du sable en fonction du contenu en vase. Les protéines des EPS liés (extraites avec résine Dowex) semble avoir un rôle crucial dans les stades pionniers de l'installation du biofilm, ce qui permet sa formation dans un environnement moins favorable causé par un enrichissement en sable. Cet effet d'EPS liés doit être contrôlé par une augmentation de la cohésion et une diminution de la perméabilité des sédiments. La teneur en glucides de la fraction liée des EPS est directement liée à l'érodabilité des sédiments, indépendamment du type de mélange ou de l'âge du biofilm. La composition du mélange semble être le principal facteur impliqué dans le phénomène de remise en suspension, avec un optimum atteint proche d'un rapport d'équilibre entre la vase et le sable. Les EPS liés permettent dans les mélanges sablo-vaseux un développement du biofilm avec de bonnes performances photosynthétiques, et ce en dépit de la résistance à l'eau et la disparition des éléments nutritifs pendant la marée basse. Cependant, l'enrichissement en sable est défavorable à la croissance des diatomées épipéliques, ainsi que leur exportation à l'eau colonne via l'érosion.

Abstract page

Intertidal areas are high energy areas, and hydrodynamics are responsible of resuspension of the sediment and associated microphytobenthos (MPB). Sediment composition and biofilm age are two major components involved in their own resuspension. However, their relative role in resuspension phenomenon has rarely been studied together in controlled conditions. To better assess their respective contribution in explaining sediment and MPB resuspension, different treatments were tested using an erodimeter flume. Pure mud to 50/50 mud-sand mixtures were tested with a presence of an epipelic MPB biofilm, and mesocosm biofilm cultures were controlled to assess different development stadium of the biofilms. The biofilm photosynthetic parameters and Extracellular Polymeric Substances (EPS) were followed as well as water content and ammonium concentration in the sediment. Between 3 and 9 first days of biofilm development, biofilm age did significantly affect erosion critical thresholds for Chl *a* and sediment resuspension for sand-mud mixtures. Chl *a* and SPiM erosion characteristics differed between treatments, biofilm being able to be eroded before sediment when they are well constituted (especially in pure mud). Sediment resuspension seemed to be mostly driven by physical constraints like differential compaction and vertical sand segregation as a function of mud content. Proteins of the EPS bound fraction (extracted with dowex resin) appeared to have a critical role in the pioneering stages of biofilm installation, allowing its formation in a less favorable environment caused by sand enrichment. This effect of bound EPS must be mediated by anincreasing cohesion and lowering sediment permeability. Carbohydrate content of the bound EPS fraction was directly related to the sediment erodability, independently from mixture type or biofilm age. Mixture composition seemed to be the main factor involved in resuspension phenomenon, with an optimum reached near a equilibrate ratio between mud and sand. Despite the resistance to water and nutrient disappearance during low-tide when sediment is enriched in sand thanks to bound EPS allowing a biofilm development with good photosynthetic performances, sand enrichment is unfavorable to the epipelic diatom growth, as well as to their exportation to the water column via erosion.

1. Introduction

Macrotidal estuaries are open ecosystems subject to hydrodynamic processes such as waves, currents and tidal rhythm. The stress generated by these physical forcing results in a more or less important resuspension of the sediment and associated microphytobenthos (MPB), disturbing the microphytobenthic communities. Benthic diatoms communities inhabiting intertidal areas are divided in two groups, according to their adaptation to the sediment habitats. Epipsamic diatoms are motile organisms firmly attached to sand grains, to prevent themselves from resuspension events. Lower energy habitats are inhabited by epipelic benthic microalgae – dominant group of microphytobenthos in intertidal mudflats (Smith and Underwood, 1998) – which are able to migrate through the sediment top layer. Photoacclimatation and light duration are responsible for the migration of diatoms (Perkins et al., 2001; Blanchard et al., 2004). It is likely mediated by the extrusion of carbohydrate-rich heteropolymers called exopolymeric substances (EPS), which as well as playing a role in the diatoms mobility are able to stabilize the sediment by limiting the erosion of the latter (Holland et al., 1974; Grant et al., 1986; Paterson, 1989b; Smith and Underwood, 1998, 2001; Friend et al., 2008). MPB development step in biostabilisation process by: (i) armouring of the sediment surface (Tolhurst et al., 2003) and (ii) production of EPS, reinforcing sediment cohesiveness. This MPB biostabilisation of sediment surface is variable upon time, since MPB has its own dynamic and growth cycle. Combination of tidal cycles, day/night cycles, and biofilm age leads to different physiological states of microalgae. Consequently MPB biomass and EPS secretion varies upon time, thus influencing the sediment erodibility.

EPS secretion is under control of abiotic factors such as light with oxygenic photosynthesis (Staats et al., 2000a) or nutrients (Staats et al., 2000b), and there is direct metabolic pathway between photosynthesis and secretion of colloidal EPS (Underwood and Smith, 1998). The biomass of MPB on intertidal flats is driven by (i) removal processes such as grazing and resuspension, (ii) factors affecting growth rate and/or health of the MPB such as light, temperature or nutrients and (iii) sediment grain-size, with interaction with both previously mentioned factors (resuspension, nutrient availability) that are drastically regulated by the respective contribution of sand and mud proportion (van de Koppel et al., 2001; Orvain et al., 2012). When factors responsible for MPB losses from sediment (resuspension, grazing) are removed, the growth of the biofilm is known to follow a logistic curve until a maximum value reached at the biotic capacity of the local environment (Blanchard et al., 2001; Orvain, et al., 2003). The number of days necessary to reach the biotic capacity appears to vary according to the authors, and has been modeled by Wolf (2007) with an initial lag phase of about 3 days, followed by an exponential growth phase until a pseudo-steady

state ‘‘mature’’ phase after approximately 13 days where biofilm growth and detachment were in equilibrium. The physiological state of the biofilm is assumed to change as a function of the biofilm age (Sutherland et al., 1998). Photosynthetic capacity and efficiency has been shown to decrease with increasing age of the biofilm (Morris, 2005), and EPS are more secreted in the late phase of the biofilm growth caused by overflow metabolism in case of nutrient limitation (Orvain et al., 2003).

Sediment properties are decisive regarding its stability against forcing environmental variables. Sandy sediments are easily transported by haulage during bed-load transport and exported in the water column during strong hydrodynamic conditions. On the contrary, cohesive sediments resist to erosion but, in the event of harsh conditions such as strong heaves, critical thresholds can be transcended leading to significant sediment erosion. Numerous experiments focusing on microphytobenthos mediation of sediment erodibility have been done in lab, but most of the time they focus on homogenous sandy (Lucas, 2003; De Brouwer et al., 2005; Friend et al., 2008) or muddy sediments (Yallop et al., 2000; Andersen and Pejrup, 2002; Tolhurst et al., 2003, 2006, 2008; Gerbersdorf et al., 2007; Spears and Saunders, 2008). However, sand and mud can be intimately mixed, and may exhibit a horizontal gradient, or can be layered in the bed (Le Hir et al., 2011). The mixture behaves like pure sand, but there is a critical mud fraction (typically 30%), above which the mixture behavior is fully cohesive (Le Hir et al., 2011). Below this critical value, the mixture shear strength depends on the relative mud concentration as stated by Migniot (1989) and Waeles et al. (2008). In fact, if physical processes such as local hydrodynamic conditions are responsible for particle grain-size selection, a succession of vertical layers of sediment from different grain-size often occurs in nature. Moreover, biological processes such as bioturbation and sediment reworking can influence the particle mean-size, leading to modify the sediment vertical structure, therefore leading to bulk sediment mixtures (Krantzberg, 1985). As a consequence, intertidal ecosystems are often characterized by mud-sand mixed sediments, with a strong spatial heterogeneity (Orvain et al., 2012; Ubertini et al., 2012). These mixed sediments must be taken into account in both microphytobenthos development and material export to the water column by erosion processes.

Erosion thresholds of sediment mixtures in relation with microbial indices have been studied *in situ* (Defew et al., 2003; Lelieveld et al., 2003; Ziervogel and Forster, 2006) or by modeling approaches (Paarlberg et al., 2005). Some experiments have been done on the effect of biofilm age on biostabilization of the sediment (Sutherland et al., 1998; Orvain et al., 2004; Droppo et al., 2007; Stone et al., 2008), but these experiments were performed with a single type of sediment (most of the time cohesive). Other experiments have been conducted on the effect of sand/mud mixture on the sediment erosion and erosion laws have been tested in different hydrosedimentary models

(Waeles et al., 2008; Le Hir et al., 2011). The influence of sand/mud mixture on the microphytobenthic biofilm development has been studied (van de Koppel et al., 2001), and the positive effect of mud proportion on the biofilm growth has been clearly evidenced.

On one hand, mud proportion lead to a higher MPB biomass in the sediment. On the other hand, the cohesive properties of mud, along with EPS secretion by MPB biofilm that are much secreted by biofilms in mud, lead to higher resistance to erosion. This is thus difficult to establish accurately the contribution of these 2 opposite effects on the Chl *a* resuspension and to assess whether the sand enrichment lead actually to an increase or a decrease of chl *a* resuspension. To better refine the interaction between sediment sand/mud mixture, the biofilm growth and MPB resuspension, the effects of sediment mixture were tested as a function of the biofilm age. The objectives were to characterize the tidal currents influence on microphytobenthos resuspension regarding the sediment grain-size, but also the development state of the microalgal biofilm by a mesocosm approach. In order to do this, mesocosm biofilm cultures were controlled to assess different development stadium of the biofilms by regulating light intensity and emersion-immersion periods.

2. Materials and Methods

2.1 Substrata and biofilm preparation

Three sediment types have been prepared from natural sediments: one of pure mud (100%) and two sand-mud mixtures (75% mud / 25% sand and 50% mud / 50% sand respectively). In order to eliminate the macrofauna naturally present, the fresh sediments have been sieved using a 1 mm mesh size. For each of these mixtures, sediment was then dispatched in twelve cores (20 cm in diameter and a depth of 20 cm). The first upper cm was enriched with a epipelic MPB inoculum collected from a mudflat in Basse-Normandie (“Estuaire de l’Orne”). The core surface was then wreathed in order to be uniform as best as possible on the whole surface. The cores were placed in a tidal mesocosm able to simulate a high/low tide alternation every 6 hours in order to simulate immersion and emersion phases. A night and day alternation (18h/6h) was applied with adapted neon lights, with a light intensity of 1200-2000 µmol photons $m^2.s^{-1}$. Each of these sediment series was tested during 2, 6 or 9 days continuous treatment.

2.2 Pigments extraction and analyses

Sediments samplings were performed at days 3, 6 and 9 during diurnal emersion periods in order to access respectively the latency, growth and stationary phases of the biofilm (Sutherland et

al., 1998; Orvain et al., 2003). The first upper cm of the sediment was sampled and mixed, and fresh sediments were weighted. After 3 days in an oven at 60°C weights measurements were also done to obtain the water content of the sediment. Microphytobenthos biomass was assessed by measuring the chlorophyll *a* (Chl *a*) content following the Lorenzen's method (Lorenzen, 1967). Chloropigments was extracted from 200 mg freeze-dried sediment subsamples with 90% acetone solution for 24 h at 4°C in the dark. After centrifugation (5 min, 2000 g), fluorescence of the supernatant was measured using a TD-700 Fluorometer (Turner **Design, USA)** before and after acidification (HCl 0.3 M for 1 mL of supernatant). Total Chl *a* and pheopigments were calculated according to Lorenzen's equations. Microphytobenthos physiological state measurements as well as photosynthetically active biomass measurements have been done using a Pulse Amplified Modulator fluorometer (PAM, Walz-Mess und Regeltechnik, Deutschland).

2.3 EPS and NH_4^+ extraction and analyses

EPS extraction was done immediately after sampling and sediment mixing on unfrozen sediments (Takahashi et al., 2010). In order to obtain the colloidal EPS, a 20 mL fresh sediment subsample was mixed with 20 mL of Artificial Sea Water (ASW 30 Practical Salinity Units), agitated during 1 hour at 4°C in dark conditions and then centrifuged at 3500 g and 4°C for 10 min**.** The supernatant containing **c**olloidal EPS was collected and stored at -20°C. In order to extract the bound EPS fraction, a 20 mL of ASW and ~3 g of activated Dowex (Marathon C, activated in Phosphate Buffer Saline for 1 h in the dark) was added to the cap. The samples were mixed gently at 4°C for 1 h in the dark and then centrifuged at 3500 g and 4°C for 10 min. The supernatant containing bound EPS was collected and stored at -20°C. The Dubois's method (Dubois et al., 1956) was applied to quantify the carbohydrate fraction with a using a UV-1700 Spectrophotometer (*Shimadzu, Japan*).The Bradford's method (Bradford, 1976) was adapted to a luminometer LB940 Mithras (Berthold Technologies, U.S.A.) and permitted to quantify the proteic fraction of EPS. The first sediment centimeter was partly sampled and centrifuged in order to measure the ammonium amount in sediment interstitial water following the Holmes fluorometric method (Holmes et al., 1999).

2.4 Rapid light response curves (RLCs)

Sediment chlorophyll *a* fluorescence was measured using a Pulse Amplitude Modulation (PAM) fluorimeter including a PAM-control unit and a WATER-EDF-universal emitter-detector unit (Walz, Effeltrich, Germany). This apparatus is equipped with a modulated blue light (LEDs with maximum emission at 450 nm), which serves as the same light source for the measuring beam, and the actinic and saturating lights. Irradiances were calibrated against a quantum sensor (LI-COR Li 190)

at a distance of 2 mm. A sediment mini-core (2 cm in diameter and depth) was taken from the mesocosm culture and place in a dark box where the PAM fiber optic probe is placed at a constant depth of 5 mm from the sediment surface. Replicated mini-cores were chosen randomly within the sediment core from the mesocosm culture. An estimation of the effective quantum yield of PSII (ΔF/Fm') was measured few seconds after positioning the probe (Serôdio et al., 2008), by applying a saturating flash of 800 ms at around 3800 µmol photons $m^{-2}.s^{-1}$. RLCs were then constructed by exposing the MPB biofilms to eight steps of increasing irradiance without prior dark acclima tion (around 70, 100, 150, 220, 310, 430, 710, 1050 µmol photons $m^{-2}.s^{-1}$). The duration of the irradiance steps was 30 s. Each experimental day, four replicates of each treatment were randomly performed in turn. The relative electron transport rate (rETR) was calculated at each level of irradiance, as the product of the effective quantum yield of PSII and the delivered irradiance: rETR = ΔF/Fm' × E. ETR_{max}, alpha et E_k have been calculated following the model of Eilers and Peeters (1988) in case of photoinhibition:

$$ETR = E/(aE^2 + bE + c)$$
$$ETR_{max} = 1/(b^2 + 2 \times \sqrt{a \times c})$$
$$\alpha = 1/c$$
$$E_k = ETR_{max}/\alpha$$

A matlab procedure has been applied to search for the best non-linear regression providing estimates of ETRmax, α and Ek by using the Nelder-Mead simplex method.

2.5 Erosion experiment

Erosion tests were executed using the ERODIMETER, a small-scale (1.20 m long, 8 cm wide and 2 cm high) straight transparent flume (Le Hir et al., 2007b). For each sampling day, 4 cores were sampled preserving their surface integrity and were placed by 2 into the flume (2 experiments per condition). Each sediment sample was directly transferred from a cylindrical core to the bottom of the flume (Le Hir et al., 2008). Sediment cores have been submitted to a controlled flow in a 15L water close-circuit. After an initial flow during 15 minutes, an increasing flow was applied every 5 minutes (32 successive levels) using a pump with a variable frequency drive (Fig. 1). The induced bed shear stress has been calibrated by eroding well-sorted non-cohesive particles and direct confrontation to the Shields threshold criterion (Le Hir et al., 2007a; Guizien et al., 2012). Flow discharge and differential pressure were also continuously recorded between upstream and downstream the sediment samples. The Bed Shear Stress (BSS) was calculated following the method by Guizien et al. (2012) to take into account for the differences in bottom roughness between

treatments by using a differential pressure gradient. The erosion parameters were measured by estimating the fine particle amounts in the water using a nephelometric probe (NTU), and estimating the Chl *a* concentration in the water using a fluorescence probe.

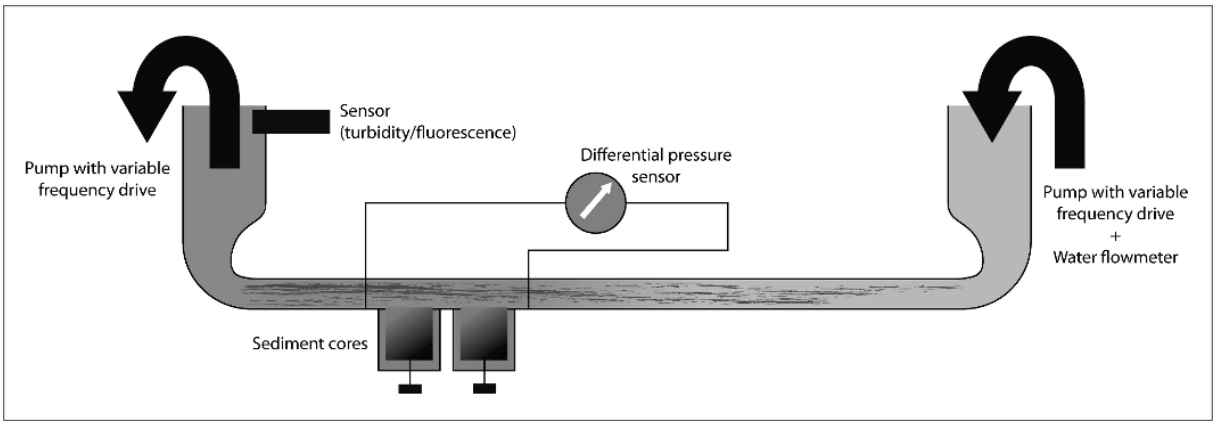

Figure 1: Schematic representation of the ERODIMETER flume

2.6 Water sampling

A duplicated volume of 0.5L was filtered at 4 different flow levels for measuring SPiM and Chl *a* (see **2.4**. SPiM data were used do determinate the erosion features of the different conditions. At 4 frequency levels corresponding to 0.166, 0.582, 1.195, 1.852 Pa (friction force), water was sampled in order to evaluate Chl *a* and suspended particulate inorganic matter (SPiM). In order to determine the SPiM content, two subsamples per level were sieved and passed through weighed and dried glass-fiber filters (Whatman GFC), washed with distilled water to avoid salt errors, packed in petrislides (Millipore, USA), and immediately stored at -20°C before analyses. The filters were dried in an oven at 50°C during 72 hours, and then during 4 hours at 450°C to estimate the organic content of resuspended material (SPoM). From the Total SPM and SPiM, the Inorganic fraction was calculated (SPiM). For Chl *a* biomass measurements, two subsamples were sieved and passed through a glass-fiber filter (Whatman GFC), fold and put in a tube at -20°C before analyses. The Chl *a* content of the sediment was extracted in 90% acetone during 24 h in the dark at 4°C. After short centrifugation, the chlorophyll extracts were measured on a Turner Designs TD 700 fluorometer (USA) following the method of Lorenzen (1967) and expressed as content ($\mu g.g^{-1}$ sediment) for the spring sampling.

2.7 Calculations and statistical tests

Fluorescence data were calibrated upon filtered Chl *a* concentration to be converted upon the basis of the most appropriate calibration curve (Fluorescence versus Chl *a*). Fluorescence data were also corrected to account for the dilution effect of sampling process, since 2 L of water was sampled for filtration at 4 successive steps all along the erosion experiment and the quantity of

filtered water was added to adjust the whole volume in the system. The rate of erosion of the chl *a* was deduced from the time derivative of the fluorescence curve, after calibration and correction for dilution effects. The mass of eroded Chl *a* was computed as the product of Chl *a* concentration (µg.L^{-1}) by the water volume (15 L), divided by this sediment area ($2 \times (\pi \times 0.045)$ in m^2. Among the 18 experiments, data of 1 experiment was not considered because of equipment failure. Erosion kinetics were analysed to determine the critical threshold for erosion by determining the intersection point with X-axis when drawing a regression line between Chl *a* (averaged for each flow step) versus log (U* +1): $\text{chl } a = \text{A} \times \log(\text{U}^* + 1) + \text{B}$, where U* is the shear velocity (in m.s^{-1}). The critical value of BSS for erosion is calculated by converting the one of shear velocity u* and by using the usual formulation between u* and τ_f, the BSS : $\tau_{f\ crit} = \rho.{\mu_{crit}}^2$. The best regression line was retained and erosion rate was determined by considering only flow steps, for which the critical BSS was reached. For the concerned data, the rate of erosion was deduced from the time derivative of the Chl *a* curve, after calibration. Erosion rates (g.m^{-2}.s^{-1}) were assessed at each step (after erosion incipient point) as the slope between the eroded chl *a* (i.e chl *a* converted in µg.m^{-2}) and Δt the time interval between each chl *a* concentration record (1 sec). The averaged erosion rate was calculated from the different values calculated per step.

Because nephelometric probe was less sensitive in the first erosion levels and problems caused by the presence of sand in the water at high flow regimes, turbidity data were not used for estimation of resuspension fluxes. Sediment erodability parameters were estimated by following the same procedure than for chl *a* but calculations relied on the filters SPiM data. Erosion kinetics calculation and representation were done using Matlab (Mathworks, USA).

GLM were performed using Minitab (Minitab inc., USA) in order to compare the results regarding to the sampling day and sediment mixture type, followed by post-hoc Tukey tests. Data were transformed when normality of distribution could not be verified. Principal Components Analyses (PCA) using the R package ADE4 (R-project) were used to identify the global effect of both mixture type and biofilm age on sediment resuspension.

3. Results

3.1 Sediment analyses

Results showed a significant difference between the benthic chl *a* concentration regarding to the sediment mixture and to the sampling day, but there was an absence of effect of the interaction between the 2 factors (Table 1). The sandier mixture (Mixture 3) was characterized by a lower chl *a* biomass than the 2 other mixtures. Even if the biomass was relatively stable from day 3 to day 9 for

the mud (Mixture 1) and sandier mixtures, the intermediate mixture (Mixture 2) was characterized by an increase of the biomass between the days 3 and 6, reaching the biomass level of the mud mixture at day 6. We must mention that the diatom biofilm growth for pure mud should be very fast (less than 3 days in fact, since the biomass was steady at a high level already at the sampled day 3). Water content varied regarding to the mixture type, increasing with the mud proportion increase, but stayed stable regarding to the day factor.

Carbohydrate content of colloidal EPS fraction differed significantly as a function of sediment mixture (Table 1), the amount of EPS increasing with the mud fraction (Fig. 2D). These EPS did not vary significantly as a function of the day of experiment (Table 1). For the bound EPS fraction, the carbohydrate content varied significantly as a function of the mixture with a larger amount for pure mud than for the 2 other mixtures. However the amount of carbohydrate from this fraction did not differ significantly at day 9 for all mixtures, with a significant effect of interaction between the 2 factors (Table 1). Indeed there was also a change in the carbohydrate amount of bound EPS (Fig. 2C) as a function of sampling days, with a significant decrease in the mud and an increase for the intermediate and sandier conditions between days 6 and 9. These two mixtures did not show significant differences either in the mixture or days of sampling. The protein component of colloidal EPS (Fig. 2B) varied significantly depending on the mixture (Table 1), with a higher proportion in the mud than for the two other mixtures in which the difference was not significant. The protein content of bound EPS (Fig. 2A) varied significantly depending on the mixture, but surprisingly this was the intermediate mixture (75%/25% of sand and mud, respectively) that showed the highest values. Protein content of bound EPS ranged from 0.061 to 0.082 $mg.gDW^{-1}$ (for the sandier to the intermediate mixture respectively), with the intermediate value of 0.075 for the pure mud. This amount did not change significantly as a function of the day factor except for the mud between days 3 and 9.

For EPS standardized by chl *a*, the protein content of bound fraction (Fig. 2E) decreased from day 3 to day 6 for the two sand-mud mixtures while it increased from day 6 to day 9 for the pure mud, reaching 8 mg EPS.µg chl a^{-1} at day 9 for all mixtures. The standardized protein amount of colloidal fraction (Fig. 2F) varied significantly as a function of mixture and day. It decreased in pure mud and sandier mixtures between day 6 and 9, but these two mixtures were characterized by higher amounts of these EPS than the intermediate mixture. Standardized carbohydrates of the bound fraction (Fig. 2G) differed as a function of mixture, day and the interaction of both. It decreased between the days 3 and 6 and remained stable between day 6 and 9 for pure mud, and inversely for the intermediate mixture. It increased continuously within the sandier mixture between

Table 1: General linear model testing the relative effect of the mixtures and day of sampling as well as their interactions for the variables measured on the cores, the erodibility characteristics, the photosynthetic parameters obtained with the PAM fluorometer, and the filtered values of Suspended Inorganic Matter (SPiM en mg.m^{-2}) obtained from the erodimeter. Significance of the statistical results is given by asterisks (* = p<0.05, ** = p<0.01, *** = p<0.001).

Variable	Mixture	M1 *vs* M2	M1 *vs* M3	M2 *vs* M3	Day	D3 *vs* D6	D3 *vs* D9	D6 *vs* D9	Mixture*Day
τ_{crit} (Chl *a*)	25.21***		***	***	0.47				2.48
Flux (Chl *a*)	3.28				0.78				0.93
τ_{crit} (SPiM)	1.72				11.88**			**	26.29***
Flux (SPiM)	15.89***	***	**		13.40**	**			20.78***
Prot. colloidal EPS	83.04***	***	***		3.95*			*	2.22
Prot. colloidal EPS (std)	11.40***	***		**	7.69**		**		0.41
Prot. bound EPS	96.10***	***	***	***	7.59***		**	**	1.64
Prot. bound EPS (std)	15.37***	***	**		5.55**	**			3.77**
Carb. colloidal EPS	38.23***	***	***	**	0.38				2.33
Carb. colloidal EPS (std)	3.23				1.40				1.25
Carb. bound EPS	63.42***	***	***		17.74***		***	***	8.67***
Carb. bound EPS (std)	32.84***	***	**	***	9.00***		**	***	6.47***
Water content	80.67***	***	***	***	2.69				1.13
Benthic Chl *a*	39.00***		***	***	7.22**	*	**		2.01
F0	4.59*			*	5.62**			**	0.34
Yield	43.66***	***	***	***	88.51***		***	***	15.19***
ETR max	2.03				0.69				2.06
Alpha	2.65				11.67***		***	**	3.56*
Ek	3.02				1.74				1.95
Filtered SPiM	1.55				0.49				0.75
Water Chl *a*	2.66				0.26				0.02

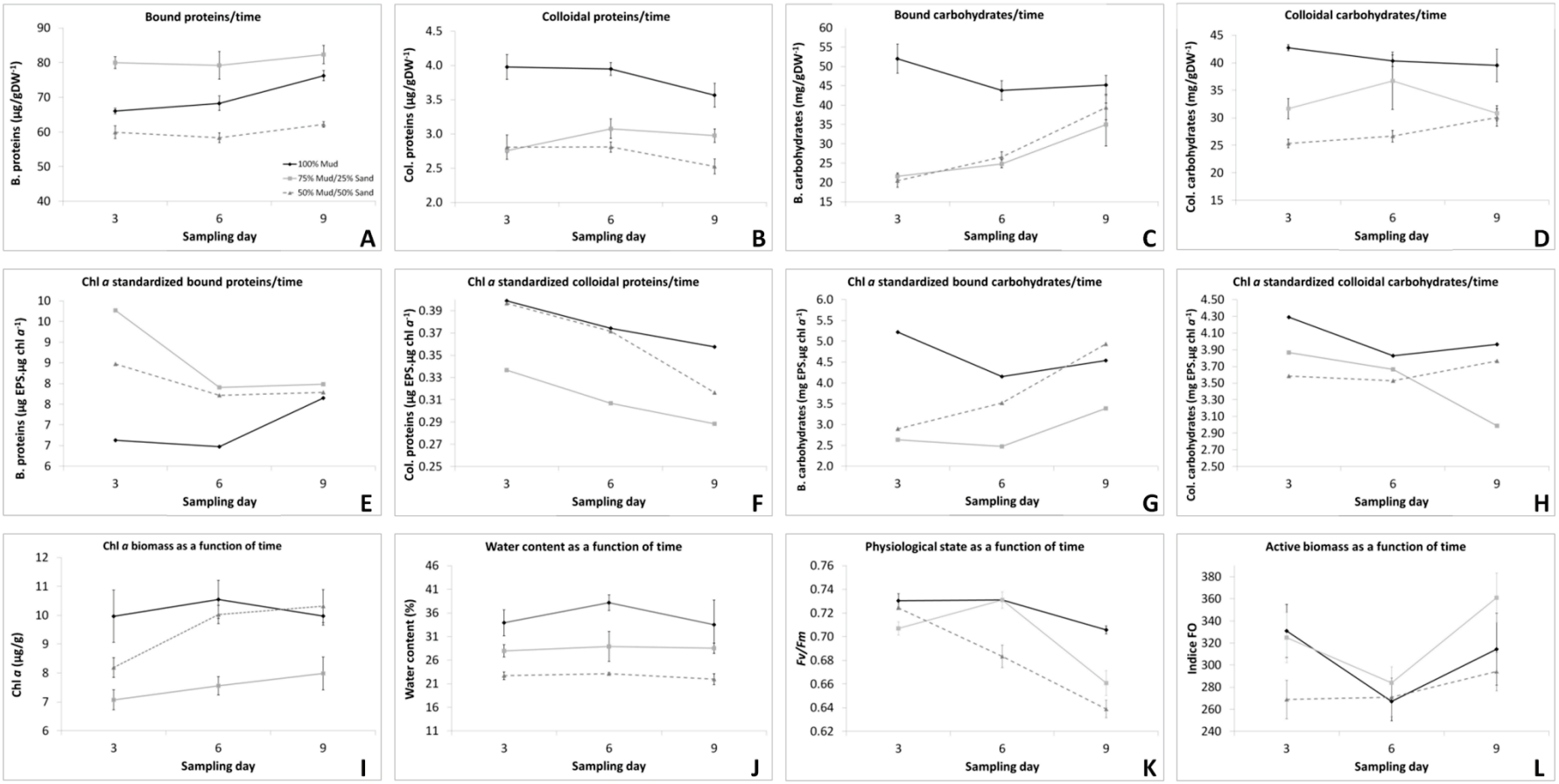

Figure 2: EPS fractions measured at the sediment core surfaces for the different sampling days. ABCD represent the different fractions (proteic and carbohydrate) of bound or colloidal EPS. EFGH represent the different fractions (proteic and carbohydrate) fractions or bound or colloidal EPS normalized by the Chl *a* biomass. I: Chl *a* as a function of time in the top first cm of the sediment. J: Water content as a function of time in the top first cm of the sediment. K: Physiological state of the biofilm as a function of time. L: Active biomass of the biofilm as a function of time.

the days 3 and 9. Standardized carbohydrates of the colloidal fraction (Fig. 2H) showed no significant differences regarding to mixture or sampling day. There was an increase in NH_4^+ concentration from porewater between day 6 and 9 for pure mud (Fig. 3). Intermediate mixture showed a slight decrease of NH_4^+ concentration between days 3 and 6 reaching a null concentration at day 6, whereas the sandier mixture showed null concentrations for all days.

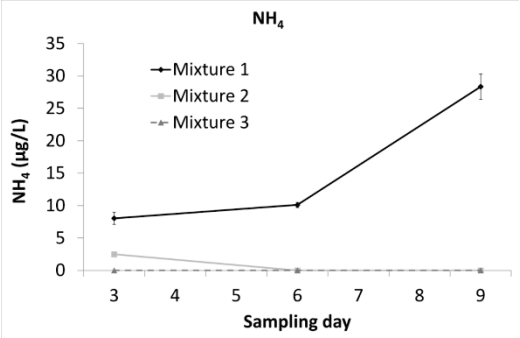

Figure 3: NH_4 interstitial sediment water content (µg.L^{-1}) as a function of time.

3.2 Photosynthetic parameters and rapid light response curves (RLCs)

The index of Photosynthetic Active Biomass (F0) was found to differ regarding to the sampling date and to the sediment mixture type (Table 1), being stable in time for the sandier mixture, decreasing between day 3 and 6 and then increasing between days 6 and 9 for the 2 other mixtures. The higher values were found for the intermediate mixture, reaching 360.95 at day 9 (Fig. 2L). The autotrophic biofilm was active with high values at day 3 for pure mud and intermediate mixture, but the biofilm was inactive during the 6 first days of the survey for the sandiest mixture. However, there was a slight increase of F0 value at day 9 for this mixture. The physiological state of microalgae given by the *fv*/*fm* ratio varied regarding to the sediment mixture type and the sampling day, decreasing for all mixtures between day 3 and 9 (Fig. 2K, Table 2). The mud mixture showed better *fv*/*fm* values than the 2 other conditions.

Table 2: Estimates of the parameters of the model of Eilers and Peeters (1988) fitted to the ETR versus PAR curves.

Mixture	Day	F_v/F_m	ETR_{max}	α	E_k
1	3	0.73 ± 0.01	561.06 ± 43.13	0.56 ± 0.04	1098.48 ± 145.67
	6	0.73 ± 0.01	571.94 ± 57.35	0.53 ± 0.01	1080.01 ± 126.87
	9	0.71 ± 0.01	564.66 ± 93.36	0.52 ± 0.02	1094.32 ± 138.69
2	3	0.71 ± 0.01	524.74 ± 19.96	0.57 ± 0.02	928.10 ± 50.79
	6	0.73 ± 0.01	571.94 ± 57.35	0.53 ± 0.01	1080.01 ± 126.87
	9	0.66 ± 0.02	601.70 ± 63.41	0.51 ± 0.03	1190.56 ± 185.35
3	3	0.72 ± 0.00	545.80 ± 16.50	0.57 ± 0.01	966.09 ± 28.29
	6	0.68 ± 0.02	559.30 ± 54.03	0.55 ± 0.03	1017.93 ± 114.15
	9	0.64 ± 0.01	482.08 ± 9.23	0.50 ± 0.02	960.18 ± 40.51

The initial slope of the RLC (α) is a measure of the light harvesting efficiency of photosynthesis and the asymptote of the curve, the maximum rate of photosynthesis (ETR_{max}), is a measure of the capacity of the photosystems to use the absorbed light energy (Marshall et al., 2000). The mixture type had no simple significant effect on α parameter, but the latter decreased as a function of the biofilm age and also the interaction between both factors (Table 1). The decrease of α as a function of culture age was more pronounced for the sandiest mixture (Fig. 4). Neither mixture type nor biofilm age had a significant effect on other parameters (ETR_{max} and E_k).

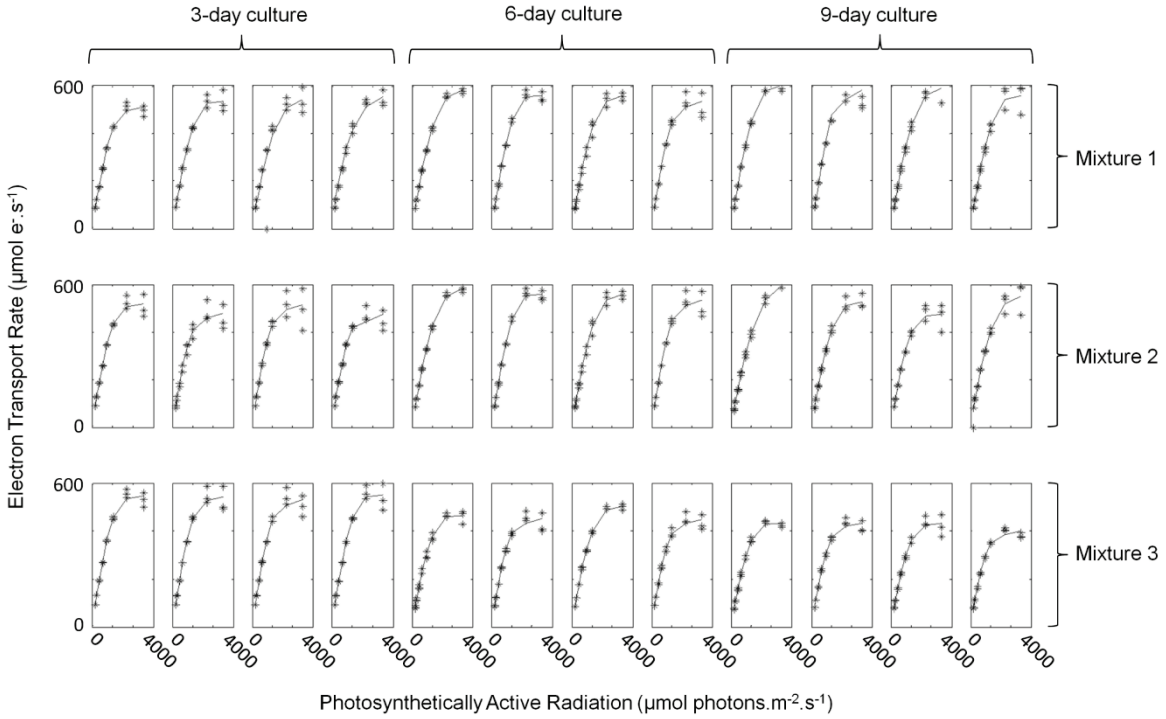

Figure 4: Rapid light response curves (RLCs) of the relative electron transport rate (rETR) of sediment core microphytobenthos (MPB) biofilms grown under 1200-2000 µmol photons $m^2.s^{-1}$ intensity. RLCs were run with 30-s light step increments. The curves were constructed using the Eilers and Peeters (1988) model.

3.3 Effect of biofilm age and mixture on erosion

Erosion kinetics of chl *a* concentration (Fig. 5) showed relatively low differences between replicates, excepted for the sandier mixture (Mixture 3) , for which the two replicates did not show high mass erosion flux. Concerning chl *a* biomass, the erosion was characterized by higher critical erosion threshold as a function of the sand content of the mixtures, and higher erosion rate for the Mixture 3 (Table 3). The pure mud is thus more

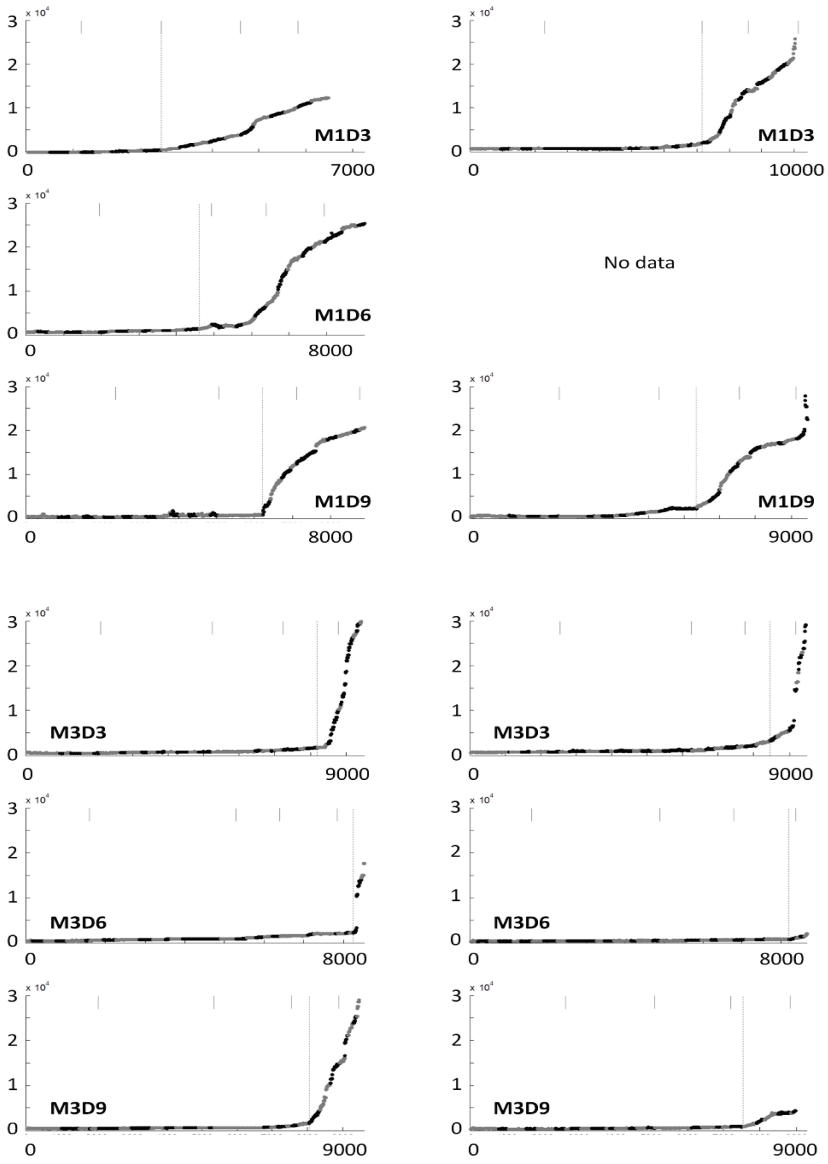

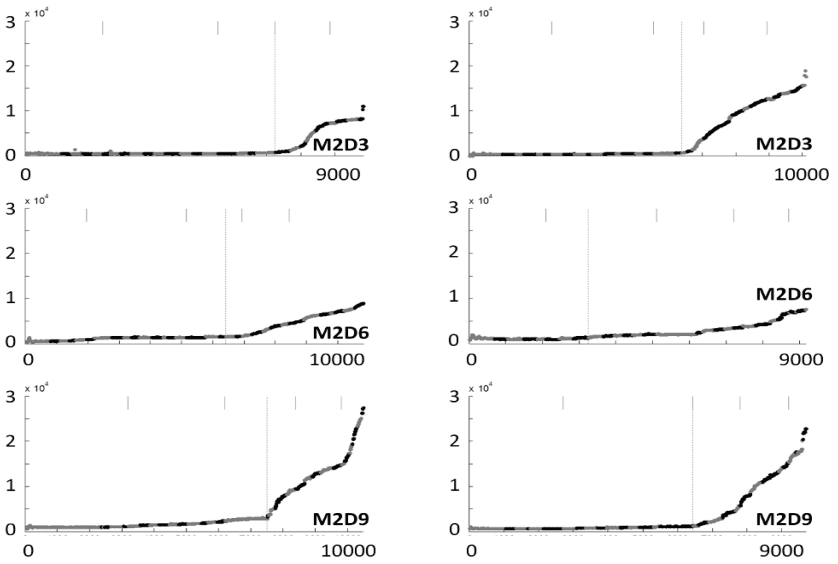

Figure 5: Erosion kinetics of chl *a* eroded (µg.m^{-2}) as a function of time (s). M = Mixture, **D** =Day. Each curve represents a replicate of simultaneous 2 cores erosion. Water samplings have been done at τ = 0.166, 0.582, 1.195, 1.852 and have been symbolized by short lines on top of the graphs.

Table 3: Flux for chl *a* (mg.m^2.s^{-1}) and SPiM (g.m^2.s^{-1}), and critical erosion thresholds "τ" (Pa).

Mixture	Sampling day	Flux (Chl *a*)	τ crit (Chl *a*)	Flux (SPiM)	τ crit (SPiM)
1	3	6.81	0.65	2.26	1.15
	6	4.77	0.46	0.20	0.60
	9	6.74	0.63	0.21	0.53
2	3	5.73	0.91	0.13	0.60
	6	1.52	0.58	0.01	0.81
	9	9.45	0.67	0.17	1.07
3	3	30.15	1.52	0.07	0.54
	6	32.31	2.48	0.04	0.58
	9	12.28	1.33	0.97	1.08

favorable for precocious erosion, while chl *a* erosion rates seem to be lower for mud compared to sandier sediments (but this effect of sediment type is not significant because of a high variability between replicates in some cases). Erosion rates were clearly more subject to variability than critical thresholds. For instance, two replicates of the sandier mixture (Fig. 5, M3D6 and M3D9) did show an absence of chl *a* erosion while high erosion fluxes were obtained for the other replicate. In the latter cases, the critical thresholds were not transcended by the applied bed shear stress in the erodimeter. For chl *a* erosion, mixture and biofilm age had no significant effect on mass erosion threshold (Table 1), and biofilm age had neither effect on erosion critical threshold (Table 1). There was an effect of mixture on chl *a* τ_{crit} (Table 1). For the SPiM, there were no significant differences between the mixtures regarding to the erosion critical thresholds, but the interaction between the 2 factors was significant. There were high values of critical threshold at the beginning of the survey for pure mud (1.15 Pa) and they showed a slight decrease at day 6 and 9, while the 2 sandy mixtures showed low values of critical threshold that progressively increased during the culture (1.07 and 1.08 Pa for mixtures 2 and 3 respectively). There was a significant increase between day 6 and 9 for Mixtures 2 and 3 (Table 1). Chl *a* erosion rate variation differed regarding to the different conditions (Fig. 2). Type I erosion can be detected by an achievement of chl *a* kinetic to an asymptotic plateau after less than 5 minutes at a given bed shear stress. For the pure mud, there was type I erosion decreasing before the end of kinetics or reaching a second state of erosion corresponding to type II erosion. The intermediate mixture was characterized by the 2 types or erosion at day 3 and 9 but only type 1 erosion on day 6. The extent of chl *a* variation was similar for the pure mud and intermediate mixture. The sandier mixture was characterized by type 2 erosion whatever the bed shear stress.

A PCA was applied to sediment and erosion variables measured (Fig. 6), and only the two first components were retained, explaining 67.15% of the total inertia. The correlation circle (Fig. 6A) showed that chl *a*, water content and EPS colloidal fraction were well represented on the 1st axis, explaining 49.13% of the total inertia. Chl *a* τ_{crit} and erosion rate were well represented on the 1st axis too, anti-correlated with the previous variables. SPiM τ_{crit} and flux were well represented on the 2nd axis explaining 18.02% of the total inertia. These variables were closely and positively related to the carbohydrates of the EPS bound fraction. The scatter-plot of individuals (Fig. 6B) showed a clear difference between the experimental conditions, which were merged into three groups corresponding to the 3 tested mixtures. Pure mud appears to be mostly characterized by higher values for all EPS extracts except EPS bound (p), whose values were higher for the intermediate sandy mixture. The sandier mixture is characterized by higher chl *a* erosion thresholds and erosion rate.

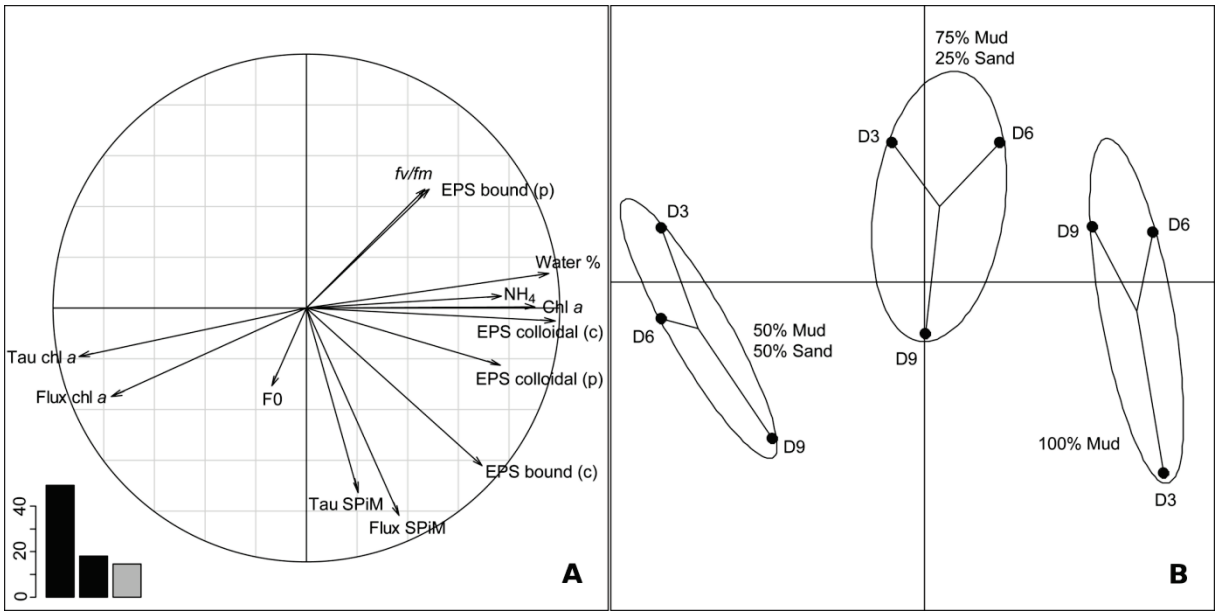

Figure 6: Principal component analyses realized on the different biological and physical variables. Tau = Critical erosion threshold, Flux = Mass erosion flux, (p) = proteins, (c) = carbohydrates, fv/fm = physiological state of the biofilm).

4. Discussion

4.1 Development and physiological state of the biofilm

There was a clear effect of mixture on Chl *a* biomass of the sediment, the sandier mixture being characterized by a lower Chl *a* biomass. Under natural conditions, cohesive sediments are known to be colonized by epipelic diatoms (Admiraal et al., 1994). On the contrary, in regions characterized by higher hydrodynamic stress, epipsammic species live attached to sediment grains. In this study, the diatom inoculum that was added to the sediment mixture came from an estuarine mudflat and they were composed of epipelic species assemblage. Since there was no hydrodynamics in the water tank we used for this experiment, this observation shows that epipelic diatom communities are less adapted to sand-mud mixtures. This assumption is confirmed by the lower *fv*/*fm* ratios found for the 2 sand-mud mixtures. A higher permeability of the sediment reduces the accumulation of regenerated nutrients in the pore water (Ehrenhauss et al., 2004), thus microphytobenthos development could be limited in the sandier mixture. This observation is in the line of observations made by van de Koppel et al. (2001).

The absence of NH_4^+ between day 6 and 9 for the intermediate mixture and its absence for the sandier mixture lead to a nutrient limitation, affecting negatively the *fv/fm* ratio for these two sand-mud mixture. Photo-biology of the biofilm is driven by nutrients and light and nutrient availability were not the same for all mixtures since the light was a controlled factor to be constant

between treatments. The decrease of α as a function of culture age was more pronounced for the sandier mixture (Table 1). Moreover, the mud mixture showed higher *fv*/*fm* values than the 2 other conditions. For these reasons, photobiology of the biofilm was likely to be affected after some days by the sand content of the sediment and this effect must be related to the decrease of water content and the rarefaction of nutrient (especially ammonium concentration of porewater that clearly disappeared from porewater). However, the *fv*/*fm* ratio was higher than 0.6 at all occasions (this critical value being considered as an index for nutrient depleted microalgal cells), so that benthic diatoms was rather affected by nutrient limitation than a strong stress due to total disappearance of a nutrient. The light harvesting efficiency of photosynthesis decreased as a function of the biofilm age, also indicating a possible loss of nutrients as a function of time and biofilm growth.

Colloidal EPS (in terms of carbohydrate as well as protein composition) confirm the interacted effects of sand enrichment and culture age affecting the photobiology. For the pure mud, the level of secreted colloidal EPS remained high all along the survey. The sandiest mixture was clearly the sediment with the lowest colloidal EPS amounts. Even though EPS losses must be amplified in sand because of a higher EPS hydrolysis and/or washaway, benthic diatoms must also secrete less colloidal EPS in sand, likely because of a decrease of photosynthesis efficiency caused by a nutrient stress. Smith and Underwood (1998) clearly showed that there is a direct linkage between photosynthesis and the metabolic pathway of colloidal EPS secretion. Contrary to Orvain et al. (2003) or Staats et al., 2000b), no overflow metabolism apparent even in the pure mud (maybe because the diatom culture was not long enough).

4.2 Sediment cohesiveness and MPB biofilm development: Role of bound EPS fraction

There was a clear relationship between the mud fraction of the sediment and the Chl *a* biomass of the sediment. Since the MPB inoculums came from mudflats, it was natural to obtain a better growth of epipelic diatom in pure mud. On field sediments, species composition of benthic diatoms often differs substantially because species are better adapted to one substrate than other substrates (Round, 1991). However, after 6 days of experiment, the biomass levels of mixture 2 were not significantly different from the pure mud condition, probably indicating: (i) a decrease of the growth rate with the sand content and (ii) a physiological adaptation of the diatoms to live in this less appropriate sediment. The *fv/fm* decreased during the experiment because of nutrient limitation (at least NH_4^+ as revealed by its rarefaction), and this effect was more pronounced for sand that cannot retain porewater and its nutrients. However, the proteic fraction of bound EPS was more secreted for the intermediate sand/mud mixture. Zetsche et al. (2011) have shown that proteins associated with the bound EPS fraction appeared to vary with the effect of EPS on permeability, with higher levels of

EPS leading to a decrease of sediment permeability. Lubarsky et al. (2010), have shown that protein fraction of the EPS plays a crucial role for adhesion/cohesion of the substratum. The higher levels of bound EPS in Mixture 2 were probably secreted in order to decrease the permeability and to better resist to unfavorable substrate, thus creating a photosynthetically active biofilm. This could explain that chl *a* biomass reached a high level after 6 days, in spite of the presence of sand. Protein fraction of bound EPS is probably involved in the pioneering stages of biofilm development (Orvain et al., n.d.), explaining their higher production - when normalized by Chl *a* biomass - in mixture 2 and 3 at day 3, and then their decrease to a normal production rate at day 9 for all mixtures.

4.3 Mixture and biofilm age effect on resuspension phenomenon

A significant effect of biofilm age on resuspension was found in this experiment in terms of physical sediment thresholds for the two sand mixtures. This result is in agreement with those of Sutherland et al. (1998), Droppo et al. (2007) or Lubarsky et al. (2010), who found that the biofilm age influenced the erosion characteristics by increasing erosion threshold during the growth stage of the biofilm. Consolidation processes alone is supposed to affect positively the sediment critical erosion threshold, but the compaction effect appears mostly almost in the first days (Stone et al., 2008). The days 3, 6 and 9 of culture may correspond to the phases of the biofilm growth stage, while biofilm mostly affect biostabilization during lag (positive effect) and senescent (negative effect) stages of its development. As a consequence, the critical erosion threshold was higher at day 3 than for the other days for pure mud, as observed by Lubarsky et al. (2010). The higher $\tau_{crit\ (SPiM)}$ for Mixture 1 at day 3 confirms the fact that initial lag stage must be determinant for stabilization of the bed (an increase of water content could then make diminish the critical threshold). These results have to be taken with caution since significant differences in growth times and microbial diversity between samples may appear (Droppo et al., 2007), underlining the difficulty to quantify a definitive critical bed shear stress for erosion based on biofilm age alone. The sediment settling process probably acts in favor of the increasing $\tau_{crit\ (SPiM)}$ within the days of experiment for mixtures 2 and 3.

Besides the biofilm age effect on resuspension phenomenon, this study clearly showed that sediment composition modifies significantly erosion resistance, with a higher $\tau_{crit\ (SPiM)}$ between 25% and 50% of sand content after 9 days of consolidation. The mud fraction therefore determines the sediment behaviour and the erosion law to be applied; however, the erosion flux of any class of sandy or muddy types is always proportional to the mass fraction of this class in the surface sediment. These results are in agreement with those of (Mitchener and Torfs, 1996), who tested 3 sand-mud mixtures (100% mud, 89% mud and 50% mud) and found that the greater sediment $\tau_{crit\ (SPiM)}$ was found for the 50/50 mixture. They estimated that the maximum $\tau_{crit\ (SPiM)}$ occurred between 30 and

50% mud content. The formula established by (Ahmad et al., 2011) also confirms this observation, with a maximum in the $\tau_{crit\ (SPiM)}$ achieved at 50 percent of sand. Panagiotopoulos et al. (1997) found increased $\tau_{crit\ (SPiM)}$ values with greater mud fractions when adding mud to pure 152.5µm sandy sediment from 0 to 50% mud. These results illustrate the interest of studying mixtures instead of pure mud or pure sand sediment, mixtures being able to behave like cement, thus enhancing erosion resistance or at least decreasing resuspension potential. The dynamic bed armouring mentioned by (Le Hir et al., 2011) explains the fact that the sand layer at the sediment surface is easily resuspended, but a large number of sand grains immediately settle, limiting or preventing the resuspension of underlying sediment, reducing significantly erosion rates. Thus sand-mud mixtures may have less erosion resistance than pure cohesive sediments, but erosion rates are lower because of this dynamical bed armouring.

The carbohydrates content within the EPS colloidal fraction were well related to the water content of the sediment. Because of their solubility in water, de Winder et al. (1999) hypothesized that they may disappear as soon as the tide comes in and therefore contribute only to a limited extent to sediment stability. On the contrary, they pointed out that the carbohydrates content within the EPS bound fraction may play a prominent role in the sediment grain cohesion. In this experiment, carbohydrates of the EPS bound fraction clearly explain variations in SPiM critical thresholds. Hydrophilic colloïdal EPS are related to the water content, thus explaining that they are not implicated in biostabilization. The adhesion properties of carbohydrates of the EPS bound fraction are directly responsible for biofilm establishment and thus biostabilization of the surface sediment. Wigglesworth-Cooksey et al. (2001) confirmed that the diatom matrix extracellular carbohydrate polymer is largely responsible for sediment stabilization and that soluble polymer implied in diatom motility plays no part in the sediment stabilization process. Our results are in agreement with the previous with the bound carbohydrates playing a predominant role in sediment erosion thresholds, which depend on the total amount of bound carbohydrates in the top layer. The Dowex extraction allow to better target the EPS implicated in biostabilization, as shown also by Gerbersdorf et al. (2009). These EPS appear to be well related to the erosion critical thresholds for every condition, with the higher concentrations corresponding to the respective higher erosion critical thresholds observed.

For the first time, $\tau_{crit\ (SPiM)}$ and $\tau_{crit\ (chl\ a)}$ were clearly differentiated for sand/mud mixtures. Concerning the chl *a* erosion, the more the sediment is rich in chl *a* the more biofilm that forms detaches quickly. Thus, the biofilm formation for pure mud results in an earlier detachment (with low $\tau_{crit\ (chl\ a)}$). Conversely, in sand mixtures the biofilm formation is more difficult and erosion of chl *a* is

also more difficult, happening for higher erosion thresholds. The biofilm constitutes a more labile armoring for pure mud, whereas sand enrichment increases chl *a* erosion thresholds. The sand vertical segregation of the sediment, along with vertical distribution of epipelic diatoms, must be the main factor responsible for the differences observed between Chl *a* and SPiM erosion.

5. Conclusion

In this study we aimed to clarify the respective roles of biofilm age and mixtures effect on resuspension phenomenon. Between 3 and 9 first days of biofilm development, biofilm age did significantly affect erosion critical thresholds for Chl *a* resuspension, and affected those of SPiM for sand-mud mixtures during biofilm growth. This experiment highlighted the difference between Chl *a* and SPiM erosion characteristics which differ between treatments, biofilm being able to be eroded before sediment, when they are well constituted (especially in pure mud). Sediment resuspension seemed to be mostly driven by physical constraints like differential compaction and vertical sand segregation as a function of mud content. Proteins of the EPS bound fraction appear to have a critical role in the pioneering stages of biofilm installation, allowing its formation in a less favorable environment by increasing cohesion and lowering sediment permeability. Carbohydrate content of the bound EPS fraction was directly related to the sediment erodability, independently from mixture type or biofilm age. This reveal the relative complexity of bound EPS heteropolymers, with different properties associated to protein and carbohydrate composition of this EPS matrix. Sediment mixture composition impacts biofilm shaping by providing a more or less favorable habitat for MPB, leading to differences in MPB biomass between mixtures. However, mixture composition seems to be the main factor involved in resuspension phenomenon, with an optimum reached near a equilibrate ratio between mud and sand. Pure mud allowed rapid growth of epipelic diatoms, but was also favorable to early erosion of the biomass due to the rapid formation of the biofilm and its higher fragility. Paradoxically, sand enrichment makes decrease the chl *a* erodability (higher critical bed shear stress and lower erosion flux). The formation of a biofilm in sand mixtures is possible through the high production of bound EPS and its composition in proteins, which consolidates the biofilm. The sandy sediments are therefore more stabilized by bound EPS than pure mud. The biofilm being less well established, it would need a high depth mass erosion to successfully pull the diatoms. The dynamic sand layer process and its protective effect evoked by Le Hir et al. (2011) have certainly explained the difficulty to erode chl *a* that is associated with the muddy fraction that is located deeper. Thus, sand enrichment is unfavorable to the epipelic diatom growth, as well as to their exportation to the water column via erosion. This explains well field observations made by Ubertini et al. (2012), since chl a

exportation in the water column was detected in the muddiest areas of the ecosystem in Bay des Veys (Normandie, France).

Acknowledgments

We would like to thank the General Council of Low-Normandy for their financial support.

Chapitre VI

Evaluation de l'impact du bioturbateur *Cerastoderma edule* sur la remise en suspension du sédiment et du microphytobenthos associé : étude en canal

© Heather Angel

« Le cerveau des poètes est un fond de mer où bien des coques reposent. »

Paul Valéry

Assessment of the bioturbator *Cerastoderma edule* impact on sediment and microphytobenthos resuspension: A flume study

Martin Ubertini[1,2], Francis Orvain[1,2,3]*, Christiane Rakotomalala[1,2], Sébastien Lefebvre[4], Johann Lavaud[5], Jean-Claude Duchêne[6]

[1] *Université de Caen Basse-Normandie, FRE3484 BioMEA, Caen, France*
[2] *CNRS INEE, FRE3484 BioMEA, Caen, France*
[3] *CNRS, UMR 7208 BOREA, Muséum d'histoire naturelle, CRESCO, Dinard, France*
[4] *Université de Lille1, UMR CNRS 8187 LOG ''Laboratoire d'Océanologie et Géosciences'', Station Marine de Wimereux, Wimereux, France*
[5] *Université de La Rochelle, UMR CNRS 6250 LIENSS, La Rochelle, France*
[6] *Université de Bordeaux 1, UMR 5805 EPOC – OASU, Station Marine d'Arcachon, France*

En préparation pour le journal :

"**Plos Biology**"
IF=11.452

PLoS BIOLOGY
a peer-reviewed open-access journal published by the Public Library of Science

Résumé

L'érodabilité du sédiment intertidal varie selon différents facteurs physiques, chimiques et biologiques. Par le processus de bioturbation, la macrofaune benthique peut déstabiliser les sédiments, induisant des événements de remise en suspension dans la colonne d'eau. Même si l'hydrodynamique (courants, vents) est considéré comme le premier facteur impliqué dans la remise en suspension de la chl *a* benthique, la bioturbation peut avoir un rôle important dans ce processus à l'échelle d'une baie. La coque *Cerastoderma edule* est un bivalve suspensivore largement distribué sur la majeure partie des côtes européennes. L'effet de la bioturbation par *C. edule* sur la remise en suspension des sédiments a été étudié par plusieurs auteurs, aboutissant à des conclusions différentes quant à son effet stabilisateur ou déstabilisateur net sur les sédiments. L'équilibre entre la stabilisation directe et indirecte peut dépendre du comportement de la coque et des concentrations alimentaires, qui peuvent dépendre tous deux de la contrainte de cisaillement au niveau du sédiment. Cette étude vise à clarifier le rôle de *C. edule* dans le phénomène de remise en suspension, y compris son effet sur le biofilm sous contrôle hydrodynamique. Un canal benthique, l'érodimètre, a été utilisé pour contrôler précisément la contrainte de cisaillement "", les seuils critiques d'érosion et les flux érosifs au sein d'un mélange sablo-vaseux enrichi en diatomées benthiques. Le dispositif a été amélioré afin de mesurer l'état physiologique du biofilm et la microtopographie de la surface sédimentaire avant et après l'érosion. Un suivi de la bioturbation par des mesures d'actographie a également pu être mené au cours du cycle d'érosion. Cette expérience nous a permis de caractériser le comportement et la capacité de *C. edule* à exporter de la chl *a* dans la colonne d'eau. L'adduction des valves semble être le principal facteur impliqué dans la remise en suspension des sédiments de masse et de la chl *a* associée. La chl *a* exportée était dépendante de la biomasse de coques. En l'absence de courant, les fortes biomasses de coques induisent une croissance accrue du microphytobenthos. Paradoxalement, sous l'influence de l'hydrodynamisme, la bioturbation des coques à des biomasses élevées accroît l'exportation de la chl *a* vers la colonne d'eau, montrant l'importance potentielle de *C. edule* en tant qu'ingénieur écosystémique dans les écosystèmes marins côtiers, capable à la fois de stimuler la production et l'exportation de MPB vers la colonne d'eau.

Abstract page

The erodibility of the intertidal sediment varies with different physical, chemical and biological factors. Through bioturbation activities, benthic macrofauna can destabilize the sediment, leading to resuspension events in the water column. Even if hydrodynamics (currents, wind) are considered as the first factor implicated in benthic chl *a* resuspension, bioturbation may have a significant role in this process at a bay scale. The common cockle, *Cerastoderma edule*, is a filter-feeding bivalve which is widely distributed along most of European coasts. Bioturbation effect of *C. edule* on sediment resuspension has been studied by some authors, leading to different conclusions about its net stabilizing or destabilizing effect on the sediment. The balance between direct stabilization and indirect stabilization may depend on the cockle behavior and food concentrations, which may depend both from the bed shear stress. This study aimed to clarify the role of the cockle *C. edule* in resuspension phenomenon, including its effect on biofilm under hydrodynamic control. An Erodimeter flume was used to precisely control bed shear stress "τ", critical erosion thresholds and erosion flux of relative fraction in mixed sediment enriched in benthic diatoms. The device was improved with multiple features in order to measure physiological state of the biofilm and µtopography of the sediment surface before and after erosion, and a bioturbation monitoring through actography measurements during the erosion cycle. This experiment allowed us to characterize the behavior and the ability of *Cerastoderma edule* to export chl *a* in the water column. Valve adduction appeared to be the main factor involved in the mass resuspension of the sediment and associated chl *a*. The exported chl *a* was dependant from cockle biomass. In the absence of current, high cockle biomass enhanced microphytobenthic growth. Paradoxically, cockle bioturbation at high biomasses also enhance exportation of MPB to the water column under hydrodynamics, showing the potential importance of *C. edule* as an ecosystem engineer in coastal ecosystem, able to both stimulate MPB production and export this production to the water column.

Introduction

For a long time disregarded or ignored, the key role of benthic macrofauna in biogeochemical cycles and in benthic-pelagic coupling is now well recognized (Lohrer et al., 2004) and integrated in ecosystem modeling (Schiffers et al., 2011). Through bioturbation activities, benthic macrofauna can destabilize the sediment (Pillay et al., 2007b; Soares and Sobral, 2009), leading to resuspension events in the water column. The erodibility of the intertidal sediment varies among different physical, chemical and biological factors. In fact, the balance between biostabilisation and bio-destabilisation is controlled by sediment properties, diatom biofilms through exopolysaccharides production (EPS) (Tolhurst et al., 2002; Consalvey et al., 2004; Spears and Saunders, 2008) as well as physical armouring (Tolhurst et al., 2003), and benthic macrofauna (Orvain et al., 2004). The distinction between stabilizer and destabilizer species is not obvious since almost all benthic organisms have a high diversity of bioturbatory mechanisms (Jumars and Nowell, 1984). For example lugworms *Arenicola marina* burrow the sediment and defecate at the sediment surface, creating an erodible biogenic fluff layer (as defined by Orvain et al., 2012), but secrete mucus that sticks grains on the burrow walls (Kristensen, 2001). Bioturbation activity is defined recently by Kristensen et al. (2012) as *all transport processes carried out by animals that directly or indirectly affect sediment matrices. These processes include both particle reworking and burrow ventilation*. These authors classified bioturbators in 4 groups as a function of their bioturbation type: biodiffusors, upward conveyors, downward conveyors and regenerators. These activities may reduce erosion thresholds and increase erosion rates at the water-sediment interface (Willows et al., 1998). Quantification of the resuspension impact is difficult due to the spatio-temporal variability of macrofauna species and densities at an ecosystem scale. However, even if hydrodynamics (currents, wind) are considered as the first factor implicated in benthic chl *a* resuspension (De Jonge and Van Beusekom, 1995), bioturbation may have a significant role in this process at a bay scale (Ubertini et al., 2012).

The common cockle, *Cerastoderma edule*, is a filter-feeding bivalve which is widely distributed along most of European coasts (Rueda et al., 2005). High densities make this mollusk predominant in terms of biomass is some ecosystems (Beukema, 1976; Ubertini et al., 2012). Bioturbation effect of *C. edule* on sediment resuspension has been studied by some authors, leading to conclusions about a destabilizing effect (Ciutat et al., 2006, 2007; Neumeier et al., 2006; Montserrat et al., 2009). Andersen et al. (2010) did not observe a significant effect of densities of *C. edule* for undisturbed sediment, and attributed that result to the fact that previous studies were carried out on manipulated sediment in lab, inducing increased bioturbation of the cockles. These studies did not take into account the size or age of the cockles; however for equivalent biomasses adult cockles may have different effects on sediment erodibility (de Montaudouin, 1997). Moreover,

bioturbation activity has to be related to microphytobenthos (MPB) biofilms which are present on the field. MPB can stabilize the sediment by EPS production, and the bioturbation activity by *C. edule* can both indirectly stimulate MPB through nutrient support (Lindström Swanberg, 1991) or directly destabilize the sediment through valve adduction and burrowing (Flach, 1996). There is also a biogenic matrix that is created when the cockle displacements handle the sediment surface around their burrows, with similar effects than for *Scrobicularia plana* even if the nature of the biogenic matrix is different (biodeposits for *S. plana* and tracks due to active movements for the cockle). The balance between direct stabilization and indirect stabilization may depend on the cockle behavior and food concentrations, which may be mediated both by bed shear stress. In fact, *C. edule* is responsible for increasing bed roughness through bioturbation and increased bed shear stress due to active valve adduction (Ciutat et al., 2007).

Macrofauna is able to control the microphytobenthic biomass and thus controls indirectly its production by maintaining low biomasses (Blanchard et al., 2001). Feedbacks between bivalve grazing and phytoplankton production has been reviewed by Prins et al. (1998), showing that the phytoplankton reduction and concomitant biodeposition may lead to increase benthic mineralization and thus nutrient availability for primary producers. The feedbacks processes may exist within the benthic environment (although not shown yet), since many species of the macrozoobenthic community feed on microphytobenthos but can also increase resuspension (Taghon et al., 1980; Nowell and Jumars, 1987). As a consequence, low biomasses are maintained both by direct feeding and indirect exportation by a mediation of resuspension processes. These 2 processes could favor primary production by facilitation processes. Sediment manipulation by macrofauna through bioturbation can modify the sediment properties and nutrient redistribution by increasing nutrient release in the water column (Biles et al., 2002). Morever, microrelief due to bioturbation increases the sediment surface (Neumeier et al., 2006) and enhance microphytobenthic biomass. Cockles have been shown to modify the properties of the sediment by reducing the fine fraction mobilization, thus increasing the sand-mud ratio of the sediment (Montserrat et al., 2009). The resulting sediment was less propitious for microphytobenthic development, and led to lowering erosion thresholds.

This study aimed to clarify the exact role of the cockle *C. edule* in resuspension phenomenon, including its effect on biofilm under hydrodynamic control. An erodimeter flume was used to precisely control bed shear stress "τ", in order to accurately evaluate critical erosion thresholds and erosion flux of relative fraction in mixed sediment. The device was improved with multiple features in order to measure physiological state of the biofilm and microtopography of the sediment surface before and after erosion, and a bioturbation monitoring through bioturbation activity recording

during the erosion cycle. *C. edule* was expected to have a negative effect on both sediment stability and a positive effect on physiological state of the biofilm as a function of its biomass.

Materials and Methods

Cockle Substrata and biofilm preparation

A sediment mixture has been prepared from natural sediments coming from the Baie des Veys (Normandy, France), consisting in 50% mud / 50% sand. This ratio was chosen as a good habitat for the cockle *C. edule* which was mostly found in those sediment types (Ubertini et al., 2012). In order to eliminate the macrofauna naturally present and shell fragments, the sediments have been dried, rehydrated, and then sieved using a 1 mm mesh size. Sediment was then dispatched in eighteen 20 cm diameter cores, with a depth of 20 cm. At each core, a well-defined cockle density was introduced. All individuals were measured and ranked per class (<5mm, 5-9mm, 9-14mm, 14-20mm for juveniles and 25-30mm for adults), and an equal number of individuals was selected to have an average size set to a constant value for adults and juveniles, by respecting a homogeneous multi-class distribution. Due to the patchy distribution of cockles within the cores, there was a different distribution between the mesocosm cores and erodimeter sub-cores. Thus, at the end of the erosion sequency, individual exact biomass present in the core were measured. Different densities of macrofauna were tested by differentiating the juveniles and adults (Table 1), in order to determine the effect of density and age of the cockles on the sediment and associated MPB resuspension in the water column. Each condition was tested twice (2 replicate experiments), with a total of sixteen experiments combining the effects of stocking density and age plus two controls without cockles were tested. A MPB inoculum was prepared with epipelic diatoms collected on a mudflat (La Rochelle, France). The latter was extracted from its originating sediments and mixed with the prepared mixture of controlled and defaunated sediment. This enriched mixture was put down within the first top cm of the cores. The core surface was then wreathed in order to be uniform as best as possible on the whole surface. The cores were placed in a tidal mesocosm able to simulate a high/low tide alternation every 6 hours in order to simulate one immersion diurnal phase and emersion nocturnal phases. For this, a night and day alternation was applied too with adapted neon lights, with a light intensity of 250-300 µmol photons $m^2.s^{-1}$ at the core surface. Each core was submitted to seven days in mesocosm i) for the MPB to create a biofilm at the surface, and being active during its exponential growth stage (Sutherland et al., 1998; Orvain, Le Hir, et al., 2003) ii) for the cockles to create their micro-environment, take a natural position in the sediment and get used to their new habitat. The temperature was set at 14°C, a temperature corresponding to spring season.

Pigments extraction and analyses

Sediments samplings were done for each core after 7 days during diurnal emersion period. The first upper cm of the sediment was sampled and mixed, and fresh/freeze dried weight measurements were done to obtain the water content of the sediment. MPB biomass was assessed by measuring the chlorophyll *a* (Chl *a*) content following the Lorenzen's method (Lorenzen, 1967). Chloropigments were extracted from 100 mg freeze-dried sediment subsamples with 90% acetone solution for 24 h at 4°C in the dark. After centrifugation (5 min, 2000 g), fluorescence of the supernatant was measured using a TD-700 Fluorometer (Turner **Design, USA)** before and after acidification (HCl 0.3 M for 1 mL of supernatant). Total Chl *a* and pheopigments were calculated according to Lorenzen's equations.

EPS extraction and analyses

EPS extraction was done immediately after sampling and sediment mixing (Takahashi et al., 2010). In order to obtain the colloidal EPS fraction, a 20 mL fresh sediment subsample was mixed with 20 mL of Artificial Sea Water (ASW 30 Practical Salinity Units), agitated during 1 hour at 4°C in dark conditions and then centrifuged at 3500 g and 4°C for 10 min. The supernatant containing **c**olloidal EPS was collected and stored at 4°C. In order to obtain the bound EPS fraction, a 20 mL of ASW and 1 g of activated Dowex (Marathon C, activated in Phosphate Buffer Saline for 1 h in the dark) was added to the cap. The samples were mixed gently at 4°C for 1 h in the dark and then centrifuged at 3500 g and 4°C for 10 min. The supernatant containing bound EPS was collected and stored at 4°C. The Dubois's method (Dubois et al., 1956) was applied to quantify the carbohydrate fraction using a UV-1700 Spectrophotometer (*Shimadzu, Japan*).The Bradford's method (Bradford, 1976) was adapted to a luminometer LB940 Mithras (Berthold Technologies, U.S.A.) and permitted to quantify the proteic fraction of EPS. Sediment was partly sampled and centrifuged in order to measure the ammonium amount in sediment interstitial water following the Holmes fluorometric method (Holmes et al., 1999).

Photosynthetic parameter monitoring

For each sampling day, one core was sampled preserving its surface integrity and directly transferred from a cylindrical core to the bottom of the flume used for erosion experiments (Le Hir et al., 2008). Before and after each of the erosion experiments, several measures were done on the sub-core used for erosion (Fig. 1). Firstly, variable chlorophyll a (Chl *a*) fluorescence was measured using a Pulse Amplified Modulation (PAM) Chlorophyll fluorometer (Walz Imaging Pam, IMAG-CM). Fluorescence was excited by a very weak (non-actinic) modulated 470 nm light beam. After 2

minutes dark-adaptation, continuous actinic light of adjustable intensity was applied for rapid light curves establishment: the irradiance was gradually increased from 0 to 700 µmol photons·m^{-2}.s^{-1} through 8 steps of 10 s each (0, 20, 55, 110, 185, 280, 395, 700 µmol photons m^{-2}.s^{-1}). 800 ms pulses of saturating blue light (2800 µmol photons·m^{-2}.s^{-1}) were used in order to monitor the evolution of maximal fluorescence during actinic light exposure at the end of each light step and 8 values of F and Fm' were obtained. F corresponds to the fluorescence, ranging from F0 which is defined as the

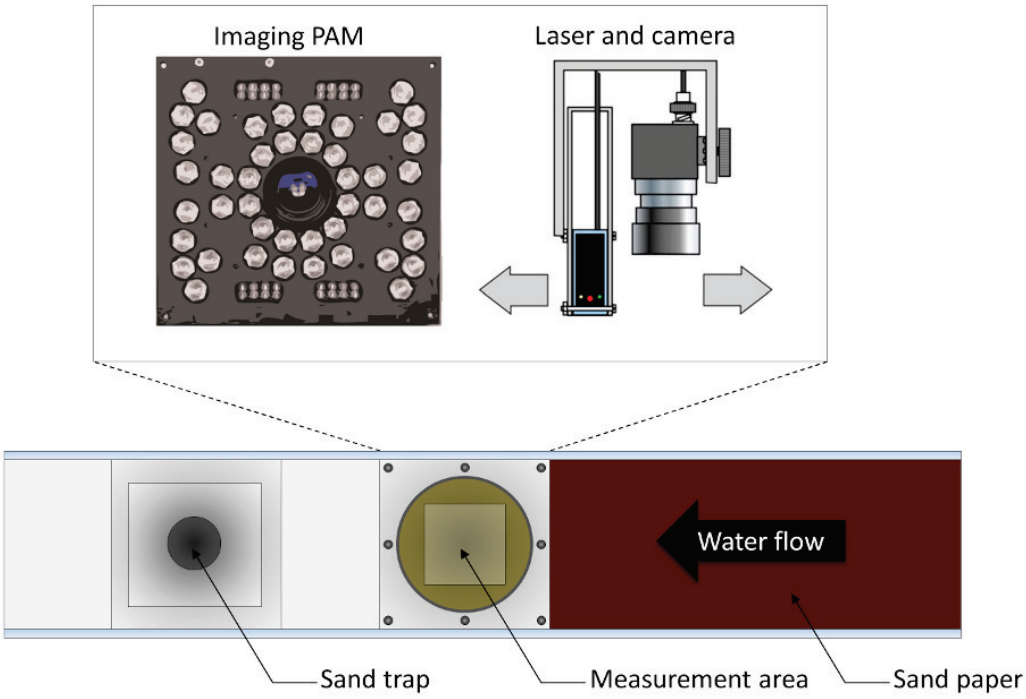

Figure 1: Additional devices used with the ERODIMETER

minimum fluorescence and Fm' which is defined by the maximum fluorescence. The relative electron transport rate (rETR) was calculated at each level of irradiance, as the product of the effective quantum yield of PSII and the delivered irradiance: rETR = ΔF/Fm' × E. The photosynthetic parameters ETR_{max}, alpha et Ek have been calculated following the Webb et al. (1974) model. The fluorescence quenching parameters NPQmax, n and E50 have been optimized with the equation of Serôdio and Lavaud (2011). At the end of erosion sequence, new measures PAM fluorometry were performed to assess the effect of cockles and hydrodynamics on both biofilm photosynthetic parameters. The method for producing maps of photosynthetic methods from Imaging PAM data comprised a first analysis of the color degree (grey intensity) for each pixel of the 8 pictures obtained for F and F'_m. The color index was then converted in F and F'_m data by using the averaged value given by the IPAM device. The first step of treatment was performed by JC Duchêne's home-made programs (using MicrosoftC software), while the second step was performed by F. Orvain's home-made programs that were developed using the Matlab software.

Microtopography

Secondly, a high resolution scan of core surface topography was done over a central 5*5 cm central area, with a horizontal resolution of 200 µm*200µm, using a laser telemeter (Sick OD80), attached under a set of motorized cross tables (401XR Parker Hannifin precision linear positioners with 5mm ball screw, connected to ViX500 Microstepper Indexer Drives with XL-PSU power supplies, providing a 1.25 µm precision). The telemeter signal was sent to an Analog Device acquisition board (PCI-6220 with NiDaq driver), converted to voltage and processed by a set of programs and drivers (MTOPO program, for MicroTOPOgraphic program, written in Microsoft C# by J.C. Duchêne). This allowed precise positioning of the scan and computation of a surface topography. This surface was defined as the vertical deviation of the core surface from an average horizontal plane measured at a 15 µm vertical resolution, and core roughness was the square root of the variance of the core topography. At the end of erosion sequence, new measures of micro-topography were performed to assess the effect of cockles and hydrodynamics on sediment topography.

Erosion procedure

Erosion tests were performed using the erodimeter (University of Caen), a small-scale (1.20 m long, 8 cm wide and 2 cm high) straight transparent flume, allowing us to apply a controlled flow in a 15L water close-circuit (Le Hir et al., 2008).

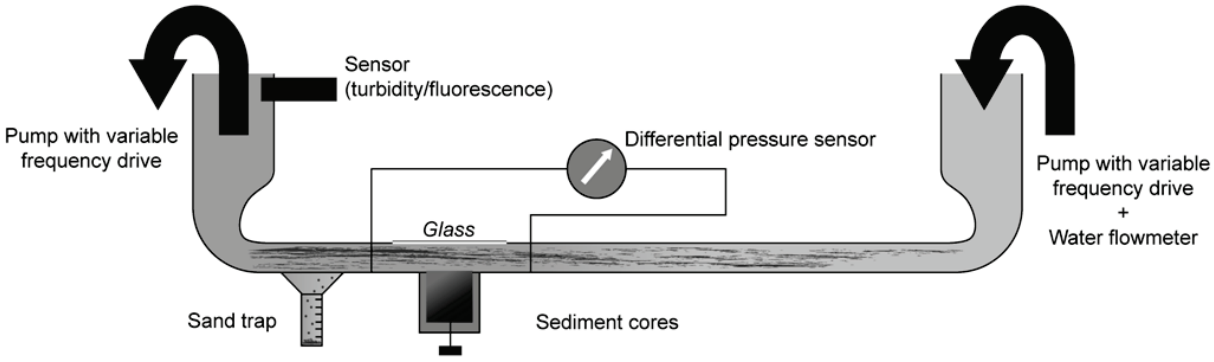

Figure 2: Schematic view of the erodimeter with the additional glass feature (University of Caen).

An additional feature was added to the flume with a transparent glass over the core, allowing camera recording during the erosion phase (Fig. 1). Then, the glass window was locked and the device was filled with filtered sea water. Every flume experiments were done at noon, after the 6 hours of an emersion phase with artificial lights. After an initial flow during 15 minutes, an increasing flow was applied every 5 minutes (32 successive levels) using a pump with a variable frequency drive

(Fig. 2). Hydraulic stress was relatively small (in the range 0 to 2.5 Pa) to avoid erosion mass, in order to identify spatial patterns of sediment and MPB biofilm characteristics after surface erosion caused by bioturbation. The induced bed shear stress has been calibrated by eroding well-sorted non-cohesive particles and direct confrontation to the Shields threshold criterion (Le Hir et al., 2008; Guizien et al., 2012).

Bed Shear Stress (BSS) was calculated following the method of Guizien et al. (2012) to take into account the differences in bottom roughness. Flow discharge, turbidity and Chl *a* were continuously recorded. The erosion was measured by estimating the fine particle amounts in the water using a nephelometric probe (NTU), and estimating the Chl *a* concentration in the water using a fluorescence probe. Because nephelometric probe was less sensitive in the first erosion levels, only fluorescence was used for estimation of resuspension fluxes. A duplicated volume of 0.5L was filtered at 4 different flow levels for measuring SPiM and Chl *a*. Fluorescence data were calibrated upon filtered Chl *a* concentration to be converted upon the basis of the most appropriate calibration curve (Fluorescence versus Chl *a*). Fluorescence data were also corrected to account for the dilution effect of sampling process, since 2 L of water was sampled for filtration at 4 successive steps all along the erosion experiment and the quantity of filtered water was added to adjust the whole volume in the system. Chl *a* fluorescence data were converted in $\mu g.L^{-1}$ by using a calibration linear curve (R^2 = 0.866) with direct confrontation to raw filter measurements (described in the further section). The rate of erosion of the Chl *a* was deduced from the time derivative of the fluorescence curve, after calibration and correction for dilution effects (during water sampling). The mass of eroded Chl *a* was computed as the product of Chl *a* concentration ($\mu g.L^{-1}$) by the water volume (15 L), divided by this sediment area $(\pi \times 0.045)$ in m^2. Among the 18 experiments, data of one experiment was not considered because of equipment failure. Erosion kinetics were analysed to determine the critical threshold for differentiating the two erosion phases: (1) Surface fluff layer erosion and (2) general bed erosion [see Orvain et al. (2003b) and Orvain (2005) for a more detailed description of the erosion phases]. The first incipient point of fluff layer erosion was considered as the point at which a significant increase in SPM between two incremental velocity steps was obtained (the u* value of the corresponding velocity step was used). The critical threshold for fluff layer erosion was determined using a statistical test which compared the means of incremental steps (n = 70) between two SPM data sets (significant at $p<0.05$). The second critical threshold for bed erosion was determined by using the intercept with X-axis when drawing a regression line between Chl *a* (averaged for each flow step) versus log (U* +1): $\mathrm{Chl}\, a = \mathrm{A} \times \log(\mathrm{U}^* + 1) + \mathrm{B}$, where U* is the shear velocity (in $m.s^{-1}$). The critical value of BSS for erosion is calculated by converting the one of shear velocity u* and by using the usual formulation between u* and τ_f, the BSS : $\tau_{f\ crit} = \rho.{\mu_{crit}}^2$. The best regression line

was retained and erosion rate was determined by considering only flow steps, for which the critical BSS was reached. For the concerned data, the rate of erosion was deduced from the time derivative of the Chl *a* curve, after calibration. Erosion rates ($g.m^{-2}.s^{-1}$) was assessed at each step (after erosion incipient point and by differentiating the two erosion phases too) as the slope between the eroded Chl *a* (i.e Chl *a* converted in $\mu g.m^{-2}$) and Δt the time interval between each Chl *a* concentration record (1 sec). The averaged erosion rate was calculated from the different values calculated per step.

Analysis sequency

During the erosion sequence (Fig. 3), bioturbation activity was recorded by actographic techniques (Maire et al., 2007a, b; Duchêne, 2012). A high resolution video sensor recorded images (IDS uEye, fitted with a 25 mm lens, with a resolution of 2560 x 1920 pixels) assembled into an Avi film. A Microsoft C# program, AviExplore, written by J.C Duchêne, cropped the image to the field dimension and processed the images to create maps of activity. Variables associated with physiology of the MPB biofilm and topography of the sediment were mapped, enabling to acquire accurate measurements of bioturbation activity, movements and feeding behavior of the cockles.

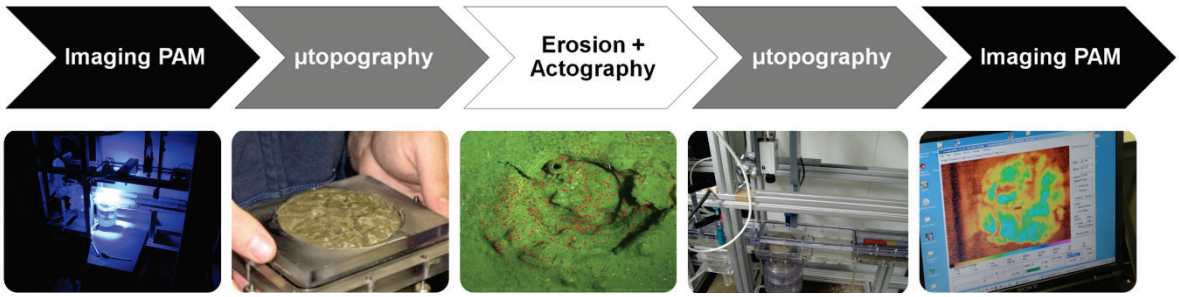

Figure 3: Summary of the erosion sequency used for this experiment

At 4 frequency levels corresponding to 0.075, 0.166, 0.352 and 0.582 Pa (friction force), water was sampled in order to evaluate Chl *a* and suspended particulate inorganic matter (SPiM). In order to determine the SPiM content, two subsamples per level were sieved and passed through weighed and dried glass-fiber filters (Whatman GFC), washed with distilled water to avoid salt errors, packed in petrislides (Millipore, USA), and immediately stored at -20°C before analyses. The filters were dried in an oven at 60°C during 72 hours, and then during 4 hours at 450°C. For Chl *a* biomass measurements, two subsamples were sieved and passed through a glass-fiber filter (Whatman GFC), fold and put in a tube at -20°C before analyses. The Chl *a* content of the sediment was extracted in 90% acetone during 24 h in the dark at 4°C. After short centrifugation, the chlorophyll extracts were measured on a Turner Designs TD 700 fluorometer (USA) following the method of Lorenzen (1967) and expressed as content ($mg.m^2$ sediment).

Statistics

Data of chl a and EPS were log-transformed before performing a Covariance analysis (ANCOVA) to detect 1) any if therewas a biomass effect on the studied variable and 2) if the biomass effect (considered as the covariable) was different between the 2 different cockles ages (juveniles and adults). Concerning EPS the same treatment was performed but an arcsinus transformation was required to obtain the residual normality (checked by a Levene test). Homoscedasticity was verified too (by using an F-test). Correlation tests were also performed to compare the sediment variables. Paired *t*-tests were used to compare variations of mean variables before and after the erosion sequence. The 3D-vizualization of the Imaging-PAM stacked maps have been done with the software Sufer (Golden Software, USA).

Results

Sediment analysis

There were no different trends between colloidal and EPS fractions (in terms of carbohydrates as well as protein contents) as a function of cockle biomass. Water content did not differ significantly as a function of biomass or age of individuals ($F_{1.44}$ = 1.71, p = 0.198 for biomass and $F_{2.44}$ = 0.47, p = 0.498 for the age effect, Fig. 4A). A significant relationship was found between both EPS carbohydrate and protein contents with the sediment water content. The increasing cockle biomass had a significant effect ($F_{1.50}$ = 6.56, p <0.05) on the chl *a* concentration of sand-mud substrate, showing that cockle bioturbation enhanced the microphytobenthic biofilm development in absence of currents in the tidal mesocosm (Fig. 4B). A positive effect of cockle age on the slope of the relationship between chl *a* concentration and cockle biomass was also observed ($F_{2.50}$ = 3.02, p <0.05). The relative colloidal and bound EPS fraction kinetics did not show any difference with factors. Neither cockle biomass nor cockle age did explain variations in measured values of EPS carbohydrates (respectively $F_{1.12}$ = 0.26, p = 0.623 and $F_{2.12}$, P = 0.939, Fig. 4D).

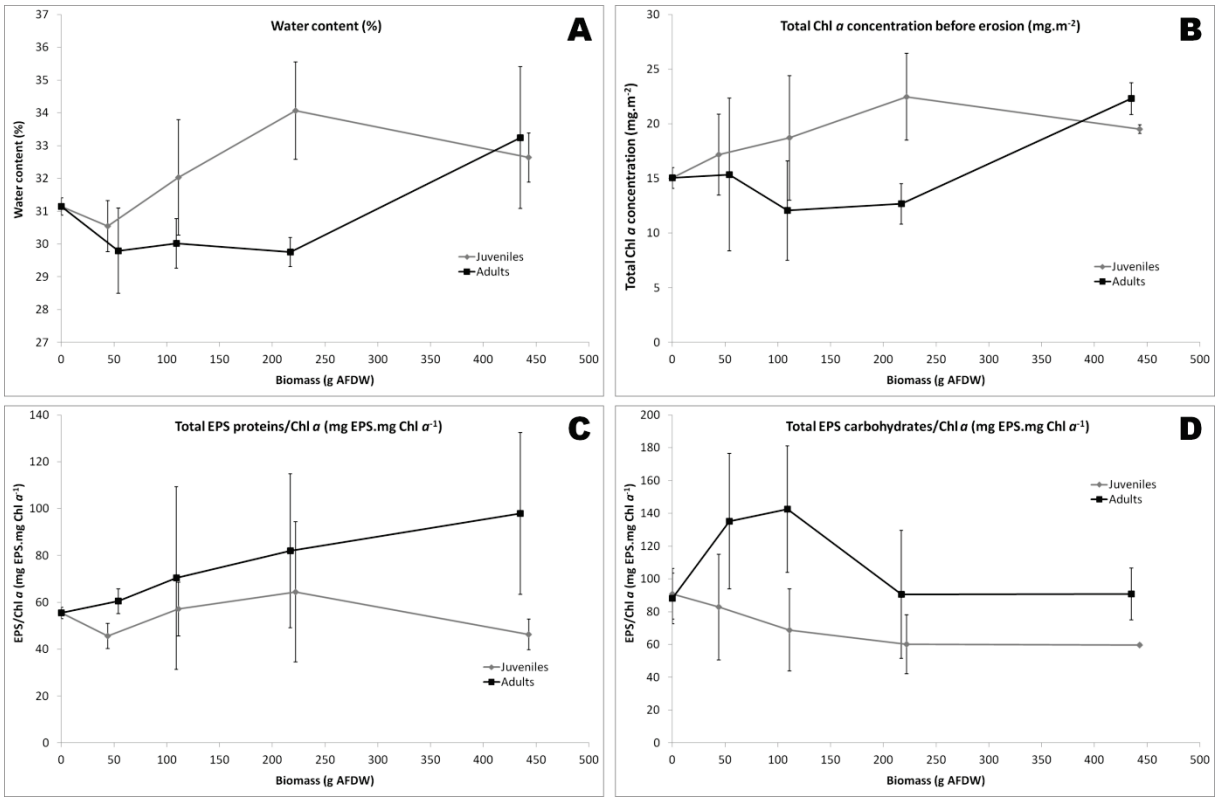

Figure 4: Sediment parameters as a function of cockle biomass measured before erosion. A: Water content (%); B: Chl *a* ($g.m^{-2}$); C: Total EPS proteins normalized by chl *a* (mg EPS.mg chl a^{-1}); D: Total EPS carbohydrates normalized by chl *a* (mg EPS.mg chl a^{-1}).

Erosion experiments

Adults and juveniles showed differences regarding to the eroded chl *a*, with adults releasing more than twice the amount of chl *a* compared to the juveniles, and this difference was more pronounced at the end of the experiments, especially with the highest cockle biomass, for which a mass Type II erosion occurred with a low critical threshold for mass erosion. Erosion kinetics were characterized by both type 0 (biogenic matrix) and type II (mass) erosion for adults, with an observed mass chl *a* erosion. For the two highest biomass conditions, erosion kinetics were characterized by early surface erosion reaching an asymptotic plateau of the eroded mass when the shear stress increased (typical of type 0 'biogenic matrix erosion'). After a very pronounced incipient point, the surface erosion was followed by mass erosion with lower thresholds than for other conditions. No or low erosion (even with low negative values in one case) was obtained in the absence of macrofauna (control condition). Conversely to adult conditions, juvenile kinetics did not show type II mass erosion but only type 0 erosion. Between 0 and 5% of the algal biomass contained in the sediment was exported to the water column after surface erosion caused by cockle bioturbation. When mass

erosion was not observed, we considered that the critical thresholds were higher than the bed shear stress range that was tested during the experiments.

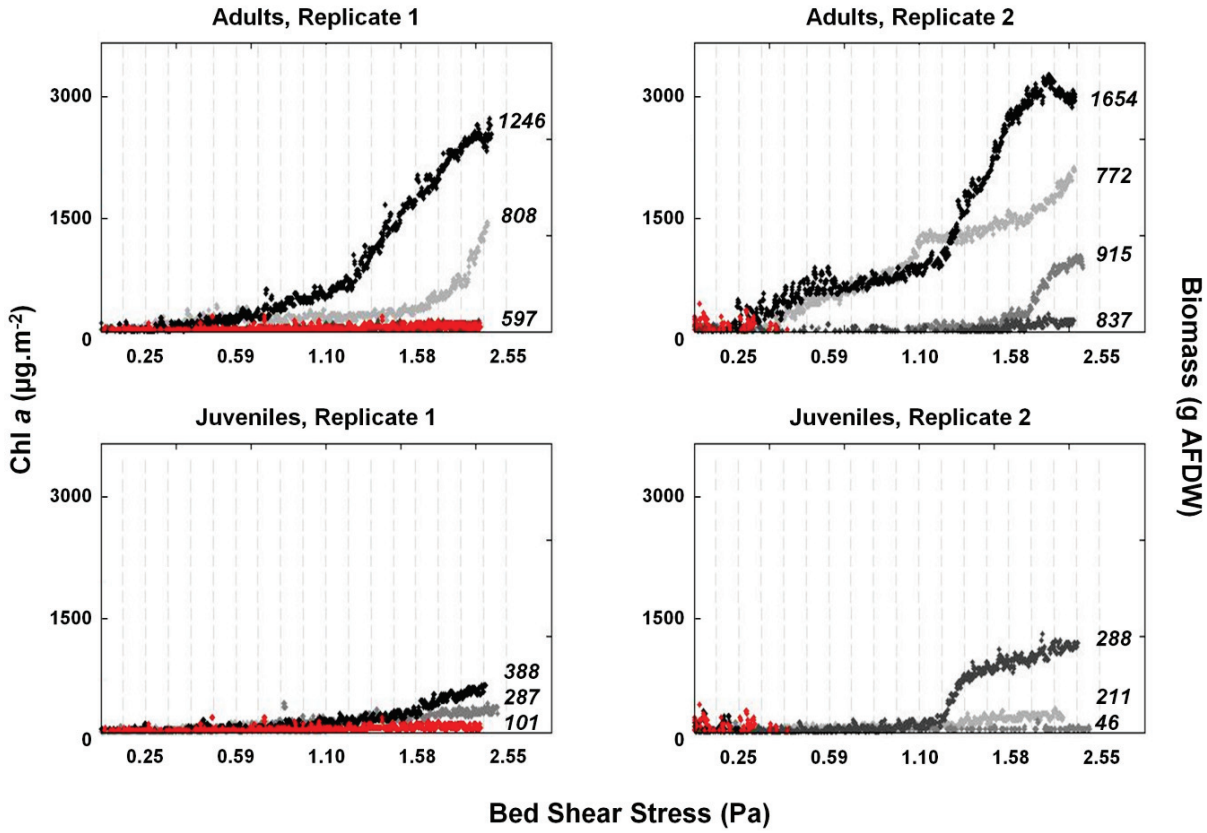

Figure 5: Water chl *a* concentration as a function of time for both "Adults" and "Juveniles" conditions. Replicates are represented by the same color, and respective biomasses have been indicated on each side of the curves. C: artificial sea water; ABD: filtered sea water.

Table 1: Core cockle biomasses and associated chl *a* critical erosion thresholds.

Age	Biomass (g.m^{-2})	Surface erosion (Pa)	Mass erosion (Pa)
Adults	772	0.138	0.792
	809	0.025	1.324
	914	0.969	1.567
	1246	0.007	1.230
	1654	0.108	overestimated
Juveniles	46	0.095	×
	101	2.653	×
	211	0.289	×
	287	0.315	×
	288	0.119	0.622
	380	1.823	×
	811	0.978	×
Control	0	1.231	×
	0	×	×

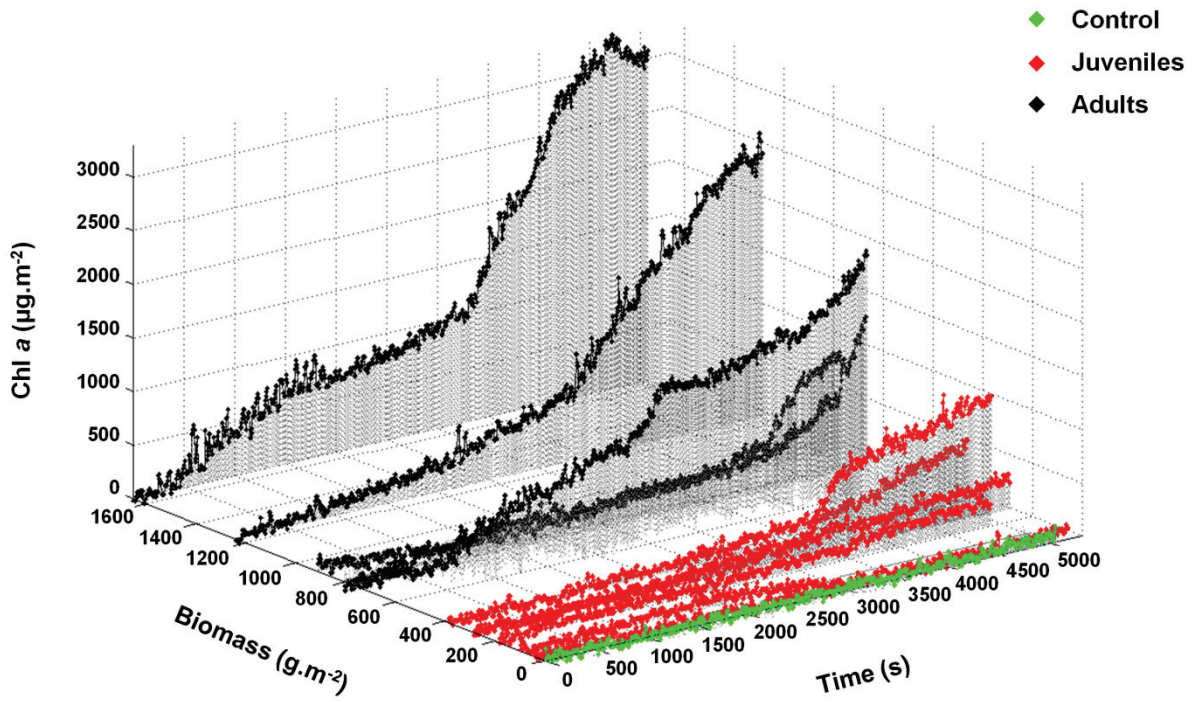

Figure 6: 3D view of the MPB resuspension kinetics as a fonction of the cockle biomass and time. The different conditions are colored.

Critical thresholds were not related to sediment chl *a*, water content or EPS content ($p>0.05$). The presence of cockles modified the sediment roughness, thus modifying the shear velocities on the bed (Fig. 6). Juveniles presence modified the bed roughness resulting in higher U^*, to a larger extent than adult individuals (Fig. 7). No size-dependent or density-dependent functions were found because of too small scale of the study.

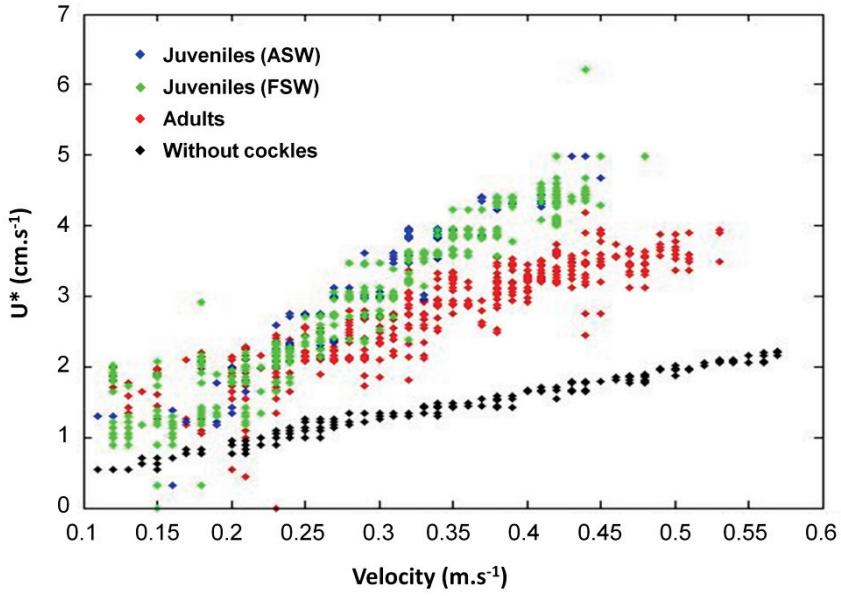

Figure 7: Shear velocity versus flume velocity as a function of cockle presence/absence.

Bioturbation activity

Biomass and bioturbation activity were well related (R^2 = 0.79). A positive correlation was observed between topography of the sediment and eroded areas, independently from both biomass and activity (Fig. 8). Thus, physical structures created by cockles were preferentially eroded (Fig. 8). The eroded surface increased as a function of cockle biomass (Fig. 8).

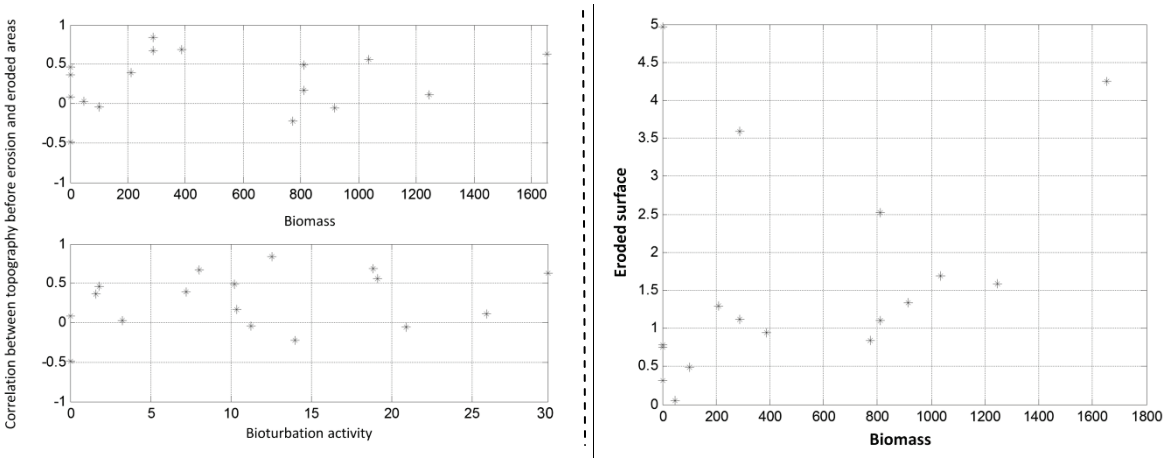

Figure 8: Spatial correlation between eroded surface and 1) topography (left panel) or 2) cockle biomass (in g AFDW, right panel). P <0.01 for all correlations.

Before erosion experiments, during water rising in the flume, cockles did react to the rising level of the seawater by burrowing in the sediment through valve adduction. Such a behavior must occur in nature as well. During the erosion sequences, valve adduction intensity showed different stages, with lagging periods followed by high intensity periods characterized by high frequency peaks. In all conditions, we can see that the first high intensity period is followed by a leap in shear velocity (Fig. 7). The adult burrowing behavior through valve adduction led to increasing shear velocity and lowering critical erosion threshold. This phenomenon was not observed for the “Juveniles” condition (Fig. 8), where that behavior was not observed during the experiments. The burrowing behavior of adult individuals digged a hole in the sediment, thus modifying roughness of the latter (Fig. 9); such a behavior was not observed with juveniles. Activity matrix (Fig. 9) showed accentuated activity in the siphon region for adult condition, putting in evidence the active filtration of cockles during the experiment. At high densities (30 and 60 individuals), juveniles were responsible for huge sediment reworking, resulting in a disturbed surface. The sediment reworking was not the same for adults, with a more “sedentary behavior” during the 7 days of installation. In fact, a few tracks were observed within the mesocosm cores.

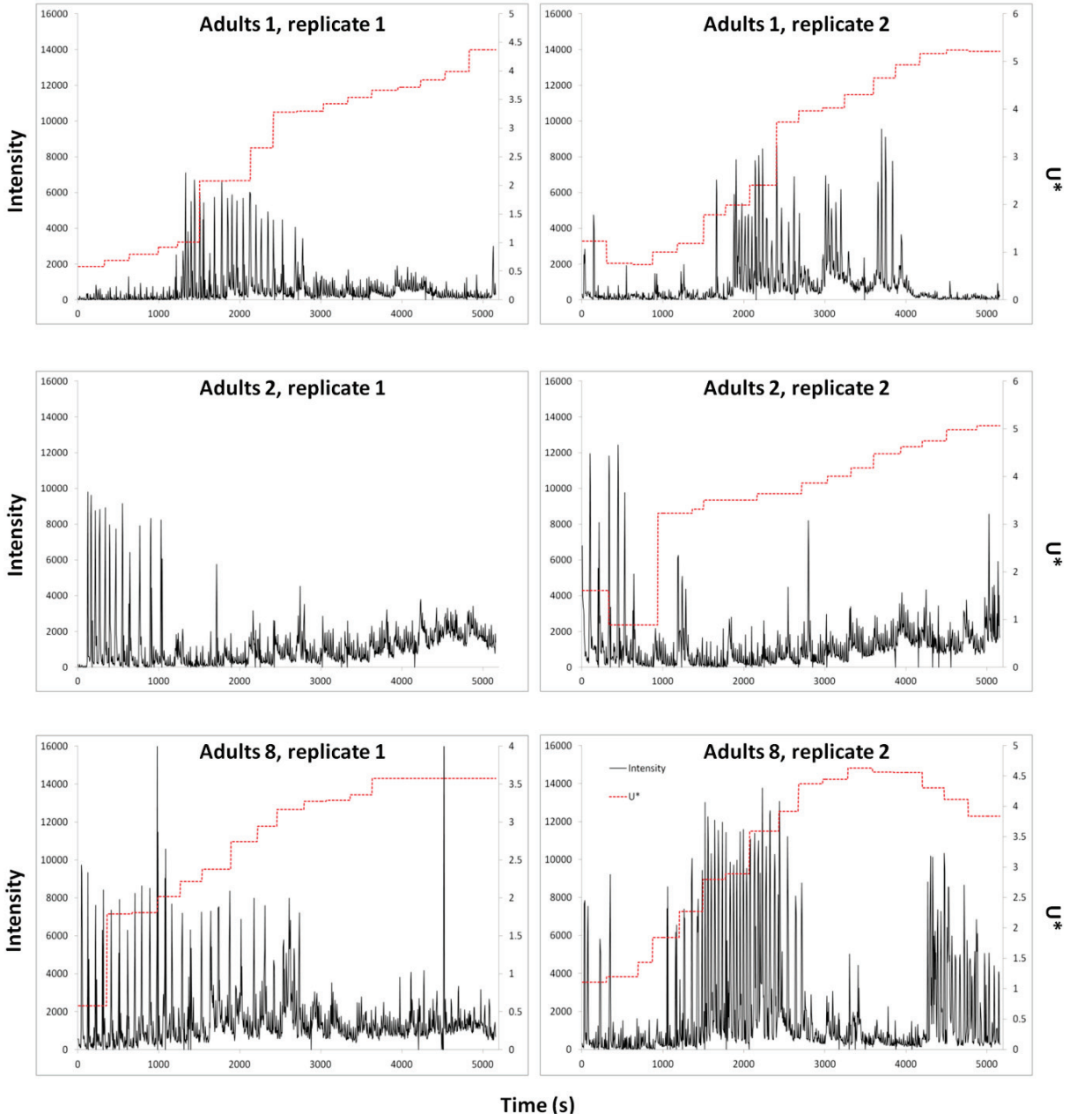

Figure 9: Intensity of biological activity as a function of time. The shear velocity has been represented by a red curve scaled on the second axis. The 2 replicates with 4 adults are not showed because of absence or death of individuals within the sub-cores. U* could not be calculated for Adults 2, replicate 1.

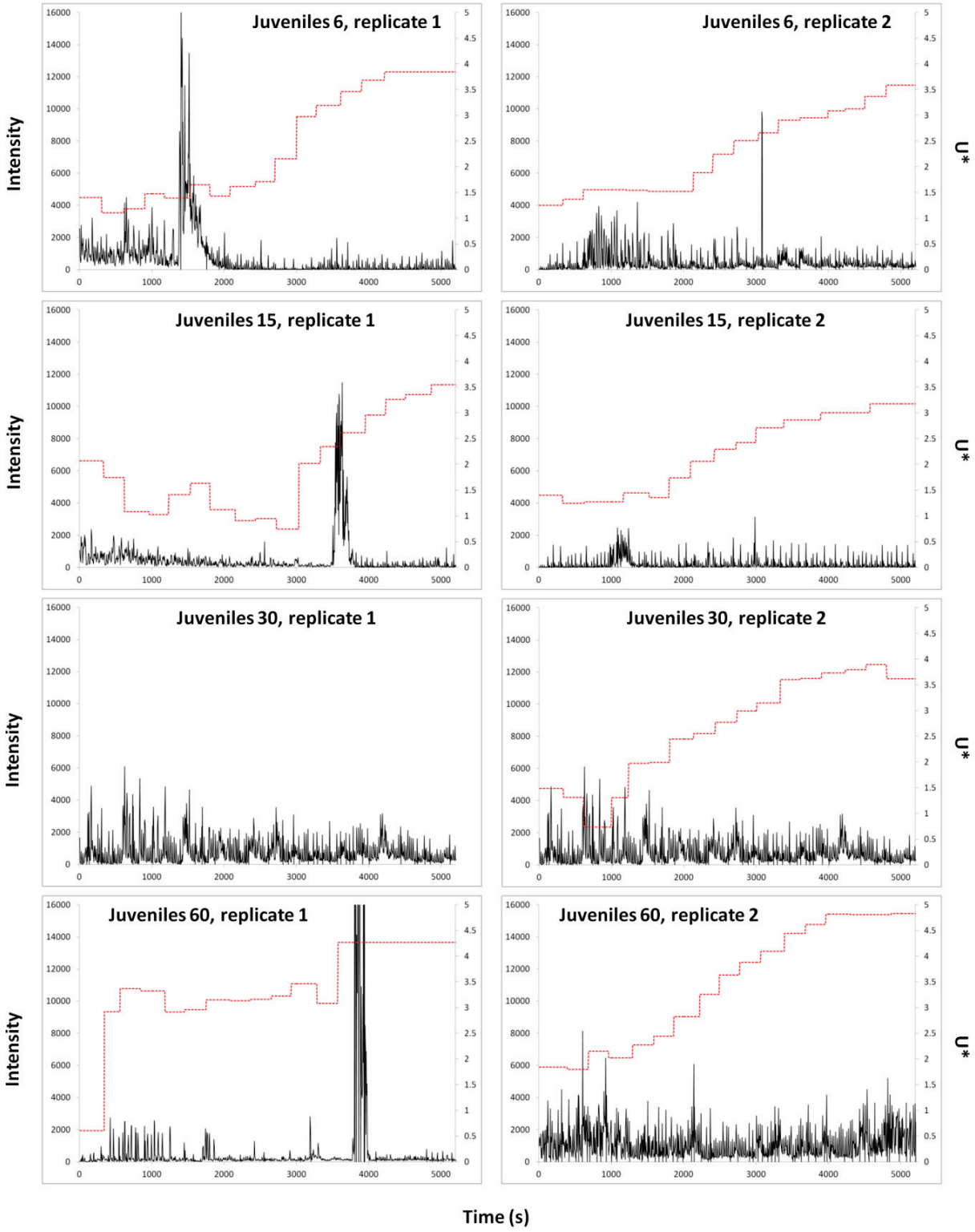

Figure 10: Intensity of biological activity as a function of time. The shear velocity has been represented by a red cure scaled on the second axis. U* could not be calculated for Juveniles 30, replicate 1.

Physiological activity

Before erosion, F0 was low in the area above the cockle individuals and was higher at the edge of the cockle burrows (Fig. 11). After erosion, F0 decreased in the same area where high erosion was observed, but systematically increased on the borders of the buried hole (Fig. 11). As a result, the averaged mean F0 within the cores increased during the erosion experiment in presence of cockles. Meanwhile, both physiological state and α decreased during the erosion experiment (Table 2). These tendencies were significant for Yield and α values within the control condition, and for α values within the adult condition.

Table 2: Mean values of the variables mesured within the 5*5 cm area.

		$\mu topo_{bef}$	$\mu topo_{aft}$	$F0_{bef}$	$F0_{aft}$	$Yield_{bef}$	$Yield_{after}$	$Alpha_{bef}$	$Alpha_{aft}$
Adults	Mean	23.981	22.189	1.373	1.506	0.603	0.530	0.546	0.278
	SD	1.242	2.400	0.415	0.900	0.029	0.112	0.284	0.197
Juveniles	Mean	23.452	22.112	1.375	1.489	0.649	0.562	0.599	0.459
	SD	0.352	1.415	0.188	0.230	0.034	0.034	0.038	0.119
Control	Mean	23.650	22.887	1.538	1.688	0.648	0.566	0.438	0.367
	SD	0.313	0.331	0.466	0.241	0.071	0.007	0.180	0.056

Table 3: Paired t-test executed on variables mesured within the 5*5 cm area (*p-value<0.05, **p-value<0.01,***p-value<0.001)**.**

Δ before-after erosion		µtopo	F0	Yield	Alpha
Adults	T-value	3.78*	-1.48	1.58	6.12***
Juveniles	T-value	60.25**	-0.30	1.50	0.81
Control	T-value	3.47*	-1.91	11.23***	3.96**

Cockles versus biofilm

The photosynthetic parameters before erosion did not rely on the erosion of the sediment; however, the areas characterized by a higher F0 seemed to be less eroded than the others (Fig. 12). There was a negative spatial correlation between erosion and the different photosynthetic parameters after erosion when considering biomass or bioturbation activity (Fig. 12). After erosion, F0 levels were negatively correlated to the eroded surfaces, and did not depend on the biomass or bioturbation activity but on the presence of cockle bioturbation. Moreover, the 2 controls did not show the same trends. The same negative correlation was observed for the Yield and α, and was more pronounced for higher biomass and bioturbation (Fig. 12).

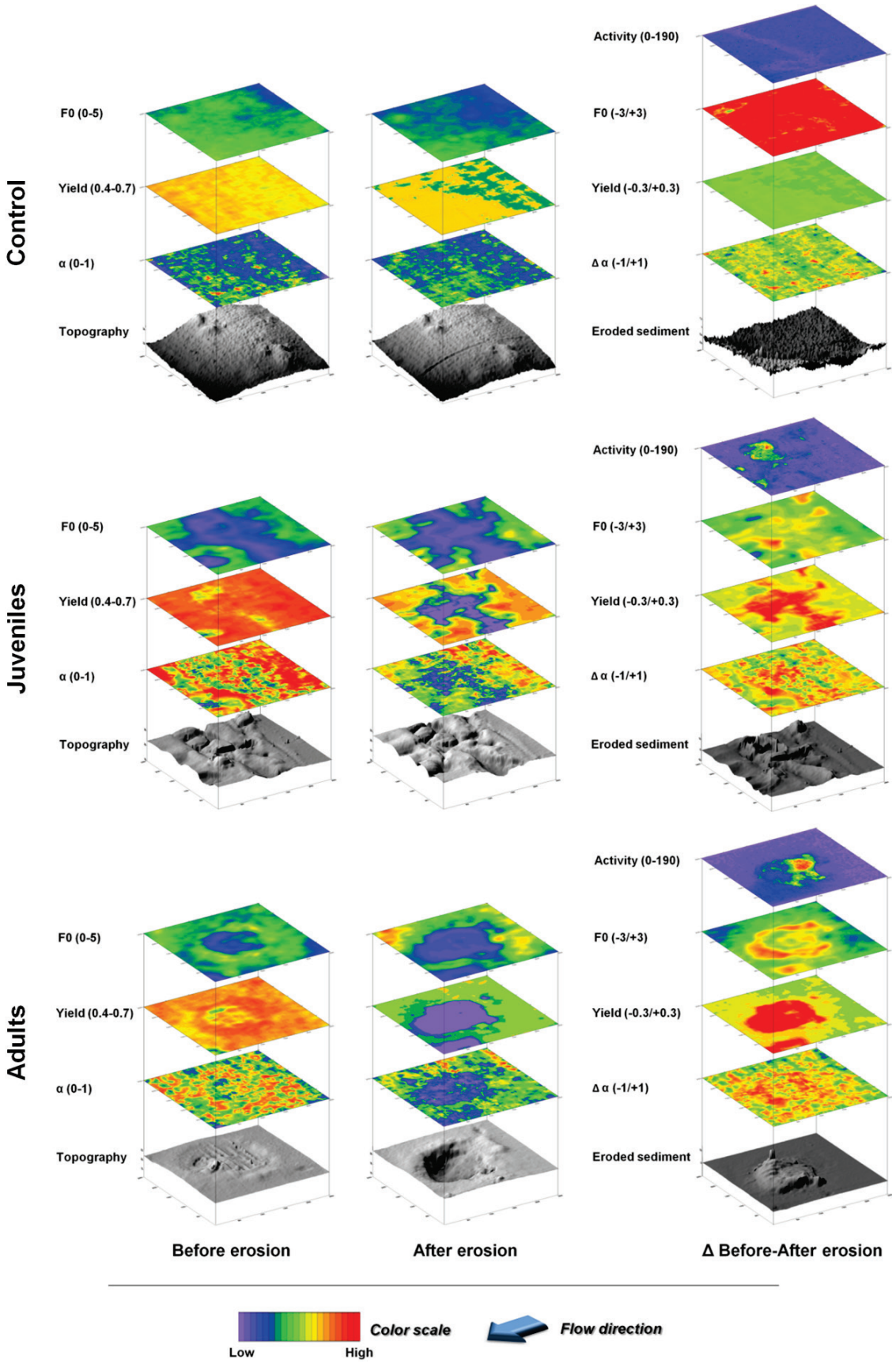

Figure 11: 3D view of the adult condition photosynthetic parameters, topography and cumulative activity for an experiment. A2-1 has been chosen as representative of the general observation made in this study.

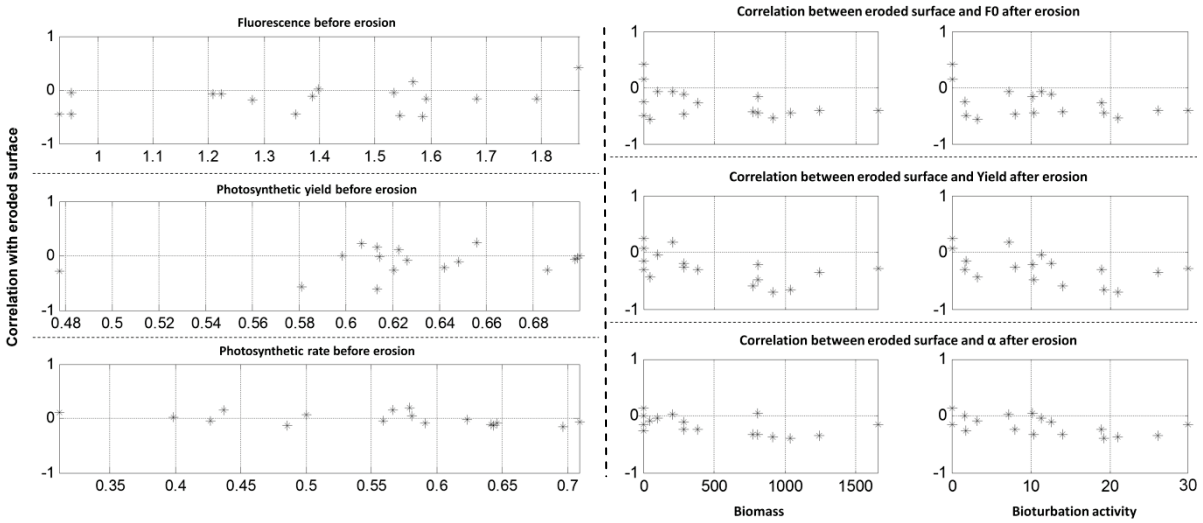

Figure 12: Spatial correlation between eroded surface 1) and photosynthetic parameters before erosion (left panel) 2) and photosynthetic parameters after erosion, as a function of biomass or bioturbation activity (right panel). P <0.01 for all correlations.

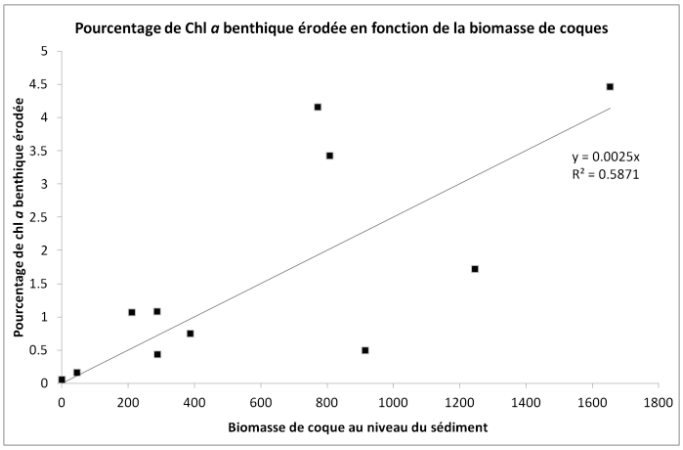

Figure 13: Percentage of the benthic chl a eroded by the cockle (as a function of biomass)

The percentage of chl *a* eroded before mass erosion was related to the cockle biomass (Fig. 13) by a linear relationship (R^2 = 0.5871).

Discussion

Cockle active and passive enhancement of both shear velocity and erosion thresholds.

During this experiment, cockles were responsible for huge surface bioturbation, leading to increased roughness of the bed. Cockle shells are responsible for increasing bed shear stress (Quaresma et al., 2007), and bioturbation intensity increased this phenomenon. Ciutat et al. (2007) did observe increased sediment resuspension as a function of cockle density, but did not observe a

significant erosion threshold decrease with cockle density. Our experiment put in evidence that both biomass and age/size were the most reliable variables related to mass erosion thresholds, with type I/II erosion systematically reached for adults. The glass rooftop allowed us to quantify valve adduction during the erosion kinetics, showing that shear velocity increased suddenly in return. Valve adduction is a natural response to depth, light, temperature, particulate matter, food availability, predator interactions or metabolic rate (Rodland et al., 2008; Robson et al., 2009). We could not link valve adduction to suspended matter concentration in this experiment. However, we observed that this behavior enhanced shear velocity, creating positive feedback on sediment disturbance and resuspension. We suggest that in addition to the predictable behavior found by Ciutat et al. (2007), there are some periods with high frequency of valve adduction behavior, which in return leads to a systematical increase of shear velocity. Siphon related bioturbation activity was linked to a higher resuspension of sediment regarding to the eroded area, highlighting the effect of exhalent siphon in sediment resuspension. Even if the juvenile activity was lower than the adult activity, their presence or tracks resulted in an increased bed roughness compared to adults. However, the burrowing behavior of adults led to higher resuspension and lower critical resuspension thresholds than juveniles. Nevertheless, we did not found a density-dependence of critical thresholds for mass erosion (ca. 0.5 Pa), because of the uncertainty in bed shear stress determination, which ranged the same (Guizien et al., 2012).

Evidence for cockle enhancement of MPB growth in absence of hydrodynamics

The higher chl *a* concentrations found in presence of the highest biomasses of cockles put in evidence their role in biofilm fertilization. These results are in agreement with those of Lindström and Swanberg (1991), who found a stimulating effect of *Cerastoderma edule* on the microphytobenthos mediated by the release of nutrients, mainly NH_4^+. Moreover, bioturbation activity linked to the biomass of cockles may increase water circulation within the superficial sediment, countering the dewatering due to the sand fraction (Ubertini et al., 2012) and thus favoring microphytobenthos development. It could be also explained by a simple sediment reworking. As a consequence the sediment reworking combined with nutrient availability mediation by the cockle *C. edule* stimulates microphytobenthos growth.

Evidence for cockle enhancement of MPB growth under hydrodynamics

If the biofilm stimulation was clear under influence of tidal cycle only (within the mesocosm), the erosion experiments results showed that MPB erosion increased under hydrodynamics. The F0 biomass index increased during erosion, but both Yield and α decreased, showing that microalgae

biomass levels were higher but that their physiological state was affected. Moreover, for adult condition, a mean of almost 2 mm of sediment was eroded at the core surface, resulting in a higher chl *a* resuspension than control condition. Thus, the only way to obtain a higher microalgae biomass after erosion must be explained by their downward migration. Between the end of the low tide emersion and the beginning of the flow corresponding to the flume water filling, diatoms may have migrated downward the superficial layer of the sediment following their chronobiological rhythm (Serôdio et al., 1997). The superficial layer has been then eroded, discovering the diatoms in surface which had migrated before erosion. This explanation is comforted by the control condition, which was the only treatment with an observed significant decrease of the photosynthetic yield. In fact, diatoms have also migrated downward in this condition, and microalgae which have not migrated are in a less good physiological state, resulting in lower values of both Yield and Alpha.

Cockle enhancement of MPB resuspension

There was a direct link between biomass of the cockles and MPB resuspension, confirming the role of *C. edule* in MPB exportation to water column observed by other authors (Ciutat et al., 2006; Neumeier et al., 2006; Widdows and Navarro, 2007). This result are opposite to those of Andersen et al. (2010), who found an indirect stabilization effect of cockles on microphytobenthos by increasing the content of fine-grained sediments at the sediment surface. They suggested that the difference observed with previous authors could be due to a modification of bioturbation activity, caused by the manipulation of individuals. Two major effects can be identified, as already found by Orvain (2005) for the bivalve *Scrobicularia plana*: Firstly, an erosion of biogenic matrix with very low critical thresholds not depending for the biomass. Chl *a* fluxes were clearly dependent on bioturbation activity on the burrow edges, as shown by the good correlation between relief (created by shell) and spatial eroded areas location which coincided well. Moreover, the correlation increased with the degree of bioturbation, as shown by the good relationship between cockle biomass and chl *a* eroded before mass erosion. Secondly, there was an effect of cockles influencing directly the mass erosion thresholds. This effect was only seen for adult individuals because the range of bed shear stress tested were not too high in order to evaluate the sediment surface photosynthetic parameters after gentle surface erosion, and to stay in realistic conditions regarding to the natural bed shear stresses found in the environment (ca. 0.5 Pa).

The present study showed an incontestable effect of cockles on MPB resuspension at local scale, cockles being acclimated to their environment for 7 days in a tidal mesocosm. Thus, the positive or negative effect of cockles on MPB resuspension may be related to the scale considered. Even if cockle bioturbation leads to destabilization of the sediment at local scale, the resuspension of

fine sediment could enhance MPB biomass at the scale of an entire bay, and thus the higher stability of the sediment observed by Andersen et al. (2010). Age and biomass of cockle can also explain the difference observed with the previous study. In fact, "Juvenile" treatment did show significant chl *a* resuspension only for one core (J6-2) in the range of bed shear stress tested by Andersen et al. (2010), between 0 and 1.5 Pa. Moreover, they measured SPM whereas the present study focused on chl *a* resuspension which can be resuspended without the underlying sediment (Orvain et al., 2004; Ubertini et al., 2012). The consumption of cockle as been demonstrated to induce chl *a* depletion in the water over the bed, at a height which decrease with current velocities (Widdows and Navarro, 2007). Consumption of cockles was not calculated during this experiment, but siphon activity recording witnessed active filtering of adult individuals. However, net resuspension was higher than consumption of the cockles, since adult cockle condition was characterized by higher MPB resuspension. Compared to other species like *Peringia ulvae* or *Scrobicularia plana*, cockles were able to resuspend high quantities of chl *a*, especially considering that the sediment was not favorable to diatom growth (Ubertini et al., *submitted*). Through siphon and valve adduction activity, *Cerastoderma edule* could achieve a self-regulation of its food supply, as seen for mussels in other studies (van de Koppel et al., 2005; Widdows et al., 2009). This valve adduction activity may occur only in case of seston depletion in the water column.

Conclusion

This experiment allowed us to characterize the behavior and the ability of *Cerastoderma edule* to export chl *a* in the water column. Valve adduction appeared to be the main factor involved in the mass resuspension of the sediment and associated chl *a*. This typical behavior was only observed for adult individuals. The erosion rate of chl *a* did depend on cockle biomass during the surface erosion (type 0). In the absence of current, high cockle biomass enhanced microphytobenthic growth, which is probably favored by the increased patchiness. Paradoxically, cockle bioturbation at high biomasses also enhance exportation of MPB to the water column under hydrodynamics, showing the potential importance of *C. edule* as an ecosystem engineer in coastal ecosystem (Montserrat et al., 2009), able to both stimulate MPB production and exporting this production to the water column. The key role evidence of bioturbation effect on sel-organisation of biofilms is now highlighted.

Acknowledgements

We would particularly like to thank Christian Portier for his help with ithe setting up of the experiment and for his help during the experiment to fix material issues. We would like to thank the General Council of Low-Normandy for their financial support.

Chapitre VII

Discussion générale, perspectives

« La vraie science est une ignorance qui se sait.»

Montaigne

Remise en suspension des diatomées benthiques et couplage benthos-pelagos

La remise en suspension des diatomées benthiques est un phénomène majeur du couplage benthos-pelagos dans les écosystèmes estuariens (Underwood and Kromkamp, 1999; Porter et al., 2010). La diversité des processus et compartiments impliqués dans cette remise en suspension induit un degré de complexité différent selon l'échelle spatio-temporelle considérée. La caractérisation et la hiérarchisation des variables impliquées est donc primordiale pour mieux définir la capacité de charge ou « *carrying capacity* » des écosystèmes côtier marins (Luckenbach and Wang, 2004), et ainsi assurer une gestion durable dans les écosystèmes conchylicoles.

L'objectif de cette thèse était d'étudier le déterminisme de la remise en suspension des diatomées benthiques au travers du couplage-benthos-pelagos, en intégrant les différents compartiments physiques, chimiques et biologiques impliqués dans ce processus et leurs interactions. L'échelle considérée est susceptible de faire varier ces interactions ; en effet s'il est apparu récemment que les diatomées benthiques participent significativement au régime alimentaire des filtreurs (Lefebvre et al., 2009), la remise en suspension peut être de nature autochtone ou allochtone (Ubertini et al., 2012). Les processus d'advection doivent donc être pris en compte et nécessitent d'envisager la remise en suspension dans son contexte spatial et comme un maillon de couplage benthos-pelagos. La remise en suspension dépend à la fois des interactions locales avec le sédiment et la macrofaune benthique (Orvain et al., 2004; Widdows et al., 2002) et des interactions avec des processus à plus large échelle que sont les courants tidaux ou le vent (de Jonge and Van Beusekom, 1995). A une échelle encore plus réduite, la micro-hétérogénéité des biofilms microphytobenthiques (Spilmont et al., 2011) permet une autorégulation de la production primaire qui est amplifiée par le stress physique (Weerman et al., 2010). Les interactions au sein du biofilm conditionnent également la remise en suspension des diatomées benthiques (Smith and Underwood, 1998). L'ensemble de ces échelles spatiales sont elles-mêmes imbriquées dans des échelles temporelles variées qui vont contraindre la remise en suspension à l'échelle d'un cycle tidal en termes d'hydrodynamisme et d'immersion-émersion (Orvain et al., 2012) comme à l'échelle interannuelle selon les années humides ou sèches (Grangeré et al., 2012). Au cours de cette thèse, nous avons démontré la pertinence de cette prise en compte multi-échelle de la remise en suspension des diatomées benthiques.

Au travers de deux approches *in situ* et *ex situ* de la remise en suspension, nous avons employé différentes et techniques pour caractériser la remise en suspension 1) à l'échelle macroscopique et d'observation en intégrant les compartiments biotiques et abiotiques ainsi que

l'aspect saisonnier et 2) au niveau des processus en intégrant spécifiquement la macrofaune benthique, les paramètres sédimentaires et le biofilm microphytobenthique.

Les processus de remise en suspension/bio-déposition dans l'écosystème

Afin d'explorer la remise en suspension dans l'écosystème décrite dans les chapitres III & IV, nous avons adopté une approche multifactorielle englobant les compartiments benthiques et pélagiques simultanément, inédite par son emprise spatiale. Au sein d'un écosystème estuarien, la cartographie des habitats benthiques et pélagiques associée à l'étude des biocénoses benthiques et pélagiques nous a permis de mettre en évidence l'influence majeure de la macrofaune benthique dans le couplage benthos-pelagos. La bioturbation par la macrofaune benthique apparait donc comme décisive pour la remise en suspension des microalgues benthiques, à l'instar de la coque *Cerastoderma edule*, organisme clé du couplage benthos-pelagos en *Baie des Veys* (Ubertini et al., 2012). Le rôle prépondérant de la macrofaune dans les échanges benthos-pelagos est directement lié à la saison, modifiant la hiérarchie des facteurs physiques et biologiques impliqués dans la remise en suspension des diatomées benthiques au cours de l'année. Cette étude nous a également permis de de mieux comprendre les processus d'advection à l'échelle de l'écosystème, mettant en avant la nécessité de considérer les zones adjacentes en termes de relations trophiques et d'advection du MPB pour une gestion durable des écosystèmes conchylicoles. La contribution des diatomées benthiques à la croissance des bivalves filtreurs avait déjà été montrée dans des écosystèmes caractérisés par de la vase pure, mais elle apparait également être importante (entre 20 et 40% en année sèche) pour un écosystème caractérisé par des mélanges sablo-vaseux comme la *Baie des Veys*. Cette estimation pourrait être revue à la hausse pour les années humides (Grangeré et al., 2012), renforçant la nécessité d'intégrer le processus de remise en suspension dans les modèles écosystémiques.

Si la remise en suspension du MPB contribue significativement au régime alimentaire des filtreurs cultivés dans les systèmes vaseux à sablo-vaseux, le processus de biodéposition semble être déterminant dans les écosystèmes sableux comme Lingreville-sur-mer. La biodéposition enrichit le sédiment en matière organique, contrôlant la production primaire benthique. La part que constituent les diatomées benthiques dans le régime alimentaire des filtreurs dans ce type d'écosystème est faible, ces derniers étant donc essentiellement alimenté par le phytoplancton ou les apports allochtones. La notion de capacité de charge intervient alors : un écosystème change

d'équilibre constamment en termes de biotopes et biocénoses, et ce en réponse à des facteurs internes et externes, biotiques et abiotiques. La faune et la flore fluctuent avec la disponibilité des ressources, la capacité de charge correspondant à l'état d'équilibre entre les ressources des consommateurs. Les écosystèmes côtiers ouverts cultivés sont susceptibles de dépasser leur capacité de charge si les sels nutritifs et producteurs primaires sont en quantité insuffisante par rapport aux mollusques cultivés (McKindsey et al., 2006). L'influence des années sèches/humides est donc d'autant plus forte pour les écosystèmes marins ouverts (Grangeré et al., 2012). La réduction de la capacité de charge des écosystèmes conchylicoles induit une compétition trophique accrue entre filtreurs sauvages et cultivés. L'exclusion marquée de suspensivores au niveau des structures conchylicoles dans les écosystèmes estuariens ou marins ouverts témoigne de la pression trophique exercée par les mollusques cultivés. Si les mollusques suspensivores sauvages ne profitent pas de la biodeposition induite par les mollusques cultivés, celle-ci profite aux déposivores de surface comme *Nassarius reticulatus*. Les mollusques suspensivores sauvages (tout comme les déposivores) sont en revanche succeptibles d'agir en tant que facilitateurs trophiques pour ces derniers via le processus de bioturbation. Celle-ci induit en effet une remise en suspension du sédiment et du MPB associé (voir section suivante), et enrichirait le compartiment pélagique en sels nutritifs.

Le processus de remise en suspension à micro-et méso-échelle

L'étude de la remise en suspension à l'échelle de l'écosystème nous a permis de mettre en avant des relations fortes entre composition sédimentaire et microphytobenthos, ainsi que l'importance de la coque pour la remise en suspension du microphytobenthos à l'échelle de l'écosystème. Le changement d'échelle par l'étude en mésocosme et en canal benthique décrite aux chapitres V & VI nous a permis d'explorer plus finement le rôle de ces variables sur la remise en suspension du microphytobenthos. La variabilité des mélanges sablo-vaseux influence la biologie du biofilm par des variations en termes de rétention d'eau, de compaction, de disponibilité des sels nutritifs (Ubertini et al., soumis, cf. Chapitre V). Cependant, nous avons mis en évidence que le MPB peut par l'intermédiaire de la production d'EPS s'adapter aux variations de substrat, et ainsi coloniser une large gamme de sédiments sablo-vaseux. Les EPS et particulièrement la fraction liée s'avèrent déterminants dans les processus de modulation de la perméabilité du substrat et de la cohésion entre les grains de sédiments. Ces EPS permettent la mise en place d'un biofilm productif même en cas d'enrichissement en sable, impactant de façon défavorable la production microphytobenthique. Les EPS colloïdaux ont souvent été reliées à l'érodabilité du substrat (Tolhurst et al., 2003), mais

semblent être plutôt liés au contenu en eau du sédiment et à la concentration en chl *a*. La composition biochimique de cette fraction explique bien son caractère hydrophile (Bellinger et al., 2005; Hanlon et al., 2006; Pierre et al., 2012). Le biofilm de surface et le sédiment sous-jacent ont des seuils critiques d'érosion différents, et la sécrétion d'EPS liées associée aux mélanges sablo-vaseux semble permettre de stabiliser ces derniers jusqu'à les rendre plus résistants que des sédiments purement cohésifs. Nous sommes les premiers à observer un tel effet des EPS liées, peut être lié à une nouvelle méthode d'extraction optimisée (Takahashi et al., 2010). En effet la composition biochimique de cette fraction a été caractérisée (Pierre et al., 2012) et révèle la dominance du rhamnose parmi les monosaccharides, ce composé possédant des propriété gélifiantes d'adhésion (Zhou et al., 1998; Giroldo et al., 2003). L'érosion précoce du biofilm permet de protéger les couches de sédiment sous-jacentes pour les sédiments vaseux. De plus, le biofilm en surface peut être doté d'une certaine élasticité qui nécessite de revoir les protocoles de mesure d'érosion en présence de biofilm (Vignaga, 2012). En conséquence, les interactions avec la faune endogée doivent être correctement envisagées dans les études de remise en suspension des sédiments benthiques. La coque *Cerastoderma edule*, modifie la vitesse de frottement au niveau du sédiment de façon différentielle selon la taille des individus, les juvéniles modifiant de façon plus prononcée les surfaces sédimentaires par leur capacité de recouvrement par rapport aux adultes. Deux mécanismes interviennent au niveau de l'érosion : 1) la taille des individus est directement liée au comportement de bioturbation, les individus adultes induisant une érosion en masse du sédiment par des comportements violents d'adduction des valves, et 2) la remise en suspension induite par cet organisme est directement liée à sa biomasse (Fig. 19), et cette relation doit être affinée et appliquée à d'autres organismes afin de mieux évaluer les processus de remise en suspension. L'implication de la remise en suspension liée à la bioturbation dans le réseau trophique est structurante et nécessite donc d'être mieux appréhendée dans les modèles écosystémiques.

Mieux intégrer la macrofaune benthique dans les modèles écosystémiques

Les différents travaux menés durant cette thèse ont permis de mieux évaluer la remise en suspension du MPB en lien avec les différents compartiments impliqués. Il apparait de façon claire que l'hydrodynamisme est un facteur clé de la remise en suspension du MPB (de Jonge and Van Beusekom, 1995). Les fractions relatives des mélanges sédimentaires en sable et en vase induisent également une remise en suspension différentielle du MPB. Les vases sont plus propices à la croissance du MPB mais aussi à son exportation. Cependant, les tensions de frottement nécessaires

pour la remise ensuspension du MPB (supérieures à 0.5 Pa) apparaissent lors d'épisodes de vagues ou de marées de vives eaux. Dans les mélanges sablo-vaseux majoritairement observés en *Baie des Veys*, le seuil critique d'érosion de la chl *a* devient très élevé (1 à 3 Pa), les flux d'érosion restant limités même en cas de dépassement de la tension critique. Dès lors, la macrofaune semble être un facteur clé et encore sous-estimé de par son impact sur une érosion quotidienne du MPB (effet de surface, matrice biogène). En effet elle permet - outre l'établissement d'un biofilm productif - la remise en suspension du microphytobenthos à des tensions de frottement inférieures (de l'ordre de 0.5 Pa), correspondant aux tensions induites par le phénomène de marées moyennes notamment.

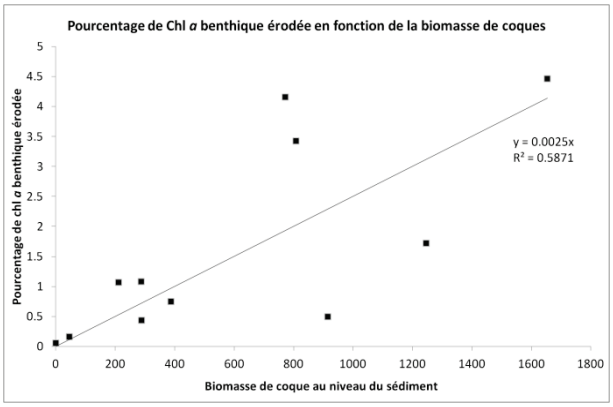

Figure 19 : Relation entre la biomasse de coques *C. edule* et le pourcentage de chl *a* benthique remis en suspension.

Cette thèse s'axait autour de 2 approches complémentaires qu'étaient l'étude des processus *in situ* et l'étude des processus *ex-situ*, permettant d'englober l'ensemble des échelles impliquées. L'étude menée en *Baie des Veys* a permis de mettre en évidence l'importance de la remise en suspension du MPB pour le régime alimentaire des huîtres cultivées *Crassostrea gigas*, et de mettre en exergue le rôle prépondérant de la macrofaune benthique et particulièrement la coque *Cerastoderma edule* dans ce processus. L'étude plus fine menée sur le comportement bioturbateur de la coque nous a quant à lui permis d'établir une relation entre la remise en suspension de la chl *a* benthique et la biomasse des coques (Fig. 19). Le couplage de ces 2 études nous a donc permis d'extrapoler la capacité de remise en suspension de la coque à l'écosystème BDV par une modélisation simple:

$$Chl\ a\ érodée\ (\mu g.L^{-1}) = (K \times Biomasse)/100 \times Chl\ a\ benthique\ (mg.m^{-2} \times z$$

Avec z la hauteur de la colonne d'eau et K l'équation linéaire correspondant au pourcentage de chl *a* benthique remis en suspension en fonction de la biomasse de coques ($K = 0{,}025$)

Avec les nouvelles valeurs théoriques, il est donc possible de créer des cartes de remise en suspension générée par la coque (Fig. 20 & 21). Ce modèle pourrait être affiné grâce aux tensions de frottement réelles observées sur le terrain. Les niveaux de chlorophylle remise en suspension sont assez importants en septembre, de 0 à 4,8 µg.m^{-2}, d'autant plus qu'il s'agit d'une intégration sur la profondeur totale de la colonne d'eau. L'exportation théorique est beaucoup moins forte en Avril, confirmant les changements saisonniers dans la balance entre des processus physiques et biologiques dominants dans la Baie (Ubertini et al., 2012). En regardant la structure spatiale de la

remise en suspension, on observe une zone de remise en suspension moyenne à l'Ouest correspondant à une déplétion en chl *a* dans la colonne d'eau, une zone au milieu de la baie avec les plus fortes remises en suspension et une déplétion moins marquée, ainsi qu'une zone au Sud-Est avec une remise en suspension moyenne et les valeurs de chl *a* dans l'eau les plus élevées. La déplétion observée à l'Ouest correspond sans doute à une consommation élevée par les coques, gommant l'effet positif de la remise en suspension dans cette zone où le courant est quasiment nul et caractérisée par un recrutement massif de *C. edule*. La deuxième zone correspond à une remise en suspension dans une zone à plus fort hydrodynamisme. La déplétion observée correspond probablement à la consommation locale des coques, mais le MPB exporté est sans doute transporté par advection dans la zone située au nord. Enfin, la zone située à l'Ouest bénéficie à la fois de la remise en suspension du MPB dans la colonne d'eau par les coques et des apports en chl *a* provenant de la *Vire*.

Cependant, il est impératif d'intégrer les autres processus mis en évidence pendant cette thèse pour modéliser l'exportation réelle du MPB vers la colonne d'eau :

1) L'effet du gradient estuarien sur le mélange sablo-vaseux : les vases pures au sud de la BDV sont les plus propices au développement du MPB et peuvent être érodées pour des seuils équivalents à 0.5 Pa. Cette érosion en masse peut expliquer les observations de Jonge and Van Beusekom (1995) sur l'effet des vagues.
2) L'érosion des mélanges sablo-vaseux sans faune n'est possible qu'à des tensions de frottement supérieures, de l'ordre de 1 à 3 Pa (50% sable, Ubertini et al., *submitted*). L'effet bioturbateur de la coque sur l'érosion en masse favorise la croissance du MPB par sa simple présence (Ubertini et al., *in prep*, cf Chapitre VI) et le rend érodable à des tensions de frottement de l'ordre de 0.5 Pa. Cet effet doit être affiné par des expériences complémentaires, en testant des biomasses plus élevées de petites coques notament.

Diversité des organismes et diversité de la bioturbation

Il apparait de façon claire que les organismes bioturbateurs agissent par différents comportements sur la remise en suspension du MPB (Kristensen et al., 2012). Le comportement de bioturbation de la coque *Cerastoderma edule* n'est donc pas généralisable à l'ensemble de la macrofaune benthique d'un écosystème. Durant cette thèse l'ensemble de la macrofaune benthique a été identifié en *Baie des Veys*, et permettra de mieux caractériser et quantifier l'exportation du MPB vers la colonne d'eau.

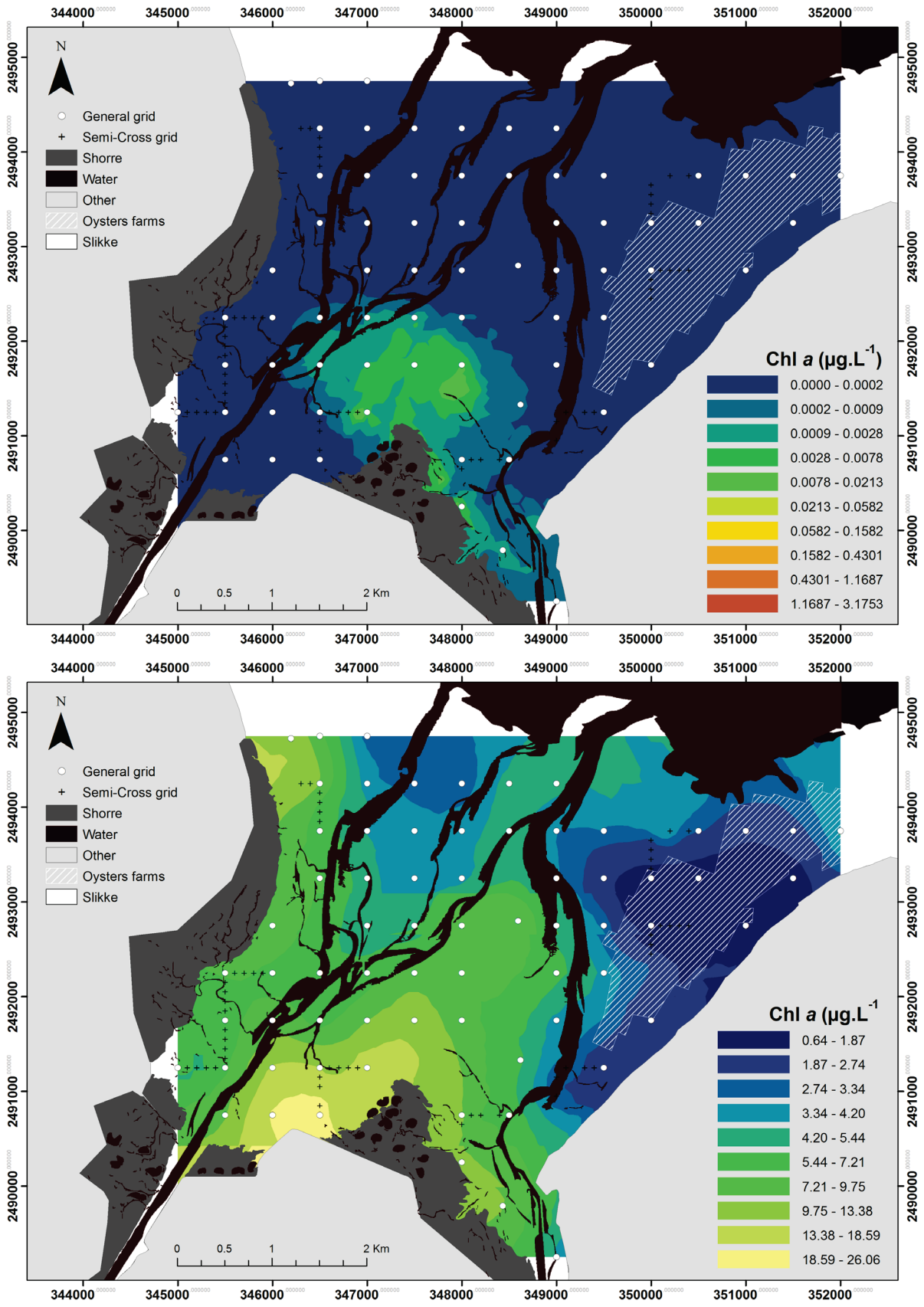

Figure 20 : Comparaison de 1) la simulation de la remise en suspension de la chl *a* benthique par les coques au jusant durant le mois d'Avril 2010 (A) et de 2) la concentration totale en chlorophylle a dans la colonne d'eau (B).

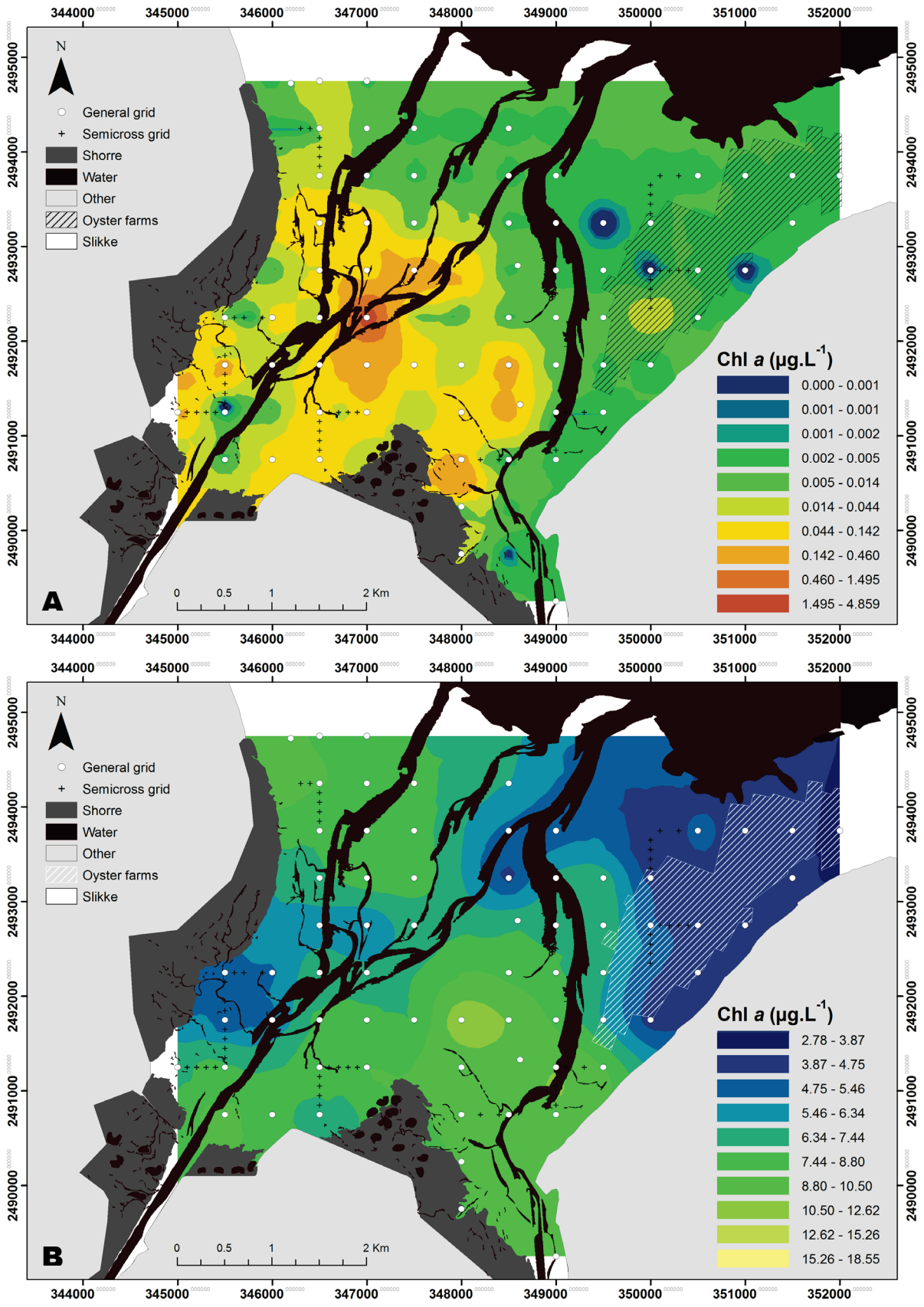

Figure 21 : Comparaison de 1) la simulation de la remise en suspension de la chl *a* benthique par les coques au jusant durant le mois de Septembre 2010 (A) et de 2) la concentration totale en chlorophylle a dans la colonne d'eau (B).

L'étude précise des remises en suspension associées aux différents organismes de la macrofaune benthique - en rapport avec la granulométrie sédimentaire et les tensions de frottement - permettrait de mieux évaluer le couplage benthos-pelagos et la capacité de charge des écosystèmes côtiers (en intégrant la dynamique spatiale de la macrofaune benthique). En Baie des Veys, le bivalve *Macoma balthica* est distribué de manière similaire à *C. edule*, ayant également une affinité pour les mélanges sablo-vaseux, et constitue le deuxième groupe de mollusques en termes de biomasse. Ce bivalve, en tant qu'ingénieur écosystémique a une action très proche de la coque puisque : 1) il stimule la croissance des diatomées benthiques (Michaud et al., 2005) et 2) il a un effect positif sur les taux d'érosion (Willows et al., 1998). Son comportement de bioturbation à micro-échelle devrait donc être étudié plus précisément, tout comme celui du bivalve *Mya arenaria*, non échantillonné pendant nos campagnes d'échantillonnage mais dont la capacité de remise en suspension est connue (St-Onge et al., 2007). L'accumulation des activités de bioturbation de l'ensemble de la macrofaune benthique pourrait expliquer la différence observée entre la chl *a* exportée par la coque (modélisation) et le ratio de 30% de microalgues benthiques en suspension trouvé en *Baie des Veys* (Ubertini et al., 2012). Cette différence peut s'expliquer également par le fait que la modélisation est basée sur une exportation au bout d'une heure de courant, mais les coques dans le milieu naturel sont soumises à des durées d'hydrodynamisme beaucoup plus long pendant le flot et le jusant. L'intégration temporelle de la dynamique tidale dans le modèle permettrait donc d'affiner ce dernier.

Ce travail de thèse a participé à une meilleure compréhension du couplage benthos-pelagos et plus particulièrement de la remise en suspension du microphytobenthos dans les écosystèmes conchylicoles. La macrofaune benthique est un facteur clé de l'exportation du microphytobenthos vers la colonne d'eau, et son importance doit être revue à l'échelle de l'écosystème en intégrant les échanges par advection pour mieux comprendre et assurer la gestion des écosystèmes conchylicoles. La caractérisation de deux écosystèmes et des processus de remise en suspension pendant ce travail de thèse permet d'ouvrir la voie à la modélisation de ces écosystèmes par des modèles de réseaux trophiques couplés benthos-pelagos.

Références

Bibliographie, liste des figures, liste des tableaux

« Une citation sans références est à peu près aussi utile qu'une horloge sans aiguilles. »

Paul Desalmand

Bibliographie

-A-

Admiraal, W., Peletier, H., Brouwer, T., 1994. The seasonal succession patterns of diatom species on an intertidal mudflat: an experimental analysis. Oikos 42, 30–40.

Ahmad, M., Dong, P., Mamat, M., 2011. The Critical Shear Stresses for Sand and Mud Mixture. Applied Mathematical and Computation 5, 53–71.

Alfaro, A.C., 2006. Evidence of cannibalism and bentho-pelagic coupling within the life cycle of the mussel, *Perna canaliculus*. Journal of Experimental Marine Biology and Ecology 329, 206–217.

Amos, C., Feeney, T., Sutherland, T., Luternauer, J., 1997. The stability of fine-grained sediments from the Fraser River Delta. Estuarine, Coastal and Shelf Science 45: 507–524.

Amos, C.L., Grant, J., Daborn, G.R., Black, K., 1992. Sea Carousel—A benthic, annular flume. Estuarine, Coastal and Shelf Science 34, 557–577.

Andersen, T., 2001. Seasonal variation in erodibility of two temperate, microtidal mudflats. Estuarine, Coastal and Shelf Science 53, 1–12.

Andersen, T.J., Lanuru, M., van Bernem, C., Pejrup, M., Riethmueller, R., 2010. Erodibility of a mixed mudflat dominated by microphytobenthos and *Cerastoderma edule*, East Frisian Wadden Sea, Germany. Estuarine, Coastal and Shelf Science 87, 197–206.

Andersen, T.J., Pejrup, M., 2002. Biological Mediation of the Settling Velocity of Bed Material Eroded from an Intertidal Mudflat , the Danish Wadden Sea. Online 737–745.

Austen, I., Andersen, T.J., Edelvang, K., 1999. The Influence of Benthic Diatoms and Invertebrates on the Erodibility of an Intertidal Mudflat, the Danish Wadden Sea. Estuarine, Coastal and Shelf Science 49: 99–111.

Avella Vasquez, A.C., 2010. Substances polymériques extracellulaires dans les procédés de traitement des eaux usées.

-B-

Bellinger, B.J., Abdullahi, A.S., Gretz, M.R., Underwood, G.J.C., 2005. Biofilm polymers:relationship between carbohydrate biopolymers from estuarine mudflats and unialgal cultures of benthic diatoms. Aquatic Microbial Ecology 38, 169–180.

Beukema, J.J., 1976. Biomass and species richness of the macro-benthic animals living on the tidal flats of the Dutch Wadden Sea. Netherlands Journal of Sea Research 10, 236–261.

Biles, C., Paterson, D., Ford, R., Solan, M., Raffaelli, D., 2002. Bioturbation, ecosystem functioning and community structure. Hydrology and Earth System Sciences 6, 999–1005.

Blanchard, G.F., Guarini, J.-M., Dang, C., Richard, P., 2004. Characterizing and quantifying photoinhibition in intertidal microphytobenthos. Journal of Phycology 40, 692–696.

Blanchard, G.F., Guarini, J.-M., Orvain, F., Sauriau, P.-G., 2001. Dynamic behaviour of benthic microalgal biomass in intertidal mudflats. Journal of Experimental Marine Biology and Ecology 264, 85–100.

Blanchard, G.F., Sauriau, P.-G., Cariou-Le Gall, V., Gouleau, D., Garet, M.-J., Olivier, F., 1997. Kinetics of tidal resuspension of microbiota:esting the effects of sediment cohesiveness and bioturbation using flume experiments. Marine Ecology Progress Series 151, 17–25.

Blanckaert, K., 2005. Hydraulique fluviale et aménagement des cours d'eau – Transport de sédiments : L'essentiel.

Bougrier, S., Geairon, P., Deslous-Paoli, J., Bacher, C., Jonquières, G., 1995. Allometric relationships and effects of temperature on clearance and oxygen consumption rates of Crassostrea gigas (Thunberg). Aquaculture 134: 143–154.

Bradford, M., 1976. A rapid and sensitive method for the quantitation of microgram quantities of protein using the principle of protein dye binding. Analytical Biochemistry 72, 248–254.

Brotas V, Cabrita T, Portugal A (1995) Spatio-temporal distribution of the microphytobenthic biomass in intertidal flats of Tagus Estuary (Portugal). Hydrobiologia: 93–104.

Bruno, J.F., Stachowicz, J.J., Bertness, M.D., 2003. Inclusion of facilitation into ecological theory. Evolution 18, 119–125.

-C-

Cadée, G.C., 2001. Sediment Dynamics by Bioturbating Organisms, in: Reise, K. (Ed.), Ecological Comparisons of Sedimentary Shores. Springer Berlin Heidelberg, pp. 127–148.

Callier MD, Richard M, McKindsey CW, Archambault P, Desrosiers G (2009) Responses of benthic macrofauna and biogeochemical fluxes to various levels of mussel biodeposition: an in situ “benthocosm” experiment. Marine pollution bulletin 58: 1544–1553.

Callier, M.D., McKindsey, C.W., Desrosiers, G., 2008. Evaluation of indicators used to detect mussel farm influence on the benthos: Two case studies in the Magdalen Islands, Eastern Canada. Aquaculture 278, 77–88.

Carpenter SR, Elser MM, Elser JJ (1986) Chlorophyll production, degradation, and sedimentation: Implications for paleolimnology. Limonology And Oceanography 31: 112–124.

Cartaxana, P., Mendes, C., Vanleeuwe, M., Brotas, V., 2006. Comparative study on microphytobenthic pigments of muddy and sandy intertidal sediments of the Tagus estuary. Estuarine, Coastal and Shelf Science 66, 225–230.

Choy EJ, Richard P, Kim K-R, Kang C-K (2009) Quantifying the trophic base for benthic secondary production in the Nakdong River estuary of Korea using stable C and N isotopes. Journal of Experimental Marine Biology and Ecology 382: 18–26.

Cibic T, Blasutto O, Falconi C, Fondaumani S (2007) Microphytobenthic biomass, species composition and nutrient availability in sublittoral sediments of the Gulf of Trieste (northern Adriatic Sea). Estuarine, Coastal and Shelf Science 75: 50–62.

Ciutat, A., Widdows, J., Pope, N., 2007. Effect of Cerastoderma edule density on near-bed hydrodynamics and stability of cohesive muddy sediments. Journal of Experimental Marine Biology and Ecology 346, 114 – 126.

Ciutat, A., Widdows, J., Readman, J.W., 2006. Influence of cockle Cerastoderma edule bioturbation and tidal-current cycles on resuspension of sediment and polycyclic aromatic hydrocarbons. Marine Ecology Progress Series 51–64.

Cloern, J.E., 1987. Turbidity as a control on phytoplankton biomass and productivity in estuaries. Continental Shelf Research 7, 1367–1381.

Cognie, B., Barille, L., 1998. Does bivalve mucus favour the growth of their main food source, microalgae? Oceanologica acta 22, 441–450.

Colijn F, De Jonge V (1984) Primary production of microphytobenthos in the Ems-Dollard Estuary. Marine Ecology Progress Series 14: 185–196.

Comte, S., Guibaud, G., Baudu, M., 2006. Relations between extraction protocols for activated sludge extracellular polymeric substances (EPS) and EPS complexation properties Part I . Comparison of the efficiency of eight EPS extraction methods. Enzyme and Microbial Technology 38, 237–245.

Consalvey, M., Jesus, B., Perkins, R.G., Brotas, V., Underwood, G.J.C., Paterson, D.M., 2004. Monitoring Migration and Measuring Biomass in Benthic Biofilms: The Effects of Dark/far-red

Adaptation and Vertical Migration on Fluorescence Measurements. Photosynthesis Research 81, 91–101.

Crowe, T., Frost, N., Hawkins, S., 2011. Interactive effects of losing key grazers and ecosystem engineers vary with environmental context. Marine Ecology Progress Series 430, 223–234.

-D-

Davoult, D., Migné, A., Créach, A., Gévaert, F., Hubas, C., Spilmont, N., Boucher, G., 2009. Spatio-temporal variability of intertidal benthic primary production and respiration in the western part of the Mont Saint-Michel Bay (Western English Channel, France). Hydrobiologia 620, 163–172.

de Brouwer, J.F.C., Wolfstein, K., Ruddy, G.K., Jones, T.E.R., Stal, L.J., 2005. Biogenic stabilization of intertidal sediments: the importance of extracellular polymeric substances produced by benthic diatoms. Microbial ecology 49, 501–12.

de Jonge, V.N., 1985. The occurrence of «epipsammic» diatom populations: a result of interaction between physical sorting of sediment and certain properties of diatom species. Estuarine, coastal and shelf science 21, 607–622.

de Jonge, V.N., Van Beusekom, J., 1995. Wind-and tide-induced resuspension of sediment and microphytobenthos from tidal flats in the Ems estuary. Limnology and oceanography 40, 766–778.

de Montaudouin, X., 1997. Potential of bivalves' secondary settlement differs with species: a comparison between cockle (*Cerastoderma edule*) and clam (*Ruditapes philippinarum*) juvenile resuspension. Marine Biology 128, 639–648.

de Montaudouin, X., Audemard, C., Labourg, P.-J., 1999. Does the slipper limpet (*Crepidula fornicata*, L.) impair oyster growth and zoobenthos biodiversity? A revisited hypothesis. Journal of Experimental Marine Biology and Ecology 235, 105–124.

de Winder, B., Staats, N., Stal, L.J., Paterson, D.M., 1999. Carbohydrate secretion by phototrophic communities in tidal sediments 42, 131–146.

Decho, A.W., 2000. Microbial biofilms in intertidal systems : an overview. Continental Shelf Research 20, 1257–1273.

Deckere, E.D., Tolhurst, T., Brouwer, J.D., 2001. Destabilization of cohesive intertidal sediments by infauna. Estuarine, Coastal and Shelf Science 53, 665–669.

Decottignies, P., Beninger, P., Rincé, Y., Robins, R., Riera, P., 2007. Exploitation of natural food sources by two sympatric, invasive suspension-feeders: Crassostrea gigas and Crepidula fornicata. Marine Ecology Progress Series 334, 179–192.

Defew, E.C., Tolhurst, T.J., Paterson, D.M., Hagerthey, S.E., 2003. Can the stability of intertidal sediments be predicted from proxy parameters? An in situ investigation. Leamington Spa: Estuarine and Coastal Sciences Association. 61–70.

Denis, L., Grenz, C., Plante-Cuny, M.-R., 1996. Etude expérimentale de la remise en suspension du microphytobenthos. Comptes rendus de l'Académie des sciences. Série 3, Sciences de la vie 319, 529–536.

Deroin J-P (2012) Combining ALOS and ERS-2 SAR data for the characterization of tidal flats. Case study from the Baie des Veys, Normandy, France. International Journal of Applied Earth Observation and Geoinformation 18: 183–194.

Dolédec S, Chessel D (1994) Co-inertia analysis: an alternative method for studying species-environment relationships. Freshwater Biology 31: 277–294.

Dreywood, R., 1946. Qualitative test for carbohydrate material. Industrial & Engineering Chemistry Analytical Edition 18, 499–499.

Droppo, I., Ross, N., Skafel, M., Liss, S., 2007. Biostabilization of cohesive sediment beds in a freshwater wave-dominated environment. Limnology and oceanography 52, 577–589.

Dubois, M., Gilles, K.A., Hamilton, J.K., Rebers, P.A., Smith, F., 1956. Colorimetric method for determination of sugars and related substances. Analytical Chemistry 28, 350–356.

Dubois, S., Barillé, L., Cognie, B., 2009. Feeding response of the polychaete *Sabellaria alveolata* (*Sabellariidae*) to changes in seston concentration. Journal of Experimental Marine Biology and Ecology 376, 168–176.

Dubois, S., Barillé, L., Retière, C., 2003. Efficiency of particle retention and clearance rate in the polychaete *Sabellaria alveolata* L. Comptes rendus biologies 326, 413–21.

Dubois, S., Blin, J-L., Bouchaud, B., Lefebvre, S., 2007. Isotope trophic-step fractionation of suspension-feeding species : Implications for food partitioning in coastal ecosystems. Journal of Experimental Marine Biology and Ecology 351, 121–128.

Dubois, S., Marin-Léal, J.C., Ropert, M., Lefebvre, S., 2007. Effects of oyster farming on macrofaunal assemblages associated with *Lanice conchilega* tubeworm populations : A trophic analysis using natural stable isotopes. Life Sciences 271, 336 – 349.

Dubois, S., Orvain, F., Marin-léal, J.C., Ropert, M., Lefebvre, S., 2007. Small-scale spatial variability of food partitioning between cultivated oysters and associated suspension-feeding species , as revealed by stable isotopes. Marine Ecology Progress Series 336, 151–160.

Duchêne, J.-C., 2012. Hydroid and serpulid recruitment patterns using a new laser microtopography technique. Journal of Experimental Marine Biology and Ecology 412, 27–36.

-E-

Ehrenhauss, S., Witte, U., Janssen, F., Huettel, M., 2004. Decomposition of diatoms and nutrient dynamics in permeable North Sea sediments. Continental Shelf Research 24, 721–737.

Eilers, P.H.C., Peeters, J.C.H., 1988. A model for the relationship between light intensity and the rate of photosynthesis in phytoplankton. Ecological Modelling 42, 199–215.

Eleftheriou, A., Holme, N.A., 1984. Macrofauna techniques, in: N.A. Holme & A.D. McIntyre (Eds.), Methods for the Study of Marine Benthos, Oxford, Blackwell Scientific. pp. 140–216.

Escapa, M., Perillo, G., Iribarne, O., 2008. Sediment dynamics modulated by burrowing crab activities in contrasting SW Atlantic intertidal habitats. Estuarine, Coastal and Shelf Science 80, 365–373.

Ettema, C.H., Wardle, D.A., 2002. Spatial soil ecology. Trends in Ecology & Evolution 17, 177–183.

-F-

Fernandes, S., Sobral, P., Alca, F., 2009. *Nereis diversicolor* and copper contamination effect on the erosion of cohesive sediments: A flume experiment. Estuarine , Coastal and Shelf Science 82, 443–451.

Fernandes, S., Sobral, P., Costa, M.H., 2006. *Nereis diversicolor* effect on the stability of cohesive intertidal sediments. Aquatic Ecology 567–579.

Flach, E.C., 1996. The Influence of the Cockle, *Cerastoderma edule*, on the Macrozoobenthic Community of Tidal Flats in the Wadden Sea. Marine Ecology 17, 87–98.

Flemming, H.-C., Wingender, J., 2010. The biofilm matrix. Nature reviews. Microbiology 8, 623–33.

Franke, H.-D., Janke, M., 1998. Mechanisms and consequences of intra- and interspecific interference competition in *Idotea baltica* (Pallas) and *Idotea emarginata* (Fabricius) (Crustacea: Isopoda): A laboratory study of possible proximate causes of habitat segregation. Journal of experimental marine biology and ecology 227, 1–21.

François, F., Dalègre, K., Gilbert, F., Stora, G., 1999. Specific variability within functional groups. Study of the sediment reworking of two *Veneridae* bivalves, *Ruditapes decussatus* and *Venerupis aurea*, Comptes Rendus de l'Academie des Sciences Series III Sciences de la Vie.

François, F., Gerino, M., Stora, G., Durbec, J.-P., Poggiale, J.-C., 2002. Functional approach to sediment reworking by gallery-forming macrobenthic organisms: modeling and application with the polychaete *Nereis diversicolor*. Marine Ecology Progress series 229, 127–136.

Friedrichs, M., Graf, G., Springer, B., 2000. Skimming flow induced over a simulated polychaete tube lawn at low population densities. Marine Ecology Progress Series 192, 219–228.

Friend, P.L., Ciavola, P., Cappucci, S., Santos, R., 2003. Bio-dependent bed parameters as a proxy tool for sediment stability in mixed habitat intertidal areas. Continental Shelf Research 23, 1899–1917.

Friend, P.L., Lucas, C.H., Holligan, P.M., Collins, M.B., 2008. Microalgal mediation of ripple mobility. Geobiology 6, 70–82.

Frølund, B., Palmgren, R., Keiding, K., Nielsen, P.H., 1996. Extraction of extracellular polymers from activated sludge using a cation exchange resin. Water Research 30, 1749–1758.

-G-

Gardner, L.R., Sharma, P., Moore, W.S., 1987. A regeneration model for the effect of bioturbation by fiddler crabs on 210Pb profiles in salt marsh sediments. Journal of Environmental Radioactivity 5, 25–36.

Gerbersdorf, S.U., Bittner, R., Lubarsky, H., Manz, W., Paterson, D.M., 2009. Microbial assemblages as ecosystem engineers of sediment stability. Journal of Soils and Sediments 9, 640–652.

Gerbersdorf, S.U., Jancke, T., Westrich, B., 2007. Sediment properties for assessing the erosion risk of contaminated riverine sites. An approach to evaluate sediment properties and their covariance patterns over depth in relation to erosion resistance. Journal of Soils and Sediments 7, 25 – 35.

Giroldo, D., Vieira, A.A.H., Paulsen, B.S., 2003. Relative increase of deoxy sugars during microbial degradation of an extracellular polysaccharide released by a tropical freshwater *Thalassiosira sp.* (Bacillariophyceae). Journal of Phycology 39, 1109–1115.

Grabowsky, R.C., 2011. The erodibility of fine sediment deposits in lowland chalk streams.

Graf, G., 1992. Benthic-pelagic coupling: a benthic view. Oceanography and Marine Biology: An Annual Review 30, 149–190.

Graf, G., Rosenberg, R., 1997. Bioresuspension and biodeposition: a review. Journal of Marine Systems 11, 269–278.

Grangeré, K., Lefebvre, S., Bacher, C., Cugier, P., Ménesguen, a, 2010. Modelling the spatial heterogeneity of ecological processes in an intertidal estuarine bay: dynamic interactions between bivalves and phytoplankton. Marine Ecology Progress Series 415, 141–158.

Grangeré, K., Lefebvre, S., Blin, J.-L., 2012. Spatial and temporal dynamics of biotic and abiotic features of temperate coastal ecosystems as revealed by a combination of ecological indicators. Estuarine, Coastal and Shelf Science 108, 109–118.

Grant, C., 2010. Rôle des installations mytilicoles dans la structuration spatiale des communautés benthiques ; cas des assemblages de sédiments grossiers de l'Est de l'archipel Chausey (France).

Grant, C., Archambault, P., Olivier, F., McKindsey, C., 2012. Influence of "bouchot" mussel culture on the benthic environment in a dynamic intertidal system. Aquaculture Environment Interactions 2, 117–131.

Grant, J., Bathmann, U.V., Mills, E.L., 1986. The interaction between benthic diatom films and sediment transport. Estuarine, Coastal and Shelf Science 23, 225–238.

Grant, J., Cranford, P., Hargrave, B., Carreau, M., Schofield, B., Armsworthy, S., Burdett-Coutts, V., Ibarra, D., 2005. A model of aquaculture biodeposition for multiple estuaries and field

validation at blue mussel (*Mytilus edulis*) culture sites in eastern Canada. Canadian Journal of Fisheries and Aquatic Sciences 62, 1271–1285.

Grebmeier, J.M., Cooper, L.W., Feder, H.M., Sirenko, B.I., 2006. Ecosystem dynamics of the Pacific-influenced Northern Bering and Chukchi Seas in the Amerasian Arctic. Progress In Oceanography 71, 331–361.

Guarini J-M, Sari N, Moritz C (2008) Modelling the dynamics of the microalgal biomass in semi-enclosed shallow-water ecosystems. Ecological Modelling 211: 267–278.

Guarini J-M, Gros P, Blanchard G, Richard P, Fillon A (2004) Benthic contribution to pelagic microalgal communities in two semi-enclosed, European-type littoral ecosystems (Marennes-Oléron Bay and Aiguillon Bay, France). Journal of Sea Research 52: 241–258.

Guillaumont, B., 1987. Cartographie biomorphosédimentaire du golfe normano-breton (1987) au 1/25000.

Guizien, K., Orvain, F., Duchêne, J.-C., Le Hir, P., 2012. Accounting for Rough Bed Friction Factors of Mud Beds Due to Biological Activity in Erosion Experiments. Journal of Hydraulic Engineering.

Guyondet, T., Roy, S., Koutitonsky, V.G., Grant, J., Tita, G., 2010. Integrating multiple spatial scales in the carrying capacity assessment of a coastal ecosystem for bivalve aquaculture. Journal of Sea Research 64, 341–359.

Gérard, F., Blanchard, G., Agion, T., Jean-Marc, G., Herlory, O., Richard, P., 2006. Analysis of the short-term dynamics of microphytobenthos biomass on intertidal mudflats, in: Proceedings of the Colloquium, Amsterdam, Functioning of Microphytobenthos in Estuaries. p. 262.

-H-

Hammerstrom, K.K., Ranasinghe, J.A., Weisberg, S.B., Oliver, J.S., Fairey, W.R., et al., 2010. Effect of sample area and sieve size on benthic macrofaunal community condition assessments in California enclosed bays and estuaries. Integrated environmental assessment and management. Integrated Environmental Assessment and Management 8: 187–198.

Hanlon, A., Bellinger, B., Haynes, K., 2006. Dynamics of extracellular polymeric substance (EPS) production and loss in an estuarine, diatom-dominated, microalgal biofilm over a tidal emersion-immersion. Limnology and Oceanography 51, 79–93.

Hansen K, King GM, Kristensen E (1996) Impact of the soft-shell clam *Mya arenaria* on sulfate reduction in an intertidal sediment. Aquatic Microbial Ecology 10: 181–194.

Hay, S.I., Maitland, T.C., Paterson, D.M., 1993. The speed of diatom migration through natural and artificial substrata. Diatom research 8, 371–384.

Hayward, P.J., Ryland, J.S., 1990. The marine fauna of the British Isles and north West Wales. Clarendon Press, Oxford 1, 1–627.

Herman, P.M.J., Middelburg, J.J., Heip, C.H.R., 2001. Benthic community structure and sediment processes on an intertidal flat results from the ECOFLAT project. Continental Shelf Research 21, 2055–2071.

Holland, A.F., Zingmark, R.G., Dean, J.M., 1974. Quantitative evidence concerning the stabilization of sediments by marine benthic diatoms. Marine Biology 27, 191–196.

Holmes, R.M., Aminot, A., Kérouel, R., Hooker, B.A., Peterson, B.J., 1999. A simple and precise method for measuring ammonium in marine and freshwater ecosystems. Canadian Journal of Fisheries and Aquatic Sciences 56, 1801–1808.

Honkoop PJC, Pearson GB, Lavaleye MSS, Piersma T (2006) Spatial variation of the intertidal sediments and macrozoo-benthic assemblages along Eighty-mile Beach, North-western Australia. Journal of Sea Research 55: 278–291.

Huot Y, Babin M, Bruyant F (2007) Does chlorophyll a provide the best index of phytoplankton biomass for primary productivity studies? Biogeosciences 4: 707–745.

-I/J-

Jesus, B., Brotas, V., Marani, M., Paterson, D., 2005. Spatial dynamics of microphytobenthos determined by PAM fluorescence. Estuarine, Coastal and Shelf Science 65, 30–42.

Jiang, W., Gibbs, M.T., 2005. Predicting the carrying capacity of bivalve shellfish culture using a steady, linear food web model. Aquaculture 244, 171–185.

Jing, L., Ridd, P.V., 1996. Wave-current bottom shear stresses and sediment resuspension in Cleveland Bay, Australia. Coastal Engineering 29, 169–186.

Johnson, B.D., Azetsu-Scott, K., 1995. Adhesion force and the character of surfaces immersed in seawater. Limnology and Oceanography 40, 802–808.

Jones, C., Lawton, J., Shachak, M., 1994. Organisms as ecosystem engineers. Oikos 69, 373–386.

Jonsson, P., Duren, L.V., Amielh, M., 2006. Making water flow: a comparison of the hydrodynamic characteristics of 12 different benthic biological flumes. Aquatic Ecology 40, 409–438.

Jumars, P.A., Nowell, A.R.M., 1984. Effects of bentbos on sediment transport: difficulties with functional grouping. Continental Shelf Research 3, 115–130.

-K-

Kang, C., Lee, Y., Choy, E., Shin, J., Seo, I., Hong, J., 2006. Microphytobenthos seasonality determines growth and reproduction in intertidal bivalves. Marine Ecology Progress Series 315, 113–127.

Kasim M, Mukai H (2006) Contribution of benthic and epiphytic diatoms to clam and oyster production in the Akkeshi-ko estuary. Journal of Oceanography 62: 267–281.

Kervella, Y., Germain, G., Gaurier, B., Facq, J., 2010. Experimental study of the near-field impact of an oyster table on the flow. European journal of mechanics 29, 32–42.

Kingston, M.B., 2002. Effect of subsurface nutrient supplies on the vertical migration of Euglena proxima (*Euglenophyta*). Journal of Phycology 38, 872–880.

Koh CH, Khim JS, Araki H, Yamanishi H, Koga K (2007) Within-day and seasonal patterns of microphytobenthos biomass determined by co-measurement of sediment and water column chlorophylls in the intertidal mudflat of Nanaura, Saga, Ariake Sea, Japan. Estuarine, coastal and shelf science 72: 42–52.

Kon K, Hoshino Y, Kanou K, Okazaki D, Nakayama S, et al. (2012) Importance of allochthonous material in benthic macrofaunal community functioning in estuarine salt marshes. Estuarine, Coastal and Shelf Science 96: 236–244.

Krantzberg, G., 1985. The influence of bioturbation on physical, chemical and biological parameters in aquatic environments: A review. Environmental Pollution Series A, Ecological and Biological 39, 99–122.

Kristensen, E., 2001. Impact of polychaetes (*Nereis spp*. and *Arenicola marina*) on carbon biogeochemistry in coastal marine sediments. Geochemical transactions 2, 92.

Kristensen, E., Penha-Lopes, G., Delefosse, M., Valdemarsen, T., Quintana, C., Banta, G., 2012. What is bioturbation? The need for a precise definition for fauna in aquatic sciences. Marine Ecology Progress Series 446, 285–302.

-L-

Larson, F., Lubarsky, H., Gerbersdorf, S.U., Paterson, D.M., 2009. Surface adhesion measurements in aquatic biofilms using magnetic particle induction: MagPI. Limnology and Oceanography Methods 7, 490–497.

Lazure P, Dumas F (2008) An external–internal mode coupling for a 3D hydrodynamical model for applications at regional scale (MARS). Advances in Water Resources 31: 233–250.

Le Hir, P., Canna, P., Waelesb, B., Jestina, H., Bassoulleta, P., 2008. Erodibility of natural sediments: experiments on sand/mud mixtures from laboratory and field erosion tests. Proceedings in Marine Science 9, 137–153.

Le Hir, P., Cayocca, F., Waeles, B., 2011. Dynamics of sand and mud mixtures: A multiprocess-based modelling strategy. Continental Shelf Research 31, S135–S149.

Le Hir, P., Monbet, Y., Orvain, F., 2007a. Sediment erodability in sediment transport modelling: Can we account for biota effects? Continental Shelf Research 27, 1116–1142.

Lefebvre, S., Marín Leal, J.C., Dubois, S., Orvain, F., Blin, J.-L., Bataillé, M.-P., Ourry, A., Galois, R., 2009. Seasonal dynamics of trophic relationships among co-occurring suspension-feeders in two shellfish culture dominated ecosystems. Estuarine, Coastal and Shelf Science 82, 415–425.

Leguerrier, D., Niquil, N., Boileau, N., Rzeznik, J., Sauriau, P.-G., Le Moine, O., Bacher, C., 2003. Numerical analysis of the food web of an intertidal mudflat ecosystem on the Atlantic coast of France. Marine ecology progre Series 246, 17–37.

Lelieveld, S., Pilditchb, C.A., Green, M.O., 2003. Variation in sediment stability and relation to indicators of microbial abundance in the Okura Estuary, New Zealand. Estuarine, Coastal and Shelf Science 57, 123–136.

Lindström Swanberg, I., 1991. The influence of the filter-feeding bivalve *Cerastoderma edule* L. on microphytobenthos: a laboratory study. Journal of Experimental Marine Biology and Ecology 151, 93–111.

Liu, H., Fang, H., 2002. Extraction of extracellular polymeric substances (EPS) of sludges. Journal of Biotechnology 95, 249– 256.

Liu, Y., Fang, H.H.P., 2003. Influences of Extracellular Polymeric Substances (EPS) on Flocculation, Settling, and Dewatering of Activated Sludge. Critical Reviews in Environmental Science and Technology 33, 237–273.

Lohrer, A.M., Thrush, S.F., Gibbs, M.M., 2004. Bioturbators enhance ecosystem function through complex biogeochemical interactions. Nature 431, 1092–5.

Lorenzen, C.J., 1967. Determination of chlorophyll and phaeopigments: spectrophotometric equations. Limnology and Oceanography 343–346.

Lowry, O.H., Rosebrough, N.J., Farr, A.L., Randall, R.J., 1951. Protein measurement with the Folin phenol reagent. The Journal of biological chemistry 193, 265–75.

Lubarsky, H.V., Hubas, C., Chocholek, M., Larson, F., Manz, W., Paterson, D.M., Gerbersdorf, S.U., 2010. The stabilisation potential of individual and mixed assemblages of natural bacteria and microalgae. PloS one 5, e13794.

Lucas, C., Widdows, J., Wall, L., 2003. Relating spatial and temporal variability in sediment chlorophyll a and carbohydrate distribution with erodibility of a tidal flat. Estuaries and Coasts 26, 885–893.

Lucas, C.H., 2003. Observations of resuspended diatoms in the turbid tidal edge. Journal of Sea Research 50, 301 – 308.

Lucas, C.H., Banham, C., Holligan, P.M., 2001. Benthic-pelagic exchange of microalgae at a tidal flat. 2: taxonomic analysis. Marine Ecology Progress Series 212, 39–52.

Lucas, C.H., Widdows, J., Brinsley, M.D., Salkeld, P.N., Herman, P.M.J., 2000. Benthic-pelagic exchange of microalgae at a tidal flat: 1. Pigment analysis. Marine Ecology Progress Series 196, 59–73.

Luckenbach, M., Wang, H., 2004. Linking watershed loading and basin-level carrying capacity models to evaluate the effects of land use on primary production and shellfish aquaculture. Bulletin of Fisheries Research Agency Suppl. 1, 123–132.

Lumborg, U., Andersen, T., Pejrup, M., 2006. The effect of *Hydrobia ulvae* and microphytobenthos on cohesive sediment dynamics on an intertidal mudflat described by means of numerical modelling. Estuarine, Coastal and Shelf Science 68, 208–220.

Lund-Hansen LC, Petersson M, Nurjaya W (1999) Vertical sediment fluxes and wave-induced sediment resuspension in a shallow-water coastal lagoon. Estuaries 22: 39–46.

-M-

MacIntyre, H.L., Lomas, M.W., Cornwell, J., Suggett, D.J., Gobler, C.J., Koch, E.W., Kana, T.M., 2004. Mediation of benthic–pelagic coupling by microphytobenthos: an energy- and material-based model for initiation of blooms of *Aureococcus anophagefferens*. Harmful Algae 3, 403–437.

Maire, O., Duchêne, J., Amouroux, J., Grémare, A., 2007. Activity patterns in the terebellid polychaete *Eupolymnia nebulosa*; assessed using a new image analysis system. Marine Biology 151, 737–749.

Maire, O., Duchêne, J., Bigot, L., Grémare, A., 2007. Linking feeding activity and sediment reworking in the deposit-feeding bivalve *Abra ovata* with image analysis, laser telemetry, and luminophore tracers. Marine Ecology Progress Series 351, 139–150.

Malet N, Sauriau P, Ryckaert M, Malestroit P, Guillou G (2008) Dynamics and sources of suspended particulate organic matter in the Marennes-Oléron oyster farming bay: Insights from stable isotopes and microalgae ecology. Estuarine, Coastal and Shelf Science 78: 576–586.

Marcus, N.H., Boero, F., 1998. The importance of benthic-pelagic coupling and the forgotten role of life cycles in coastal aquatic systems. Limnology and oceanography 43, 763–768.

Marshall, H.L., Geider, R.J., Flynn, K.J., 2000. A mechanistic model of photoinhibition. New Phytologist 145, 347–359.

Marín Leal, J.C., Dubois, S., Orvain, F., Galois, R., Blin, J.-L., Ropert, M., Bataillé, M.-P., Ourry, A., Lefebvre, S., 2008. Stable isotopes (δ13C, δ15N) and modelling as tools to estimate the trophic ecology of cultivated oysters in two contrasting environments. Marine Biology 153, 673–688.

McKindsey, C., Thetmeyer, H., Landry, T., Silvert, W., 2006. Review of recent carrying capacity models for bivalve culture and recommendations for research and management. Aquaculture 261, 451–462.

McKindsey, C.W., Archambault, P., Callier, M.D., Olivier, F., 2011. Influence of suspended and off-bottom mussel culture on the sea bottom and benthic habitats a review. Canadian Journal of Zoology 89, 622–646.

Mehta, A., Partheniades, E., 1982. Resuspension of deposited cohesive sediment beds. Eighteenth Conference Coastal Engineering 1569–1588.

Mermillod-Blondin, F., François-Carcaillet, F., Rosenberg, R., 2005. Biodiversity of benthic invertebrates and organic matter processing in shallow marine sediments: an experimental study. Journal of Experimental Marine Biology and Ecology 315, 187–209.

Mermillod-Blondin, F., Rosenberg, R., François-Carcaillet, F., Norling, K., 2004. Influence of bioturbation by three benthic infaunal species on microbial communities and biogeochemical processes in marine sediment. Aquatic Microbial Ecology 36, 271–284.

Michaud, E., Desrosiers, G., Mermillod-Blondin, F., Sundby, B., Stora, G., 2005. The functional group approach to bioturbation: II. The effects of the *Macoma balthica* community on fluxes of nutrients and dissolved organic carbon across the sediment-water interface. Journal of Experimental Marine Biology and Ecology 337, 178–189.

Migniot, C., 1989. Tassement et rhéologie des vases, 1ère partie. La Houille Blanche 1, 11–29.

Mitbavkar, S., Anil, A., 2004. Vertical migratory rhythms of benthic diatoms in a tropical intertidal sand flat: influence of irradiance and tides. Marine biology 145, 9–20.

Mitchener, H., Torfs, H., 1996. Erosion of mud/sand mixtures. Coastal Engineering 29, 1–25.

Montserrat, F., Van Colen, C., Provoost, P., Milla, M., Ponti, M., Van den Meersche, K., Ysebaert, T., Herman, P.M.J., 2009. Sediment segregation by biodiffusing bivalves. Estuarine, Coastal and Shelf Science 83, 379–391.

Morris, E.P., 2005. Quantifying primary production of microphytobenthos: application of optical methods. Univ. Groningen.

-N-

Neumeier, U., Lucas, C.H., Collins, M., 2006. Erodibility and erosion patterns of mudflat sediments investigated using an annular flume. Aquatic Ecology 40, 543–554.

Newell, R., 2004. Ecosystem influences of natural and cultivated populations of suspension-feeding bivalve molluscs: a review. Journal of Shellfish Research 23, 51–61.

Newell RIE, Cornwell JC, Owens MS (2002) Influence of simulated bivalve biodeposition and microphytobenthos on sediment nitrogen dynamics: A laboratory study. Limonology And Oceanography 47: 1367–1379.

Ni Longphuirt S, Clavier J, Grall J, Chauvaud L, Leloch F, et al. (2007) Primary production and spatial distribution of subtidal microphytobenthos in a temperate coastal system, the Bay of Brest, France. Estuarine, Coastal and Shelf Science 74: 367–

Nixon, S.W., Oviatt, C.A., Frithsen, J., Sullivan, B., 1986. Nutrients and the productivity of estuarine and coastal marine ecosystems. Journal of the Limnological Society of Southern Africa 12, 43–71.

Nowell, A., Jumars, P., 1987. Flumes: theoretical and experimental considerations for simulation of benthic environments. Oceanography and Marine Biology 25, 91–112.

Nybakken, J.W., Bertness, M.D., 2004. Marine Biology: An Ecological Approach (6th Edition). Benjamin Cummings.

-O-

Odebrecht, C., Abreu, PC., Fugita, C. BM (2003) The Impact of Mud Deposition on the Long Term Variability of the Surf-Zone Diatom *Asterionellopsis glacialis* (Castracane) Round at Cassino Beach, Brazil. Journal of Coastal Research: 486–491.

Orvain, F., 2005. A model of sediment transport under the influence of surface bioturbation: generalisation to the facultative suspension-feeder *Scrobicularia plana*. Marine Ecology Progress Series 286, 43–56.

Orvain, F., De Crignis, M., Guizien, K., Lefebvre, S., Mallet, C., Takahashi, E., Dupuy, C., n.d. Tidal and seasonal effects on the consortium of bacteria, microphytobenthos and exopolymers in natural intertidal biofilms (Brouage, France). Aquatic Microbial Ecology.

Orvain, F., Galois, R., Barnard, C., 2003a. Carbohydrate production in relation to microphytobenthic biofilm development: An integrated approach in a tidal mesocosm. Microbial ecology 45, 237–251.

Orvain, F., Le Hir, P., Sauriau, P., 2003b. A model of fluff layer erosion and subsequent bed erosion in the presence of the bioturbator *Hydrobia ulvae*. Journal of Marine Research 823– 851.

Orvain, F., Lefebvre, S., Montepini, J., Sébire, M., Gangnery, A., Sylvand, B., 2012. Spatial and temporal interaction between sediment and microphytobenthos in a temperate estuarine macro-intertidal bay. Marine Ecology Progress Series 458, 53–68.

Orvain, F., Sauriau, P., Hir, P.L., 2007. Spatio-temporal variations in intertidal mudflat erodability: Marennes-Oléron Bay, western France. Continental Shelf Research 27, 1153–1173.

Orvain, F., Sauriau, P.G., Sygut, A., Joassard, L., Le Hir, P., 2004. Interacting effects of *Hydrobia ulvae* bioturbation and microphytobenthos on the erodibility of mudflat sediments. Marine Ecology Progress Series 278, 205–223.

-P-

Paarlberg, a, Knaapen, M., Devries, M., Hulscher, S., Wang, Z., 2005. Biological influences on morphology and bed composition of an intertidal flat. Estuarine, Coastal and Shelf Science 64, 577–590.

Pan, X., Liu, J., Zhang, D., Chen, X., Li, L., Song, W., Yang, J., 2010. Five extraction methods for extracellular polymeric substances (EPS) from biofilm by using three-dimensional excitation-emission matrix (3DEEM) fluorescence. Water SA 36, 111–116.

Panagiotopoulos, I., Voulgaris, G., Collins, M.B., 1997. The influence of clay on the threshold of movement of fine sandy beds. Coastal Engineering 32, 19–43.

Pannard A, Bormans M, Lagadeuc Y (2008) Phytoplankton species turnover controlled by physical forcing at different time scales. Canadian Journal of Fisheries and Aquatic Sciences 65: 47–60. doi:10.1139/F07-149.

Paterson, D., 1989a. Short-term changes in the erodibility of intertidal cohesive sediments related to the migratory behavior of epipelic diatoms. Limnology and Oceanography 34, 223–234.

Paterson, D.M., 1989b. Short-term changes in the erodibility of intertidal cohesive sediments related to the migratory behaviour of epipelic diatoms. Limnology and Oceanography 34, 223–234.

Paterson, M.S., 1982. The determination of hydroxyl by infrared absorption in quartz, silicate glasses and similar materials. Bulletin de Minéralogie 105, 20–29.

Peine, F., Friedrichs, M., Graf, G., 2009. Potential influence of tubicolous worms on the bottom roughness length z 0 in the south-western Baltic Sea. Journal of Experimental Marine Biology and Ecology 374, 1–11.

Peninsula, D., Reay, W.G., Gallagherl, D.L., Simmons, G.M., 1995. Sediment-water column oxygen and nutrient fluxes in nearshore environments of the lower Delmarva Peninsula, USA. Marine Ecology Progress Series 118, 215–227.

Perissinotto, R., Nozais, C., Kibirige, I., Anandraj, A., 2003. Planktonic food webs and benthic-pelagic coupling in three South African temporarily-open estuaries. Acta Oecologica 24, 307–316.

Perkins, R., 2003. Changes in microphytobenthic chlorophyll a and EPS resulting from sediment compaction due to de-watering: opposing patterns in concentration and content. Continental Shelf Research 23, 575–586.

Perkins, R.G., Underwood, G.J.C., Brotas, V., Snow, G.C., Jesus, B., Ribeiro, L., 2001. Responses of microphytobenthos to light : primary production and carbohydrate allocation over an emersion period. Marine Ecology Progress Series 223, 101–112.

Phillips, D.L., Gregg, J.W., 2003. Source partitioning using stable isotopes: coping with too many sources. Oecologia 136, 261–9.

Pierre, G., Graber, M., Rafiliposon, B.A., Dupuy, C., Orvain, F., De Crignis, M., Maugard, T., 2012. Biochemical composition and changes of extracellular polysaccharides (ECPS) produced during microphytobenthic biofilm development (Marennes-Oléron, France). Microbial Ecology 63, 157–69.

Pillay, D., Branch, G.M., Forbes, A.T., 2007a. The influence of bioturbation by the sandprawn *Callianassa kraussi* on feeding and survival of the bivalve *Eumarcia paupercula* and the gastropod *Nassarius kraussianus*. Journal of Experimental Marine Biology and Ecology 344, 1 – 9.

Pillay, D., Branch, G.M., Forbes, A.T., 2007b. Effects of *Callianassa kraussi* on microbial biofilms and recruitment of macrofauna : a novel hypothesis for adult – juvenile interactions. Marine Ecology Progress Series 347, 1–14.

Porri, F., Jordaan, T., McQuaid, C.D., 2008. Does cannibalism of larvae by adults affect settlement and connectivity of mussel populations? Estuarine, Coastal and Shelf Science 79, 687–693.

Porter, E., Mason, R., Sanford, L., 2010. Effect of tidal resuspension on benthic–pelagic coupling in an experimental ecosystem study. Marine Ecology Progress Series 413, 33–53.

Prins, T., Smaal, A., Dame, R., 1998. A review of the feedbacks between bivalve grazing and ecosystem processes. Aquatic Ecology 31, 349–359.

Prins, T.C., Dankers, N., Smaal, A.C., 1994. Seasonal variation in the filtration rates of a semi-natural mussel bed in relation to seston composition. Journal of Experimental Marine Biology and Ecology 176, 69–86.

-Q-

Quaresma, V. da S., Amos, C.L., Bastos, A.C., 2007. The Influence of Articulated and Disarticulated Cockle Shells on the Erosion of a Cohesive Bed. Journal of Coastal Research 236, 1443–1451.

-R-

Riera, P., Stal, L.J., Nieuwenhuize, J., 2002. δ13C versus δ15N of co-occurring molluscs within a community dominated by *Crassostrea gigas* and *Crepidula fornicata* (Oosterschelde, The Netherlands). Marine Ecology Progress Series 240, 291–295.

Riera, P., Stal, L.J., Nieuwenhuize, J., Richard, P., Blanchard, G., Gentil, F., 1999. Determination of food sources for benthic invertebrates in a salt marsh (Aiguillon Bay, France) by carbon and nitrogen stable isotopes: importance of locally produ ced sources. Marine Ecology Progress Series 187, 301–307.

Riisgårdet, H.U., Kamermans, P., 2001. Switching Between Deposit and Suspension Feeding in Coastal Zoobenthos. Ecological Studies 151, 73–101.

Roberts JJ, Best BD, Dunn DC, Treml EA, Halpin PN (2010) Environmental Modelling & Software Marine Geospatial Ecology Tools: An integrated framework for ecological geoprocessing with ArcGIS , Python , R , MATLAB , and Cþþ. Environmental Modelling and Software 25: 1197–1207.

Robson, A., Thomas, G., Garcia de Leaniz, C., Wilson, R.P., 2009. Valve gape and exhalant pumping in bivalves: optimization of measurement. Aquatic Biology 6, 191–200.

Rodland, D.L., Schone, B.R., Baier, S., Zhang, Z., Dreyer, W., Page, N.A., 2008. Changes in gape frequency, siphon activity and thermal response in the freshwater bivalves *Anodonta cygnea* and *Margaritifera falcata*. Journal of Molluscan Studies 75, 51–57.

Rörig, L.R. & Garcia VMT (2003) Accumulations of the surf-zone diatom *Asterionellopsis glacialis* (Castracane) in Cassino Beach, Southern Brazil, and its Relationship with Environmental Factors. Journal of Coastal Research: 167–177.

Rossi, F., Herman, P., Middelburg, J., 2004. Interspecific and intraspecific variation of δ13C and δ15N in deposit and suspension-feeding bivalves (*Macoma balthica* and *Cerastoderma edule*): evidence of ontogenetic changes in feeding mode of Macoma balthica. Limnology and Oceanography 49, 408–414.

Round, F.E., 1991. Diatoms in river-monitoring studies. Journal of Applied Phycology. Journal of Applied Phycology 3, 129–145.

Rueda, J.L., Smaal, A.C., Scholten, H., 2005. A growth model of the cockle (*Cerastoderma edule* L.) tested in the Oosterschelde estuary (The Netherlands). Journal of Sea Research 54, 276–298.

-S-

Saburova, M., Polikarpov, I., 2003. Diatom activity within soft sediments: behavioural and physiological processes. Marine Ecology Progress Series 251, 115–126.

Saburova M, Polikarpov I (1995) Spatial structure of an intertidal sandflat microphytobenthic community as related to different spatial scales. Marine Ecology Progress Series 129: 229–239.

Safi KA (2003) Microalgal populations of three New Zealand coastal locations: forcing functions and benthic-pelagic links. Marine Ecology Progress Series 259: 67–78.

Schaaff, E., Grenz, C., Pinazo, C., Lansard, B., 2006. Field and laboratory measurements of sediment erodibility: A comparison. Journal of Sea Research 55, 30–42.

Schelske, C.L. and Odum EP (1962) Mechanisms maintaining high productivity in Georgia estuaries. Gulf and Caribbean Fisheries Inst Proc: 75–80.

Schiffers, K., Teal, L.R., Travis, J.M.J., Solan, M., 2011. An Open Source Simulation Model for Soil and Sediment Bioturbation. PLoS ONE 6, e28028.

Serôdio, J., Lavaud, J., 2011. A model for describing the light response of the nonphotochemical quenching of chlorophyll fluorescence. Photosynthesis Research 108, 61–76.

Serôdio, J., Vieira, S., Cruz, S., 2008. Photosynthetic activity, photoprotection and photoinhibition in intertidal microphytobenthos as studied in situ using variable chlorophyll fluorescence. Continental Shelf Research 28, 1363–1375.

Serodio J, Coelho H, Vieira S, Cruz S (2006) Microphytobenthos vertical migratory photoresponse as characterised by light-response curves of surface biomass. Estuarine, Coastal and Shelf Science 68: 547–556.

Serôdio, J., da Silva, J., Catarino, F., 1997. Nondestructive tracing of migratory rhythms of intertidal benthic microalgae using in vivo cholorophyll a fluorescence. Journal of Phycology 33, 542–553.

Shimeta, J., Amos, C., Beaulieu, S., Ashiru, O., 2002. Sequential resuspension of protists by accelerating tidal flow: implications for community structure in the benthic boundary layer. Limnology and Oceanography 47, 1152–1164.

Shimeta, J., Amos, C., Beaulieu, S.E., Katz, S.L., 2003. Resuspension of benthic protists at subtidal coastal sites with differing sediment composition. Marine Ecology Progress Series 259, 103–115.

Smith, C.R., Jumars, P.A., DeMaster, D.J., 1986. In situ studies of megafaunal mounds indicate rapid sediment turnover and community response at the deep-sea floor. Nature 323, 251–253.

Smith, C.R., Mincks, S., DeMaster, D.J., 2006. A synthesis of bentho-pelagic coupling on the Antarctic shelf: Food banks, ecosystem inertia and global climate change. Deep Sea Research Part II: Topical Studies in Oceanography 53, 875–894.

Smith, D., Underwood, G., 1998. Exopolymer production by intertidal epipelic diatoms. Limnology and Oceanography 43, 1578–1591.

Smith, D., Underwood, G., 2001. The production of extracellular carbohydrates by estuarine benthic diatoms: the effects of growth phase and light and dark treatment. Journal of Phycology 333, 321–333.

Smith, P.K., Krohn, R.I., Hermanson, G.T., Mallia, A.K., Gartner, F.H., Provenzano, M.D., Fujimoto, E.K., Goeke, N.M., Olson, B.J., Klenk, D.C., 1985. Measurement of protein using bicinchoninic acid. Analytical Biochemistry 150, 76–85.

Snoeijs P, Busse S, Potapova M (2002) The importance of diatom cell size in community analysis. Journal of Phycology 38: 265–281.

Soares, C., Sobral, P., 2009. Density-dependent effects of bioturbation by the clam, *Scrobicularia plana*, on the erodibility of estuarine sediments. Marine and Freshwater Research 737–744.

Spears B, Saunders J, Davidson I, Paterson DM (2008) Microalgal sediment biostabilisation along a salinity gradient in the Eden Estuary, Scotland: unravelling a paradox. Marine And Freshwater Research 59, 313–321.

Spilmont, N., Seuront, L., Meziane, T., Welsh, D.T., 2011. There's more to the picture than meets the eye: Sampling microphytobenthos in a heterogeneous environment. Estuarine, Coastal and Shelf Science 95, 470–476.

Spooner N, Harvey HR, Pearce GES, Eckardt CB, Maxwell JR (1994) Biological defunctionalisation of chlorophyll in the aquatic environment. II: Action of endogenous algal enzymes and aerobic bacteria. Organic geochemistry 22: 773–780.

St-Onge, P., Miron, G., Moreau, G., 2007. Burrowing behaviour of the softshell clam (*Mya arenaria*) following erosion and transport. Journal of Experimental Marine Biology and Ecology 340, 103–111.

Staats, N., Stal, L., Mur, L., 2000. Exopolysaccharide production by the epipelic diatom Cylindrotheca closterium: effects of nutrient conditions. Journal of Experimental Marine Biology and Ecology 249, 13–27.

Staats, N., Stal, L.J., De Winder, B., Mur, L.R., 2000. Oxygenic photosynthesis as driving process in exopolysaccharide production of benthic diatoms. Marine Ecology Progress Series 193, 261–269.

Stevenson, R.J., Peterson, C.G., Kirschtel, D.B., King, C.C., Tuchman, N.C., 1991. Density-dependent growth, ecological strategies, and effects of nutrients and shading on benthic diatoms uccession in streams. Journal of Phycology 27, 59–69.

Stone, M., Krishnappan, B.G., Emelko, M.B., 2008. The effect of bed age and shear stress on the particle morphology of eroded cohesive river sediment in an annular flume. Water research 42, 4179–87.

Sutherland, I.W., 2001. Biofilm exopolysaccharides: a strong and sticky framework. Microbiology 147, 3–9.

Sutherland, T.F., Amos, C.L., Grant, J., 1998. The effect of buoyant biofilms on the erodibility microtidal estuary of sublittoral sediments of a temperate Lunenburg Bay. Limnology and Oceanography 43, 225–235.

Sylvand, B., 1995. Sylvand B., La Baie des Veys, 1972–1992: Structure et évolution à long terme d'un écosystème benthique intertidal de substrat meuble sous influence estuarienne.

-T-

Taghon, G.L., Nowell, A.R., Jumars, P.A., 1980. Induction of suspension feeding in spionid polychaetes by high particulate fluxes. Science (New York, N.Y.) 210, 562–4.

Takahashi, E., Ledauphin, J., Goux, D., Orvain, F., 2010. Optimising extraction of extracellular polymeric substances (EPS) from benthic diatoms: comparison of the efficiency of six EPS extraction methods. Marine And Freshwater Research 1–10.

Thornton, D.C.O., Dong, L.F., Underwood, G.J.C., Nedwell, D.B., 2002. Factors affecting microphytobenthic biomass , species composition and production in the Colne Estuary (UK). Aquatic Microbial Ecology 27, 285–300.

Tolhurst TJ, Jesus B, Brotas V, Paterson DM (2003) Diatom migration and sediment armouring – an example from the Tagus Estuary , Portugal. Marine Ecology: 183–193.

Tolhurst, T.J., Black, K.S., Shayler, S.A., Mather, S., Black, I., Baker, K., Paterson, D.M., 1999. Measuring the in situ Erosion Shear Stress of Intertidal Sediments with the Cohesive Strength Meter (CSM). Estuarine, Coastal and Shelf Science 49, 281–294.

Tolhurst, T.J., Defew, E.C., Brouwer, J.F.C.D., Wolfstein, K., 2006. Small-scale temporal and spatial variability in the erosion threshold and properties of cohesive intertidal sediments. Continental Shelf Research 26, 351–362.

Tolhurst, T.J., Gust, G., M Paterson, D., 2002. The influence of an extracellular polymeric substance (EPS) on cohesive sediment stability, in: Fine Sediment Dynamics in the Marine Environment. Elsevier, pp. 409–425.

Tolhurst, T.J., Jesus, B., Brotas, V., Paterson, D.M., 2003. Diatom migration and sediment armouring – an example from the Tagus Estuary , Portugal. Marine Ecology 183–193.

Tolhurst, T.J., Watts, C.W., Vardy, S., Saunders, J.E., Consalvey, M.C., Paterson, D.M., 2008. The effects of simulated rain on the erosion threshold and biogeochemical properties of intertidal sediments. Continental Shelf Research 28, 1217–1230.

Trevethan, M., Cater, J., Coleman, S., 2010. Low Reynolds Number Bed Shear Stress Measurements Behind a Backward-facing Step Using PIV, in: 17th Australian Fluid Mechanics Conference. pp. 1–4.

Trotsenburg, M., 2011. Estuarine ecosystem engineering: biogeomorphology in the estuarine intertidal.

-U-

Ubertini, M., Lefebvre, S., Gangnery, A., Grangere, K., Le Gendre, R., Orvain, F., 2012. Spatial Variability of Benthic-Pelagic Coupling in an Estuary Ecosystem Consequences for Microphytobenthos Resuspension Phenomenon. Plos ONE 7, 1–17.

Ubertini, M., Rakotomalala, C., Orvain, F., n.d. Impact of sediment grain-size and biofilm age on microphytobenthos resuspension. Submitted to Journal of Sea Research.

Underwood, GJC, Barnett M (2006) What determines species composition in microphytobenthic biofilms? Functioning of microphytobenthos in estuaries. Kromkamp J, editor. Microphytobenthos symposium. Amsterdam, The Netherlands: Royal Netherlands Academy of Arts and Sciences. pp. 121–138.

Underwood, G.J.C., Kromkamp, J., 1999. Primary production by phytoplankton and microphytobenthos in estuaries. Advances In Ecological Research 29, 93–153.

Underwood, G., Smith, D., 1998. Predicting Epipelic Diatom Exopolymer Concentrations in Intertidal Sediments from Sediment Chlorophyll a. Microbial ecology 35, 116–25.

Underwood, AJ, Chapman, M., 1996. Scales of spatial patterns of distribution of intertidal invertebrates. Oecologia 1996, 212–224.

Utermöhl von H (1931) Neue Wege in der quantitativen Erfassung des Planktons. (Mit besondere Beriicksichtigung des Ultraplanktons). Verh Int Verein Theor Angew Limnol 5: 567–595.

-V-

Valdemarsen, T., Wendelboe, K., Egelund, J.T., Kristensen, E., Flindt, M.R., 2011. Burial of seeds and seedlings by the lugworm Arenicola marina hampers eelgrass (Zostera marina) recovery. Journal of Experimental Marine Biology and Ecology 410, 45–52.

van Duren, L. a., Herman, P.M.J., Sandee, A.J.J., Heip, C.H.R., 2006. Effects of mussel filtering activity on boundary layer structure. Journal of Sea Research 55, 3–14.

van de Koppel, J., Herman, P., Thoolen, P., Heip, C., 2001. Do alternate stable states occur in natural ecosystems? Evidence from a tidal flat. Ecology 82, 3449–3461.

van de Koppel, J., Rietkerk, M., Dankers, N., Herman, P.M.J., 2005. Scale-dependent feedback and regular spatial patterns in young mussel beds. The American Naturalist 165, E66–77.

van der Wal, D., Wielemaker-van den Dool, A., Herman, P.M.J., 2010. Spatial Synchrony in Intertidal Benthic Algal Biomass in Temperate Coastal and Estuarine Ecosystems. Ecosystems 13, 338–351.

van der Wal D, Herman P, Forster R, Ysebaert T, Rossi F, et al. (2008) Distribution and dynamics of intertidal macrobenthos predicted from remote sensing: response to microphytobenthos and environment. Marine Ecology Progress Series 367: 57–72.

Vignaga, E., 2012. The effect of biofilm colonization on the stability of non-cohesive sediments.

Volkenborn, N., 2007. Effects of bioturbation and bioirrigation by lugworms (*Arenicola marina*) on physical and chemical sediment properties and implications for intertidal habitat succession. Estuarine, Coastal and Shelf Science 74, 331–343.

-W-

Waeles, B., Hir, P.L., Lesueur, P., 2008. Sediment and Ecohydraulics, in: INTERCOH 2005. Elsevier.

Waite AM., Thompson PA., Harrisson PJ. (1992) Does energy controls the sinking rates of marine diatoms ? Limnology and Oceanography 37: 468–477.

Webb, M.N., Warren, L., Starr, D., 1974. Carbon dioxide exchange of Alnus rubra. Oecologia 4, 281–291.

Webster, R., Welham, S.J., Potts, J.M., Oliver, M.A., 2006. Estimating the spatial scales of regionalized variables by nested sampling, hierarchical analysis of variance and residual maximum likelihood. Computers & Geosciences 32, 1320–1333.

Weerman, E.J., van de Koppel, J., Eppinga, M.B., Montserrat, F., Liu, Q.-X., Herman, P.M.J., 2010. Spatial self-organization on intertidal mudflats through biophysical stress divergence. The American Naturalist 176, E15–32.

Welschmeyer, N.A., 1994. Fluorometric of chlorophyll a in the presence of analysis b and pheopigments chlorophyll. Limonology and Oceanography 39, 1985–1992.

Wentworth, C.K., 1922. A scale of grade and class terms for clastic sediments. Journal of Geology 30, 377–392.

Whitehouse, R.J.S., Bassoullet, P., Dyer, K.R., Mitchener, H.J., Roberts, W., 2000. The influence of bedforms on flow and sediment transport over intertidal mudflats. Continental Shelf Research 20, 1099–1124.

Widdows, J., Brinsley, M., 2002. Impact of biotic and abiotic processes on sediment dynamics and the consequences to the structure and functioning of the intertidal zone. Journal of Sea Research 48, 143 – 156.

Widdows, J., Navarro, J., 2007. Influence of current speed on clearance rate, algal cell depletion in the water column and resuspension of biodeposits of cockles (*Cerastoderma edule*). Journal of Experimental Marine Biology and Ecology 343, 44 – 51.

Widdows, J., Pope, N.D., Brinsley, M.D., Gascoigne, J., Kaiser, M.J., 2009. Influence of self-organised structures on near-bed hydrodynamics and sediment dynamics within a mussel (*Mytilus edulis*) bed in the Menai Strait. Journal of Experimental Marine Biology and Ecology 379, 92–100.

Wigglesworth-Cooksey, B., Berglund, D., Cooksey, K.E., 2001. Cell–cell and cell–surface interactions in an illuminated biofilm: Implications for marine sediment stabilization. Geochemical Transactions 2, 75.

Willows, R.I., Widdows, J., Wood, R.G., 1998. Influence of an infaunal bivalve on the erosion of an intertidal cohesive sediment: A flume and modeling study. Limnology and Oceanography 43, 1332–1343.

Wolf, G., 2007. Kinetic modeling of phototrophic biofilms: The PHOBIA model. Biotechnology and Bioengineering 97, 1064–1079.

Wood, R., Widdows, J., 2002. A model of sediment transport over an intertidal transect, comparing the influences of biological and physical factors. Limnology and oceanography 47, 848–855.

-X/Y-

Yallop, M., Paterson, D., Wellsbury, P., 2000. Interrelationships between rates of microbial production, exopolymer production, microbial biomass, and sediment stability in biofilms of intertidal sediments. Microbial Ecology 39, 116–127.

Ysebaert, T., Hart, M., Herman, P.M.J., 2009. Impacts of bottom and suspended cultures of mussels Mytilus spp. on the surrounding sedimentary environment and macrobenthic biodiversity. Helgoland Marine Research 63, 59–74.

-Z-

Zetsche, E., Paterson, D., Lumsdon, D., Witte, U., 2011. Temporal variation in the sediment permeability of an intertidal sandflat. Marine Ecology Progress Series 441, 49–63.

Zhou, J., Mopper, K., Passow, U., 1998. The role of surface-active carbohydrates in the formation of transparent exopolymer particles by bubble adsorption of seawater. Limnology and Oceanography 43, 1860–1871.

Ziervogel, K., Forster, S., 2006. Do benthic diatoms influence erosion thresholds of coastal subtidal sediments? Journal of Sea Research 55, 43–53.

Liste des figures

Figure 1 : Biofilm de surface avec diatomées épipéliques (Source : Barreto et Meyer, 2006). 6

Figure 2 : Rythme de migration verticale des diatomées benthiques épipéliques, adapté de Gérard et al. (2006). 6

Figure 3 : Particules ferromagnétiques fluorescentes remises en suspension lors d'une expérimentation au MAGPI (Source : http://www.partrac.com)..... 13

Figure 4 : Illustration des différents types de dispositifs d'étude de la remise en suspension (Source : Jonsson et al., 2006)..... 15

Figure 5 : Schéma simplifié du fonctionnement de l'érodimètre développé par IFREMER 17

Figure 6 : Diagramme conceptuel des interactions entre les bivalves cultivés et l'écosystème, en lien avec : (A) l'impact de la filtration sur la déplétion en MES (seston); (B) la biodéposition de la matière organique non digérée dans les fèces et pseudofèces; (C) l'excrétion d'ammonium et d'azote; and (D) l'enlèvement de matériaux (sels nutritifs) lors de la récolte des bivalves (Cranford et al. 2006)..... 19

Figure 7 : Modes de déplacement des particules solides lors d'épisodes d'érosion (Source : Blanckaert, 2005). 20

Figure 8 : Illustration des vitesses et tensions inhérentes au niveau du fond pendant un écoulement de fluide turbulent (Source : Blanckaert, 2005)..... 21

Figure 9 : Écoulement sur surface lisse (A), avec un profil de vitesse logari-thmique caractéristique. Lorsqu'il rencontre des irrégularités de surface (b), l'écoulement devient turbulent (c) et une combinaison de forces de poussée et traction entraîne les particules de sédiments à s'éroder (Trotsenburg, 2011). 21

Figure 10 : Microstructure d'un sédiment cohésif, montrant les matrices créées par les composants biotiques et abiotiques (Source : Grabowsky, 2011)..... 25

Figure 11 : Illustration du phénomène de bioturbation au niveau de la zone intertidale. On y observe les différents taxons ainsi que les différents types de perturbation du sédiment par la faune endogée. 27

Figure 12: Les 4 types de remaniements sédimentaires par la macrofaune benthique. A. Biodiffuseurs, B. Convoyeurs vers le haut, C. Convoyeurs vers le bas, D. Régénérateurs (Source : Kristensen et al., 2012) 28

Figure 13 : Situation géographique de la baie des veys..... 31

Figure 14 : Vues d'altitude de la Baie des Veys. Les chenaux d'Isigny et Carentan apparaissent respectivement à gauche et à droite de la photo (Sources : http://www.basse-normandie.developpement-durable.gouv.fr pour l'image de gauche, Homeexhange.com pour l'image de droite)..... 32

Figure 15 : Localisation géographique de Lingreville sur mer (Source : Lefebvre et al., 2009)..... 335

Figure 16 : A gauche, embouchure de la Sienne et en arrière plan embouchure de la Vanlée (Source : http://www.parachutisme-chutelibre.fr). A droite Havre de la Vanlée (Source : http://manche.fr)..... 33

Figure 17 : Modélisation du panache de la Vanlée (à gauche) et de la Sienne (à droite). Simulation sans vent, coefficient de marée 75, rejet continu, lâché à pleine mer. L'échelle de dilution est symbolisée du rouge (moins dilué) au bleu (plus dilué) (Source : http://www.ifremer.fr/envlit, 2008). 33

Figure 18 : Approches utilisées durant la thèse pour répondre à la problématique générale..... 34

Figure 19 : Relation entre la biomasse de coques C. edule et le pourcentage de chl a benthique remis en suspension correspondant. 145

Figure 20 : Comparaison de 1) la simulation de la remise en suspension de la chl *a* benthique par les coques au jusant durant le mois d'Avril 2010 (A) et de 2) la concentration totale en chlorophylle a dans la colonne d'eau (B). 147

Figure 21 : Comparaison de 1) la simulation de la remise en suspension de la chl *a* benthique par les coques au jusant durant le mois de Septembre 2010 (A) et de 2) la concentration totale en chlorophylle a dans la colonne d'eau (B). 148

Liste des tableaux

Tableau 1 : Les différents types de systèmes permettant de mesurer l'érosion du sédiment 16

Tableau 2 : Fonctions des EPS dans les biofilms, tiré de Flemming and Wingender (2010). 24

Tableau 3 : Travaux menés depuis 2000 concernant l'influence du microphytobenthos sur la stabilité sédimentaire 26

Tableau 4 : Etudes menées depuis les années 2000 quant aux effets de la bioturbation sur les paramètres d'érodabilité à l'interface eau-sédiment 30

Tableau 5 : Différences notoires entre les deux écosystèmes modèles étudiés pendant la thèse 35